Comprehensive risk-perspective for flood defence system management

den Heijer, F.

DOI
10.4233/uuid:dd4f8c22-c57b-44b8-9dd5-75f4b152a599

Publication date
2025

Document Version
Final published version

Citation (APA)
den Heijer, F. (2025). *Comprehensive risk-perspective for flood defence system management*. https://doi.org/10.4233/uuid:dd4f8c22-c57b-44b8-9dd5-75f4b152a599

Comprehensive risk-perspective for flood defence system management

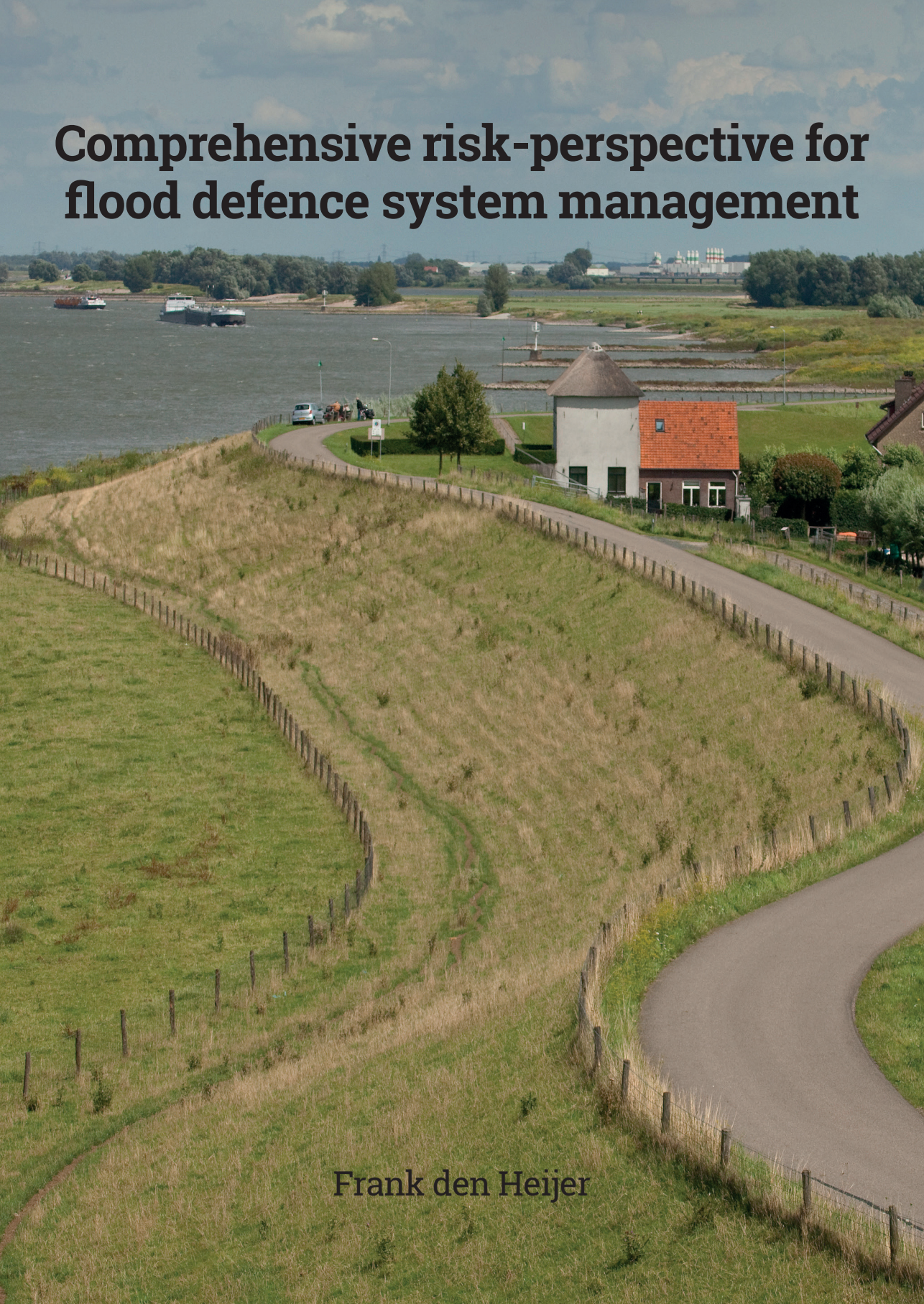

Frank den Heijer

Comprehensive risk-perspective for flood defence system management

Comprehensive risk-perspective for flood defence system management

Dissertation

for the purpose of obtaining the degree of doctor
at Delft University of Technology
by the authority of the Rector Magnificus, prof. dr. ir. T.H.J.J. van der Hagen,
chair of the Board for Doctorates
to be defended publicly on
Wednesday 17 September at 15:00 o'clock

by

Frank den HEIJER

civil engineer, Delft University of Technology, the Netherlands
born in Voorburg, the Netherlands

This dissertation has been approved by the promotors.

Composition of the doctoral committee:

Rector Magnificus,	chairperson
Em. prof. dr. ir. M. Kok	Delft University of Technology, *promotor*
Prof. dr. ir. P.H.A.J.M. van Gelder	Delft University of Technology, *promotor*

Independent members:

Prof. dr. ir. S.N. Jonkman	Delft University of Technology
Prof. dr. ir. P. Willems	Catholic University of Leuven
Prof. dr. ir. D. den Hertog	Tilburg University
Dr. ing. E.M. Hahn	University of Twente
Prof. dr. mr. ir. N. Doorn	Delft University of Technology, *reserve member*

Other member:

Dr. ir. J.S. Rijke,	HAN University of Applied Sciences, *non-independent member*

Keywords: flood defences, reinforcement, structural robustness, asset management, flood risk, risk based planning, system reliability, system management, optimization, organisation, cooperation

Printed by: Ridderprint

Cover by: Ridderprint, cover photo ©Rijkswaterstaat | Ruben Smit

ISBN 978-94-6384-803-9

An electronic copy of this dissertation is available at
https://repository.tudelft.nl/.

"*Lorsque la sureté d'une nation est si prochainement et si totalement menacee il n'y a pas d'efforts trop grands pour une telle enterprise.*"

(When the safety of a nation has recently been under such severe and complete threat, no effort is too large for such an undertaking)

Lodewijk Napoleon, about flood risk reduction measures after the Rhine river flood disaster in 1809

SUMMARY

'Flood risk management' can be defined as the continuous and holistic societal analysis, assessment and reduction of flood risk. From all opportune flood risk reduction measures, structural and non-structural, flood defence management is the most important for those areas protected by a system of flood defence assets like dikes. Asset management of flood defences systems includes strategic, tactic and operational decision levels. Since risk is a key parameter for asset management, risk management capabilities are important for the maturity and quality of flood defence asset management.

The main objective of this thesis is *to develop and test methods for risk analysis in flood defence system management subject to deterioration and climate change*. It focusses on three questions which elaboration can improve the risk-based management of flood defences, one at each of the three asset management decision levels. The questions are related to the three key topics of this thesis. Key topic 1 (operational decision level) concerns optimization of dike design: How can the structural robustness of the flood defence contribute to flood risk reduction? Key topic 2 (tactical decision level) concerns portfolio prioritisation of measures in system: How can planning of measures contribute to effective system risk reduction? Key topic 3 (strategic decision level) concerns flood risk standards: How can risk-based standards for flood defences reflect the benefits of structural robust designs?

Flood risk concerns both the probability of flooding and its consequences. For flood risk in low lying areas protected by dikes, the undesired event is a flooding, most likely due to dike breach due to natural hazards anywhere along the flood defence protecting the area. The assessment of probabilities of flood defence failure depends on the hydraulic loads and the flood defence strength. The consequences are dependent on failure, breach and flood characteristics, and on the exposed values in the considered area. Consequences of flooding are expressed in economic damage, number of victims and number of affected people. Upper limits for the individual and economical risks provide a risk-based target or standard to keep a system safe under changing conditions. To assess when, where and how to intervene, different asset managers may differently develop and apply intervention criteria and conditions, leading to different plans. In this thesis the interventions are narrowed to dike

reinforcements, since its objective concerns flood defences.

For key topic 1 an integrated risk analysis has been set up. Present risk analyses often consist of decoupled calculations of probabilities of dike failure and calculation of consequences of flooding. However, the flood defence design determines not only the probability of failure, but influences the consequences of flooding as well. Especially when the dike is structural robust, which is reflected by a ductile failure and breach growth behaviour, the consequences of flooding reduce. In this thesis an assessment method of risks and investments is presented, valuing the risk reduction due to the structural robustness of a construction type, represented by its ductile behaviour during high loads. Therefore, the consecutive occurrence of initial dike failure mechanisms, failure path development, breach growth and consequences is modelled integral and time dependent. The investments consist of the costs to reinforce or reconstruct the flood defence to behave relatively ductile. This new method enables to compare flood impacts of different construction types and design dimensions. The results of a case study show the total societal costs and the individual risks on victims strongly depend on the construction type. The brittle sand dike with a clay cover in the case, requires larger dimensions than the more ductile dike with a clay core. Applying an integrated risk analysis enables to consider the dike construction as an additional and highly relevant alternative main option for risk reduction, next to the existing ones such as load decrease, strength increase and consequence decrease.

For key topic 2 the interventions or measures are studied for a system of dikes in flood-prone areas, which are continuously required to mitigate changes such as ageing and climate change. Planning costly measures requires proper insight into system risk effects. Tactical plans define the planning of consecutive measures to implement a flood risk reduction strategy, which may take decades. The plans may differ due to choices such as a prioritisation metric, planning conditions and budget. A method is developed to compare different tactical plans to prioritize and plan measures in interdependent systems of dikes, to reduce risks most effectively and efficiently. A case study is carried out for the reinforcement of about 500 km of dikes along the Rhine River branches in the Netherlands. The effects of 12 different tactical plans on the aggregated risks over time have been studied. The economic risks differ by up to about 40%, and the risks on victims differ by up to 70%, which underpins that tactical planning and corresponding decisions are important for reduction of time-aggregated system flood risks. This time-aggregated risk reduction can be introduced as a decision variable for evaluation of tactical plans.

For key topic 3 is studied how economic optimal probabilities of dike failure, can be updated to reflect the impact of structural robust dike designs. The context elaborating this topic is the Netherlands. First, the analytic approach to assess the economic optimal flood probability by Van Dantzig, used by the Dutch Delta Committee (1958), is adapted to enable comparison to the numerically derived dynamic (saw-tooth-like) optimal probabilities, used as input for the recently formalized standards (2017). Second, building on the finding the comparison appeared to be rather good, the failure mechanism piping is added in the analytic derivation. Therewith, the effect is researched of the use of only the failure mechanism wave overtopping, which was the starting point of both former analyses. The effect on the optimal flood probabilities appeared to be small. Third, an analytical relation is developed for economic optimal design horizons. Finally, using the adapted Van Dantzig relation, a simple approach has been developed to update the economically optimal failure probability, based on a proposed design and planning. This can serve to check whether the reliability standard is still adequate. Therewith, it is practical possible to keep a dynamic and risk aware focus on the economic optimal flood defence reliability.

Risk analysis is an indispensable element in risk-informed decision making on each of the asset management decision levels used in asset management practices. The in the key topics elaborated dynamic connected risk analyses are combined with this concept of decision levels, and with the concept of the Deming circle as an organisational concept for continuous capability improvement. Coherent use of this dynamic connected risk analyses, can bridge the practical disconnections between the decision levels. Due to fragmented responsibilities the decisions are to be taken by different actors, increasing complexity. Practical bottlenecks and dilemmas arise that need to be solved. This prompts flood defence asset management to mature. In case an escalation step is not opportune, because a central authority does not exist for the management of complex multi-managed systems in public space, sound cooperation is required. The success of asset management of flood defence systems depends on the practical implementation of cooperation and the ability and agility to choose and change the shape of cooperation dependent on the situation. As shown by existing literature this is better accommodated by an Agile process than by a Waterfall process. If such a process is continuously related to societal acceptability, the risk perspective focuses on the ALARA risk management principle.

The main contribution of this thesis is that it provides a comprehensive perspective for the utilization of risk analysis as a tool supporting efficient flood defence system management. Further steps are recommended to develop and enhance the approach and implementation of

the findings in this thesis and to mature the application. These steps focus on utilization of structural robustness, set up of tactical plans for system planning, and on investigation of the effects of risk-based updating of performance requirements. A dynamic process can be introduced to continuously focus on effective and efficient risk reduction.Therefore, a sound cooperation between flood defence system management actors is indispensable, tailored to the situation.

SAMENVATTING

'Overstromingsrisico management' kan worden gedefinieerd als de continue en holistische maatschappelijke analyse, de beoordeling en de reductie van overstromingsrisico's. Van alle mogelijke overstromingsrisico reducerende maatregelen, structureel en niet-structureel, is het beheer van de waterkeringen het belangrijkst voor die gebieden die worden beschermd door een systeem van waterkeringen zoals dijken. Assetmanagement van systemen van waterkeringen omvat strategische, tactische en operationele beslissingsniveaus. Aangezien risico een belangrijke parameter is voor assetmanagement, is risico management belangrijk voor de volwassenheid en kwaliteit van het beheer van waterkeringen.

Het hoofddoel van dit proefschrift is *het ontwikkelen en testen van methoden voor risicoanalyse in het beheer van waterkeringen die onderhevig zijn aan veroudering en klimaatverandering*. Het richt zich op drie vragen waarvan de uitwerking het op risico's gebaseerde beheer van waterkeringen kan verbeteren, één op elk van de drie beslissingsniveaus van assetmanagement. De vragen zijn gerelateerd aan de drie kernthema's van dit proefschrift. Kernthema 1 (operationeel beslissingsniveau) betreft optimalisatie van dijkontwerp: Hoe kan de structurele robuustheid van de waterkering bijdragen aan reductie van overstromingsrisico's? Kernthema 2 (tactisch beslissingsniveau) betreft portfolioprioritering van maatregelen in het systeem: Hoe kan de planning van maatregelen bijdragen aan effectieve systeemrisicoreductie? Kernthema 3 (strategisch beslissingsniveau) betreft normen voor overstromingsrisico's: Hoe kunnen op risico gebaseerde normen voor waterkeringen worden geactualiseerd, zodat ze de voordelen van structureel robuuste dijkontwerpen weerspiegelen?

Overstromingsrisico heeft zowel betrekking op de kans op overstromingen als op de gevolgen ervan. Voor overstromings-risico in laaggelegen gebieden die worden beschermd door dijken, is de ongewenste gebeurtenis een overstroming, die in de meeste gevallen wordt veroorzaakt door dijkdoorbraken door hoogwater ergens langs de waterkering die het gebied beschermt. De beoordeling van de faalkans van de waterkering is afhankelijk van de hydraulische belastingen en de sterkte van de waterkering. De gevolgen zijn afhankelijk van faal-, bres-, en overstromingskenmerken, en van de waarden in het beschouwde gebied. Gevolgen van overstromingen worden uitgedrukt in economische schade, slachtoffers

en aantal getroffen personen. Bovengrenzen voor de individuele en economische risico's bieden een op risico's gebaseerde norm om een systeem veilig te houden onder veranderende omstandigheden. Om te beoordelen wanneer, waar en hoe er moet worden ingegrepen, kunnen verschillende asset managers verschillende interventiecriteria en voorwaarden ontwikkelen en toepassen, wat leidt tot verschillende plannen. In dit proefschrift worden de interventies beperkt tot dijkversterkingen, aangezien het doel ervan betrekking heeft op waterkeringen.

Voor kernthema 1 is een geïntegreerde risicoanalyse opgezet. Huidige risicoanalyses bestaan vaak uit ontkoppelde berekeningen van de faalkans van een dijk en de berekening van de gevolgen van overstromingen. Het ontwerp van de waterkering bepaalt echter niet alleen de kans op falen, maar beïnvloedt ook de gevolgen van overstromingen. Vooral wanneer de dijk structureel robuust is, wat tot uiting komt in een ductiel faal- en bresgroeigedrag, worden de gevolgen van overstromingen gereduceerd. In dit proefschrift is een beoordelingsmethode van risico's en investeringen gepresenteerd, waarbij het risico reducerend effect wordt gewaardeerd van de structurele robuustheid van een constructietype, vertegenwoordigd door het ductiele gedrag tijdens hoge belastingen. Daartoe is het opeenvolgende optreden van initiële faalmechanismen, faalpadontwikkeling, bresgroei en gevolgen integraal en tijdsafhankelijk gemodelleerd. De investeringen bestaan uit de kosten om de waterkering zodanig te versterken of te reconstrueren dat het zich relatief ductiel gedraagt. Deze nieuwe methode maakt het mogelijk om de gevolgen van overstromingen van verschillende constructietypen en ontwerpdimensies te vergelijken. De resultaten van een case study laten zien dat de totale maatschappelijke kosten en de individuele risico's voor slachtoffers sterk afhankelijk zijn van het constructietype. De brosse zanddijk met een kleidek in de case study, vereist grotere afmetingen dan de meer ductiele dijk met een kleikern. Door een geïntegreerde risicoanalyse toe te passen, kan de dijkconstructie worden beschouwd als een extra en zeer relevante alternatieve hoofdoptie voor risicoreductie, naast de bestaande opties zoals reductie van de belasting, vergroting van de sterkte en reductie van de gevolgen.

Voor kernthema 2 zijn de interventies of maatregelen bestudeerd voor een systeem van dijken in overstromingsgevoelige gebieden, die continu nodig zijn om veranderingen zoals veroudering en klimaatverandering te mitigeren. Het plannen van kostbare maatregelen vereist een goed inzicht in de effecten van systeemrisico's. Tactische plannen defini-ëren de planning van opeenvolgende maatregelen om een strategie voor het reduceren van overstromingsrisico's te implementeren, wat tientallen jaren kan duren. De plannen kunnen verschillen door keuzes zoals een prioriteringsmaatstaf, planningsvoorwaarden en budget. Er is een meth-

ode ontwikkeld voor de vergelijking van verschillende tactische plannen voor het prioriteren en plannen van maatregelen in onderling afhankelijke dijksystemen, om risico's zo effectief en efficiënt mogelijk te reduceren. Er is een case study uitgevoerd voor de versterking van ongeveer 500 km dijken langs de Rijntakken in Nederland. De effecten van 12 verschillende tactische plannen op de in de tijd geaggregeerde risico's zijn bestudeerd. De economische risico's verschillen tot ongeveer 40% en de risico's op slachtoffers verschillen tot 70%, wat onderstreept dat tactische planning en bijbehorende beslissingen belangrijk zijn voor het reduceren van in de tijd geaggregeerde overstromingsrisico's in het systeem. Deze in de tijd geaggregeerde risicoreductie kan worden geïntroduceerd als een beslissingsvariabele voor de evaluatie van tactische plannen.

Voor kernthema 3 is bestudeerd hoe economisch optimale faalkansen van de dijk kunnen worden geactualiseerd om de impact van structureel robuuste dijkontwerpen te weerspiegelen. De context waarin dit onderwerp wordt uitgewerkt, is Nederland. Ten eerste is de analytische benadering van de economisch optimale overstromingskans van Van Dantzig, gebruikt door de Nederlandse Deltacommissie (1958), aangepast om vergelijking mogelijk te maken met het numeriek afgeleide dynamische (zaagtandachtige) verloop van optimale faalkansen, gebruikt als input voor de recent geformaliseerde normen (2017). Ten tweede, voortbouwend op de bevinding dat de vergelijking redelijk goed bleek te zijn, is het faalmechanisme piping toegevoegd aan de analytische afleiding. Daarmee is het effect onderzocht van het gebruik van alleen het faalmechanisme golfoverslag, dat het uitgangspunt was van beide eerdere analyses. Het effect op de optimale overstromingskans bleek gering. Ten derde is een analytische relatie ontwikkeld voor de economisch optimale ontwerphorizon. Tenslotte, met behulp van de aangepaste Van Dantzig-relatie is een eenvoudige aanpak ontwikkeld waarmee de economisch optimale faalkans kan worden geactualiseerd, op basis van een voorgesteld ontwerp en planning. Deze kan dienen om na te gaan of de faalkansnorm nog steeds adequaat is. Daarmee is het praktisch mogelijk om een dynamische en risico-bewuste focus te houden op de economische optimale faalkans.

Risicoanalyse is een onmisbaar element in risico-geïnformeerde besluitvorming op elk van de assetmanagement beslisniveaus dat wordt gebruikt in de praktijk van assetmanagement. De in de kernthema's uitgewerkte dynamisch verbonden risicoanalyses zijn gecombineerd met dit concept van beslisiveaus, en het concept van de Deming-cirkel als een organisatorisch concept voor continue competentie verbetering. Coherent gebruik van deze dynamische verbonden risicoanalyses kan de praktische knip tussen de beslisniveaus overbruggen. Vanwege gefragmenteerde verantwoordelijkheden moeten de beslissingen door verschil-

lende actoren worden genomen, wat de complexiteit vergroot. Er ontstaan praktische knelpunten en dilemma's die om een oplossing vragen. Dit leidt ertoe dat assetmanagement van waterkeringen volwassen wordt. Indien een escalatiestap niet mogelijk is, omdat er geen centrale autoriteit bestaat voor het beheer van complexe multi-managed systemen in de openbare ruimte, is een goede samenwerking vereist. Het succes van assetmanagement van waterkeringen hangt af van de praktische implementatie van samenwerking en de competentie en de wendbaarheid om de vorm van samenwerking te kiezen en te veranderen, afhankelijk van de situatie. Zoals blijkt uit de bestaande literatuur, wordt dit beter geaccommodeerd door een Agile proces dan door een Waterval proces. Als een dergelijk proces continu gerelateerd is aan maatschappelijke aanvaardbaarheid, richt het risicoperspectief zich op het ALARA-risicomanagementprincipe.

De belangrijkste bijdrage van dit proefschrift is dat het een samenhangend perspectief biedt voor het gebruik van risicoanalyse als hulpmiddel voor efficiënt waterkeringssysteembeheer. Er worden verdere stappen aanbevolen om de aanpak en implementatie van de bevindingen in dit proefschrift te ontwikkelen en te verbeteren en de toepassing te laten rijpen. Deze stappen richten zich op het benutten van structurele robuustheid, het opzetten van tactische plannen voor systeem planning, en op onderzoek naar de effecten van risico bewust actualiseren van de normen. Er kan een dynamisch proces worden ingezet om continu te focussen op effectieve en efficiënte risicoreductie. Een goede samenwerking tussen de actoren in waterkeringssysteembeheer, afgestemd op de situatie, is daarbij onontbeerlijk.

ACKNOWLEDGEMENTS

Al lange tijd liep ik rond met het idee om te willen promoveren. Voordat ik in 2019 begon bij de Hogeschool van Arnhem en Nijmegen (HAN) heb ik meer dan 25 jaar gewerkt bij Rijkswaterstaat en Deltares en haar voorgangers. In die tijd voelde ik meer en meer enige goedbedoelde jaloezie voor de promovendi, die zich geheel konden vastbijten in een onderwerp, en daardoor en daarmee toevoegden aan de kennisbasis van waterkeren.

Die jaren voordat ik begon aan m'n PhD waren belangrijk voor me, omdat de ideëen ontluikten. Mijn rol was weliswaar veelal die van projectleider, programmaleider, kennisambassadeur of een andere trekkende rol, maar de inhoud van de waterbouw stond bij mij steeds voorop. Al die projecten hebben in de loop van die jaren bijgedragen aan de ideëen die op de achtergrond groeiden. Alle discussies, met vele mensen - nationaal en internationaal, sommigen ondertussen gepensioneerd, met sommigen vaker, met anderen eenmalig - hebben hun zaadjes geplant, of we het nu eens waren of niet. En eerlijk gezegd waren het zoveel mensen dat ik zowiezo mensen ga vergeten als ik ze allen bij naam zou willen noemen. Dus bij deze wil ik allen bedanken voor de inspirerende gesprekken en gedachten.

Dit proces is ook in de laatste 5 jaar voortgezet. Vlak voor de coronatijd kreeg ik goedkeuring van de HAN om met mijn promotiewerk te beginnen. Ik gaf in die eerste corona-periode geen lessen, zodat ik vanuit een dynamische periode vol drukte als programmaleider, plotseling op m'n kamertje zat. Wat voor velen een eenzame periode was, was voor mij een vruchtbare tijd. De (gedeeltelijke) vrijstelling van de HAN gedurende 5 jaar, was een onmisbare voorwaarde om het voor u liggende werk te kunnen doen, en ik wil vanaf deze plaats daar mijn dank voor uitspreken.

De coronatijd ligt alweer geruime tijd achter ons, en in de loop van de afgelopen jaren hebben verschillende mensen bijgedragen door feedback, advies, of daadwerkelijke support. En natuurlijk zijn er een aantal mensen die ik vanaf deze plaats met name wil bedanken. Allereerst Matthijs Kok, die ik al lange tijd kende voordat hij mijn promotor werd. Waar we al vakvrienden waren, werd hij mijn wetenschappelijke coach. Ons contact heb ik altijd als prettig en stimulerend ervaren. Wat eens begon in een restaurantje in Delft, kreeg een lang vervolg van teamsgesprekken. Zijn inhoudelijke vragen en commentaren, opmerkingen en overwegingen, hebben me telkens weer aangezet tot denken en verbeteren. Maar ook zijn adviezen over rolvastheid en het kunnen afron-

den van een stuk werk (ook al is het nooit af) heb ik zeer op prijs gesteld. Pieter van Gelder, die ik ook al lange tijd kende vanaf mijn eerste betrekking bij Rijkswaterstaat, heeft het laatste deel van het traject mede begeleid. Ondanks dat hij pas later betrokken werd, was zijn inbreng heel goed en erg prettig. Hij reflecteerde met theoretische en praktische beschouwingen, alsmede op de verbinding met de proceskant en met toepassingen in andere risico-velden. Dat was belangrijk voor de inbedding en zorgvuldige afronding. Als derde noem ik Jeroen Rijke. Wat al begon voordat ik bij de HAN kwam, kreeg een mooi vervolg. Hij heeft het laatste zetje gegeven om het promotie-werk daadwerkelijk bij de HAN op te pakken, heeft de eerste plannen van commentaar en koers voorzien, en heeft me gedurende de gehele periode gestimuleerd en vanuit de HAN begeleidt. Zijn vragen hadden vaak een dimensie die me weer op een andere manier aan het denken zette.

Verder wil ik diverse anderen bedanken die op verschillende manieren hebben bijgedragen. Voor het onderwerp taaie dijken heeft vooral Rob Brinkman van Deltares goed werk verricht om de probabilistic toolkit (PTK) uit te breiden. Al discussierende over mijn resultaten kwamen we tot een krachtige aanpak in de familie van Monte Carlo methoden, voor het geautomatiseerd zoeken naar een startpunt voor Important Sampling. Rob heeft dit in de PTK ingebouwd en ik heb daar veel baat bij gehad. Hij was onvermoeibaar om telkens weer kleine verbetering door te voeren en me toegang te geven tot nieuwe versies. Jarl Kind van De Waterwerkers (voorheen collega bij Deltares) stuurde data van het project Waterveiligheid 21e eeuw, en Kymo Slager van Deltares stuurde de basisdata die onder de LIWO database liggen. Maarten Podt van de HAN hielp met het maken van enkele mooie kaarten. Marten Hoeksema van Waterschap Vallei en Veluwe verstrekte data voor de case studie Grebbedijk, en verzorgde toestemming om deze locatie als casus te mogen gebruiken. Uiteraard dank ik ook de collega’s die tijdens mijn onderzoek in meer incidentele gesprekken feedback gaven. Verder dank ik de platforms waar ik welkom was om m’n verhaal te vertellen, zoals het Adviesteam Dijk Ontwerp voor HWBP, en het samenwerkingsverband met Waterschap Rivierenland.

Tenslotte ben ik veel dank verschuldigd aan mijn vrouw en kinderen. Het spreekt voor zich dat zij voor mij de belangrijkste plaats innemen. Ze hebben me altijd gesteund in mijn streven om het onderzoek te doen en het proefschrift tot een goed einde te brengen, terwijl ze mij er in de afgelopen drukke jaren alleen maar meer mee misten. Woorden van dank schieten hiervoor tekort.

Nu ligt er een proefschrift, maar er zijn nog steeds vele ideëen om de kennis weer verder te brengen. Het is een eindpunt, maar ook een beginpunt voor verder onderzoek.

Frank den Heijer, Harskamp, 2025

CONTENTS

1

INTRODUCTION

There this miserable race inhabits raised pieces ground or platforms, which they have moored by hand above the level of the highest known tide.

Gaius Plinius Secundus, 78

'Flood risk management' can be defined as the continuous and holistic societal analysis, assessment and reduction of flood risk. Despite flood risk management consist of several structural and non-structural measures, flood defence management remain the most important for those areas protected by a system of flood defence assets like dikes. The different components of adaptive asset management of flood defences systems consists of aspects on strategic, tactic and operational decision levels. Since risk is a key parameter in asset management, risk management capabilities are important for the maturity and quality of flood defence asset management. This thesis focusses on three key topics which can improve the risk-based management of flood defences, one in each of the three asset management decision levels, concerning optimization of dike design, portfolio prioritisation of measures in system, and flood risk standards. The main objective of this thesis is: to develop and test methods for risk analysis in flood defence system management subject to deterioration and climate change. The cases used for application of the methods are situated in the Netherlands. The main contribution of this thesis is that it provides a comprehensive perspective for the utilization of risk analysis as a tool to obtain efficient flood defence system management.

Parts of Section 1.5 has been published in F. den Heijer, J. Rijke, M. Bosch-Rekveldt, A. de Leeuw, and María Barciela-Rial. "Asset management of flood defences as a co-production – An analysis of cooperation in five situations in the Netherlands". In: Journal of Flood Risk Management (2023). doi: 10.1111/jfr3.12909

1

1.1. BACKGROUND AND RATIONALE

Living in low-lying deltaic areas means living flood prone, due to natural flood hazards like a storm surge at sea caused by hurricanes, cyclones or windstorms, or like river flood waves caused by high river discharges due to snowmelt or precipitation. The risk on victims, damage or other consequences due to floods is referred to as 'flood risk'.

Despite the risk, locations near coasts and rivers are the most inhabited ones, since water is a basic need. In ancient days water was used to drink and to fish for food. For centuries it is increasingly used for irrigation and for transport. Infrastructure is build to manage our use of natural water bodies such as weirs, inlets, ports and locks [1].

Dealing with flood risk for those who lived in deltaic, flood prone river, or lake areas has developed dependent on the possibilities and opportunities in time or place. In early days this took place by living on higher places, earthen dwelling mounds ('terpen') near sea and current ridges in river environments [1–3]. Later, dikes have been built to be able to obtain space for agriculture and settlements (in Europe from about 1000AD [1], in China even far earlier [3]). In the 20th century closure dams and storm surge barriers were build. Nowadays, about 1.8 billion of people, which is 23% of worlds population, are exposed to a flood with a probability of occurence of 1/100 per year [4].

'Flood risk management' can be defined as the continuous and holistic societal analysis, assessment and reduction of flood risk [5–7]. In the early days the probability of flooding was attempted to be controlled by living on 'terpen' and later by building dikes. From the early days the dikes breached regularly [8, 9]. Van Kempen & van Baars [10] provided a number of 1735 dike failures in the Netherlands between 1134AD and 2006AD. Dikes were repaired and enhanced continuously [11, 12]. 'Flood defence management' became an increasingly important part of flood risk management.

Sayers et al. [13] present the development of flood risk management in the second half of the twentieth century as a 'new approach [..] that utilized the concept of risk in decision-making in practice'. Despite flood risk management has been evolvingly practised before, see Figure 1.1, last decades more and more the consequences were attempted to be reduced by spatial planning, communication and early warning. The use of quantitative risk assessments in flood risk management, which came up in the second half of the twentieth century, enabled the explicit trade-off between efforts and risk effect [14]. Sayers et al. [13] gives characteristics for good flood risk management:

- whole system understanding and societal goals
- knowledge of risk and uncertainty to take risk-informed decisions
- a portfolio of measures and instruments

- operation as a continuous and adaptive process

Despite flood risk management consist of several structural and non-structural measures [13], flood defence management remain the most important for those areas protected by a system of flood defence assets like dikes, dunes and hydraulic structures like storm surge barriers, locks and pumping stations [15]. This holds not only for a single polder. In deltaic areas, flood hazards threats a system of several polders, situated along sea, rivers, lakes or estuaries. This requires 'Flood defence system management' to reduce flood risks and maximise the benefit of limited investments available for measures to flood defences. This is the subject of this thesis.

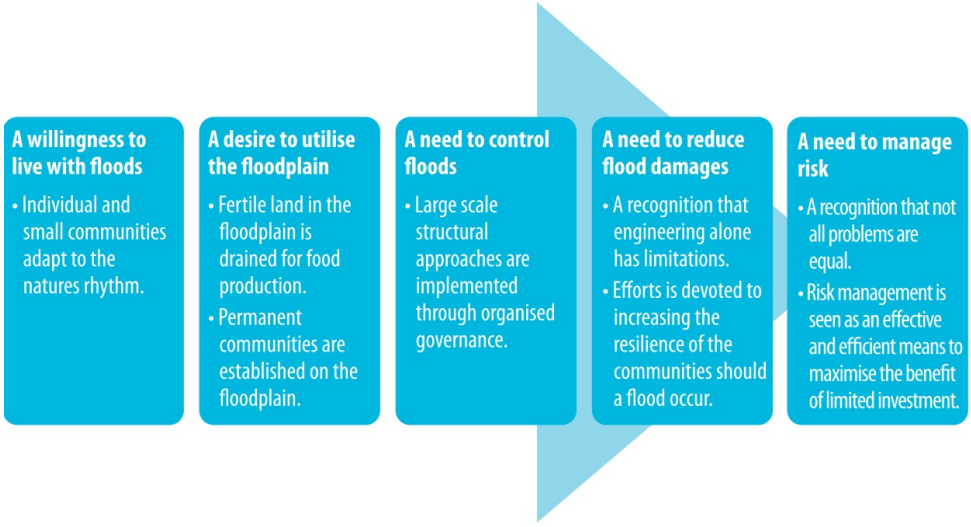

Figure 1.1.: *The evolution of flood risk management practice (source:[13]).*

1.2. FLOOD DEFENCE SYSTEM MANAGEMENT

1.2.1. ASSET MANAGEMENT

The key objective of flood defence assets is to reduce flood risk [16]. Once build flood defences age just as other man-made constructions [15]. This holds for dikes, for example due to subsidence, just as for civil constructions due to ageing concrete or fatique. Worldwide the flood risks have been increasing over the last decennia. Zbigneiw et al. [17] researched the global flood losses and trends due to climate. They presented losses 'from an average of US$7 billion per year in the 1980s to

some US$24 billion per year in the period 2001–2011'. Climate change projections propose the hazard will increase over the coming era [18]. Continuously asset management of the flood defences in the system is needed to prevent flood risks will increase as a result.

Good practices in asset management have evolved from financial, industrial and engineering sources, converging over the last 30 to 40 years to increasing international consensus [19]. The ISO 55000 series standardized asset management in 2014 [20], defining asset management as the "coordinated activity of an organization to realize value from assets". Flood defence assets are physical assets, mostly managed by public institutions without any commercial objective. Therefore, for Infrastructure Asset Management (IAM) the United States Army Corps of Engineers (USACE) accentuated this definition as a disciplined corporate approach for the management of the asset portfolio [21]. Pathirana et al. [19] provided a more practical interpretation for IAM as the process by which decisions are made and resources allocated to ensure organisations' assets continue to deliver the required systems functionality. Brown & Humphrey [22] define IAM as the 'art of balancing performance, cost and risk in the long term'. All these definitions pinpoint the importance of adaptivity as a feature of IAM.

The different components of adaptive asset management of flood defences systems consists of aspects on strategic, tactic and operational decision levels [23]. On the strategic level, it is important to understand the actual system performance and the potential impacts of threats, based on which can be decided on policies, performance standards and measures on a system level. On the tactical level, the development of an adaptive plan for system development is key, which should be based on the actual performance of the individual assets. On the operational level, actual performance assessments are the basis for decisions on requirements and design of individual measures (in asset management jargon also referred to as interventions). The rationale of the coherence between the levels are performance, cost and risk, see Figure 1.2.

Flood defence management has a very large time scale. Since flood defence systems are build in deltaic areas, society has invested in towns, villages, agriculture, industries and private properties in the hinterland. Those investments and corresponding functions affect the asset management decisions for flood defence systems. The maturity of the asset management of the institutions [25] and the cooperation between the responsible institutions are important for the quality of asset management of the flood defence system [26].

1.2.2. RISK MANAGEMENT

Since risk is a key parameter in asset management, risk management capabilities are important for the maturity and quality of flood defence

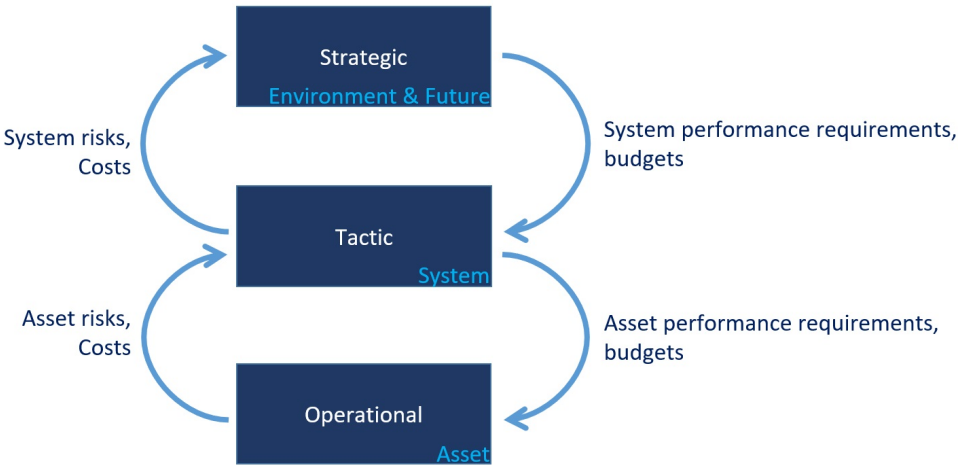

Figure 1.2.: *Asset management decision levels, their focus and their connection (adapted from [23] and [24]).*

asset management. Just as asset management as described in [23], risk management is presented as an endless process [27], see Figure 1.3. In [27] three dimensions of risk management capability are given: Technical, Financial and Administrative. For each of them below the context is provided of present challenges of flood defences system management, which is the key theme of this thesis:

- The technical capability dimension. In [27] this capability dimension is specified by expertise, data, methodologies and technical systems. Since the first known quantitative flood safety level optimization by the Dutch Delta Commission, performed after the 1953 disaster [14], risk assessment approaches pursue increasingly to support risk informed decision making with reliability methods [28–32] and full risk analyses [33], following the source-pathway-receptor framework [13].
- The financial capability dimension. In [27] this capability dimension is specified by the capacity to budget, manage and implement measures. Management contains maintenance, reinforcement or renew flood defences and needs allocation of budgets. On a national level these budgets compete with other sectors such as healthcare. Once allocated, a prioritizing system allocates budget for measures over time. The system to manage and implement measures is allocated to this dimension as well.
- The administrative capability dimension. In [27] these capability dimension is specified by the capacity to define a vision, formulate

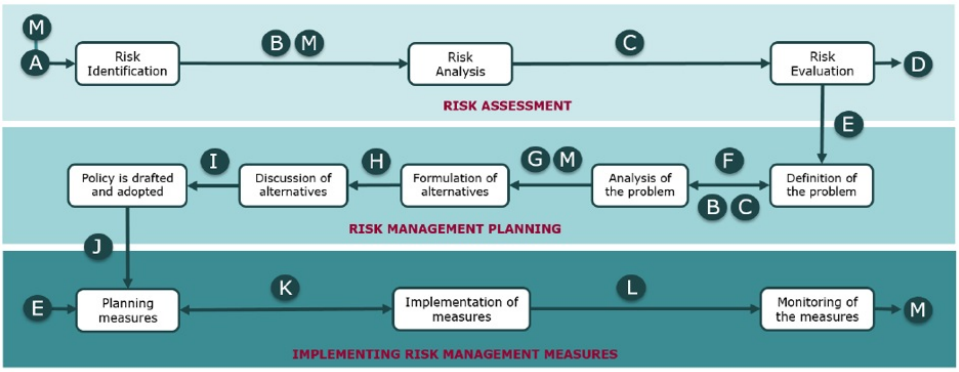

A	Loss and damage data, Projections, Research projects, Contextual information, etc.
B	Risk components are analysed, drivers and conditions that lead to impact are well stated
C	Likelihood of events and their related impacts (direct and indirect)
D	Risk Report
E	Risk Report, with the risks to prioritise (full version)
F	Disaster risk to treat is defined with clear objectives to be reached
G	Causes, background information, interest at stake, relevant actors in decision-making, etc.
H	Alternatives are formulated in order to reach the objective(s
I	Preferred alternative(s) of action are selected and ranked
J	Measures are drafted in order to reach the policy objective(s)
K	The resources and times for each of the measures are allocated and documented
L	The indicators for monitoring the implementation of the measures are designed
M	The values of the indicators on the outcomes and the impact of the measures planned

Figure 1.3.: *Policy cycle for the implementation of integrated disaster risk management (adapted from [27]).*

policies and strategies, engage stakeholders and learn and improve. The knowledge system, including education, research and innovation, is allocated to this dimension as well. This is pivotal for the capability of the institutions involved. The assignment of responsibilities to institutions differs per country [13, 23] and develops in time. For example: in the Netherlands the first Water Authorities are established in the 13^{th} century [12]; at the time of the 1953 disaster about 2500 Water Authorities exist; nowadays 20 Water Authorities and a national agency manage the Dutch flood defences. In [3] the relation between floods in the twentieth century and the impact on policy development is analysed, resulting in needs for basin scale infrastructure and coordination, clear roles and (national) responsibility, need for better understanding of flood defence performance, warning, emergency planning and spatial planning. The Floods Directive (2007/60/EC) [34] stimulates member states to map and

plan risk reduction. Nevertheless, development and mainstream a vision and the corresponding approach is especially a challenge in case of fragmented organisations [26].

These capabilities are needed in each of the three asset management decision levels, in Section 1.2.1 referred to as operational, tactical and strategic respectively. In this thesis topics are chosen out of these three decision levels and capabilities to enhance the flood defence system management by enhanced utilization of flood risk analysis, with a focus is on the technical an economical approach.

1.3. KNOWLEDGE GAPS

This thesis elaborates knowledge gaps in each of the three asset management decision levels, to improve the risk-based management of flood defences.

OPERATIONAL DECISION LEVEL

A lot of studies show applications for risk-based assessment of optimal flood probabilities and probability assessment for design of flood defences, such as [29, 33, 35–38]. Common simplifications in the applications are to use a) the maximum loads and flood level during a flood event, neglecting dike-erosion development in time, b) fault trees to combine dike failure mechanisms, neglecting their interdependencies or their parallel development during the event, c) the occurrence of initial damage caused by a failure mechanism as an estimator for failure, neglecting residual strength, and d) single polders [33] neglecting the effect of the larger system. Some of these are already mentioned as knowledge gaps in [39]. Most studies use practical assumptions such as steady loads during an event, and pre-calculation of a limited number of hydraulic simulations and dike stability simulations. Furthermore, the dike design optimizations in these studies focus mostly on the probability of flooding and not on the consequences of flooding. This complicates to take into account additional aspects reflecting the structural robustness of a dike, such as the effect of the dike construction containing materials to delay the breach or to decrease the breach discharges, reducing consequences. Little studies are found which consider the time dependent development of failure paths from the occurrence of initial damage to a starting breach [40]. No studies has been found which consider the simultaneous development of the failure paths in time. Therefore, the knowledge gap is the assessment of the effect of time-dependent behaviour of structural robust flood defences on risk reduction.

TACTICAL DECISION LEVEL

Much work has been done on flood risk system analysis [33, 41, 42], strategies for the long term and adaptive strategies to cope with climate change [38, 43, 44], and prioritisation [45–47]. Herein, the modelling of the systems is increasingly improved with respect to scale, failure mechanisms, and mathematic-computational methods, and prioritisation of interventions is done more and more risk-based. Time-dependent reliability methods arise [48]. However, in a system of dikes, especially in a riverine area, the performance of assets affects the performance of other assets in the same system. No studies has been found relating system measures planning to the development of system flood risk over time. Therefore, the knowledge gap is the assessment of the effect of tactical planning to system risk reduction.

STRATEGIC DECISION LEVEL

Flood risk standards deliver the reason for the organisations involved in flood risk management to invest when and where, in a complex portfolio of flood risk reducing assets. Managing their flood defences, different countries use different approaches for standardization and performance assessment [16, 23, 49]. In the Netherlands the flood risk standards are introduced by the first Delta Committee [50], based on the analysis of Van Dantzig [14] and more recently by the second Delta Committee, based on analysis of Eijgenraam and Kind [51, 52]. These standards are set in the Dutch Law as acceptable probabilities on flooding per year. The basis of the methods used is that the investments are to be in balance with the corresponding risk reduction obtained. Despite not fixed in Law, in other countries standards are present as well [23], in most cases load exceedance frequencies, which in risk analyses are interpreted as acceptable probabilities of flooding per year. Urged by competition, contractors strive for investment cost optimality given the standard. Since the consequences are not expressed in the standard, the contractor will use materials which are cheapest to use in place. There are no practical opportunities to value consequence reduction by a structural robust design. Therefore, the knowledge gap is the risk-based assessment of the effect of structural robust designs on the standards expressed as acceptable probabilities of flooding per year.

1.4. OBJECTIVE, KEY TOPICS AND OUTLINE

As introduced in the previous section, present application in each of the decision levels is partly risk-based. In this thesis methodologies are developed to further enhance and utilize risk analysis as a tool for efficient flood defence system management. The developed methodologies are applied with case studies in the Netherlands. Therewith, the main

objective of this thesis is: *to develop and test methods for coherent risk analysis in flood defence system management subject to deterioration and climate change.* The knowledge gaps in the previous section are taken as the key topics for this thesis. The following questions are answered and illustrated with application on cases:

1. How can the structural robustness of the flood defence contribute to flood risk reduction?
2. How can planning of measures contribute to effective system risk reduction?
3. How can risk-based standards for flood defences reflect the benefits of structural robust designs?

Figure 1.4 presents the general structure of this thesis. After the introduction, Chapter 2 outlines the concept of flood risk analysis, flood risk standards and actual application. Chapters 3, 4 and 5 deal with the questions on the key topics outlined here above. Chapter 3 presents a risk-based design optimization methodology for the time dependent simultaneous development of several failure paths integrated with consequence analysis (key topic 1). Chapter 4 presents a risk based methodology to compare tactical plans for measures (or interventions) in time in a changing system, in which the performance of assets affects the performance of other assets in the same system, as is the case for a system of dikes in a riverine area (key topic 2). Chapter 5 describes an approach to relate an existing standard with an economic optimal design enabling to take into account the value of structural robust designs (key topic 3). Chapter 6 contains the discussion to synthesize the presented research to obtain a comprehensive perspective for risk-based flood defence system management. Chapter 7 present the key conclusions and recommendations for further research. In the chapters, reference is made to several appendices to prevent the main text from too detailed explanations or information which is not directly needed to understand the presented methodologies.

Since the cases in this thesis originate from the Netherlands, next paragraph 1.5 outlines the Dutch flood defence management. However, the application of the presented risk-based concepts is not limited to the Dutch context.

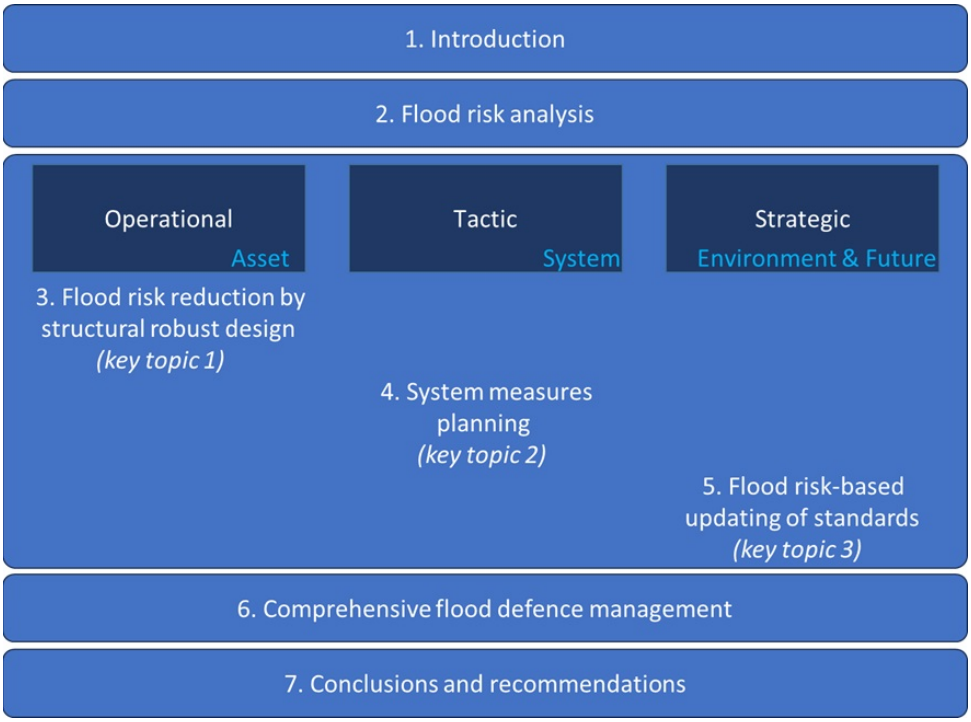

Figure 1.4.: *General outline of this dissertation. Numbers and descriptions are chapter titles.*

1.5. CONTEXT OF CASES IN THE NETHERLANDS

The key topics are of general importance for application of risk analysis in flood risk management. Especially key topic 3 relates to the organisation of flood risk management in the Netherlands. Therefore, the cases in this thesis are situated in the Netherlands. The situation, risk analysis developments, organisation and locations are briefly described, to enable understanding of the context of case studies.

1.5.1. DEVELOPMENT OF RISK ASSESSMENT IN THE NETHERLANDS

About 60% of the Netherlands is flood prone (Figure 1.5). At present, about 3500 km flood defences prevent from flooding from rivers the large lakes and sea, the so-called primary flood defences. In the Netherlands dikes have been built from the early middle ages. In former days, the height and construction of dikes were mainly based on experience, e.g. the requirement of the Province of Gelderland in the early 20th century to design the dike reinforcements at 1 meter above the highest known water level [53].

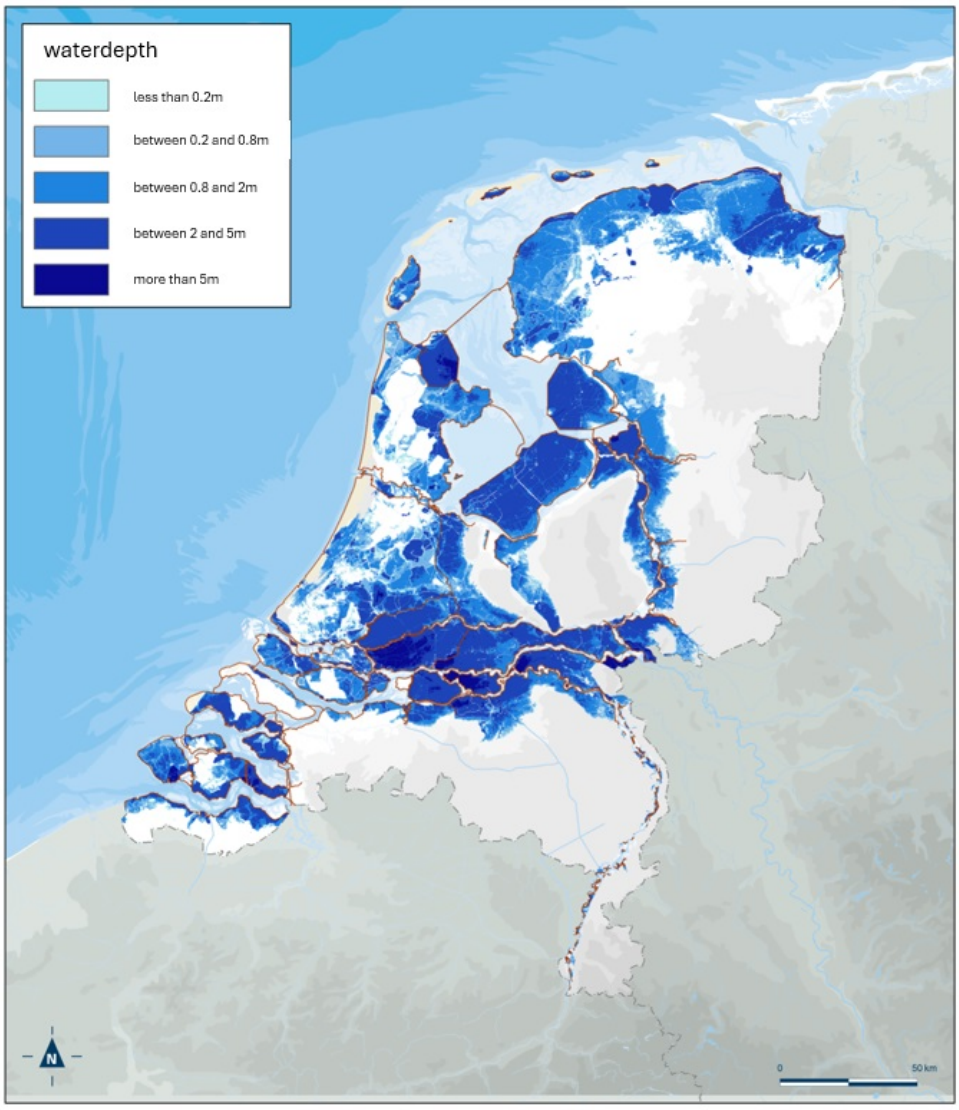

Figure 1.5.: *Overview of the flood prone are in the Netherlands, based on the flood simulations in the National database flood simulations [54, 55].*

After the disaster in 1953, during which 1836 people died, a more scientific and quantitative approach was developed. Safety standards were established, expressed as probabilities of exceedance of water levels at which the flood defence should be certainly safe [12]. Among others these standards have been based on a cost-benefit analysis for a

large low lying country part in South Holland [14]. Design rules were developed and dikes were reinforced to meet these standards, and storm surge barriers have been built [1]. To secure safety on the standard level, these levels were established by law since 1996. A periodic assessment is required by law as well.

Developing insights in hydraulic boundary conditions, dike strength, dike breach process and modelling of floodings, provided potential improved calculation of flood risks. In 1993, the Dutch Technical Advisory-Committee on Water Defences proposed the preparation of standards based on these (by then) actual insights and data, the so-called 'Marsroute' [56]. The Marsroute contained four milestones for standardization, respectively based on exceedance of water levels (the current situation by then), exceedance of load levels (including wave overtopping), probability levels of flooding, and flood risk levels. National flood risk studies delivered the actual probabilities of flooding and corresponding risks (FLORIS, in Dutch abbreviated by VNK [33]) and the acceptable probabilities of flooding based on risk analyses (in Dutch abbreviated by WV21 [57]. New standards, representing the acceptable probability of flooding, are re-established in the Water Act in 2017 [58].

1.5.2. ORGANISATION OF FLOOD DEFENCE MANAGEMENT

Asset management of the primary flood defences is a joint legal task of the Ministry of Infrastructure and Water Management (from here on denoted as "The Ministry") and 20 regional Water Authorities. Water Authorities are responsible for the management of the majority of the primary flood defences in their respective regions, consisting of dikes and hydraulic structures. The Ministry is responsible for the maintenance of dunes, storm surge barriers and large dams protecting low-lying western parts of the country against storm surges. These organizations have three main clusters of tasks in flood defence asset management.

The first cluster of tasks aims to the operational or daily management of flood defences. It includes inspection, maintenance, licensing and management of the revetments. Daily management during high water events includes high water inspection, implementing emergency measures if needed, and collecting and communicating information between organizational levels within the Water Authorities and regional crisis management teams headed by the safety region [55]. During high water events, the Ministry is responsible for flood forecasting and warning, and the Ministry, provinces, and safety regions are responsible for evacuation.

The second cluster of tasks aims to the periodic safety assessment, which has to be reported every 12 years to Parliament. The Ministry

is responsible to provide hydraulic boundary conditions and to provide design and assessment rules and the tools to perform the calculations [58]. The Water Authorities are responsible to perform the assessments. Most Water Authorities outsource the preparatory work, such as data collection and calculations. The Ministry performs the assessments for the flood defences under their responsibiblity, checks the assessments, summarizes outcomes on the national level and reports the national overview to the Dutch parliament.

The third cluster of tasks aims to the reinforcement of flood defences based on the outcomes of the periodic safety assessments. Since 2008 the allocation of budget for dike reinforcements is centralised in the National Flood Protection Program (in Dutch abbreviated by HWBP; [59]), which is an alliance between the Ministry and the Water Authorities. The ambition of HWBP is to meet the status 'dike system safe on standard level' before 2050. The HWBP stimulates innovative design to optimize reinforcement costs and dike footprint. The Ministry is responsible for the actual reinforcements of dunes, dams and most storm surge barriers. The Water Authorities are responsible for the actual reinforcements of the flood defences under their responsibility. They apply for budget to HWBP. They often outsource large parts of the design to the consultancy market. The implementation is procured by contractors, under the supervision of the Water Authorities.

With these clusters of tasks tasks, the organisation is focussed to satisfy the standard level. The majority of the budget for flood risk management is needed for the third main task, to reinforce the flood defences. The total dike length to be reinforced is continuously changing. Reinforcements are delivered, and new dikes to be reinforced are upcoming. Furthermore, new knowledge, climate change and new measurements change our perception on actual safety. In fact, the risk is continuously changing as well, not only due to climate change and subsidence of the flood defence, but also due to the changes in land use and number of inhabitants, as well as by enhanced planning of evacuation. The changes in risk levels are expected to be accommodated by updates of standards.

The managing institutions, mostly the Water Authorities, are responsible to meet the standards. The Ministry has the responsibility for the system as a whole. Based on the total length of 3500 km and an average life cycle of 50 years each year about 70 km should be reinforced, considered on the long run. Although the standards are based on the risk of flooding, due to the expression of the standard in terms of maximum acceptable probabilities of failure for each individual dike segment, the managing institutions focus on meeting these probability levels.

1.5.3. CASES

The elaborations on the key topics are illustrated with case studies in the Netherlands. Figure 1.6 provides an overview of the locations and areas used in the case studies. The location for the elaboration of the first key topic (integrated risk-based optimization of dike design) is the Grebbedijk, situated in the centre of the Netherlands along a branche of the river Rhine. The river area, containing the Rhine from the Dutch border, and the branches Waal, Nederrijn and IJssel, is used for elaborating the second key topic (integrated portfolio prioritisation of measures in system). For the third key topic almost all dike segments along the Dutch primary flood defences are used, with a special attention for 7 locations spread over the country. Herewith, the applications are spread over different hydraulic regimes and different regions in the Netherlands.

1.6. CONTRIBUTION

The main contribution of this thesis is that it provides a comprehensive perspective for the utilization of risk analysis as a tool to obtain efficient flood defence system management.

Although the EU Floods Directive stimulates a risk-based approach [34], in the state-of-the-art methods for flood defence assessment and design, probability and consequences are mostly decoupled, which is beneficial for practical reasons. Integrated risk-based optimization of dike design (key topic 1, Chapter 3) provides a methodology and application for dike design, in which the probability and consequence part are mutual dependent on the dike construction type. The method provides comparative insight in the investment and risk for alternative designs, for example for designs which differ with respect to structural robustness. Especially at densely populated locations a dike construction in combination with materials which can contribute to delay of flooding and decrease of flood volume, reducing the expected number of victims, could be an valuable design alternative. This research contributes to decisions in such situations.

Tactical plans determine when and where to intervene in flood defence systems to reduce the risks in system until they reach an acceptable level. The order of measures or interventions affects the pattern of system risks over time. Integrated portfolio prioritisation of measures in system (key topic 2, Chapter 4) provides a methodology and application to compare the system risk patterns for different tactical plans. The importance is shown for a case study in a riverine area in which the performance of assets affects the performance of other assets in the same system, including the system changes over time due to climate change and subsidence.

Standards used for flood risk reduction are in many cases expressed as limits on probability of failure of the flood defences, introducing a focus

Figure 1.6.: *Overview of the case-locations in the Netherlands, per key topic.*

to satisfy the probability limit. In case the pre-imposed probability limit is based on an optimization of investments and risks, a design meeting that limit can be economic optimal. However, in all cases the design deviates from the starting points used to derive the probability limits, the design is not economic optimal, for example in case of increased structural robustness. In (key topic 3, Chapter 5) a risk based method

has been developed to include the risk-effect of the dike design in the reliability standard. This enables to value a construction which is robustly designed to reduce risks even after breaching, with a milder reliability standard than less robust constructions. A practical formula has been developed which is easy to use for different applications.

In Chapter 6 the coherence between the risk analyses for these three key topics is indicated, together with the process they can be used in practice.

The contribution of this thesis is summarized in the conclusions and recommendations (Chapter 7).

2

FLOOD RISK ANALYSIS

I never worry about action, but only about inaction

Winston Churchill
in a letter to General Dill, 7 December 1940

Flood risk concerns both the probability of flooding and its impact. The expected value is the sum of the risk for all possible events leading to an undesired event. For flood risk in low lying areas protected by dikes, the undesired event is flooding, most likely due to dike breach due to natural hazards anywhere along a dike segment which protects the area. The definition of the event and the corresponding limit state differs for the key topics, concerning a dike breach on a location or segment (key topics 1 and 3 respectively), or a dike breach anywhere in the system (key topic 2). The determination of probabilities of flood defence failure depends on the hydraulic loads and the flood defence strength. The consequences are dependent on failure and breach characteristics as well. Consequences of flooding are expressed in economic damage, victims and number of affected people, dependent on the exposed values in de considered area. The consequences of flooding are site specific. Limits for the individual and economical risks provide a risk-based target or standard to keep a system safe under changing conditions. To determine when, where and how to intervene different asset managers may differently develop and apply intervention criteria and conditions, leading to different plans. Common steps are inventory of possible interventions, prioritisation, and planning them in time. In this thesis the first step is narrowed to dike reinforcement.

2.1. FRAMEWORK FOR QUANTITATIVE RISK ANALYSIS

Flood risk is a concept that concerns both the possible impact of flooding and the probability that these impacts will occur [14, 55]. To analyse flood risks several frameworks exist. Most frameworks consists of combinations of hazards, vulnerability, exposure and resilience [7, 60] to assess these probabilities and consequences. Thywissen [61] provided a comprehensive overview of the terminology of these components of risk, see Figure 2.1, which is in line with the usual terminology in the international flood risk community [62] and the international flood defence community, such as in the International Levee Handbook [16].

Hazard:
'is a threat [having] the notion of probability, or a likelihood of occurring'.

Exposure:
'the number of people and/or other elements at risk that can be affected by a particular event'.

Vulnerability:
'indicates a damage potential and [..] is an intrinsic characteristic of a community that is always there.

Resilience:
'act directly upon damage during the event [..], adaptive strategies [..] to circumvent or avoid damaging effects [..] plus the capability to remain functional during an event and to completely recover from it'.

Risk:
'is understood as a function of hazard, vulnerability, exposure, and resilience' [and] 'involves the notion of probability of occurrence'.

Figure 2.1.: *Interpretation of terminology used in risk analyses, and cohesion between these terminologies (source: [61]).*

In their paper in 1981 Kaplan and Garrick [63] proposed the concept of risk as a product of probability and consequences with the possibility of multiple consequence scenarios to take uncertainties into account. The expected value $E(D)$ is the sum of the risk for all possible events leading to that undesired event [32]:

$$E(D) = \sum_{j=1}^{j=n} P_j \cdot D_j \tag{2.1}$$

In which:

$E(D)$	Expected value of risk due to an undesired event	unity of $D/year$

P_j	Probability of an undesired event j	–
D_j	Consequences of undesired event j	e.g. €, *victims*
j	Indicator of an undesired event	–
n	Number of undesired events	–

The principles of the first scientific papers of about 50 years ago are still the basis of the field of risk analysis today [64]. Nowadays, these are widely used in flood risk analysis. Aven [64] provides different qualitative definitions of risk which all are compositions of both probability of an undesired event and the consequences of it. He provides an overview of types of uncertainties taken into account in risk assessments. Furthermore, he stresses the importance to integrate risk analysis with the fields of robustness and resilience concepts (in this thesis addressed by key topic 1). Pasman [65] reviewed many studies and concludes the way forward is a dynamic risk analyses, supported by increasing IT possibilities, because risks develop in time (in this thesis addressed by key topic 1, 2 and 3). These aspects would enhance the risk communication with decision makers. Sayers [3] proposes strategic flood risk management, based on the whole physical system and portfolio of assets, which is adaptive to respond to uncertainties or changes (in this thesis addressed by key topic 2 and 3).

For flood risk in low lying areas protected by dikes, the undesired event is flooding, most likely due to dike breach due to natural hazards anywhere along a dike segment which protects the area [55, 66], although it may be caused by man as well. Therefore, the probability of flooding is expressed as the probability per year P_f of dike breach. The consequences of flooding depends on the exposed elements, such as number of inhabitants, economic activity, critical infrastructures, potential pollutive sources. They can be expressed by economic damage, number of affected people and victims [27, 55]. In fact, the number of flooding scenarios is infinite. Kaplan and Garrick [63] already proposed to take them into account, and the corresponding uncertainties. Nevertheless, they understand the need to get a single value for the risk. Using equation (2.1) in its basic shape for each scenario without a special weight for scenarios, probabilities or consequences reflects a risk neutral approach. To reflect risk aversion, Kaplan and Garrick [63] proposed to use utility functions to trade-off different types of consequences. Although probability and consequences may be weighed in different ways, flood risk is mostly defined as a risk neutral function of the probability of failure of the flood defences along a flood prone area and the consequences in case the area is flooded [32, 55]. The use of the expected value in equation (2.1) reflects this risk-neutral approach which is usual for economic optimizations in flood risk management [51, 67]. For flood risk applications

where flood defences are in place to prevent flooding, the general risk in equation (2.1) can be written as:

$$E(D) = \int_{\vec{h}} P_f \cdot D(\vec{h})\, d\vec{h} = \int_{\vec{h}} f_{\vec{h}} \cdot P_{f|\vec{h}} \cdot D(\vec{h})\, d\vec{h} \tag{2.2}$$

In which:

$\vec{h}$	Set of variables determining the loads such as water levels and wave attack	e.g. $m+SWL$, m
$f_{\vec{h}}$	Multi dimensional frequency distribution of the loads	*per year*
$P_{f\|\vec{h}}$	Probability of dike segment failure given the set of loads	*per event*
P_f	Probability of dike segment failure	*per year*
$D(\vec{h})$	Consequences of flooding due to dike failure given the set of loads	*e.g. €, victims*

2.2. FLOOD DEFENCE BEHAVIOUR

The determination of probabilities of flood defence failure depends on the hydraulic loads and the flood defence strength [16, 55]. The consequences may be dependent on failure and breach characteristics as well [68].

Key topics 1 and 2 in this thesis focus on riverine areas protected by dikes. The loads on the dikes in these areas consists of river flood waves and wind waves. To describe these loads a lot of literature has been written, such as by Van Rijn [69] and the application for specific applications such as for the Rhine river in the Netherlands [70] as well as its physical and statistical modelling [71, 72].

The strength of the dikes depends on its construction and dimensions. Dikes may fail due to several failure mechanisms, see Figure 2.2. Some are mainly dependent on water level, such as piping, and some are mainly dependent on wave attack, such as wave overtopping [73]. In many applications assessing failure probabilities the failure mechanisms are assumed to occur mutual independent [29, 33, 74], which is a practical starting point.

After the occurrence of a failure mechanism the dike is damaged. The damaged dike may still resist the loads, or delay dike breach. In case of a damaged dike construction the failure mechanisms may affect each other, since overtopping may lead to increased freatic levels in the dike increasing the macro-instability, or macro-instability may cause a slide plane through or onto the aquifer increasing the opportunities for piping. Recently, there is upcoming attention for the so-called failure paths,

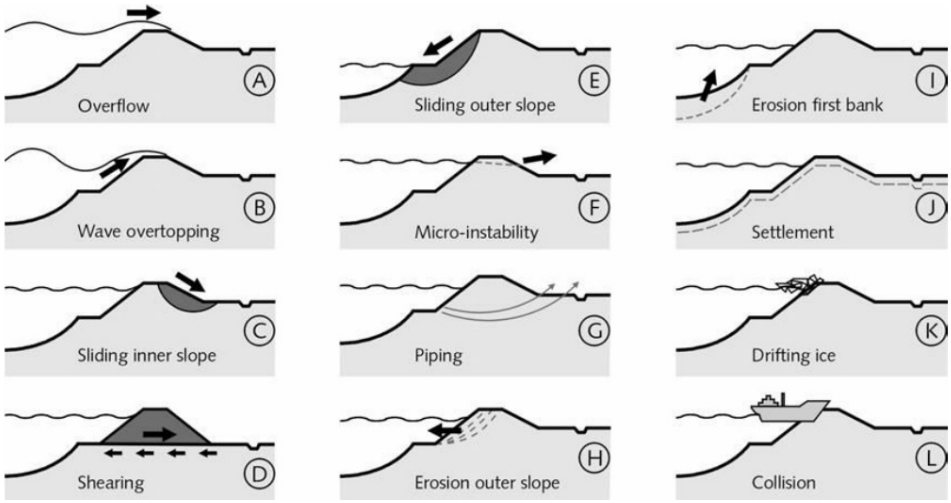

Figure 2.2.: *Overview of failure mechanisms (source: [75]).*

to assess the residual strength after occurrence of a failure mechanism [76]. In the cases in this thesis the failure mechanisms overflow, overtopping and piping are considered, and their corresponding failure paths, see Figure 2.3.

After failure in a dike cross section the breach will grow over time depending on the head over the dike and the dike core material [77]. In Table 2.1 an overview is provided with the character of 759 breaches in riverine areas in the Netherlands, available in the National database flood simulations [54]. For 319 (42%) of the simulations the breach-widths are not registered (right column). For 261 (34%) of the simulations the breaches are based on breach growth calculations (middle column). For the other 179 (24%) of the simulations the breach-widths have been chosen as input (left column). In the majority of the simulations the material is not registered (65%). In the registered part the material is more or less equally distributed (sand 20% and clay 15%). The column with calculated breach-widths show the final breach width in a dike with a clay core is expected to be much smaller than in case of a sand core. The calculated breach widths for sand dikes are about twice as wide as the ones for clay dikes. A clay core is expected to delay breach-growth more than a sand core will do, but the data does not provide information about the breach growth process. Note, the chosen breach-width for clay dikes (210m) are contra intuitive with respect to the chosen breach-width for sand dikes (67m) and with respect to the calculated widths (30m), but take in mind a lot of the flood calculations

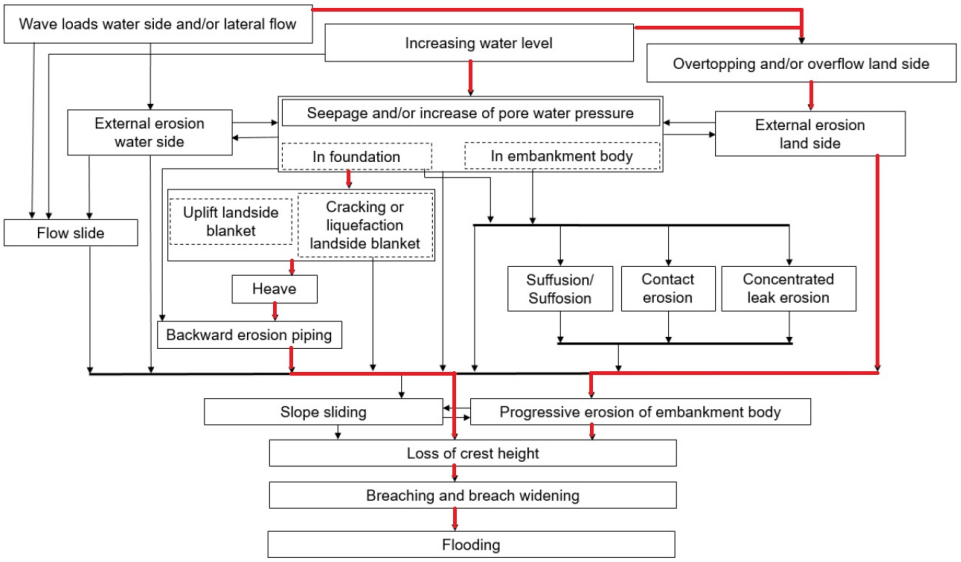

Figure 2.3.: *Overview of the common physical phenomena that can lead to flooding as a result of an event, with the paths considered in this thesis highlighted in red (adapted from: [76]).*

took place in the 90ties or early this century. They were mainly based on assumptions and the scarce experiments and experiences, and took place before the development of the breach growth formula in 2003 [77]. Note, the breach growth formula is based on limited data as well, thus despite it provides a structured way to assess breach widths, it should still be interpreted as an approximation.

Table 2.1.: *Number of breaches for which flood calculations are available in the Dutch National database flood simulations [54] for the riverine areas, depending on the dike material and the method to choose the breach-widths. Between brackets the average breach-widths in the flood calculations (in italics).*

Material	**Breach-widths based on assumption**	**Breach-widths calculated with [77]**	**Breach-widths not registered**
Sand	9 *(67m)*	124 *(58m)*	18
Clay	10 *(210m)*	102 *(30m)*	5
Not registered	160 *(197m)*	35 *(83m)*	296

2.3. PROBABILITY AND CONSEQUENCE ANALYSES

2.3.1. PROBABILITY ASSESSMENT

Following section 2.1 the flood risk is a multiplication of the probability of an event and its consequences.

In areas protected by flood defences the event can be defined as the occurrence of a flooding. To quantitatively assess its probability on an event many applications use the reliability function Z, defined as $Z = R - S$ with R containing the strength variables and S containing the load variables [32]. In this definition the limit state function $Z = 0$ distinguishes flooding and no flooding, mostly assessed by the failure anywhere along the flood defence system [32, 45, 55]. Therewith, the probability of flooding due to failure of the flood defence is $P_f = P(Z < 0)$ [32].

In this thesis the definition of the event and the corresponding limit state differs for the key topics. Therefore, in this thesis the common formulation $P_f = P(g(\vec{X}(i)) < 0)$ is used, with $Z = g(\vec{X}(i))$, corresponding with the probability of failure in year i, The vector $\vec{X}(i)$ contains the variables determining the flood characteristics, including loads, strength, and breach characteristics.

- In the case of derivation of an economic optimal safety standard (key topic 3) the event in year i is defined as the flooding of a polder protected by a flood defence segment, the limit state is defined by all combinations of parameters in vector $\vec{X}(i)$ distinguishing flooding and no flooding. In this case the probability reflects the probability of flood defence failure:

$$P_f(i) = P(g(\vec{X}(i)) < 0) \tag{2.3}$$

In which:

$P_f(i)$	Probability of flooding in year i	*per year*
i	Year indicator, relative to the start year of analysis	—
$g(\vec{X}(i))$	Reliability function in year i	
$\vec{X}(i)$	Vector of variables determining the flood characteristics, including loads, strength, and breach characteristics	

- In the case of an integrated dike design optimization (key topic 1) the event in year i is defined as an event-maximum water depth $\hat{h}_p$ in the protected area. With $h_p(\vec{X}(i))$ relating the parameters in $\vec{X}(i)$ to the event-maximum water depth the corresponding probability of exceedance of a polder water level $\hat{h}_p$ in year i is:

$$P(h_p(\vec{X}(i)) > \hat{h}_p) = P(\hat{h}_p - h_p(\vec{X}(i)) < 0) \tag{2.4}$$

In which:

$h_p(\vec{X}(i))$	Polder water level in year i, dependent on vector $\vec{X}(i)$	$m+SWL$
$\hat{h}_p$	Limit value of polder water level defining the event	$m+SWL$

Except for an event-maximum water depth $\hat{h}_p = 0$ this probability is not the same as the probability of failure of the flood defence in equation (2.3). Nevertheless, both probabilities are related because the water depth in the protected area can only exceed zero in case of flooding. Because different values for the event-maximum water depth $\hat{h}_p$ lead to different probabilities and different consequences a series of events has to be considered to assess the risks.

- In the case of integrated portfolio prioritisation (key topic 2) the event is even less unambiguous: in a system with multiple dike segments and multiple polders there is no singular event leading to consequences. The event is multiple. Therefore, the risk analysis takes in account multiple combinations of loads and strengths in the system and determines the consequences in the different polders (see equation (2.17).

In case of an event defined as the flooding of a polder protected by a flood defence segment (used for key topic 3) the probabilities can be calculated with:

$$P_f(i) = \int_{g(\vec{X}(i))<0} f_{\vec{X}(i)} d\vec{X}(i) \tag{2.5}$$

Since $\vec{X}(i)$ contains a number of stochastic variables, among others representing loads and strength, solving equation (2.5) may be rather complex. In literature three classes of methods are distinguished [32]:

- exact methods (Level III) assessing the full multi-variate probability distributions.
- approximating methods (Level II) linearising the limit state function in a so-called design point and transform the probability distributions to normal distributions (enabling analytic calculation).
- partial safety factors (Level I) determining representative loads and strengths as used in Eurocodes [78].

Level II methods has been used in the VNK project [33], for which the linearisation is assumed to be sufficiently accurate [79]. The limit state functions defining an event-maximum water depth in the polder (key topic 1) and the multiple events in system (key topic 2) are assumed to be far more non-linear than the limit state functions used in the VNK project. Therefore, level II methods are not used in this thesis. An example of a level III method is the Monte Carlo Simulation method, in which N random samples are drawn from the entire set of random variables $\vec{X}$, leading to N_{event} cases for which the draw lead to $g(\vec{X}) < 0$. The probability calculation for year i is rather straight forward:

$$P_f(i) = \frac{N_{event}(i)}{N} = \frac{1}{N} \cdot \sum_{n=0}^{n=N} I_{MC}(n,i) \tag{2.6}$$

In which:

N	Number of random samples	–
N_{event}	Number of samples for which $g(\vec{X}^{(n)}(i)) < 0$ indicating occurence of the undesired event	–
$I_{MC}(n,i)$	Indicator function indication whether draw n leads to the undesired event in year i: $I = 0$ for $g(\vec{X}^{(n)}(i)) \geqslant 0$ and $I = 1$ for $g(\vec{X}^{(n)}(i)) < 0$	–
$\vec{X}^{(n)}(i)$	Draw n from $\vec{X}(i)$ in year i	

Due to the absence of a clear singular event for the key topics 1 and 2 the existing level III methods are not applicable straight forward. Therefore, in this thesis level IV methods has been developed, described in [32] as 'risk-based [..] consequences of failure are also taken into account', enabling to integrate risks for multiple events. In a Level IV approach the probability of occurrence of an event is not calculated separately by a Level I, II or III approach, e.g. by integration of the marginal probability distributions. The marginal distributions are used to calculate marginal risks, which are integrated. From here the level IV approach is denoted as an 'integrated risk analysis'. Again using the Monte Carlo simulation method this lead to the shape:

$$E(D,i) = \frac{1}{N} \cdot \sum_{n=0}^{n=N} I_{MC}(n,i) \cdot D(n,i) \tag{2.7}$$

In which:

$D(n,i)$	Consequences of flooding for draw n from $\vec{X}(i)$ in year i	e.g. €, *victims*

2.3.2. CONSEQUENCE ASSESSMENT

Consequences of flooding are mostly expressed in economic damage, victims and number of affected people [51, 80], dependent on the exposed values in de considered area such as the number of inhabitants, economic activity, and potential pollutive installations or activities, as well as their vulnerability and the character of the hazard [27]. In flood defence protected areas the hazard depends on the characteristics of load, strength and breaches. Therefore, the consequences of flooding are site specific.

In the Netherlands, the country in which the cases in this thesis are taken, a National database flood simulations [54] is available containing the results of calculations with 2D-Hydraulic models and the corresponding consequences with respect to economic damage, victims and number of affected people for several load scenarios and breach locations. Maximum local water depth is taken key for economic damage. Maximum local water depth, its increase rate and local flow velocity are taken key for victims [80].

For the elaboration of key topic 1 'integrated risk-based optimization of dike design' which use the level IV approach to assess the risks, the consequences are required for a variety of load, strength and breach characteristics to assess $g(\vec{X})$. Since the National database flood simulations [54] contains only a limited series, in this thesis a proxy has been derived. To enable elaboration of the effect of dike design on risks, the total volume of water entering the polder is chosen, since it includes the effect of load water level, timing of failure and breach characteristics. Therefore, the data of 652 simulations in the riverine polders were taken for analysis. The volumes are derived as the sum of all available maximum water depths per cell in the numerical calculations. A relation has been derived between the consequences and the total flood volume in the shape:

$$D = c_D \cdot V^{b_D} \tag{2.8}$$

In which:

c_D	Coefficient for consequences per m^3 of flood volume, depending on type of consequences	$€/m^3$ vict./m^3
b_D	Exponent for consequences	-
V	Flood volume	m^3

In Figure 2.4 the data showed the relation between flood volume and consequences. There are some outliers with very large flood volumes and zero or low damage, without a clear cause, and some with high numbers of victims in situations with very low flood volumes, which are

flood scenarios due to failure of hydraulic structures in towns. For assessments of dikes these outliers can be eliminated, which resulted in a linear relationships of the shape:

$$D = c_D \cdot V \tag{2.9}$$

with $c_D = 18.6$ €/m^3 for assessment of economic damage and $c_D = 1.2 \cdot 10^{-6}$ victims/m^3 for the assessment of victims. Especially for economic damage the data underpins the linear relationship. NB. In Appendix A.5 an additional analysis is presented to support the assumption of a linear relationship for victims as well.

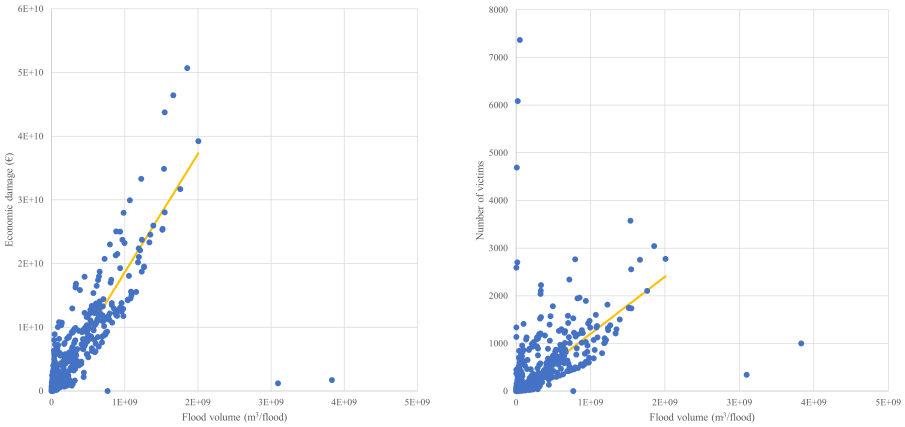

(a) *Economic damage* (b) *Victims*

Figure 2.4.: *Overview of data of consequences of river floods in the National database flood simulations [54]. The line in orange provides the linear relation of equation* (2.9).

2.4. MANAGEMENT OF INTERVENTIONS

In this thesis the focus is on interventions in flood defence management, which are a part of the total portfolio of opportunities to reduce flood risks, next to load reduction and consequence reduction. Interventions are a substantial part of flood defence management since climate change such as sea level rise and river flood waves with increasing maximum discharges normally lead to increasing loads, and since ageing mechanisms lower strengths, such as subsidence lowering the dike crest heights.

Interventions take resources (budget, capacity, material, space) [24]. Decisions whether, when, where and with which design-effect they are

implemented in a portfolio of assets to optimally use the scarce resources require insight in the performance [20]. For flood defences their reliability is often used as a performance indicator [32, 49, 51] because of the large impacts in case of flooding. Next to that 'the levee should ideally have a measure of resilience to breach even if overtopped' [16].

To evaluate whether measures to reduce flood risks are beneficial with respect to risk reduction the performance is related to the risks. The actual risk of flooding and the risk after intervention are compared and weighed with respect to the investment cost of measures. In case all resources and effects of interventions could be translated to financial means, optimization over the possible portfolio of measures and the opportune intervention times will lead to an optimal intervention scheme [46]. However, the consequences of floods are not only economic and tangible. The critical review on flood management measures in Tariq et al. [60] shows clearly that many consequence types such as victims and pollution are intangible. They present a variety of hazard focussed, vulnerability focussed and resilience based approaches to shortlist and combine measures to effectively reduce risks.

For the tactical management of interventions [23] in a system of flood defences it is key to determine when, where and how to intervene [24]. In case the resources would be no boundary for the 'when' a decision framework can be used to determine whether the performance decreases under a pre-defined limit (section 2.4.1). However, since the resources are boundaries, the 'when', 'where' and 'how' can be treated simultaneously as presented for a series of bridges in [46] (section 2.4.2).

2.4.1. RISK-BASED DECISION FRAMEWORK

Approaches to limit the risks are sometimes simply chosen by limit the flood hazard P_f to e.g. 10^{-2} or 10^{-3} per year, as used to be the case in countries like Belgium, Germany [81], and Romania. In those approaches a qualitative estimate has been made that the risks corresponding with a dike breach for those extreme events are not acceptable. In the recent decades developments to assess risks more quantitatively has been undertaken in the countries in the Northsea region [23].

Because 60% of the people in the Netherlands are at risk for floods [1] risk management is existential. A quantitative assessment has been developed after the 1953 disaster by Van Dantzig [14] which is updated recently [51, 82]. The safety standards in the Netherlands are expressed as acceptable probabilities of flooding for a dike segment, based on a risk-framework consisting of criteria for the individual risk, group risk (groups of victims due the same event) and economical risks [35, 83]. The line of thought in [35] is to use the most stringent of those criteria as input for the categorization of a flood safety standards which are reg-

ulated by Law [82]. Since the group risk is not generally used in decision frameworks in other countries, below only the individual and economical risks are presented.

For the individual risk, the consequences D are expressed in equation (2.2) in the probability of a victim per year D_{nv} on a location. The criterion on individual risk limits the acceptable probability of occurrence of an individual victim being on a location (Local Individual Risk, LIR). Referring to the general equation (2.2) this leads to:

$$LIR = E(D_{nv}) = \int_{\vec{h}} f_{\vec{h}} \cdot P_{f|\vec{h}} \cdot P_{nv|f}(\vec{h}, a) \cdot (1 - f_E)\, d\vec{h} \tag{2.10}$$

In which:

$E(D_{nv})$	Expected value of the probability per year of a victim on a location in the polder protected by the dike segment of interest	*victims per year*
$P_{nv\|f}(\vec{h}, a)$	Conditional probability on a victim on location a given a flood (mortality), depending on the characteristics of flooding $\vec{h}$, see section 2.3.2	*per year*
f_E	Evacuation fraction	–

In the Netherlands the LIR is defined as the postal code average, with LIR_{max} equal to 10^{-5} per year. In each postal code in the considered area the LIR should meet this limit. Given the conditional probability on a victim this provides a maximum acceptable value for P_f per postal code. The minimum of all acceptable values for P_f, taken over a polder protected by a dike segment, is the criterion as input for the categorization of a flood safety standard for P_f to limit individual risks.

For the economic risk, the consequences D are expressed in equation (2.2) in the damage D_{Ec} in € per year. The economic risk is defined as the sum of the expected value of economic damage and the expected values of human lives lost in the polder with flood prone surface A [51]. Referring to the general equation (2.2) this leads to:

$$E_A(D_{Ec}) = \int_{\vec{h}} f_{\vec{h}} \cdot P_{f|\vec{h}} \cdot \int_{a \in A} \left(D_{Ec}(\vec{h}, a) + P_{nv|f}(\vec{h}, a) \cdot (1 - f_E) \cdot VOHL\right) da\, d\vec{h} \tag{2.11}$$

In which:

$E_A(D_{Ec})$	Expected value of the economic risk in a polder with surface A behind the dike segment of interest	€/year
$D_{Ec}(\vec{h}, a)$	Economic damage depending on the flood effect based on loads $\vec{h}$ on location a in a polder with surface A protected by the dike segment of interest	€/year
$VOHL$	Economic value of a human life	€

The total societal costs C_{soc} are the sum of investments and the Present Value (PV) of the remaining risk after implementing the measure [32]:

$$C_{soc} = I + \frac{E_A(D_{Ec})}{r} \tag{2.12}$$

In which:

C_{soc}	Present Value (PV) of the societal costs of investments and remaining economic risk	€
I	Investment costs	-
r	Interest rate	-

In fact, the criterion on economic risk is an optimization of the societal costs. In for example [51] and [32] the decision parameter in this optimization is the probability of failure of a dike, P_f. In the Netherlands, the probabilities corresponding to the minimal societal costs are input for the categorization of flood safety standards for P_f, to limit economic risks.

Bischiniotis et al. [37] used a set of decision parameters in the optimization, taking in account three different failure mechanisms. This approach is used in Chapter 3 in which the decision parameters are the dimensions and construction types of the dike, which are related to the construction costs.

2.4.2. INTERVENTIONS IN SYSTEM

The limits such as described in the previous section 2.4.1 provide a risk-based target or standard to keep a system safe under changing conditions. To determine when, where and how to intervene different asset managers may differently develop and apply intervention criteria and conditions, leading to different plans. Common steps are inventory of possible interventions, prioritisation, and planning them in time.

In this thesis the first step, the inventory of possible interventions, is narrowed to dike reinforcement. The intensity of the intervention depends on the performance level which is pursued [45] and the time horizon of the measure.

For the second step, the determination of prioritisation, the effect of the possible interventions is ranked for all dike sections k, below denoted as $\forall k$. Several metrics may be used to rank the different measures. A first example of a metric reflects the relative deviation of the actual safety performance of the dike section to a safety standard:

$$\forall k : \; ratio\, P(k,i) = \frac{P_{f_k}(i)}{P_{f_k\, standard}} \tag{2.13}$$

In which:

$ratio\, P(k,i)$	Ratio between the actual probability and the standard as a measure to rank measures	–
k	Indicator for a dike section	–
$P_{f_k}(i)$	Actual probability of failure of a dike section k in year i	per year
$P_{f_k\, standard}$	Standard for the acceptable probability of flooding of a dike section k	per year

A second metric enables to rank the risk effects of an intervention on system performance. For each dike section k the risk contribution is recalculated with a simulated reinforcement in year i with a design horizon $i + T_{plan}$. This metric uses for all dike sections the differences between the risk in the actual state and the risk in the potential reinforced state of dike section k. It reflects the risk difference due to breaching of a dike section before and after execution of a measure to meet the standard:

$$\forall k : \Delta\, R^{PV}(k,i) = R^{PV}(k,i) - R^{PV}(k_{\text{re}},i) \tag{2.14}$$

In which:

$\Delta\, R^{PV}(k,i)$	Difference between the present value of the flood risks of the potential reinforced and the actual dike section k in year i	€, *victims*
$R^{PV}(k,i)$	Present value of the flood risks with the actual dike section k in year i	€, *victims*

$R^{PV}(k_{re}, i)$	Present value of the flood risks in the potential case of a reinforced dike section k in year i, reinforced to be compliant until a year $i + T_{plan}$	€, *victims*
T_{plan}	Design horizon of a reinforcement	*year*

A third metric is the ratio between benefits and costs, in which the benefits of a measure are the corresponding decrease of the present value of the risk:

$$\forall k : BC(k, i) = \frac{\Delta R^{PV}(k, i)}{C_k(i)} \tag{2.15}$$

In which:

$BC(k, i)$	Ratio between the benefits of reinforcement of dike section k and the corresponding costs in year i	€
$C_k(i)$	Present value of the potential costs of dike section k in year i, reinforced to be compliant until a year $i + T_{plan}$	€, *victims*

The third step, planning the actual measures in the system in time based on the ranking derived in the second step, contains a check whether a planning criterion is met (e.g. exceedance of safety level), and a check on planning constraints such as available budget per year or other resources needed to perform an intervention.

2.5. RISK ANALYSES APPLICATION

The European Union established the Floods Directive 2007/60/EC [34] to stimulate the member states to manage their flood risks based on the same rationale to map risks, plan and take measures, and monitor. Nevertheless, despite the Floods Directive stimulated the application of quantitative approaches, still differences in risk approach are present [3, 23]. The guidance by the EU for all kinds of risk (floods, wildfires, chemical, nuclear etc.) is extensive but conceptual [27]. The rationale is that the application of risk analysis depends on the objective and on available data and site specifications. The same holds for the risk analysis within the floods domain. In this thesis three applications are elaborated for each of the key topics. Each uses the general definition in equation (2.2), however, applied differently.

For the integrated dike design optimization (key topic 1) the consequences in this general equation (2.2) are reflected by the effect of the flood on the maximum water depth in a polder due to the set of variables $\vec{X}$ of loads, strength and dike breach in year i:

$$E(D,i) = \int_{\vec{X}(i)} P_{\vec{X}(i)} \cdot D\left(\hat{h}_p(\vec{X}(i))\right) d\vec{X} \tag{2.16}$$

In which:

$\vec{X}(i)$	Set of variables determining the flooding in year i: loads, strength and dike breach	–
$P_{\vec{X}(i)}$	Probability of flooding in year i	*per year*
$D\left(\hat{h}_p(\vec{X}(i))\right)$	Consequences of flooding in year i dependent on the maximum polder water level based on set of variables determining the flooding	e.g. €, victims
$E(D,i)$	Expected value of consequences of flooding in year i	*e.g. €/year, victims per year*

For the integrated portfolio prioritisation (key topic 2) the loads in this general equation (2.2) are applied dependent on possible flooding anywhere in an area of several polders along a series of dike sections k, covering several dike segments K. The loads and consequences are dynamic over time i:

$$E(D_{\forall k},i) = \sum_{k \in \forall K} \int_{\vec{h}(i)} f_{\vec{h}(i)} \cdot P_{f|\vec{h}(i)}(k) \cdot D(\vec{h}(i),k)\, d\vec{h}dk \tag{2.17}$$

In which:

$E(D_{\forall k},i)$	Expected value of consequences of flooding due to failure of dike segments protecting the polders in a region in year i	*e.g. €/year, victims per year*
$\vec{h}(i)$	Set of variables determining the loads such as water levels and wave attack in year i	e.g. $m+SWL$, m
$f_{\vec{h}(i)}$	Probability distribution of the set of variables determining the loads such as water levels and wave attack in year i	*per year*
$P_{f\|\vec{h}(i)}(k)$	Probability of failure of dike segment k given the set of loads in year i	*per year*
K	Indicator for a dike segment	–

$D(\vec{h}(i,k))$	Consequences of flooding due to failure of dike segment k given the set of loads in year i	e.g. €, victims

For the strategic analysis determining the adaptive application of standards (key topic 3) this general equation (2.2) is used per dike segment K and per year i using the probability of flooding in stead of the multiplication of the distribution of loads and the probability distribution of dike breaches given the loads:

$$E(D,K,i) = \int_{\vec{h}(i)} P_{f_K}(\vec{h}(i)) \cdot D_K(i)\, d\vec{h} \tag{2.18}$$

In which:

$P_{f_K}(\vec{h}(i))$	Probability of failure of dike segment K due to load vector $\vec{h}$ in year i	–
$D_K(i)$	Consequences of flooding due to failure of dike segment K in year i	e.g. €, victims
$E(D,K,i)$	Expected value of consequences of flooding due to failure of dike segment K in year i	*e.g. €/year, victims per year*

The three applications of the general risk formula presented by equations (2.16), (2.17) and (2.18) are all in the shape of a multiplication of probability and consequences, following the general shape in equation (2.2). They are further elaborated and applied in the following chapters.

3

FLOOD RISK REDUCTION BY STRUCTURAL ROBUST DESIGN

The introduction of pre-determined criteria may give the wrong focus – meeting these criteria rather than obtaining overall good solutions and measures.

Terje Aven [84]

Present risk analyses often consist of decoupled calculations of probabilities of dike failure and calculation of consequences of flooding. However, the flood defence design determines not only the probability of failure, but influences the consequences of flooding as well. Especially when the dike has a ductile failure and breach growth behaviour the consequences of flooding reduce. In this chapter an assessment method of risks and investments is presented, valuing structural robustness of a construction type, represented by its ductile behaviour during high loads. Therefore, the consecutive occurrence of initial dike failure mechanisms, failure path development, breach growth and consequences is modelled integral and time dependent. The investments consist of the costs to reinforce or reconstruct the flood defence to behave relatively ductile. This method enables to compare flood impacts of different construction types and different dimensions of designs. The method is applied on a case in a riverine area in the Netherlands. The results show the total societal costs and the individual risks on victims strongly depend on the construction type. The brittle sand dike in the case requires larger dimensions than the more ductile dike with a clay core.

The majority of this chapter has been published in F. den Heijer and M. Kok. "Assessment of ductile dike behaviour as a novel flood risk reduction measure". In: Risk Analysis (2022), pp. 1–16. doi: 10.1111/risa.14071

3.1. INTRODUCTION

Dikes are crucial for flood risk management in the lower reach of rivers [1]. Ageing, climate change and human and faunal activities urge to maintain and reinforce or adapt them. Increase of data, knowledge, and innovations provide the opportunity to manage these activities in a contemporary manner. At present, mainly three categories of flood risk reduction measures are practised: reduction of loads, increase of strength, both reducing the probability of failure, and reduction of consequences of dike failure. In this chapter a fourth one is presented: structural robustness by design of the dike construction.

Baker et al. introduced a framework for assessing robustness [85]. Klerk investigated stuctural robustness of dike revetments [49]. In this chapter the structural robustness of the dike related to flood risks is elaborated. Structural robustness can be increased by a ductile behaviour of the construction. In this thesis ductile behaviour is defined as the slow failure process of a dike, and a relatively slow or depth-limited breach growth, both leading to reduced breach dimensions and reducing flood impacts. It is the opposite of brittle behaviour, with a sudden occurrence of a breach, increasing flood impacts. Thus, a more ductile dike is not necessarily larger than a brittle dike but it has another construction with e.g. a clay core instead of a sand core, leading to less flood impact. A method is developed to evaluate the potential benefits, and it is applied on a location in the Dutch river area.

The first motive of this chapter is to enable an evaluation and enrichment of the present practice, e.g. in the Netherlands, see Section 1.5. In [66] the Source-Pathway-Receptor framework figures out a route to an effective flood risk management. However, in case standards are in place for the probability of dike failure, the focus is on meeting these standards [84]: the practice is to design mainly to meet the standards with minimal financial efforts, leading to a preference of brittle dikes with a sand core. This may have worked out this way due to the standards and rules for safety assessment as provided in [75], or due to financial constraints. The approach used in the development of the standards, to propose more stringent standards at high-risk locations, leads to stronger but still brittle dikes. Barely research has been found on whether this is an optimal choice [37, 68]. However, the practice before standards were established was to build dikes, especially on high-risk locations, with a core of clay [86], such as the Grebbedijk. The Deltacommission [87] introduced in 2008 the so-called Delta dikes, which are so high, strong and wide that dike failure probability is very small with respect to other dikes. The elaborations of Delta dikes are a step to search for alternative construction types for high-risk locations [88, 89], and field tests with a sheetpile in the dike, at Eemdijk, showed the ductile (or: tough) failure

behaviour [90]. This research responds to the growing awareness of the importance of dike construction at high risk locations, with an approach providing comparative insights in its societal benefits.

Second motive is to provide an extra opportunity for the utilization of the recently updated safety standards in the Netherlands. The standards are based on an improved and extended risk analysis [51, 82], expressed as acceptable flooding probabilities of dike segments. The segments consist of a series of dike sections. Only the failure mechanism overtopping is considered, assuming that this would be normative for the dike dimensions. Since the basic approach for risk-based standards could not be optimal for some specific situations, the Dutch policy provides the so-called decision for 'exchange' between measures for reduction of failure probability and reduction of consequences, persevering the same risk level [55]. The fourth category of risk reduction measures, referred to in the preamble of this section, may provide an opportunity to take benefit of this 'exchange'-policy, reflected in adapted dimensions, adapted construction type or adapted optimal flood risk level. This provides the opportunity to incorporate consequences of failure in the design process, due to taking into account the failure behaviour in time, dependent on initial failure mechanism or construction type.

Third motive is to enrich the present elaboration of time dependent failure processes in the reliability analyses of dikes [39, 91–94], describing the residual strength after occurrence of initial damage due to a failure mechanism. The present methods for system analysis of probabilities of failure, developed in the last decades, does not support time dependent failure approaches. Loads are schematized by extreme value statistics of maximum water levels during storm or river floods. In essence, the present analysis is compiled by a combination of a probabilistic analysis per failure mechanism per dike section, and a system analysis of all known failure mechanisms and dike sections in a flood defence segment [31, 74, 95, 96]. To embed time dependent developments of initial failure mechanisms and time-dependent failure paths to flooding require artificial assumptions, such as the average duration of a water level or storm maximum [94]. This chapter provides a method set up to handle time dependency, avoiding the uncertainties connected to such artificial assumptions.

The objective of this chapter is to develop and test a method which will enable the evaluation of the risk reduction potential of dike construction types. This chapter presents consecutively the theoretical background of flood risk assessment, risk-based criteria as a basis for trade-offs, the methodology and application of the proposed evaluation of ductile behaviour, a case study, and finally the discussion and conclusions.

3.2. THEORETICAL BACKGROUND FLOOD RISK ASSESSMENT

Referring to equation (2.1) flood risk can be defined as the expected value $E(D)$ calculated as the sum of the risk for all possible scenarios leading to the undesired flood event [32]. In the application in the Netherlands, due to a smart choice of the dike segments, the consequences of dike breach are almost independent of the location of dike breach along a dike segment. Only a few dike breach scenarios are chosen, expressing the effect of different load levels on the consequences: some individual breaches and one with multiple breaches as a worst case. This simplifies the risk calculation, distinguishing the calculations of dike failure probabilities and consequences of flooding [80]:

$$E(D) = P_f \sum_{j=1}^{j=n} \alpha_j \cdot D_j \tag{3.1}$$

In which:

α_j	Weighting factor dependent on the chosen flooding scenarios j	—

A typical time pattern of the water level in the polder is given in Figure 3.1a. The consequences are in [80] related to the maximum water level and the maximum rate of water level increase during a flood. In this way the calculations for dike failure are disconnected from the calculations of consequences. This simplified risk calculation contains pre-defined loads in time, the moment of dike failure, and breach growth in time. Since these are chosen independent of dike construction type the risk calculation in [80] will not provide insight in the risk-effects of construction type.

Therefore, in this chapter is sticked to the basic definition of risk in equation (2.1), applying it for flood risk, equation (2.2), in such a way insight in the effects of construction type could be provided, see equation (2.16). The undesired event j is defined as the occurrence of a flood at a location a, see Figure 3.1b, resulting in a certain water level in time $h(t)$ during the flooding at that location, see Figure 3.1c. The consequences d are defined as damage and victims during the event at a location a in a polder with surface and bathymetry A_b. The flood patterns $h(t)$ at a contain the characteristics of the loads on the dike system $S(t)$, the strength and construction of the dike R, the breaching behaviour $B(t)$, and the bathymetry of the polder A_b:

$$h_{\vec{X},a}(t) = f(S(t), R, B(t), A_b) \tag{3.2}$$

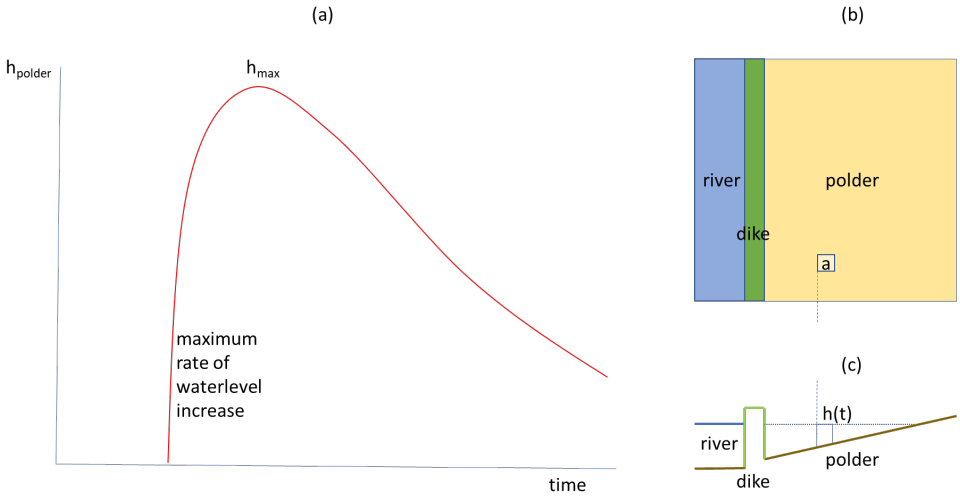

Figure 3.1.: *Typical time course of the water level in the polder a) during a flood; b) in a polder in a riverine area c) at location a.*

In which:

$h_{\vec{X},a}(t)$	Water level in the polder over time on location a due to flooding	$m+SWL$

with $\vec{X}$ the set of variables determining loads, strength and breach growth. In Appendix A these variables and the physical relationships for determination of $h_{\vec{X},a}(t)$ are given as used in this thesis. The derivation of the probability of occurrence of a flood on a location in a polder is similar to the derivation of the probability of failure of a dike, based on loads and strength. The difference is the introduction of a chain of relationships following initial failure mechanisms, covering the whole pathway from 'source' (hazard) to 'receptor' (consequences) [66]. The probability of a flood pattern $h_{\vec{X},a}(t)$ depends on the set of uncertain variables $\vec{X}$ in the relations in equation (3.2). In general equation (2.1) for the flood risk in a polder then looks like:

$$E(D) = \int_{a \in A} \int_{\vec{X}} \left(f_{\vec{X}}(h_{\vec{X},a}(t)) \cdot D(h_{\vec{X},a}(t)) \right) d\vec{X}\, da \tag{3.3}$$

In which:

$f_{\vec{X}}(h_{\vec{X},a}(t))$	Probability density of the flooding at location a with the flooding characteristics $h_{\vec{X},a}(t)$	-
$D(h_{\vec{X},a}(t))$	Consequences of the flooding at location a with the flooding characteristics $h_{\vec{X},a}(t)$	€, *victims*

Note, since $\vec{X}$ contains breach characteristics next to loads and strength variables the probability of failure of the dike is no longer a separate and disconnected part of this relation. Dike breaching is integrated in the derivation of the probability density function. Consequently the probability density in equation (3.3) contains the characteristics of the loads on the dike system, the strength and construction of the dike and the characteristics of the polder.

A typical profile of the relation between river hazards and flood impact due to dike breach is given in Figure 3.2. The profile is based on the simplification to assume only maximum water level during a flood event as a cause for dike breach. River flood waves with relatively low maxima does not lead to any flood impact. When the maximum water level during a river flood wave exceeds a certain level, the dike breaches and the polder will be flooded, resulting in a sudden increase of maximum water level in the polder. This maximum water level will only slightly increase with increasing maximum river water level (Figure 3.2a), see also [97]. The frequency of exceedance decreases for higher maximum river water levels (Figure 3.2b). The consequences of flooding correspond with the polder water level, occurring suddenly at a certain exceedance frequency and increasing slightly with decreasing exceedance frequency (Figure 3.2c). Note: still assuming the exceedance frequency of maximum water level in the river is directly related to the probability of dike breach, the surface below the profile of Figure 3.2c) is equal to the risk of flooding, corresponding to equations (2.16) and (3.3). Note that the consequences D are multi-dimensional, mostly represented by economic damage and victims. The shape of Figure 3.2c) is referenced to as F_N-curve for groups of victims and F_D-curve for economical damage.

3.3. APPLICATION

3.3.1. CALCULATION OF MAXIMUM POLDER WATER LEVEL

Loads, strength, breach, flooding and consequences are to be calculated time dependent during a load event, for each of which numerical models could be used. Especially the calculation of equation (3.2) is time consuming. To be able to apply it for a proof of concept in a concrete riverine situation, simplifications have been made on the following physical relations and modelling:

- Loads during breach: the effect of the breach on the local water level is analytically derived. It is based on available pre-calculated polynomic relationships between discharge at the country-border and local water level [72], and the logic that the sum of discharges through the breach and in the river downstream should be equal to

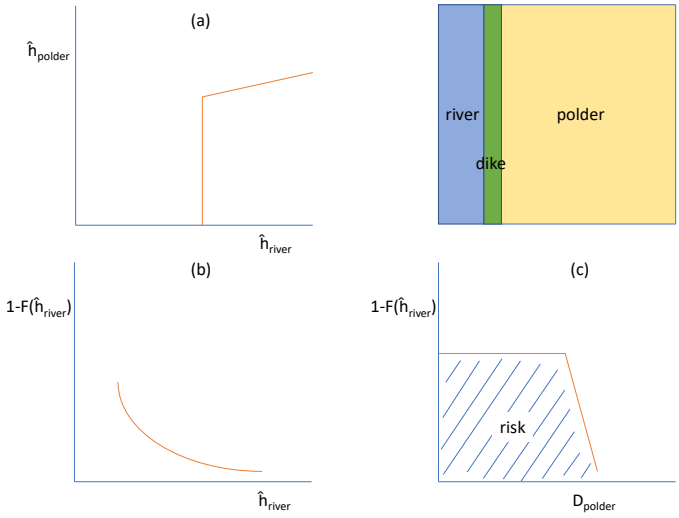

Figure 3.2.: *Typical relations in an riverine area protected by dikes between a) maximum polder water level and maximum river water level; b) maximum river water level and its exceedance frequency* $(1 - F(\hat{h}_{river}))$*; and c) damage in the polder and exceedance frequency of water level in the river. The surface below the curve in (c) is the risk assessed by equation* (3.3).

the upstream river discharge. See the load model in Appendix A for the physical relations.

- Dike system: the dike system consists of one dike segment, and the dike segment consists of exactly one dike section. Only two relevant initial failure mechanisms are considered, which are overtopping and piping. The piping mechanism is a regressive tunnel erosion process. The point at the riverside of the dike where the pipe shortcuts with the water system is called the entrance point, the point at the polderside the exit point. Two possible exit points are considered: the inner toe of the berm, and the inner toe of the inner slope.

- Breaching: The dike failure path due to overtopping as an initial failure mechanism occurs when consecutively the inner revetment is eroded, the clay layer below the revetment is eroded, and the core is eroded. The dike failure path due to piping as an initial failure mechanism occurs when a pipe propagates entirely from exit backwards to entrance point. See Appendix A for the physical relations.
- Flooding: The flooding in the polder area is schematized as a 0-D hydraulic model, and the polder is flat. Thus, each inflow is directly spread over the polder with surface A, translating $h_{\vec{X},a}(t)$ into $h_{\vec{X}}(t)$.
- Consequences: the consequences of flooding are directly related to the flood inflow V, the total volume of water entering the polder during an event, see equation (2.9) in Section 2.3.2 with $c_D = 18.6$ €/m^3 for economic risks D_{Ec} and $c_D = 1.2 \cdot 10^{-6}$ victims/m^3 for the individual risk D_{nV}.

The simplifications mean that water depth in the polder is uniform distributed and the consequences of a flooding are only related to the maximum water depth in the polder during an event.

$$D = c_D \cdot V = c_D \cdot A \cdot H = c_D \cdot A \cdot (\hat{h}_{\vec{X},A} - d_A) \tag{3.4}$$

In which:

H	Maximum water depth in the polder during an event	m
A	Surface of the polder	m^2
$\hat{h}_{\vec{X},A}$	Maximum water level in the polder with surface A during an event	$m+SWL$
d_A	Ground level of the polder with surface A	$m+SWL$

Equation (3.2) can be rewritten to process the effect of time dependent breach behaviour, the core of this chapter:

$$\hat{h}_{\vec{X},A} = MAX(h_{\vec{X},A}(t)) \tag{3.5}$$

The time dependent development of polder water level during a flood event is modelled by a chain of physical relations, operationalized in a Python script and tested for a location along the Rhine river. For each of the physical relationships explained in Appendix A the script is checked separately before use in the model chain. In Figure 3.3 a set of intermediate results shows the propagation of the event in time in the physical space. The Figure on top shows the development of the local water levels in time. The green line presents the undisturbed river water level in case of no breach. The river water level (red line) shows a jump when dike

breach occurs at about t=220 hours. The polder water level (blue line) increases after dike breach and decreases when it exceeds the river water level. The second part of Figure 3.3 shows the erosion of the dike due to increasing loads. It shows the prelude of dike breach. At about 190 hours the piping mechanism starts with uncontrolled pipe growth (blue line). At that moment the pipe has grown to half the available length (fraction 50%). The green line shows the erosion of the grass cover on the inner slope due to overtopping. A fraction of 100% means the cover is damaged in a way the underlying core material cannot be protected anymore. Erosion of the core starts after such an eroded cover (red line). The two failure paths piping and overtopping develop simultaneously. In this case dike breach is initiated by piping because the blue line reached 100% while the core is only eroded for about 10% (red line at t=220). The third part of Figure 3.3 shows the development of breach width. The last part of the Figure shows the inflow in the polder during the event. The total inflow during the event, in this case between t=220 hours until t=500 hours, is the volume V which can be used in equation (2.9) to calculate the consequences.

3.3.2. CALCULATION OF RISKS

Substituting these simplifications in equation (3.3) leads to:

$$E(D) = A \cdot \int_{\vec{X}} \left(f_{\vec{X}}(\hat{h}_{\vec{X},A}) \cdot D(\hat{h}_{\vec{X},A}) \right) d\vec{X} \tag{3.6}$$

In which:

$f_{\vec{X}}(\hat{h}_{\vec{X},A})$	Probability density of the flooding with maximum flood level $\hat{h}_{\vec{X},A}$	-
$D(h_{\vec{X},A})$	Consequences of the flooding with maximum flood level $\hat{h}_{\vec{X},A}$	€, *victims*

Substituting equation (3.4) for a given level H gives the risk due to floodings causing a polder water depth of H :

$$E(D \mid \hat{h}_{\vec{X},A} = d_A + H) = A \cdot \int_{\vec{X}} \left(f_{\vec{X}}(d_A + H) \cdot c_D \cdot H \right) d\vec{X} \tag{3.7}$$

with $f_{\vec{X}}(d_A + H)$ the probability density of occurrence of water depth H. Reordering equation (3.7) and integration over all possible polder water levels H gives:

$$E(D) = A \cdot c_D \cdot \int_H H \cdot \left(\int_{\vec{X}} f_{\vec{X}}(d_A + H)\, d\vec{X} \right) dH \tag{3.8}$$

with between brackets the probability of exceedance of polder water level H.

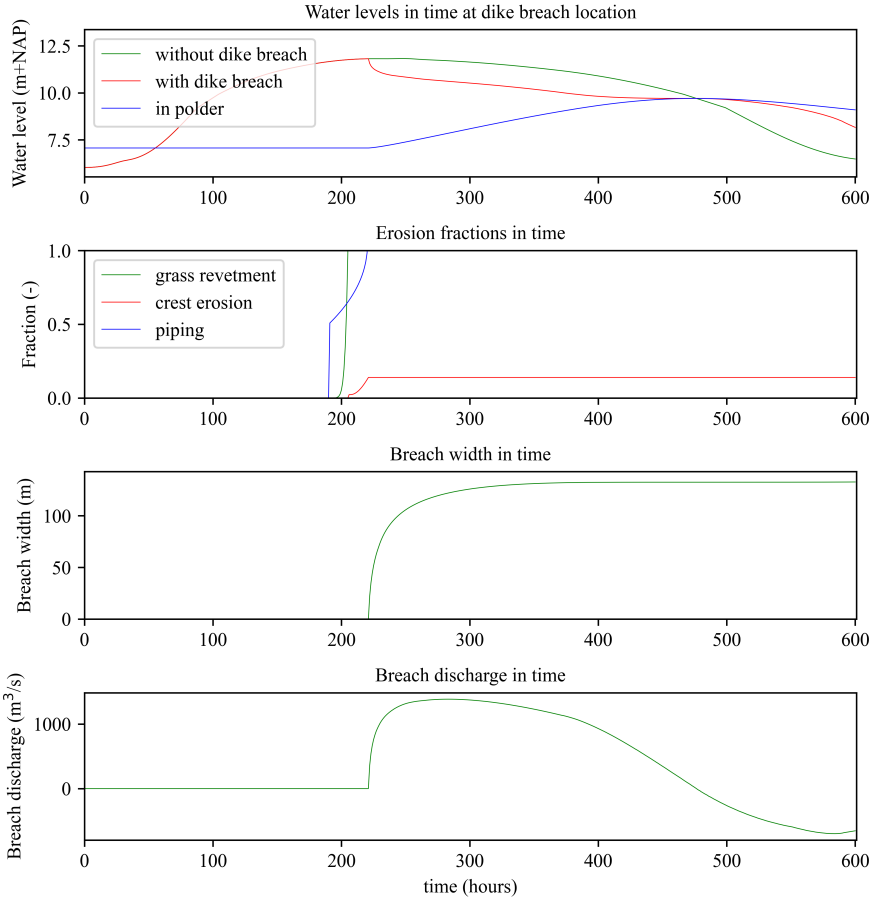

Figure 3.3.: *Example of calculation of respectively water levels in the river and in the polder as a part of the limit state function, erosion fractions in time, breach width in time and breach discharge in time, for a location at Rhine river km 906.3, and a dike with a clay core, a height of 12.05 m+NAP (Dutch reference level) and a berm width of 6m.*

3.3.3. CALCULATION OF FLOOD LEVEL EXCEEDANCE PROBABILITIES

The limit state function for exceedance of level H is:

$$Z(H) = d_A + H - \hat{h}_{\vec{X}} \tag{3.9}$$

with $P(Z < 0)$ the probability of exceedance of polder water depth H : $P(\hat{h}_{\vec{X}} > d_A + H)$. For application in equation (3.8) this probability has to

be calculated for all H, which is in practice the domain 0<H<dike crest:

$$\forall H \in (0, dike\ crest) : P(\hat{h}_{\vec{X}} > d_A + H) = \int_{\vec{X}} \left(f_{\vec{X}}(d_A + H)\right) d\vec{X} \tag{3.10}$$

An example of the result of calculation of equation (3.10) is showed in Figure 3.4, for two different horizons for a location along the Rhine river, km 906.300. In this example a series of calculations has been carried out for discrete values of H starting with $H_{min} = 0.1m$ and a step $\Delta H = 0.2m$. Note, the relationship with existing approaches use the probability of failure of the dike P_f. This is a specific case of equation (3.10) with $H \downarrow 0$, the intersection of the curve with the vertical axis:

$$P_f \approx \lim_{H \downarrow 0} P(\hat{h}_{\vec{X}} > d_A + H) \tag{3.11}$$

For H smaller than H_{min} we assume $= P(\hat{h}_{\vec{X}} > d_A + H) = P(\hat{h}_{\vec{X}} > d_A + H_{min})$. This means the probability for water depths smaller than H_{min} is assumed to be equal to the probability at H_{min}, which is a reasonable assumption in case H_{min} is small, see Figure 3.4. With the result of this calculations, the risk in equation (3.8) can be calculated easily by numerical integration:

$$E(D) = A \cdot c_D \cdot \left(H_{min} \cdot P(\hat{h}_{\vec{X}} > d_A + H_{min}) + \Delta H \cdot \sum_{m=1}^{m=n} P(\hat{h}_{\vec{X}} > \overline{H}) \right) \tag{3.12}$$

with $n = \frac{H_{dikecrest}}{\Delta H}$, D and c_D indicating the type of risk, $P(\hat{h}_{\vec{X}} > \overline{H})$ the mean probability in the water depth interval $(H - \Delta H, H)$, and $H = H_{min} + m \cdot \Delta H$. The relationship in equation (3.10), presented in Figure 3.4 as well, is the equivalent of the F_D-curve and F_N-curve as used in [32] and as schematic given in Figure 3.2c. In the following to these curves are referred to as F_H-curves. As applied in equation (3.4), H has a linear relation with the consequences. Therefore, in this application the risk in equation (3.3) is equal to the surface below this Figure multiplied by the polders surface A and damage coefficient c_D.

3.3.4. PROBABILISTIC APPROACH

Even with the simplifications as presented in the sections before, the calculation of equation (3.12) is time consuming. Furthermore, because of the discontinuity of $\hat{h}_{\vec{X}}$, due to a possible dike breach during an event, a FORM technique is not applicable without significant additional measures for numerical stability. Therefore, the probabilities of exceedance are assessed by a Monte Carlo importance sampling (MC-IS) method. The benefit of a Monte Carlo approach is the independence of calculation time from the number of stochastic variables. Implementation of this approach requires some additional starting points:

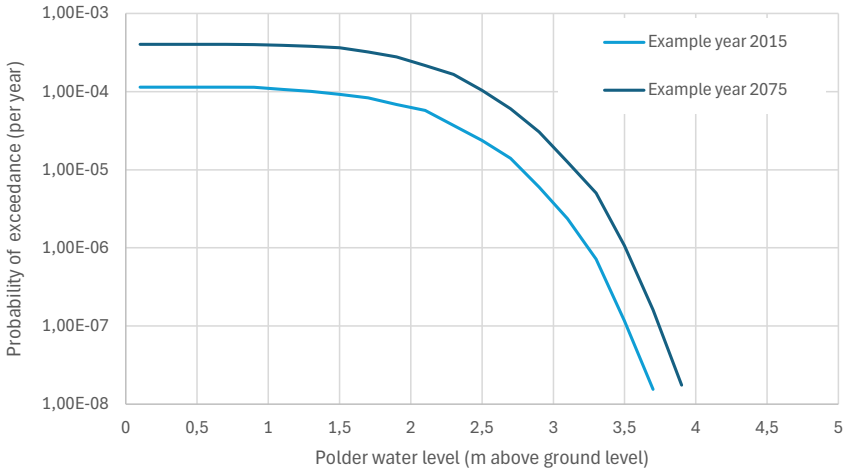

Figure 3.4.: *Example of a series of probabilities of exceedance of polder water level H.*

- Package: The free available software package Probabilistic ToolKit (PTK) [98] developed by Deltares is used. This package calculates probabilities for a given limit state function for a variety of probabilistic techniques including MC-IS.
- Importance Sampling: the choice of the important $\vec{X}$-space around a central IS-point is subjective and for each value of H this may shift a bit. Therefore, an iterative procedure has been used which is developed in PTK, in which in several loops the IS-point is adjusted to get a sufficient accurate result. This is done for each individual calculation in the series of calculations in equation (3.10).
- Time base: The duration of the load event on the system is taken as long as the longest load event involved, T_{max}. For a riverine area that is the period of a river flood wave, for the Rhine in the Netherlands about 1 month [70]. Consecutive flood waves are considered to be independent. Upscaling of probabilities to a year, the time unit mostly used for flood risk analyses is a simple analytical transformation of equation (3.10):

$$\forall H \in (0, dike\ crest) : P_{yr}(\hat{h}_{\vec{X},A} > H) = 1-(1-P_{T_{max}}(\hat{h}_{\vec{X}} > d_A + H))^{\frac{T_{year}}{T_{max}}} \tag{3.13}$$

- Combining loads with different time scales: During a river flood event there may be several load events with a shorter time base. Windstorms are included, causing waves which may damage the dike. These windstorms are modelled at random in time occurring once during a flood event. This is an underestimation because there may be more windstorms during one event, but in a riverine situation the discharge of the river flood wave is by far the most important stochastic variable, so this inaccuracy is expected to be very small.
- Wind direction: Each sample represents a flood event, composed based on the different load variables. The wind direction is one of them. For practical reasons only one wind direction is chosen for the whole flood event.

Following this starting points, the load model has been compared with the load model HYDRA-NL as given by [99] used for assessments and designs for the National Flood Protection Program in the Netherlands, for a location along the Rhine river, km 906.300, see Figure 3.5.

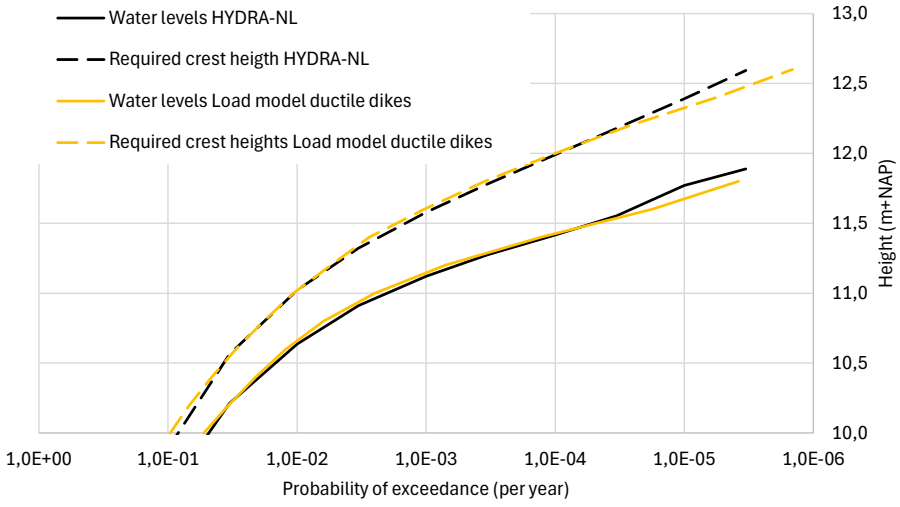

Figure 3.5.: *Comparison between the model HYDRA-NL [99] (black lines) and the model in this chapter (orange lines) for water levels (solid lines) and required dike crest heights (dike heights corresponding with a required limit for overtopping discharges, in this case 1 l/m/s). Dike slope 1:3.*

The comparison is pretty good for both water levels (solid lines) and required crest heights to reduce overtopping discharges to 1 l/m/s (dashed). From probabilities of about 10^{-5} and smaller the results of the load model (orange) still look stable, deviating a bit from the results from HYDRA-NL (black). In Figure 3.6 the calculation process for the MC-IS-analysis is schematized. For each drawn sample the limit state function is evaluated, requiring a calculation of the physical model showed in Figure 3.3, resulting in $\hat{h}_{\vec{x},A}$.

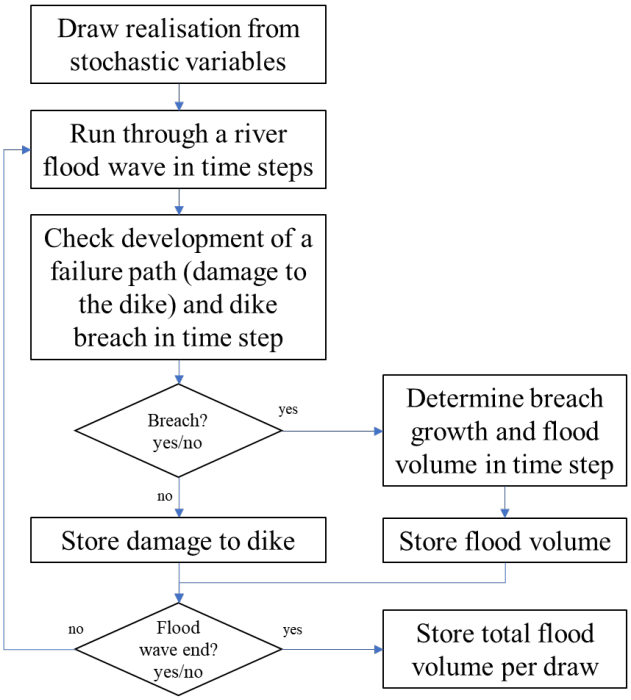

Figure 3.6.: *Flowchart for evaluation of an individual limit state function*

3.4. APPLICATION IN CASE GREBBE

3.4.1. LOCATION

The location for the case is the 'Grebbedijk', along the river Rhine branch 'Nederrijn', at river kilometer 906.300, between dike marks 46 and 47, at the Paris coordinates (170757,440168), see Figure 3.7. For this case location is chosen based on several criteria:

- the location has to be on a primary dike in the Netherlands, along a large and independent source of risk [55].

- for a proof of concept of the methodology a relatively simple load regime is preferred. Therefore, the riverine area has been chosen, with river flood waves as major load, without near-sea effects of high tides, and with windspeeds causing waves as secondary load.
- the dike has a risk deficit, urging the dike manager to reinforce.

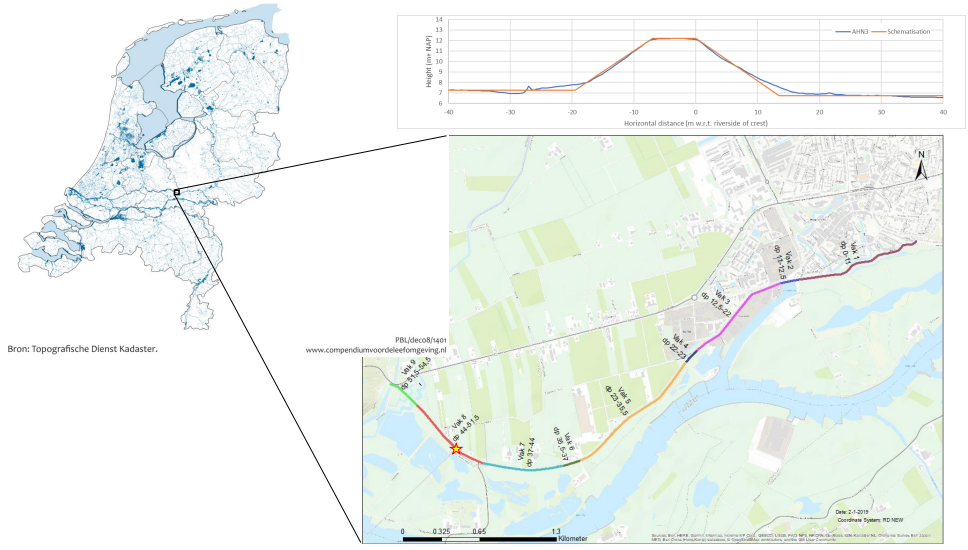

Figure 3.7.: *Map of the Netherlands (left) and the location with dike segment, dike section and dike cross-section of interest (right below). Profile of dike cross-section: the national digital terrain model AHN3 in blue and the schematization in this thesis in orange (right above).*

3.4.2. CASE SPECIFIC STARTING POINTS

To operationalize the concept for a riverine case the following assumptions and starting points are made:

- Six dike construction types are considered, referring to [100], [90] and the second Dutch Deltacommission [87] who recommended to consider Delta dikes: a traditional dike, a dike stabilized with a sheetpile, and a width dike, all with cores of sand or clay, see Figure 3.8. These types are chosen because of the expected difference in ductility and corresponding risks. Types a and d are typical for the Dutch river area.
- Two chosen design dimensions characterise the difference between the construction types in the calculations: the toplevel of the sheet-

pile in construction types c and f is 1.5m above the landward polder level, and the extra crest width of the construction types b and e with respect to the other types is 10m.

- Loads and strengths are assumed to be homogeneous over the length of the dike segment of 5.5 km.
- Climate change and subsidence are deterministically coupled to the chosen design horizon in 2075, assuming climate scenario G+ [101] and subsidence of 0,17 m/50 year [102]. The effect of climate change on the river discharge is based on Smale [101] which is representative for the year 2015. The effect is represented in a transformation of the probability distribution of the river discharge with:

$$Q = Q_{2015} \cdot \left(1 + c_{cl} \cdot (horizon - 2015)^{b}\right) \tag{3.14}$$

In which:

Q_{2015}	Discharges base value in 2015	m^s/s
$horizon$	Year of interest	–
b	Parameter depending on climate scenario	–
c_{cl}	Parameter depending on climate scenario	–

in which $c_{cl} = 1.68 \cdot 10^{-3}$ and $b = 0.1$ reflect the climate scenario G in [103]. Subsidence is assumed to occur evenly for the whole cross-section:

$$h_x = h_{x,\,2015} - \frac{dh_x}{dt} \cdot (horizon - 2015) \tag{3.15}$$

In which:

$h_{x,2015}$	Dike height in 2015 for location x in the dike cross section	$m+SWL$
h_x	Dike height for location x in the dike cross section in the year *horizon*	$m+SWL$
$\frac{dh_x}{dt}$	Subsidence rate per year	$m/year$

- The probability distribution of the water level on the location of interest is based on the distribution of discharge in the Rhine river, which is based on the statistics at the Dutch border at Lobith, available from load events [70]. Floodings upstream are assumed to prevent flood waves exceedance of discharges 18000 m^3 [104].

- The Rhine branch 'Nederrijn' discharges 21%, independent of the exact discharge [104]. Analytical relations are used between the national borders and the location of interest, derived based on a series of numerical calculations with SOBEK [72].
- A flood wave on the Rhine river has a duration T_{max} of about 1 month, 675 hour [70]. The probability in summer is assumed to be zero, thus, with T_{year} is 6*30*24=4320 hours, about 6 independent flood wave events occur per year. The timestep in the calculation of each MC sample is chosen as 1 hour, which is small with respect to the event duration.
- The investments I to take measures in the cross section are based on initial investments, which are independent of degree and type of reinforcements, and the marginal investments due to supply, replace or removal of volume of materials used for the reinforcement, renewal of the pavement on the dike, or change of construction type such as the use of a sheetpile. In Appendix A the full equation is given. The application of the marginal costs and parameters in this equation is based on exercises with cost model KOSWAT [105], the model used in the Dutch Flood Protection Program.
- Interest rate is assumed to be 3% and the value of a human live is based on [51] 6.7 M€.

3.4.3. CALCULATIONS, RESULTS AND ANALYSIS

The risks for the present situation (year 2015) have been assessed with the physical relations of equation (3.4) and (3.5) in Section 3.3. The results are presented in Table 3.1. Two variants of the existing situation are presented: the existing dike with a clay core, and a semi-existing situation, representing the same dike with a sand core. For both variants no investment costs I are needed to reach the existing situation. Therefore, the societal costs are in this case only the costs due to the risk of flooding. Table 3.1 presents as well the situation in 2075 when no measures are taken. In case of no measures, the net present value (NPV) and the number of victims would increase significantly in 60 years. Note, the individual risks (LIR) are expressed as the number of victims per hectare (ha). This deviates from the LIR as presented in the decision framework in Section 2.4.1, because a LIR could not be derived from this proof of concept schematisation (hypothetical flat polder, 0-D hydraulic model) for which no postal code areas are available.

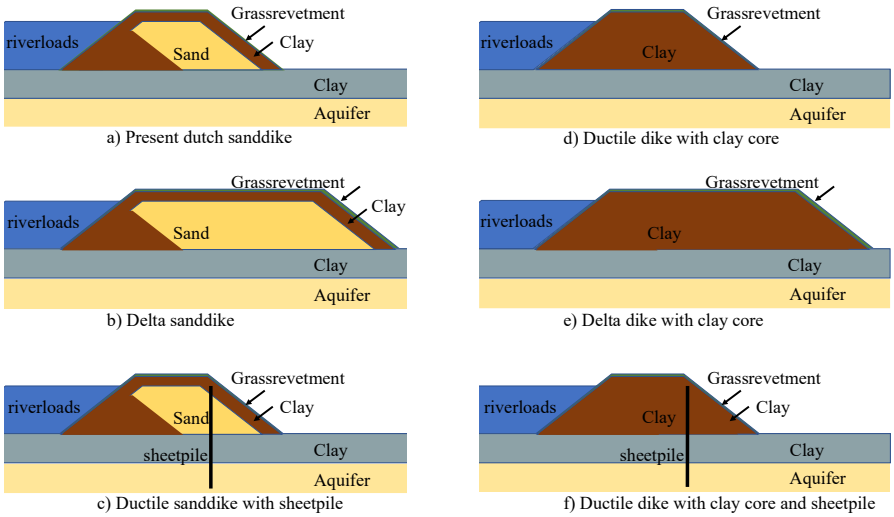

Figure 3.8.: *Six dike cross sections used, typical to express the effect of ductile behaviour on flood risk*

Table 3.1.: *Results of assessment for 2015 for existing dike at case location, with polder level 7.25 m+NAP. Second line in the rows represents the costs and risks in 2075 without measures taken with respect to the present situation.*

Construction type (see Figure 3.8)	**dike height** (m+NAP)	**inner slope** (-)	**berm width** (m)	**berm height** (m+polder gr. level)	**Soc. costs (total/I/ER)** (M€, NPV)	**Indiv.risk (vict./ha)** ($\cdot 10^{-5}/yr$)	**prob.dike failure** ($\cdot 10^{-5}/yr$)
Existing (d)	12.20	2.5	0	0	51.8 / 0 / 51.8 200 / 0 / 200	0.20 0.77	10.4 38.6
Semi-existing (a)	12.20	2.5	0	0	72.1 / 0 / 72.1 269 / 0 / 269	0.28 1.04	11.4 40.2

In case measures are considered to reduce the risks, investments have to be made. Usually optimizations of dike design as presented in [32], [51] and [68] are used, searching for a dike failure probability resulting

in minimal societal costs, or other criteria such as reduction of individual risks. For this optimization mostly a limited number of design degrees of freedom is considered. In [51] and [68] the most important design variable is the dike height. The optimization searches for the dike failure probability resulting in the minimal societal cost. However, the dike failure probability or dike height is not sufficient informative to assess the consequences of floods protected by dikes with different ductile behaviour. The concept presented in this chapter, summarized by equation (3.12), even does not explicitly require the dike failure probability. Furthermore, for non-economic criteria such as individual risks optimization of dike failure probability does not hold, since no economic benefits exist for non-economic criteria.

An optimization process had been set up, similar to [32], [51] and [68], without the need of an explicit dike failure probability, and with the opportunity to compare the performance of different dike construction types. The heuristic optimization process for this approach is rather straight forward, but time consuming:

- For each of the dike construction types in Figure 3.8 a matrix of several combinations of dimensions has been taken, step by step enlarged with respect to the existing dimensions.
- For each construction-dimension-combination (in the following referred to as CDC) the exceedance curves of water levels F_H in the polder are calculated with equation (3.10), and the corresponding risks are calculated with equation (3.12).
- Each CDC corresponds to an investment as well. The investments I follow from the difference between the CDC with the existing situation.
- The costs and risks of all CDC's are graphical presented with the individual risks as the average number of victims per ha per year on the x-axis, and the societal costs on the y-axis.

The varied dimensions are crest height, berm width, berm height and inner slope. Figure 3.9 gives examples for some F_H-curves for the different construction types in Figure 3.8. The shape of the F_H-curves is mainly a decreasing probability for increasing exceedance levels. Despite the slight angularity which is caused by the limited number of MC samples with minor effect on the risks, the curves are more or less smooth. Having the same dike dimensions, all construction types face a different probability of failure (intersection with y-axis). The sand dikes (blue, 3 types) are all above the equivalent clay dikes. All surfaces below the curves differ, indicating the differences in risk between the construction types and accordingly their ductility and structural robustness.

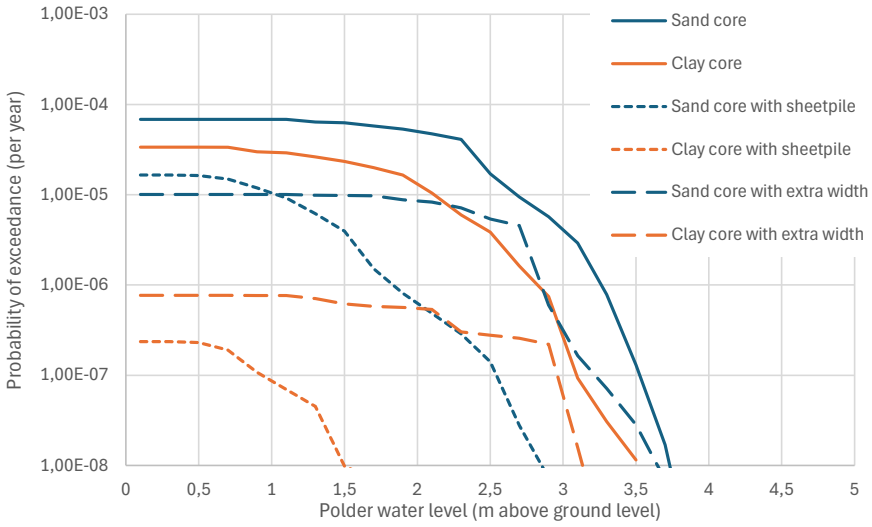

Figure 3.9.: *Examples of a series of probabilities of exceedance of polder water level H, for different construction types. Crest height = 12.2 m+NAP, Berm width = 10m, Berm height = 0.75m, inner slope 1:2.5.*

The curves for the sand core with sheetpile (short-dashed) and the sand dike with extra width (dashed) are interesting. Firstly, they intersects on a lower probability with the y-axis than the original sand dike (solid line), indicating the sheetpile and extra width prevents piping, which decrease the dikes' failure probability significantly. Secondly, the decrease of the curve starts at lower polder water level, than the original sand dike. Since overtopping causes dike breach, it appears the time needed to erode the revetment and the crest is longer than the development of a pipe, leaving less time to cause a large flood volume. Third, the dike with the core with sheetpile has a larger probability of failure than the dike with extra width, but due to the sheet pile the curve start decreasing at lower polder water levels, indicated by the crossing curves at a polder water depth of 1 m. The sheetpile reduces the flood volume significantly more than the width dike. The surface between the F_H-curves for the sand dike with sheetpile and the sand dike reflect the difference in risks: a sheetpile in the dike is a measure to increase the ductility of the dike and thus its structural robustness.

The results for numerous CDCs (construction-dimension-combinations) are calculated. In Figure 3.10 the results for different CDC's for construction type 'dike with sand core' are presented. A triple of dots in red, blue

and green represents one CDC, referring to respectively its risk, investment cost, and total economic cost, on the y-axis, and its corresponding individual risk on the x-axis. The red dots representing the economic and societal risks do not scatter, because of their common source in the F_H-curve: following equation (3.12) there is a fixed relation between them $c_{D_{Ec}}/c_{D_{nv}}$.

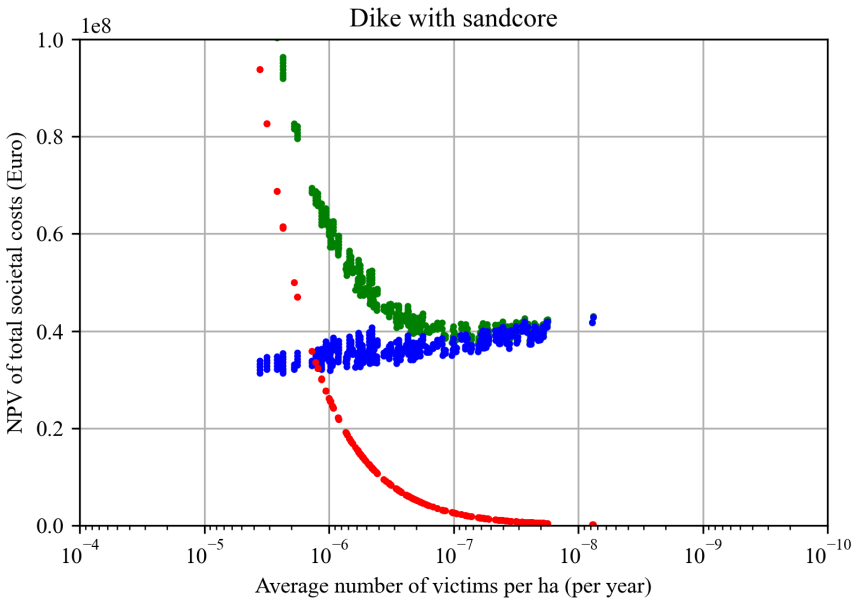

Figure 3.10.: *Results for a matrix of dike dimensions, as input for heuristic optimization*

Figure 3.11 shows the bottom of the envelop of the total societal costs of all CDCs, together with the corresponding risks and investments. It shows clearly the similarity with well-known economic optimization practices [51]. However, the x-axis does not contain a singular physical decision parameter. The neighbours of a CDC-dot with a certain position on the x-axis may be the result of a rather different combination of dike dimensions. Because of the discontinue multi-dimensional matrix of calculations the envelop does not look that fluently in the high societal risk-zone. However, the low societal risk-zone is in this case more important for the determination of the optimum.

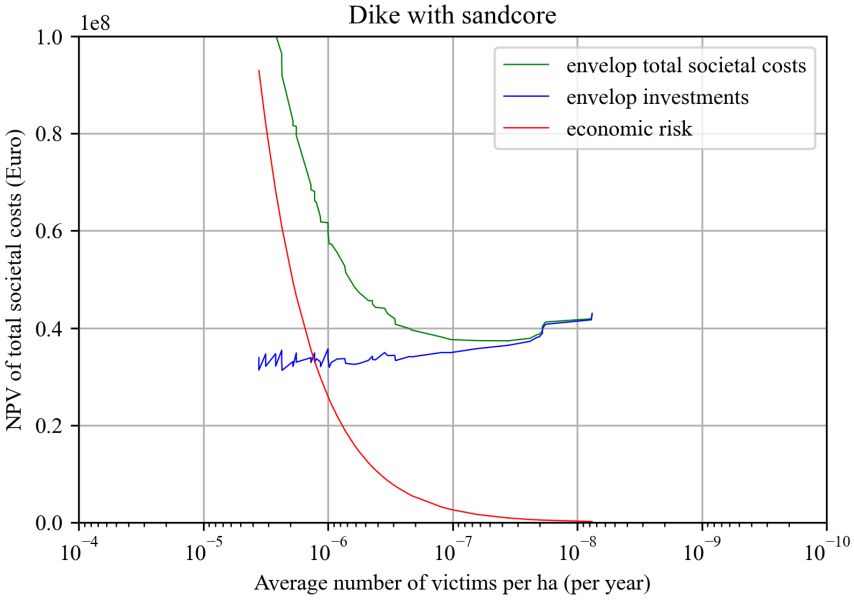

Figure 3.11.: *Bottom of envelop of societal costs, and corresponding investments and risk.*

Figures 3.12 and 3.13 show only the envelop of the total societal cost for all construction types. Figure 3.12 shows the results for design options with the existing clay dike as a starting point. The cost-optimal measure given a construction type, is the CDC with minimal societal costs on a curve. For each construction type these are given in Table 3.2. For some of the curves the optimum is the left edge of the curve. Just the change from the existing construction type to e.g. a dike with extra crest width will lead to minimal costs for that construction type. Enlarging one of the dike dimensions will increase societal costs. The overall cost-optimal measure is the CDC with the lowest societal costs over all curves. NB. For some curves the edges are shaped vertical, such as the right end of the curve for the dike with sheetpile, which is caused by the limited size of the matrix with dimensions calculated.

Figure 3.13 shows the results for design options with a semi-existing dike with a sand core as a starting point. The cost-optimal measures are given in Table 3.3 for each construction type. In this case the option for widening the crest becomes more competitive as well. In all cases a change of core material is far too expensive.

The existing dike at the case location is a dike with a clay core, which is in this case the type resulting in lowest net present value. However, the reduction of the individual risk on victims may be a reason to change

construction type, regardless of the extra costs. In this case the construction type with a sheetpile (in dotted-red) reduce the individual risk by a factor of about 50, requiring only a rather small budget extra.

Table 3.2.: *Results of design calculations for existing clay dike at case location, with polder level 7.25 m+NAP.*

Construction type (see Figure 3.8)	**dike height** (m+NAP)	**inner slope** (-)	**berm width** (m)	**berm height** (m+polder gr. level)	**Soc. costs (total/I/ER)** (M€, NPV)	**Indiv.risk (vict./ha)** ($\cdot 10^{-5}/yr$)	**prob.dike failure** ($\cdot 10^{-5}/yr$)
Sand core (a)	12.50	2.50	18	0.75	37.4 / 36.4 / 0.9	0.0036	0.11
Clay core (d)	12.20	2.50	18	0.75	9.6 / 8.5 / 1.1	0.0041	0.16
Sand core with sheetpile (c)	12.30	2.50	0	0	46.1 / 44.5 / 1.5	0.0059	0.42
Clay core with sheetpile (f)	12.20	2.50	0	0	15.6 / 15.5 / 0.1	0.0004	0.03
Sand core with extra width (b)	12.40	2.75	6	0.50	46.9 / 45.4 / 1.5	0.0058	0.19
Clay core with extra width (e)	12.20	2.50	9	0.25	19.8 / 18.7 / 1.2	0.0046	0.18

Table 3.3.: *Results of design calculations for semi-existing sand dike at case location, with polder level 7.25 m+NAP.*

Construction type (see Figure 3.8)	**dike height** (m+NAP)	**inner slope** (-)	**berm width** (m)	**berm height** (m+polder gr. level)	**Soc. costs (total/I/ER)** (M€, NPV)	**Indiv.risk (vict./ha)** ($\cdot 10^{-5}/yr$)	**prob.dike failure** ($\cdot 10^{-5}/yr$)
Sand core (a)	12.50	2.75	15	0.50	15.0 / 13.3 / 1.7	0.0064	0.20
Clay core (d)	12.20	2.50	18	0.75	41.1 / 1.1 / 40.1	0.0041	0.16
Sand core with sheetpile (c)	12.20	2.75	0	0	20.6 / 16.2 / 4.3	0.0167	1.10
Clay core with sheetpile (f)	12.20	2.50	0	0	47.2 / 47.1 / 0.1	0.0004	0.03
Sand core with extra width (b)	12.20	3.50	0	0	22.4 / 15.0 / 7.5	0.0287	1.06
Clay core with extra width (e)	12.20	2.50	9	0.25	51.3 / 50.2 / 1.2	0.0046	0.18

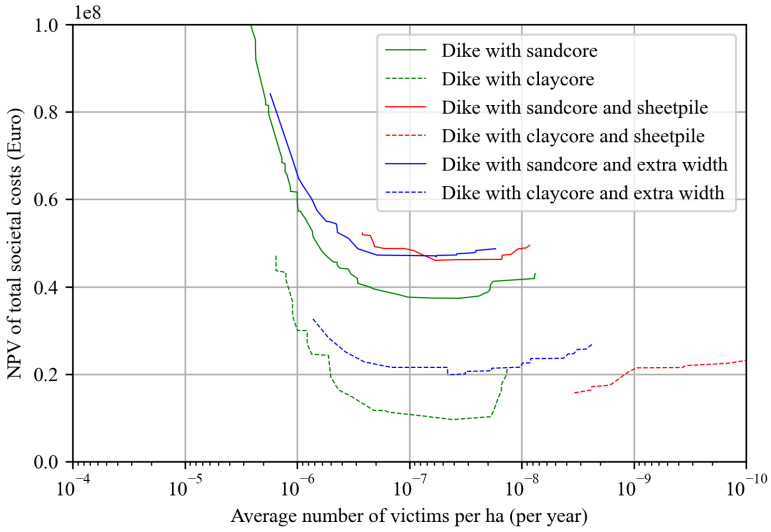

Figure 3.12.: *Envelops of societal costs for the different dike construction types from Figure 3.8 for existent clay dike*

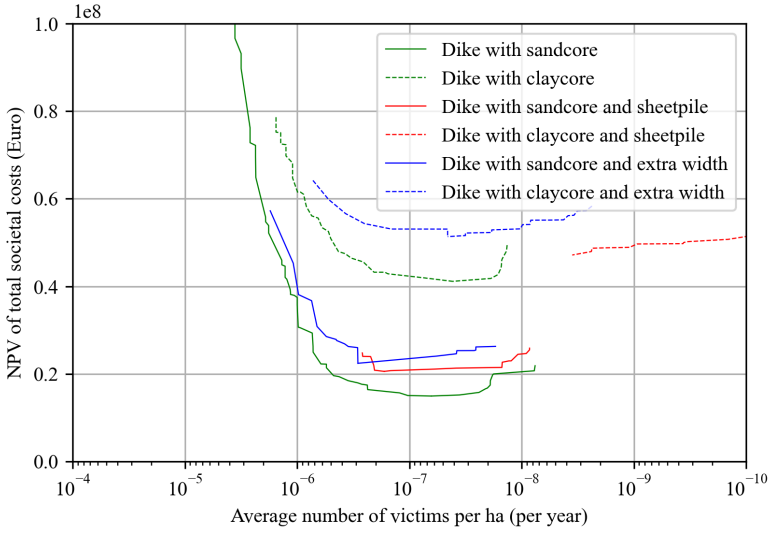

Figure 3.13.: *Envelops of societal costs for the different dike construction types from Figure 3.8 for semi-existent sand dike*

3.5. DISCUSSION

The objective of this chapter is to enable the evaluation and comparison of the risk reduction potential of dike construction types, as a fourth measure next to lower loads, increase dike dimensions and reduce vulnerability in the flood prone area behind the dike.

This chapter demonstrates the possibility to perform an analysis providing insight in the relation between dike construction types, dike dimensions, societal costs and societal risks. To value different construction types with respect to their effect on consequences of flooding, the whole chain from loads, strength, dike breach, flooding and consequences is modelled time dependent. In this concept, the widely used practical cut between calculations of dike failure and consequences [37, 96] is not needed. Still, the decision framework presented in section 2.4.1 is applicable. In the following some benefits of this approach will be discussed, its limitations, and some recommendations.

First, this integrated modelling enables the use of the risk concept in [32] and [63] in a basic way, using the number of MC-samples as the flooding scenarios, which are directly used to take into account uncertainties in loads, strength and consequences. Although failure of the dike is of major impact on a flooding, the physical processes are treated in the same way as other physical processes such as hydraulic modelling of the river, it has no preferred position in the set-up of the risk calculation. This approach prevents the introduction of assumptions to assess the time dependent boundary conditions for flooding scenarios. Furthermore, in the approach used in this chapter the mechanisms determining dike stability (in most literature referred to as failure mechanisms) develop parallel to each other. The benefit is that no compilation has to be made of failure probabilities per failure mechanism, preventing assessment of their correlations due to correlated loads and dike material.

Second, an effect of the practical cut between dike failure and consequences is it enables standardization of dike failure probabilities, as formalized in e.g. the Netherlands. Although not formalized, standards in terms of probabilities related to dike failure are common practice in many flood risk studies in Deltas worldwide, using them as a starting point for dike design. However, since the objective of a designer is to deliver a most efficient design compliant with these standards, a design with a construction type deviating from the one used for standardisation, this is per definition sub-optimal. Due to the practical simplifications to assess dike failure and flooding separately, and this sub-optimalisation, this common practice will not per definition comply to the most efficient risk reduction. Due to the practical cut between probability of dike failure and consequences, a brittle dike is often valued just as good as a ductile dike. This chapter shows an approach on how to value dikes on its risk reduction capacity, due to its degree of ductility, leading to more

opportunities for structural robust design interventions.

Third, each model requires simplifications of reality, such as to cut parts of the physical processes, to simplify modelling of physical relations, to make choices to simplify the process in time, or to calculate probabilities. However, the approach in this chapter does not require simplifications due to the approach itself. The simplifications in this proof of concept can be extended, having only effect on calculation time. The approach in this chapter aims to hand over opportunities to choose simplifications based on their effect on dike dimensions, combined with practical applicability and accuracy.

Fourth, with this approach, some techniques or practices are no longer needed, reducing the number of design choices. For example techniques used to explicitly calculate or assess the dike failure probability, such as a fault tree analysis to combine different dike failure mechanisms, or to explicitly choose representative flooding scenarios to calculate the risk.

A limitation is the application on only one case location situated in a riverine area, using a limited number of dike failure mechanisms. Consequently, only one dike breach location is used. In theory, along a dike segment more breaches could occur (NB. In a riverine area this is unlikely due to the water level effect as a result of breaching which decreases the loads downstream of a breach, see Figure 3.3 upper part). The concept can be extended to a series of dike locations. In equation 3.8 the part between brackets, representing the F_H-curve, has to be evaluated for all dike sections in a dike segment searching for its maximum, and in $\bar{X}$ the independent variables per dike section should be added.

A second limitation is the 0-D representation of the flood simulation and the analytical coupled consequences in (3.4). Especially when the dike section would be expanded to a gradually descending dike segment enabling more breaches along the river, this representation should be changed in the real bathymetry of the polder and a flood simulation model should be used.

Only the flood waves during winter periods are taken into account in this chapter. Despite this is no conceptual limitation, the extreme discharges along the Meuse river in July 2021 showed this starting point needs to be re-evaluated.

3.6. CONCLUSIONS

In this chapter a novel assessment method is presented for evaluating the risk reduction potential of dike construction types. Next to reduction of loads, increase of strength, both reducing the probability of failure, and reduction of consequences of dike failure, this opens the route for a fourth category of risk reduction measures: structural robust dike de-

sign. It is showed that the risk profile of different construction types may differ significantly. Next to the method and its application on a case, a graphical representation is presented to compare designs based different construction types.

An important novel element included in the approach is the absence of the need to explicitly calculate the dike failure probability to assess the flood risk. The risk is assessed by integration of the probability of flood levels at a location in the polder and the consequences of that flood levels, the F_H curve. Assessment of those flood levels is accommodated by an integrated and time dependent modelling of the whole process of loads by the water system, strength- and erosion development of the dike, breaching, and flooding in the physical domain. Due to the integrated approach a sub-optimal application of the risk approach can be prevented. As a side result this provides a novel insight of the simultaneously propagation of the development of the failure mechanisms in time, including possible interactions. In the Grebbe case, this approach led to significantly different risk profiles in case the polder is protected by a brittle or a ductile dike.

The main conclusion of this chapter is that an integrated risk assessment, based on a time dependent physical model, provides the insight in the difference in risks between brittle and ductile dikes, enabling the trade-offs of dike designs and corresponding risks and investments.

The implementation of the approach shows a simple understandable result: a set of dike constructions and dike dimensions leads to corresponding flood level-probability curves, which are the base for the corresponding economic and individual risk. The presented graphical connection between the societal costs and the individual risks provides a powerful insight to enable trade-offs between construction types.

The method is implemented for a riverine water system. For the implementation in a proof of concept, some simplifications are made to be able to perform a case study to show the analysis and results of the method. The main simplifications, such as the implementation of only two dike failure mechanisms, and the use of a 0-D flood model, are easily extendible. However, enhancements of optimization routines and calculation power need to be considered.

This conclusion is interpreted as that evaluation of structural robustness should be standard in dike design. This further matures the flood risk approach, leading to well-considered designs, with a ductility dependent on the potential consequences. Fully implemented, with ductile dikes at high-risk locations, the consequences could be mainly economic damage, simplifying the trade-offs. Therefore, further steps are recommended to develop the method for other than riverine systems, and to operationalize the method for application in Flood Protection Programs.

4

SYSTEM MEASURES PLANNING

What can it profit, that sciences and practices, that commerce and freedom flourish, yes even that we enjoy the most pleasant peace through a wise management of the country's government, as long as year after year we are threatened to lose all the fruitful consequences of these benefits through the unbridled violence of the inland waters?

Christiaan Brunings, Inspector-General of Dutch rivers and first head of the *Bureau voor Waterstaat*, the predecessor of *Rijkswaterstaat*, could hardly understand that the wrong priorities were being set, because a region as developed and prosperous as Holland should give high priority to the river problems (end of 18th century).

A system of dikes in flood-prone areas continuously requires measures to mitigate changes such as ageing and climate change. Planning costly measures requires proper insight into system risk effects. Tactical plans define the planning of consecutive measures to implement a flood risk reduction strategy, which may take decades. They may differ due to choices such as a prioritisation metric, planning conditions and budget. A method is developed to compare different tactics to prioritize and plan measures in interdependent systems of dikes to reduce risks most effectively and efficiently. A case study meant as a proof of concept is carried out for the reinforcement of about 500 km of dikes along the Rhine River branches in the Netherlands. The effects of 12 different tactical plans on the aggregated risks over time have been studied. The economic risks differ by up to about 40%, and the risks on victims differ by up to 70%, which underpins that tactical planning and corresponding decisions are important for reduction of time-aggregated flood risks.

The majority of this chapter has been published in F. den Heijer and M. Kok. "Risk-based portfolio planning of dike reinforcements". In: Reliability Engineering & System Safety 242 (Feb. 2024), p. 109737. issn: 0951-8320. doi: 10.1016/J.RESS.2023.109737

4.1. INTRODUCTION

Deltaic areas are often protected against flooding by defence systems of dikes, dunes and hydraulic structures near the sea, and more upstream along rivers mostly by systems of dikes. Flood defences are ageing, due to subsidence or deterioration of revetment material. As well, the performance of flood defences decreases due to the increase of loads caused by climate change. Therefore, as long as the area has to be protected against flooding, interventions are required in the flood defence system to mitigate increasing risks.

Management of large portfolios of dikes consists of several decision levels [23, 24, 106], based on the ISO 55000 series. Operational management contains aspects such as regular inspections, maintenance and reinforcements [55], in the taxonomy of maintenance strategies described by [107] referred to as condition-based or predictive maintenance. Strategic management contains aspects such as how to prepare for uncertain climate change, and development of safety standards and long-term spatial developments [6, 13, 51]. Tactic management connects the strategic and operational management [23], containing aspects such as prioritisation and planning of reinforcements in the system. The planning of reinforcements and other interventions takes place within the boundaries given by the flood risk strategy. Following the terminology in [23] and [19] 'tactical' asset management is used in this thesis to prevent confusion with strategic asset management. When a strategy is a plan in outline to achieve a goal, a tactic is a way to implement the strategy to achieve that goal.

The main objective of proper asset management is to balance risks, performance and cost over time, to align asset-related spending to institutional goals [19, 22, 108]. A dike system is not in balance in case of sudden changes such as the adoption of more stringent safety standards or new knowledge. Dike reinforcements may be required in the whole system to become compliant. This is also the case when new climate projections, or new spatial development goals are adopted. The corresponding efforts are large relative to planning issues for a system in balance. Since budgets, outsourcing and contractors' execution capacity are limited, it will take time to become compliant and restore a balanced system. In Figure 4.1 this is schematically presented. The portfolio risk is defined as the total risk in the system, and the risk deficit as the surface between the actual portfolio risk in time and the compliant risk level, which is the portfolio risk in case all dikes in the system are exactly compliant. The larger the risk deficit relative to executing capacity, the longer the period the system does not satisfy the pursued compliant risk level.

A tactical plan leads to a programme of interventions in a portfolio. Different tactical plans lead to different intervention schemes. In Figure 4.2 a programme is schematically presented. It propagates in time,

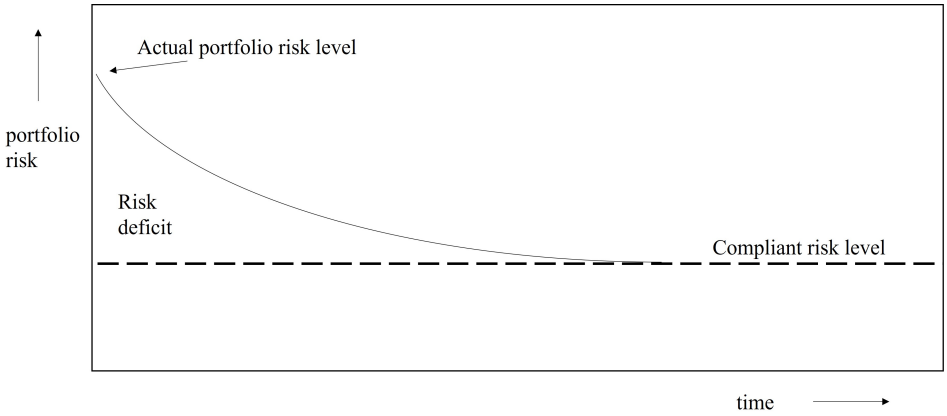

Figure 4.1.: *Schematic representation of actual portfolio risk level and risk deficit in time in case measures are effective.*

changing each timeframe due to realisation, new, postponed or withdrawn projects.

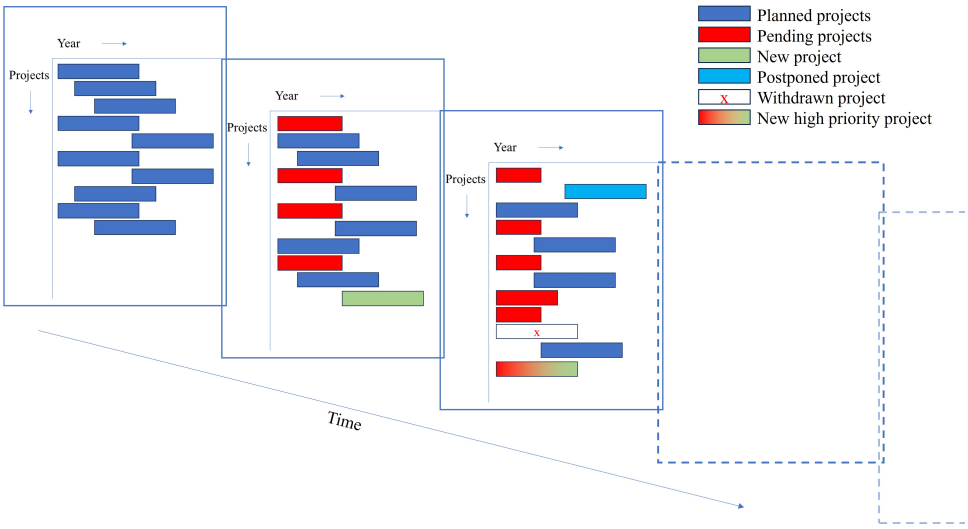

Figure 4.2.: *Schematic representation of a programme window with projects (vertical axis) and planning (horizontal axis) propagating in time.*

Especially in a riverine dike system, the risk contributions of individual assets to the flood risk in the system are not independent [42, 109]. Reinforcement of a dike upstream increases the risks downstream. In the classification of infrastructure interdependencies in [110] a riverine

dike system could be best described as episodic (dependency only during floods and dike breaches). Thus, a dike reinforcement upstream reducing a small risk, may even increase the total system risk. Therefore, the relation between the individual asset risk contributions and system risks is very non-linear. This specifically leads to continuous changing contributions of individual assets risks to system risks, depending on the measures executed in time and space.

Therefore, to reduce system risks in time the order and planning of reinforcements matters. In this chapter a method is presented to compare the aggregated risks over time of tactical plans to prioritize and plan compliance measures, and an application for a portfolio of dikes in a riverine system. The novel contribution to literature is the physiscs-based dependence-modeling for the tactical intervention management over time. To focus on the effect of tactical asset management decisions, this study is based on a single flood risk strategy to pursue compliance with standards by dike reinforcements.

Consecutively is presented the theoretical background of planning flood risk systems, the development of a risk-based method for prioritisation and planning of a system of dikes and the metrics to enable comparison, and a case study meant as a proof of concept, which is carried out for the dikes along the Rhine River branches which is planned to last for decades. The chapter closes with the discussion and conclusions.

4.2. LITERATURE OVERVIEW

Meteo and water systems cause loads along large flood defences systems, and consequences could affect a large area. Derivation of maintenance policies for a portfolio of degrading assets under climate change with budget constraints, needs thorough system analyses [38, 44, 111].

Quantitative risk-based system approaches have been widely adopted in the practice of flood defence management. In [14] an optimal flood defence system safety level is derived for a large polder in the Netherlands based on the economic risk. Based hereon the Dutch safety standards have been established [50] for other polders, also referred to as the criteria determining soft failure [111]. The present Dutch safety standards were re-established in 2017 based on an enhanced economic [52, 67] and technical approach [51], based on probabilities of failure for dike overtopping. An extensive risk analysis has been performed taking all failure mechanisms into account [33]. In [66] and [112] the source-pathway-receptor framework is proposed to systematically assess risks. In [41] a conceptual approach is developed and applied to quantify the effects of river system behaviour on probabilities of dike breach and flood risk, for a reduced set of failure mechanisms, concluding that for proper flood risk assessment all relevant dike failure mechanisms, uncertainties as well as all proposed safety improvement measures are to be jointly

taken into account. Vorogushyn [113] developed and applied probabilistic flood hazard maps, taking dike breaches in a river branch into account, and considering three failure mechanisms. Domeneghetti [114] improved the approach adding the effect of uncertain boundary conditions. Bachmann [115] developed a risk-based model for decision support on measures on the scale of a catchment area. Bachmann [116] took into account the effect of dike breaches in the system and [117] improved the hydrological modelling of dependencies in the river branches and cascade effects of polders. The presented system risk analyses all refer to the actual status of the flood defences to consider the risks and effects of potential measures.

In [23] the poor interconnection between strategic and operational flood defence asset management is addressed, emphasizing the need to streng-then the interconnecting tactical handshake to better factor deterioration into planning. In [42] a time-dependent economic flood risk optimization is performed to determine the optimal development of safety standards in the long term in a small interdependent river system, however, without planning constraints such as budget. Klerk et al. [45] elaborated on the cost-optimal prioritisation of interventions for reinforcement of non-homogeneous segments of dikes. They showed the considerable effect of intervention tactics on Life Cycle Costs (LCC). However, they focused on prioritisation, simplified the risk analysis and did not study the planning of measures in time.

Prioritisation and planning of costly measures in large infrastructure systems requires proper insight in system risk effects [118]. It requires to look forward to uncertain circumstances at the design horizon. Buijs et al. [119] performed time-dependent reliability analysis for flood defences in the Thames estuary and [120] did so for corrosion analyses of quay walls. Mens [121] researched the system robustness of one of the branches of the Rhine River, comparing system risks for different strategies. Haasnoot [43] developed a qualitative approach for decision-making under deep uncertainty called ‘Dynamic Adaptive Policy Pathways’ (DAPP). They introduced the opportunity to consider different perspectives to choose a robust strategy. Manocha [122] and Toimil [123] added quantitative elements to DAPP for the management of storm water infrastructure and coastal erosion. The DAPP approach does not provide intervention planning, and requires discrete chosen scenarios and strategies.

In research on related water infrastructure, the tactical interconnection based on time-dependent risk analyses is increasingly addressed to prioritize measures. Young and Hall [124] performed a systems perspective on investments in the Thames Estuary region, including infrastructure asset interactions. Smet [47] developed a proactive planning approach for water resource infrastructure investments taking into account uncertain external drivers like climate change as well as uncertain structure-

specific drivers like deterioration. Van den Boomen [125] focused on the optimal timing of replacements of public infrastructures with respect to life cycle costs, taking price uncertainty into account. Both focus on individual and independent hydraulic structures rather than systems of assets. Yang and Frangopol [46] developed a robust risk-based single-objective optimisation approach to portfolio management under deep uncertainties, for a set of individual and independent assets like bridges. The method uses proxies for loads, climate change and deterioration in time and allows one intervention per asset. Fluixá-Sanmartín et al. [126] propose an approach for dam risk management in the long term that considers the time-dependent evolution of risk, ranking the priority of present measures to optimally reduce dam risks. Liu et al. [118] presents a probabilistic measure for the potential risk of regional roads exposed to landslides, providing guidance for spatial and hierarchical risk management.

Systems with many components in different states are elaborated extensively with mathematical models, e.g. in [127, 128], e.g. using fault tree analysis, failure mode analysis, bow-tie analysis, and Markov models. In these approaches it is important to find solutions reducing the explosive number of samples in reliability analyses. Model-based approaches gain increasing attention [129]. Especially when cascading effects may occur [130], or in case of integrated reliability analysis, remaining useful life analyses and maintenance actions [131], the model based approaches support reducing the explosive number of combinations of state and space [132].

To summarise, much work has been done on flood risk analysis, system analysis, strategies for the long term, adaptive strategies to cope with climate change, and prioritisation. The modeling of the systems is increasingly improved with respect to scale, failure mechanisms, and mathematic-computational methods. Prioritisation of interventions is done more and more risk-based. However, no work has been found on time-dependent risk-based medium-term planning of interventions in an interdependent, deteriorating system of dikes under climate change. This figures out a clear knowledge gap for flood risk analyses: how to plan interventions in time in a changing system, in which the performance of assets affects the performance of other assets in the same system, as is the case for a system of dikes in a riverine area. In this chapter, as especially the physical system dependency affects flood risks, a physical-model-based approach is used to assess space-dependency applied in an integrated system risk analysis and reinforcement planning approach.

4.3. METHODOLOGY

In [46] the portfolio risk is given as the sum of all risks per asset per year, which assets are independent of the performance of others:

$$R_p(t_L) = \sum_{i=1}^{t_L} \sum_{k=1}^{K} R(k,i) = \sum_{i=1}^{t_L} \sum_{k=1}^{K} P_k(i) \cdot D_k(i) \tag{4.1}$$

In which:

$R_p(t_L)$	Portfolio risk from present to year t_L	*€/year, victims/year*
i	Indicator of year	-
t_L	Time horizon of interest	year
k	Indicator of asset, in this study dike section	-
K	Number of assets in the portfolio	-
$R(k,i)$	Risk for asset k in year i	*€/year, victims/year*
$P_k(i)$	Probability of failure of asset k in year i	per year
$D_k(i)$	Consequences due to failure of asset k in year i	*€/year, victims/year*

In this thesis, the objective is to enable an analysis of portfolio risks in time for a system of dikes. The system state is given by $P_k(i)$: the probabilities of failure of the dikes in the system in year i. Since the system state changes due to interventions, the risks $R(k,i)$ of dike breach at dike section k in year i are intertwined with the interventions on other dike sections in the system. Therefore, the methodology consists of two main steps that are followed over a period of time: the determination of portfolio risks in a year given a system state, and the determination of interventions in the system state given the compliance requirements (e.g. safety standard) and given planning constraints, see Figure 4.3. In the following subsections is firstly elaborated on a system consisting of a single dike section, secondly to expand to a system of dike sections, and thirdly to determine the interventions based on system states.

4.3.1. A SINGLE DIKE IN THE SYSTEM

The risk for a single dike section k in year i is the probability of failure multiplied by consequences $P_{f_k}(i) \cdot D_k(i)$. Herein, the water level is the dominant load for both the probability of failure and consequences. The probability of failure for dike section k in year i is assessed by integration of the probability density function (pdf) of water level and a fragility

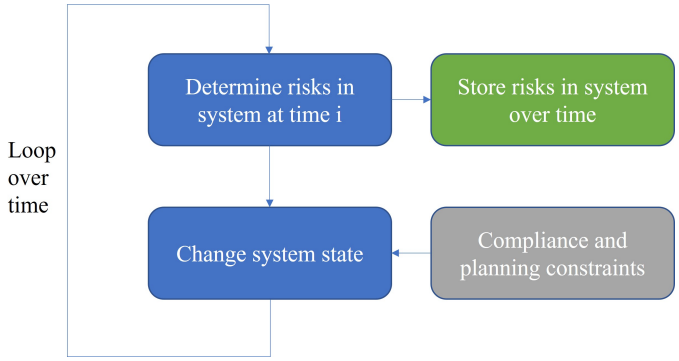

Figure 4.3.: *Schematic overview of methodology to assess the sum of risks over time.*

curve, see Figure 4.4, as increasingly used in flood risk assessments since the '90s as shown by [133]:

$$P_{f_k}(i) = \int_{h_k(i)} f(h_k(i)) \cdot p_{f|h_k}(i)\, dh \tag{4.2}$$

In which:

$P_{f_k}(i)$	Probability of flooding for dike section k in year i	per year
$f(h_k(i))$	Probability density function of water level $h_k(i)$ along dike section k in year i	per year
$h_k(i)$	Water level along dike section k in year i with respect to reference level SWL (Sea Water Level)	$m+SWL$
$p_{f\|h_k}(i)$	Conditional probability of failure of dike section k during a flood wave with water level $h_k(i)$ in year i	–

The fragility curves reflect the strength of a dike section, expressed as a curve of conditional probabilities of dike failure for given water levels. Thoroughly derived, this curve includes not only the strength of a dike section, but also secondary loads such as wave impacts. An advantage of fragility curves is they can be precalculated based on knowledge and detailed models, and are practical to use in probabilistic models [134, 135]. This also enables operational flood risk management during flood waves, supporting decision making in situations under time pressure [136, 137], as policy analysis and planning decisions [138]. For planning issues as addressed in this chapter, the fragility curve is time-dependent

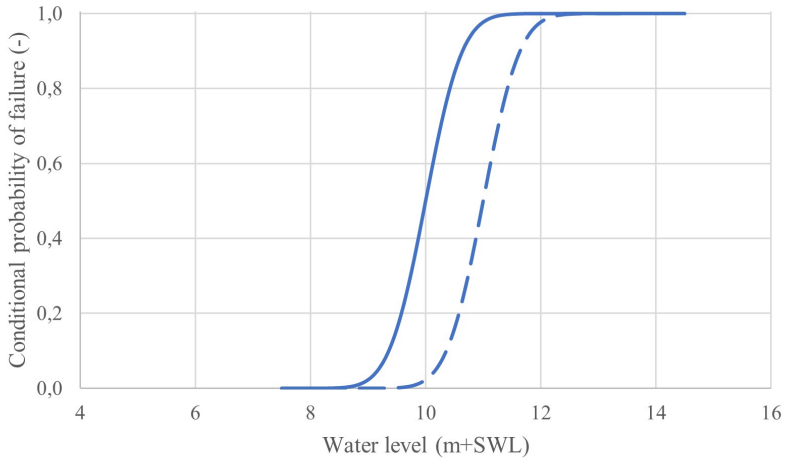

Figure 4.4.: *Example of a fragility curve, here simplified as a normal distribution with a mean of 10m+SWL and a standard deviation of 0.5m (solid line) and a curve representing a dike heightening of 1m (dashed line).*

because of subsidence, and subsequently, the pdf of water level is time-dependent due to climate change. Deterioration due to subsidence is modelled as a shift of the entire fragility curve, in Figure 4.4 to the left, gradually in time. Reinforcements are modelled as a sudden shift of the entire fragility curve, in Figure 4.4 to the right. In fact, herewith only the measure of dike heightening is considered. Thus, the mean value of the fragility curve for dike section k in year t_L is:

$$\mu_{frag_k}(t_L) = \mu_{frag_k}(0) - s_k \cdot t_L + \sum_{i=0}^{i=t_L} \Delta h_k(i) \tag{4.3}$$

In which:

$\mu_{frag_k}(i)$	Mean value of the fragility curve for dike section k in the system in year i	m+SWL
$\mu_{frag_k}(0)$	Mean value or 50% percentile of the fragility curve for dike section k at the start of the analysis, year $i = 0$	m+SWL
s_k	Yearly subsidence of dike section k	m/year
$\Delta h_k(i)$	Increase of mean value of fragility curve due to reinforcement of dike section k in year i	m

In practice, the planning process starts after detailed reliability analysis, delivering the components of equation (4.2): the probability of failure $P_{f_k}(0)$ at the start year of the analysis, the pdf of water level $f(h_k(0))$ and the shape of the fragility curve $p_{f|h_k}(0)$. With these components, $\mu_{frag_k}(0)$ is known.

The interventions $\vartriangle\ h_k(i)$ in time are based on the assessed performances over time. In case the probability in year i rises above the standard and other constraints such as budget are fulfilled a dike reinforcement $\vartriangle\ h_k(i)$ is performed. This reinforcement has to be compliant until the design horizon $i + T_{plan}$. Since exactly one reinforcement is planned between year i and year $i + T_{plan}$ this reinforcement can be designed based on the difference of equation (4.3) between year $i + T_{plan}$ and i:

$$\vartriangle\ h_k(i) = s_k \cdot T_{plan} + \left(\mu_{frag_k}(i + T_{plan}) - \mu_{frag_k}(i)\right) \tag{4.4}$$

In which:

T_{plan}	Design horizon of a reinforcement	*year*

The values for $\mu_{frag_k}(i + T_{plan}))$ are derived based on equation (4.2). The probability of failure $P_{f_k}(i + T_{plan}))$ is equal to the required standard to be compliant. The pdf of water level $f(h_k(i + T_{plan}))$ is based on a climate change projection. The location $\mu_{frag_k}(i + T_{plan}))$ of the fragility curve is solved using the present shape of the fragility curve, which is a reasonable starting point for planning issues since detailed designs are in practice performed as a follow-up. Therewith, the probability of flooding for a single dike section is known in time.

The consequences of failure of a dike section in the system are based on pre-calculated consequences of floods occurring at different flood characteristics. The economic consequences per year are discounted to the present value. Victims in the future are assumed to be as important as victims nowadays, thus, the 'present value' for victims is a simple sum over the years of interest. Thus, the following equation is used for the risk for a single dike section k in year i:

$$R^{PV}(k, i) = \int_{h_k(i)} f(h_k(i)) \cdot p_{f|h_k}(i) \cdot D(h_k(i)) \cdot \exp\left(-I_d \cdot r' \cdot i\right) dh \tag{4.5}$$

In which:

$R^{PV}(k,i)$	Present value of the flood risk for a single dike section k in year i	€, *victims*
$D(h_k(i))$	Consequences due to a breach in dike section k during a flood wave with water level maximum $h_k(i)$ in year i	€, *victims*
I_d	Indicator for type of consequences (for economic consequences: 1; for victims: 0)	-
r'	Discount rate minus inflation	-

4.3.2. MULTIPLE DIKES IN THE SYSTEM

The risk assessment for a portfolio of dikes along a water system is more complex. Firstly, the loads along the dike system depend on a set of water levels, depending on system loads. In river areas these system loads are mainly river discharges. Near the sea, in estuaries and in coastal environments they depend also on tides and wind-driven storm surge. Here, these system loads are denoted by $\vec{S}$. The contribution of a single dike section to the flood risk for the entire system in year i is slightly adapted with respect to equation (4.5) to take into account the effect of system loads on local water levels:

$$R^{PV}(k,i) = \int_{\vec{S}(i)} f_{\vec{S}(i)}(h_k) \cdot p_{f|h_k}(i) \cdot D(h_k(i)) \cdot \exp\left(-I_d \cdot r' \cdot i\right) d\vec{S}(i) \qquad (4.6)$$

In which:

$\vec{S}(i)$	System loads, e.g. combination of river discharge and sea water level.	
$f_{\vec{S}(i)}(h_k)$	Probability density function of system loads in year i, causing local water levels (h_k) at dike sections k.	-

Secondly, the risks of different potential dike breaches interrelate because the water levels along the water system affect each other in case of a failure of one of the stretches. A breach upstream a river lowers the downstream water levels and thus affects both the probabilities of failure of stretches downstream and their consequences. Therefore, a simple sum of risks per individual dike stretch in equation (4.6) does not hold. In this proof of concept for planning issues, the effect of breach discharges on downstream river water levels is estimated with the spillway formula at critical flow [139, 140]:

$$Q_{breach} = C_e \cdot B \cdot \frac{2}{3}\sqrt{2g} \cdot (h_k - h_{b_k})^{1.5} \tag{4.7}$$

In which:

C_e	Spillway discharge coefficient, here assumed to be the minimal value in [139] of $1/\sqrt{3} \approx 0.58$.	–
B	Breach width.	m
h_{b_k}	Bottom level at breach location.	m

Note, with (4.7) the effect of a breach on downstream river water levels is over-estimated, because the breach volume is assessed as a suddenly occurring breach with a width B at the event water level maximum, neglecting the backwater effect of polder water levels. Note, equation (4.7) is not used for the estimation of consequences $D(h_k(i))$ since backwater effects are considered to be important for consequence estimates.

With breach effects the load distribution $f_{\vec{S}(i)}(h_k)$ is transformed in $f_{\vec{S}'(i)}(h_k)$. The risks are summed for the whole portfolio of dikes k given an individual load event $\vec{S}(i)$, taking into account the transformed water-level distributions and then is integrated over the pdf of system load events in year i:

$$R_p^{PV}(i) = \int_{\vec{S}(i)} \sum_{k=1}^{K} f_{\vec{S}'(i)}(h_k) \cdot p_{f|h_k}(i) \cdot D(h_k(i)) \cdot \exp\left(-I_d \cdot r' \cdot i\right) d\vec{S}(i) \tag{4.8}$$

In which:

$R_p^{PV}(i)$	Present value of flood risk for the entire portfolio of dikes in the system in year i	€, *victims*
$f_{\vec{S}'(i)}(h_k)$	Probability density function of system loads in year i, causing local water levels (h_k) at dike section k, taking into account the effect of breaches elsewhere in the system	-

4.3.3. INTERVENTIONS IN SYSTEM

Deliberately chosen interventions in system are based on criteria and metrics, see Section 2.4.2. With a chosen metric the possible interventions are ranked. Starting with the measure with the highest rank, the measures with lower ranks can be taken as long as the planning criterion and constraints are met. The reinforcements $\Delta h_k(i)$ are solved with equations (4.2), (4.3) and (4.4).

Therewith the discounted risks in a year in equation (4.8) can be calculated and summed over years i until t_L like in equation (4.1):

$$R_p^{PV} = \sum_{i=1}^{t_L} R_p^{PV}(i) \tag{4.9}$$

In which:

R_p^{PV}	Present value of flood risk for the entire system over the period of interest, taking into account the system effects of the entire portfolio of dikes in the system	€, *victims*

4.4. CASE STUDY MODEL

The model in section 4.3 is built and applied on a case study: the Rhine River area in the Netherlands, see the red box in Figure 4.5. For centuries, the Dutch policy has been to ensafe the country by dikes. The strategy is to standardize the dike safety level, based on risks, and to pursue compliance to that level. The standards have been set recently [82], based on risks per dike segment [51]. Furthermore, the strategy is to maintain safety levels by dike reinforcement taking into account ageing and climate change. About 1500 km of the dikes is not compliant with these standards [141]: the system is not in balance. The dutch Flood Protection Programme has been installed to reinforce dikes (in Dutch called 'HoogWaterBeschermingsProgramma', abbreviated as HWBP). The reinforcements in the Rhine River area are a major part of HWBP.

4.4.1. PHYSICAL SYSTEM

The case study area in the red box in Figure 4.5 is schematised in Figure 4.6. The named blue lines are the river branches. The polders along the branches are presented as green boxes. Each polder can be flooded via one of the potential dike breach locations.

The main loads are represented by waterlevels. The strengths of the dike sections are represented by fragility curves. The waterlevels in river branches depend mainly on the discharge of the main branch. The translation from these system loads $\vec{S}$ to local water levels is modelled by analytical relationships, which are based on available numerical simulations [72]. The local water level corresponding with the flood wave maxima is added with a model uncertainty factor:

$$\hat{h}_k = g_k(\hat{Q}_u(m_Q)) + m_h \tag{4.10}$$

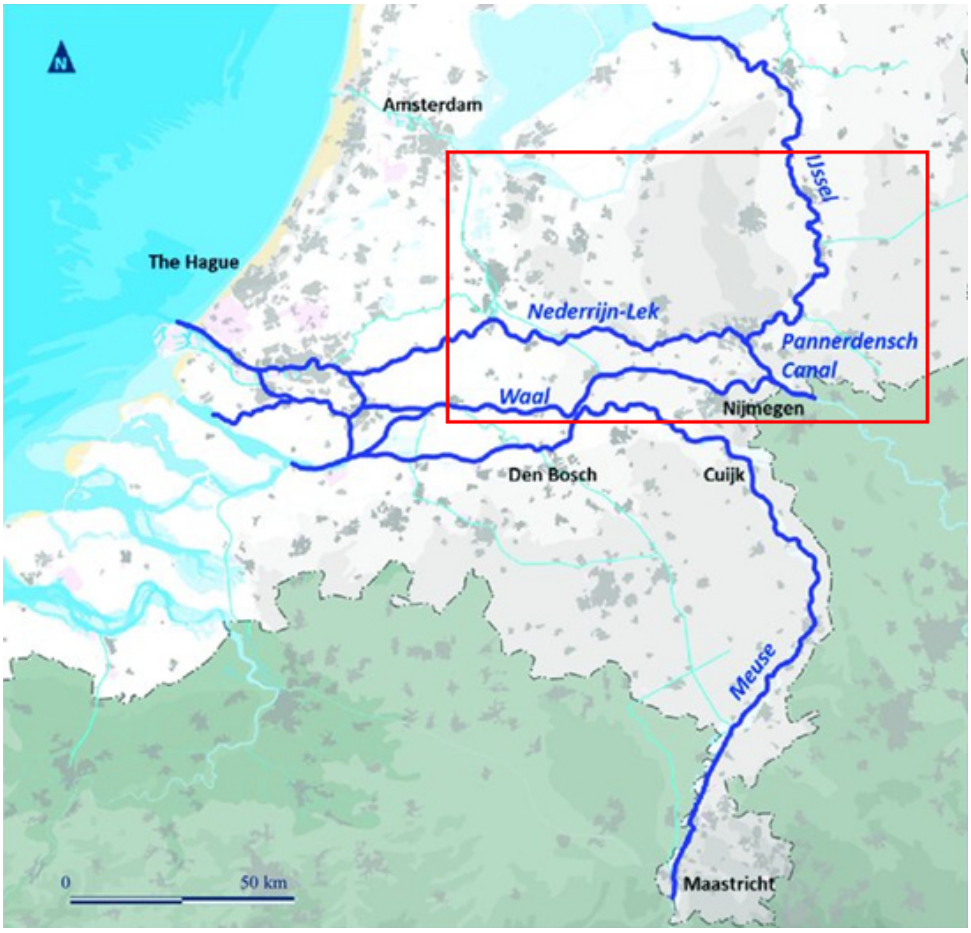

Figure 4.5.: *Overview of the study area of the Rhine and its branches (in red).*

In which:

$\hat{Q}_u$	Upstream discharge	m^3/s
$g_k(\hat{Q}_u)$	Local water level maximum at dike section k for a discharge $\hat{Q}_u$ based on [72]. These levels are given relative to the Dutch reference level NAP (in Dutch: Normaal Amsterdams Peil)	$m + NAP$
$\hat{h}_k$	Local water level maximum at dike section k during flood wave	$m + NAP$

m_h	Unbiased model uncertainty of local waterlevel	m
m_Q	Unbiased statistical uncertainty of upstream discharge	m

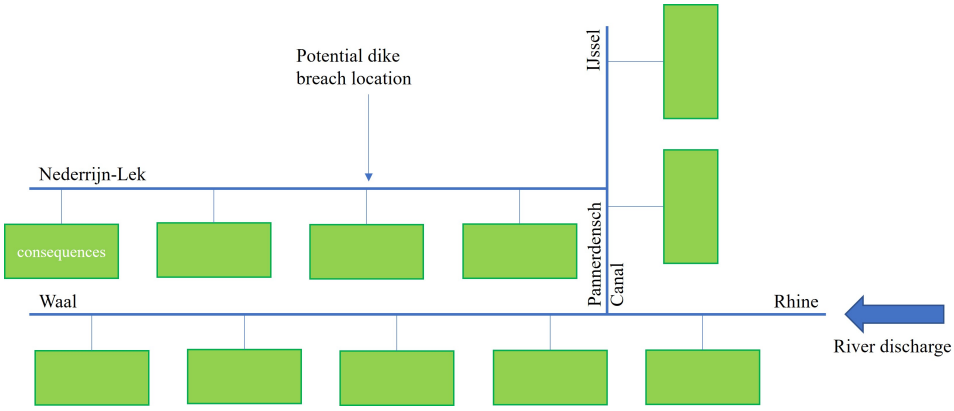

Figure 4.6.: *Overview schematisation of the Rhine, its branches, potential breach locations, and the polders in which consequences occur in case of floods.*

The consequences of failure of a dike section are based on the results of about 1800 flood calculations [54], performed until the year 2015. In the Rhine River area upstream from influence by sea water levels, calculations are available for 63 potential breach locations in 24 dike segments, see Figure 4.7. A dike segment is a length of dikes of about 25 km which is standardized in the Dutch law. A dike segment consists of different dike sections. In this study the separation between dike sections is chosen between these breach locations because for further detail no flood calculations would be available. For each location are one or more records of consequences available (damage and victims) resulting from a breach occurring at a waterlevel referred to with a return period. These return periods are assessed with the pdf based on the year 2015. Due to the effects of climate change the return period of these waterlevels will decrease for events in years after 2015.

Furthermore, the local water level is influenced by upstream disturbances due to breaches. In that case, a part of the discharge flows into an upstream polder, causing a decrease of the maximum water level downstream. The derivation of the correction for these situations is based on the law of preservation of discharge in the river branch where the breach takes place:

$$\hat{Q}_u \cdot b_Q = Q_{b,downs} + Q_{breach} \tag{4.11}$$

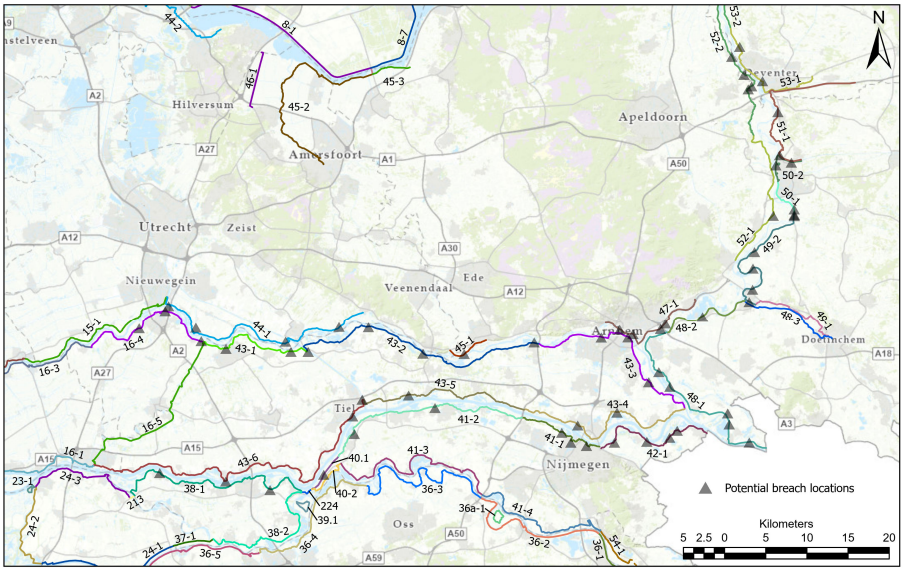

Figure 4.7.: *Segments (colored and numbered lines) and breach locations (grey triangles) in the study area.*

In which:

Q_{breach}	Breach discharge into the polder, see equation (4.7).	m^3/s
b_Q	Fraction of discharge Q_u flowing into branch b.	-
$Q_{b,downs}$	Discharge downstream of a breach in branch b.	m^3/s

The downstream water level h_k at breach location k is determined with the analytical relations in [72] for which numerous numerical SOBEK calculations have been carried out, based on the upstream Rhine discharge. In equation (4.11) the local waterlevel h_k is the only unknown in both $Q_{b,downs}$ and Q_{breach}, which can be iteratively determined. Note, a breach in one of the branches is assumed to not affect the discharge in the other branches, which assumption neglects the more complex effects near bifurcation points.

A typical result for the waterlevel along a river branch is presented in

Figure 4.8. The blue line is the undisturbed water level, representing the situation without dike breaches. The dots on this line represent the potential dike breach locations on both sides of the river branch. The orange dots represent a Monte Carlo draw from the fragility curves, which characterise dike strength for that specific draw. The draws at each potential dike breach location along the river branch are independent and its course therefore looks random. The flood wave, propagating from upstream, first exceeds at km 887.5 an orange dot (strength). There a dike breach occurs, affecting the downstream water levels, represented by the grey line. Further downstream, between kilometers 910 and 920, two orange dots are below the undisturbed water level again, but no second breach occurs, because these dots are above the disturbed waterlevel. Would one of them have been drawn below the disturbed water level, a second breach would have occurred. In that case the process to find the downstream discharge and the water level at the breach with equations (4.7) and (4.11) is carried out again. In this way, each drawn event is processed from upstream to downstream to find the accompanying breaches and water levels in the system.

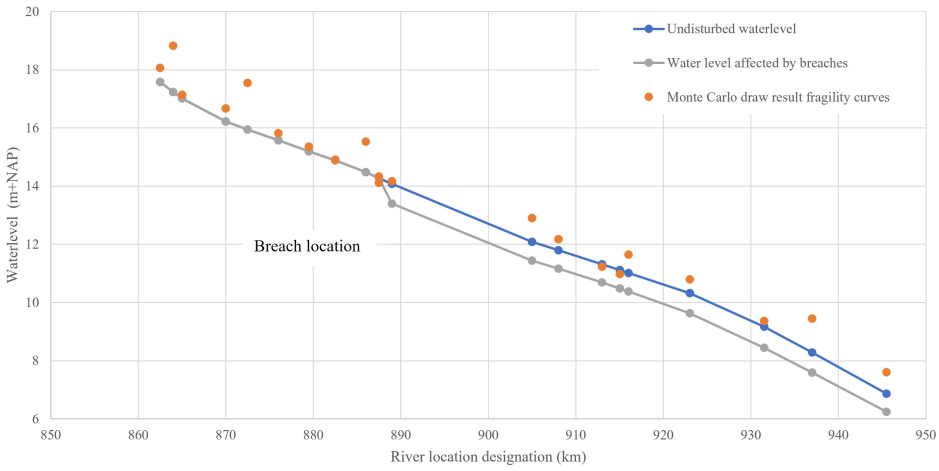

Figure 4.8.: *Typical course of water level along the branch Rhine-Waal (see Figures 4.5 and 4.6).*

4.4.2. PROBABILISTIC MODEL

RISKS PER YEAR

The stochastic load variables are the yearly maximum river discharge ($\hat{Q}_u$), the statistical uncertainty of its distribution (m_Q) and the model uncertainty (m_h). The stochastic strength variables are the fragility curves for the 63 potential breach locations.

For the system risk assessment, a Monte Carlo Important Sampling method (MC-IS) has been used. This is an accurate method because flooding in a river area is only possible at large discharges. In Figure 4.9 the flowchart of the calculations is presented. The central column is the core of the flowchart, containing a yearly update of the location of the fragility curves corresponding to equation (4.3), risk calculations and a propagating prioritisation and planning.

For a system consisting of one dike section and one breach location, the portfolio analysis for year i is a calculation of equation (4.8) with K=1. Firstly, a draw is performed from the pdf of the stochastic load variables, translate them to a local load $h(i)$ with equation (4.10), and draw from the fragility curve for the dike section representing dike strength ($h_{frag}(i)$). Secondly, the risks in year i are weighed and summed over all N events. Therewith, the calculation scheme for equation (4.8) is:

$$R_p^{PV}(i) = \frac{\sum_{n=1}^{n=N} I_{MC}(n,i) \cdot w(n) \cdot D(h(n,i))}{\sum_{n=1}^{n=N} w(n)} \cdot \exp\left(-I_d \cdot r' \cdot i\right) \tag{4.12}$$

In which:

$I_{MC}(n,i)$	Indicator function indicating whether draw n leads to failure in year i: I=0 if $h(n,i) < h_{frag}(n,i)$ and I=1 if $h(n,i) > h_{frag}(n,i)$.	–
$h(n,i)$	Local load for the dike section in a system based on draw n from ($\hat{Q}_u$, m_Q, m_h), in year i	$m+NAP$
$h_{frag}(n,i)$	Draw n from the fragility curve for the dike section in the system, in year i	$m+NAP$
$w(n)$	Weight of the n^{th} MC-IS draw event of the river discharge $\hat{Q}_u(n)$: the probability density of that river discharge event divided by the probability density of the sampling function for that event.	–
N	Number of draws	–

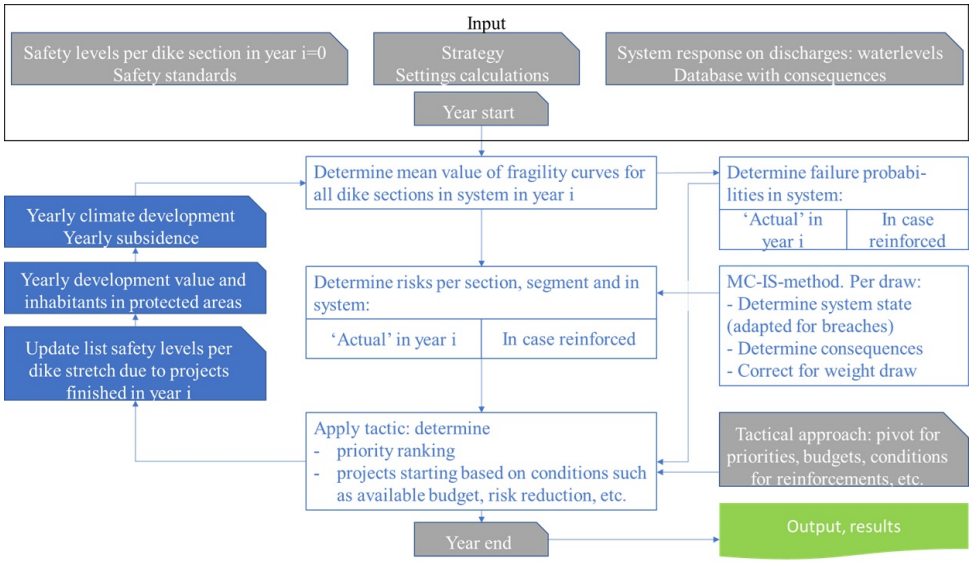

Figure 4.9.: *Flowchart of the calculations for portfolio management of dikes. Input in grey, updates in blue, calculation steps in white, and results in green.*

For a system consisting of multiple interdependent dike sections, the first step is the same, except the draw is performed from the fragility curves for all dike sections in the system. A second step is inserted: a system analysis is performed to determine where the breaches would occur for this drawn event, and to adapt the downstream local water levels, see Figure 4.8. Third, the risks per dike section k in year i are calculated based on the adapted water levels, summed over the system, weighed and summed over all N events. The calculation scheme for equation (4.8) is:

$$R_p^{PV}(i) = \frac{\sum_{n=1}^{n=N}\sum_{k=1}^{K} I_{MC}(n,k,i)\cdot w(n)\cdot D(h_k'(n,i))}{\sum_{n=1}^{n=N} w(n)} \cdot \exp\left(-I_d \cdot r' \cdot i\right) \quad (4.13)$$

In which:

$I_{MC}(n,k,i)$	Indicator function indicating whether draw n leads to failure in dike section k in year i: I=0 if $h_k'(n,i) < h_{frag_k}(n,i)$ and I=1 if $h_k'(n,i) > h_{frag_k}(n,i)$.	–

$h'_k(n,i)$	Local load for dike section k based on draw n from ($\hat{Q}_u$, m_Q, m_h), in year i, adapted for breaches upstream	$m+NAP$
$h_{frag_k}(n,i)$	Draw from the fragility curve for dike section k in the system, in year i	$m+NAP$

FAILURE PROBABILITIES ON DIFFERENT SCALES

In this chapter dike sections are defined in between the potential breach locations, with average lengths of about 8 km. For different reasons the translation of probabilities of failure is enabled for different dike lengths:

- The actual failure probabilities are used as input for the derivation of realistic fragility curves, which are available per dike subsection in [33] with lengths of about 1 km
- The reinforcements are based on the standards, expressed as probability of failure, which are defined per dike segment, with lengths of about 25 km.
- The check of the risk-calculations is based on the system analyses in [33], which are based on detailed probabilistic modeling [31]. These are provided for entire polders, with dike lengths up to 200 km.

For this translation, an approximation is used which is rather good for small and not fully dependent probabilities of failure [142]:

- full dependence for the translation between dike subsections and dike sections, for which the correlation is very large,

$$P_{f_k}(i) = \max_{1 \le s \le m} P_{f_s}(i) \tag{4.14}$$

In which:

$P_{f_s}(i)$	Probability of failure of a dike subsection s in year i	—

- independence for the translation between dike sections and dike segments:

$$P_{f_j}(i) = 1 - \prod_{\forall k \in j} \left(1 - P_{f_k}(i)\right) \tag{4.15}$$

In which:

$P_{f_j}(i)$	Probability of failure of dike segment j in year i	–

Similarly, to compare the results of these approximations with the system analysis in [33], the results per dike segment are translated to an entire polder:

$$P_{f_{polder}}(i) = 1 - \prod_{\forall j \in polder} \left(1 - P_{f_j}(i)\right) \tag{4.16}$$

In which:

$P_{f_p}(i)$	Probability of failure of a polder p in year i	–

These translations are applied to those polders in the study area for which [33] determined failure probabilities. The comparison is rather good, see Figure 4.10.

4.4.3. DERIVATION OF PROBABILITY DENSITY FUNCTIONS OVER TIME

The pdf's for loads and strength in equation (4.8) are time-dependent. The system loads $\vec{S}$ are represented by river discharge. The strengths by fragility curves.

RIVER DISCHARGE

In a riverine area, the maximum river discharge during a flood wave is the most important stochastic variable to assess flood risks. The representation of the pdf of the discharge of the Rhine River at the border of the Netherlands is given in [71]. In this thesis, this river discharge $\hat{Q}_u$ is represented by a Gumbel distribution, transformed as described in detail in Appendix A to get a realistic pdf in the time frame of the case study.

FRAGILITY CURVES

The fragility curves are required for the actual situation ($i = 0$) and for reinforcements in year i to solve equations (4.3) and (4.4). However, not in all cases fragility curves are available since flood probabilities can be derived via other methods than equation (4.2), such as [33] which provides probabilities of failure per dike section. For testing the proof of concept in this chapter, these probabilities are used as a starting point for the derivation of the fragility curves. A normal distribution is used like Figure 4.4. Given this shape the required fragility curves are represented

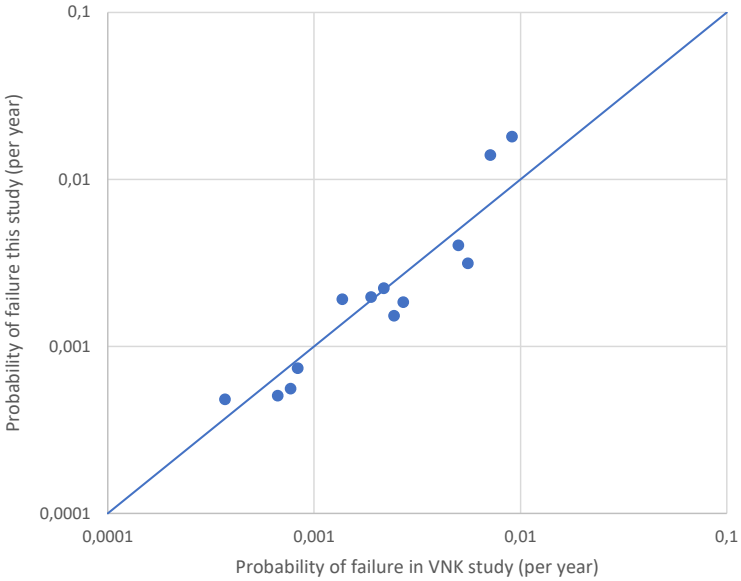

Figure 4.10.: *Comparison between the results in [33] (denoted as VNK study) for 13 polders (38, 40, 41, 42, 44, 45 and 47-53) and the approach in this study.*

by $\mu_{frag_k}(0)$ and $\mu_{frag_k}(i + T_{plan})$ for the actual and reinforced situation respectively.

For the actual situation ($i = 0$) the available results per dike subsection in [33] are merged to the larger dike sections used in this chapter based on full dependence within the dike section, see equation (4.14). For the derivation of the fragility curve for reinforcements in year $i + T_{plan}$ the probability of failure per dike section is obtained from the standards for flood probabilities which are to be met per dike segment j, consisting of several dike sections. The flood probabilities per dike section k are obtained based on independence between the dike sections in the dike segment, see equation (4.15), which for small probabilities is approximated by:

$$P_{f_k}(i) = P_{f_j}(i) \cdot \frac{L_k}{L_j} \tag{4.17}$$

In which:

L_j	Length of dike segment j	km
L_k	Length of dike section k	km

For both the actual and the reinforced situation a Newton-Raphson method is used to solve the location $\mu_{frag_k}(i)$ iteratively, leading to these probabilities of failures for dike section k in equation (4.2). As a heuristic prior estimate herein the waterlevel is used which corresponds to an exceedance frequency equal to the actual probability of failure. In each iteration numerical integration is used to solve equation (4.2).

4.4.4. BUDGET AND COSTS OVER TIME

The budget for measures is calculated as the base budget at the start of the period of interest, increased with inflation:

$$B(i) = B(i=0) \cdot (1 + infl)^i \tag{4.18}$$

In which:

$B(i)$	Budget for flood risk measures in year i	€
$B(i=0)$	Yearly budget for flood risk measures at the start year of the analysis $i=0$	€
$infl$	yearly inflation	–

The costs of measures are based on key numbers for ensafing tenfold [143], again corrected for inflation:

$$C_k(i, T_{plan}) = f_C(k, i) \cdot \left(\frac{\Delta\, h_k(i)}{h_k^{10}} \right) \cdot C_k^{10} \cdot L_k \cdot (1 + infl)^i \tag{4.19}$$

In which:

$C_k(i, T_{plan})$	Cost of a reinforcement in year i, targetting to reinforce for the year $i + T_{plan}$	€
h_k^{10}	Water level difference with a tenfold decreased probability of exceedance	m

C_k^{10}	Costs per km for dike reinforcement required for a tenfold decrease in probability of flooding	€/km
$f_C(k,i)$	Reduction factor on costs for dike section k in year i	-

The actual strengths may vary significantly along a dike section [33]. Some parts should be more reinforced than others to comply with the standard. In case the costs of reinforcement would be based on the maximum probability of failure along a section according to equation (4.14), they would be overestimated. Therefore, the costs $C_k(i, T_{plan})$ are reduced by a factor f_C to compensate for that overestimation. Figure 4.11 provides a schematic representation of the cost reduction.

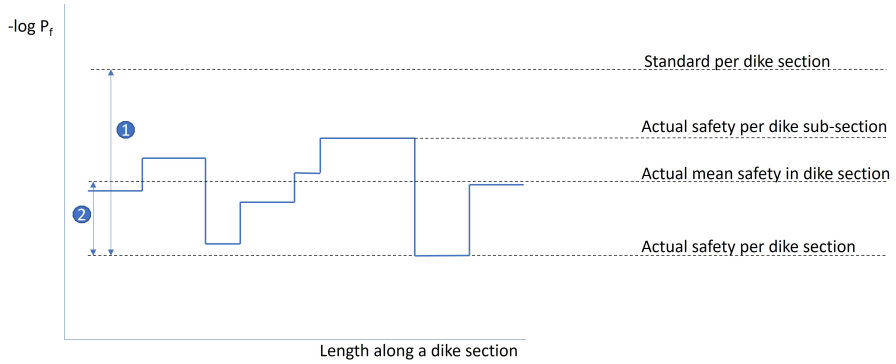

Figure 4.11.: *Schematic cost reduction due to existing differences in safety level along dike sections.*

Equation (4.20) provides the cost reduction factor f_C. It is approximated based on the proportionality of reinforcements $\Delta h_k(i)$ to $log\, P_{f_k}$, which is in line with the use of an extreme value distribution for discharges and water levels.

$$f_C(k,i) = 1 - \frac{\sum_s \frac{L_s}{L_k} \cdot \left(logP_{f_s} - log \max_s P_{f_s} \right)}{logP_{f_{k,standard}} - log\, P_{f_k}(i)} \tag{4.20}$$

In which:

L_s	Length of dike subsection s	m
$P_{f_{k,standard}}$	Standard for dike section k based on the formal standard for dike segments by equation (4.17)	$-$

The counter in equation (4.20) sums a length-weighed distance to the maximum probability of failure, the lowest point in Figure 4.11, represented by arrow (2). The denominator represents the distance between the actual and the required probability of failure, which is arrow (1). Note, in advance it is unknown at what actual safety level $P_{f_k}(i)$ the intervention will take place, due to its unknown timing. Therefore, the denominator of the reduction factor f_C is dependent on the year i. Assuming an even aging along the dike section after reinforcement, this reduction by f_C is applied only when the dike section is reinforced for the first time in the simulation period.

4.5. APPLICATION AND RESULTS

4.5.1. NUMERICAL SETTINGS AND MODEL CHECK

Several model runs have been carried out to choose numerical parameters leading to stable flood risk calculations. The performance of the case study model is compared with the results of a detailed national study (from here denoted as VNK) on actual risk assessments in the Netherlands [33, 79]. VNK provides probabilities per polder, which are in most cases enclosed by several dike segments. Each polder consists of dozens of small dike sections delivering a high level of detail for assessment of actual safety. For the comparison in this section the starting points of the calculations in VNK [33] are used. For the year of comparison 2015 is chosen, the year VNK reported. The results for 5 polders are used which are entirely in the model area (see Figure 4.6). Table 4.1 provides the starting points for the comparison, the pdf's for probabilistic calculations and the numerical parameters.

The results are shown in Figure 4.12. The comparison is good for flood probabilities (grey), economic risks (blue) and individual risk on victims (yellow). Note, for one of the examined polders for which [33] provided a value for the probability of failure denoted as '>0.01 per year' a value of 0.01 per year is taken. This is the most right grey bullet in Figure 4.12, which would shift right a bit resulting in an even better comparison with the result in this study. Thus, despite the use of a less detailed dike section schematisation, a hybrid numerical analytical modeling of the water levels in the river system, probabilistic modeling without dependency between dike sections, and a calculation of consequences for each MC draw instead of only a few, the results are comparable. This comparison serves as a check for the modeling and implementation.

Since the standard deviation of the fragility curves ($\sigma = 0.50m$) is based on expert opinion, the effects of different values of the standard deviation used in the fragility curves are examined. The comparison for $\sigma = 0.25m$ is more or less the same and for $\sigma = 1.00m$ it is significantly less. Therefore, $\sigma = 0.50m$ is kept.

Table 4.1.: *Overview of numerical starting points for the case study model, and the adapted case study specific ones for a proper model check with VNK.*

Starting points	**Case study (sections 4.5.2 and 4.5.3)**	**Model check (only section 4.5.1)**
System effects on probabilities of failure due to breaches upstream polder	Yes	No
Evacuation fraction	56% [143]	
Dutch National database with consequences [54]	For water levels higher than the highest in the database, the consequences corresponding to the highest water level are chosen. For water levels lower than the lowest in the database, the consequences are truncated to zero	
Value of a human life (per victim)	6,7 M€ [51]	Neglected
Consequences (per affected person)	12500 € [51]	Neglected
Sampling Function (SF) for $\hat{Q}_u$	normal distribution with (μ, σ) is (16000,2000) m^3/s	
Number of draws	10000	
m_h	Normal distribution with (μ, σ) is (0,0.15) based on [101, 144] truncated at $\mu - 2.9\sigma$ and $\mu + 2.9\sigma$	
m_Q	Normal distribution with (μ, σ) is (0,1) based on [71], truncated at $\mu - 2.9\sigma$ and $\mu + 2.9\sigma$, see Appendix A	
Fragility curves	Normal distribution with σ is 0.5m	
Step size $\hat{Q}_u$	$50 m^3/s$	
Step size m_h,m_Q	$5/6 \cdot \sigma$	

4.5.2. ELABORATIVE CALCULATIONS

Some elaborative calculations are made to get an understanding of the model behaviour and the results and tactical planning settings. In this subsection the results for risks and costs are not discounted to get a clear insight into the course of the results in time. Table 4.2 provides the case-specific parameters which are used together with Table 4.1.

In Figure 4.13 the model result is shown. The prioritisation of interventions is based on the maximum decrease in economic risks (see section 2.4.2). Consequently, the economic risks (grey) decrease at each reinforcement. The cost increases at each reinforcement (brown) until all dikes reach their standard. The total budget (blue) is proportional and increases due to the yearly added budget and inflation.

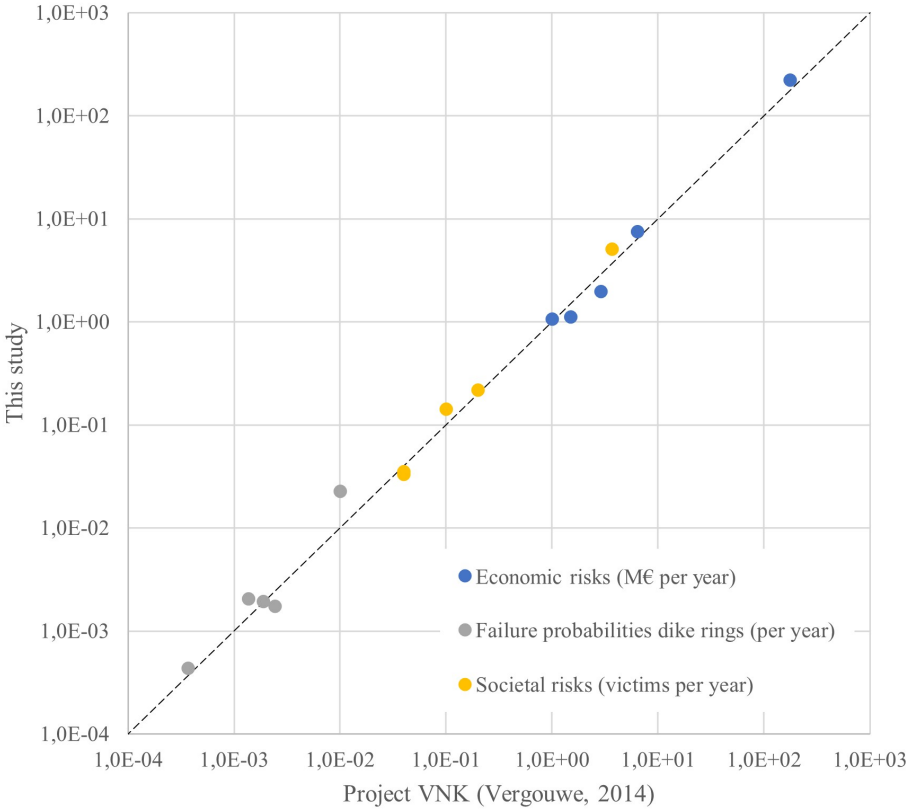

Figure 4.12.: *Comparison model of this study with results of project VNK, dike ring areas 42, 43, 47, 48 (except dike segment 48-3), and 50 [33] for the probability of failure, economic risks and risks on victims. NB. The most right grey bullet would shift right a bit, because it is reported as '>0.01 per year' in [33].*

In Figure 4.14 the model result is shown for the situation as in Figure 4.13, however, the budget constraint is more flexible due to acceptance of some overplanning, as long as the execution costs (the last 2 years of each reinforcement, see Table 4.2) fit in the budget (grey). The risks are smoother in time, and even a small increase occurs around 2035, due to the fact a top-ranked dike can not be reinforced due to budget shortage and a reinforcement upstream causes increased risks downstream. A variant in which the top 3 ranked dikes are forced to be planned first shows a more continuously descending course of risks in time (yellow), in this thesis referred to as a priority condition. Before 2035 the risks of this variant are somewhat higher with respect to the grey line due to

Table 4.2.: *Overview of case study specific starting points.*

Starting points	**Case study (sections 4.5.2 and 4.5.3)**
Period of analysis	100 years, starting from 2015
Breach width and depth	150 m based on historic floods [77], head $h_k - h_{b_k}$ of 5m based on the extreme water levels and polder levels in the study area
Population growth rate	0,33% per year
Subsidence rate	0.1 m per 50 years
Climate scenario	G+ [103]
Budget at the start of the analysis	The budget is based on the national budget of HWBP of 362 M€/year. Since the study area contain 498.9km from the national 3437km of dikes, the length-proportional budget is taken as 50 M€/year, in this thesis referred to as the proportional budget.
Reinforcement cost division over preparation and execution years	HWBP pursuits reinforcement in 7 years. Five preparation years are used together for 25% of the cost. In the last 2 execution years the actual reinforcement takes place, using the other 75%.
Costs per reinforcement unit C_k^{10} (in: equation (4.19))	[143]
Cost reduction factor f_C	Correct costs of first reinforcement for dike sections in which actual safety level differs along the length, minimized by a chosen value of 0.25 for minimal required fixed costs
The price level at the start	2015
Inflation	2%
Discount	5% (2% in section 4.5.2)

the fact no expenditures on other dikes are made before the top-ranked dikes are reinforced. After 2035 the risks are considerably lower.

In Figure 4.15 the model result is shown in case of system changes in population growth rate, subsidence rate and climate scenario (see Table 4.2 in time (grey). As a reference the yellow line is the same as in Figure 4.14. The risks show a clear difference. Just from the start in 2015 they increased, because the first reinforcements only become effective after the construction period of 7 years. From 2022 they decrease, however, considerably higher risks are present, and more time is needed to reduce the risks until they stabilize around 2080. The costs consequently follow the budget during this time. The stable risk level of the variant with changes (grey, after 2080) is some lower than that of the completely stable variant without system changes (yellow), for which the reinforcements will lead to an exactly compliant system. This is because, in a changing system a reinforcement meant to be compliant with circumstances a design horizon ahead leads to a surplus of risk reduction at the time of reinforcement. Over the full portfolio this leads to some extra risk

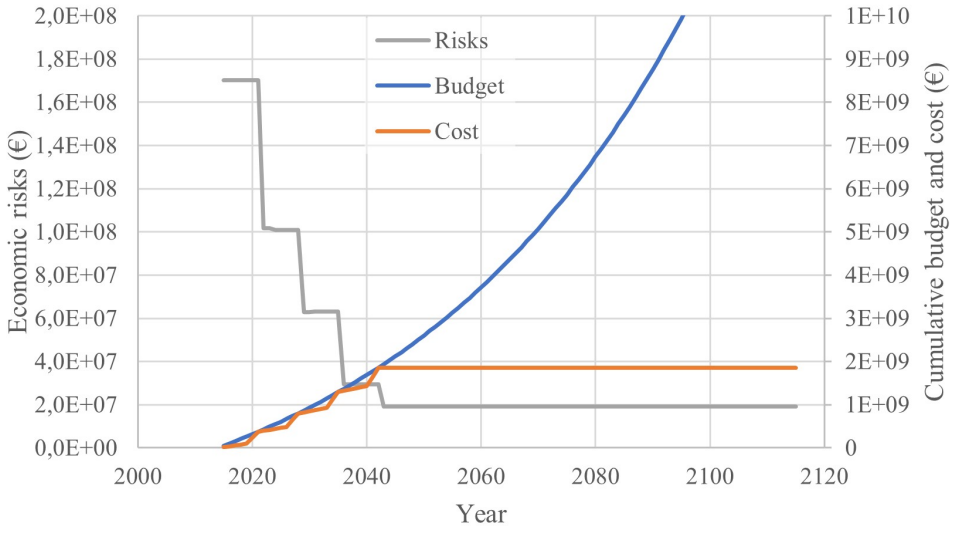

Figure 4.13.: *Model result for general starting points, for prioritisation based on decrease of economic risks.*

reduction.

In Figure 4.16 again the model result is as in Figure 4.15 (grey). The effect of a physical discharge limit of 18000 m^3/s due to breaches upstream the study area is presented as well (yellow). It shows clearly the effect is not that large. This is because the actual safety is rather low, causing breaches far below this discharge level. Nevertheless, since it is more realistic and in correspondence to this research on system effects in the study area, this setting is used as a starting point for the calculation of different tactics.

In Figure 4.17 the model results are presented for different prioritisation metrics in section 2.4.2: decrease of economic risk (yellow), individual risk on victims (black, right axis), safety level (green) and benefit cost ratio (grey). The course of the risks in time is comparable.

All incremental changes in the presented results of the elaborative calculations develop in time in an understandable course. This serves as a second check on the proper implementation, next to the comparisons with [33] in the previous subsection.

4.5.3. RESULTS FOR DIFFERENT TACTICAL MANAGEMENT PLANS

A tactical management plan defines the planning of consecutive measures to implement a strategy. Tactical plans may differ due to several choices such as:

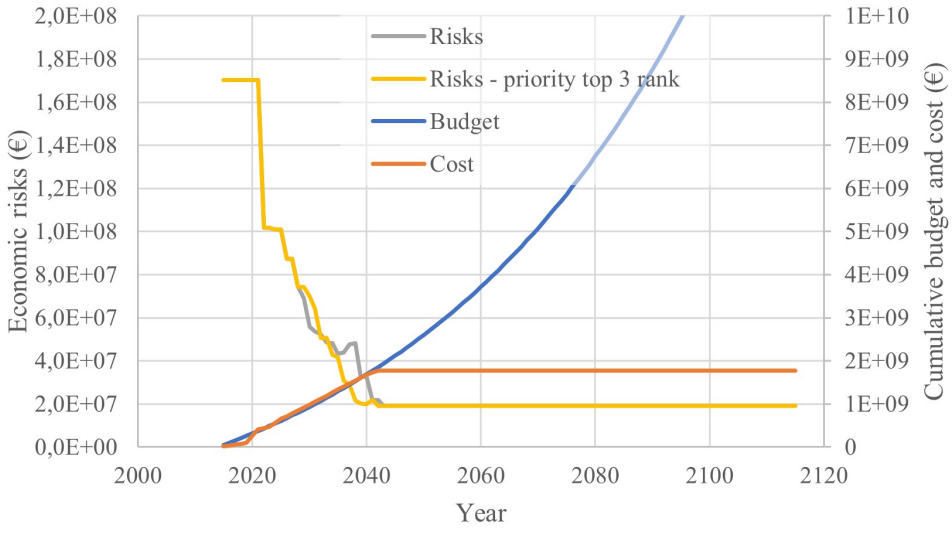

Figure 4.14.: *Model results as in Figure 4.13 and planning with tolerance for overplanning (corresponding risks in grey) and a priority condition for the top 3 ranked dikes (corresponding risks in yellow).*

- The criterion to include reinforcement in the program planning, e.g. exceedance of a safety level.
- Metric for prioritisation: order on decreasing risk per year, on decreasing differences between actual and required safety level, or on benefit-cost ratio.
- A priority condition, is to give priority to plan a number of top-ranked dikes first, which holds no others are planned as long as for these dikes is no room on programme.
- Available budget per year, and the division of the budget over the period of interest
- Minimal risk reduction rate per reinforcement is relative to the measure with maximum risk reduction in a year, to postponing the reinforcements which have small risk effects.
- Planning window shifting through the period of interest (see Figure 4.2). In planning, this is the time for which reinforcements were actually planned and executed.

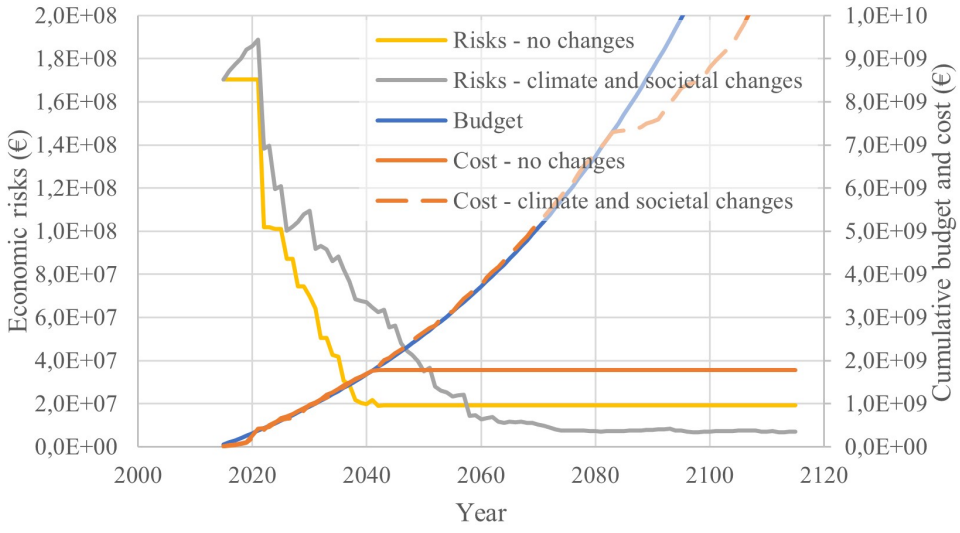

Figure 4.15.: *Comparison of model results without (yellow, as in Figure 4.15) and with system changes (grey).*

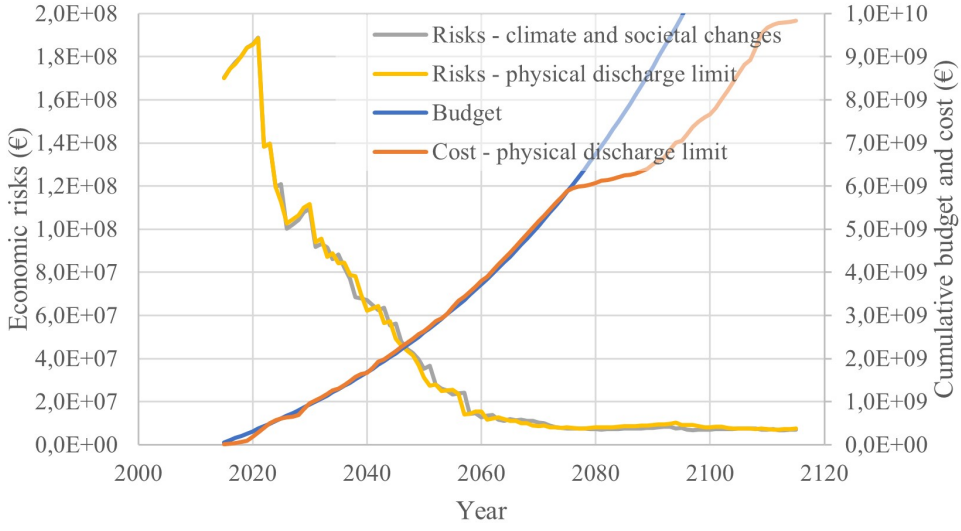

Figure 4.16.: *Model results without (grey, as in Figure 4.15) and with a physical river discharge limit (yellow).*

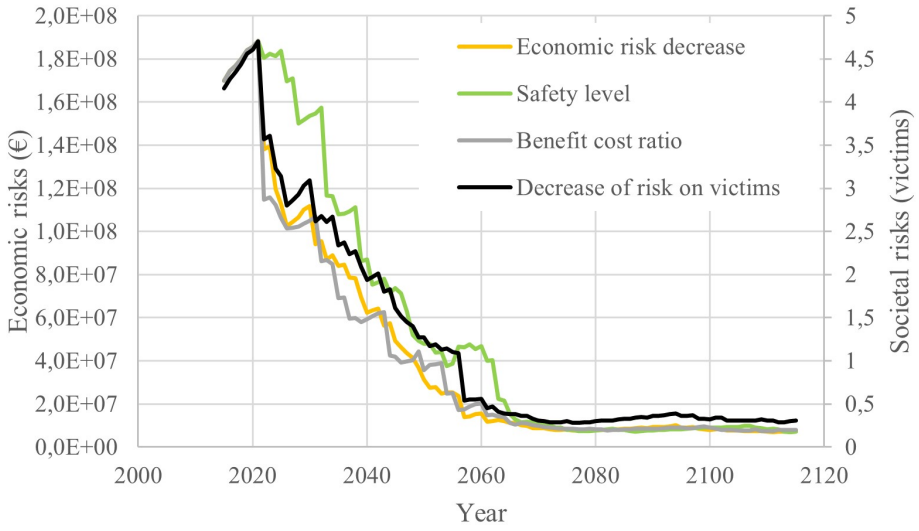

Figure 4.17.: *Model result for different prioritisation metrics: Economic risk decrease (as in Figure 4.16, yellow), Safety level (green), Benefit cost ratio (grey) and Decrease of individual risk on victims. The first three refer to the left axis, the last to the right axis*

- The degree of reinforcement. In some models the intensity of reinforcement is a degree of freedom [46], or partial reinforcement is enabled [45].
- Design horizon of a reinforcement.
- Provisions for overplanning: In most models the budget limits all activities, however, in practice mostly at least preparations for the next projects are allowed because of low costs.
- Intangible starting points such as to pursue regional spread.

The Dutch Flood Protection Programme (HWBP) is actually active in the case study area and uses a mix of different tactics for planning: difference between actual safety and standard, regional spread, and available budget per year. In this study different tactical plans are defined based on the list above. The first item in the list is fixed, because the criterion for planning is based on the Dutch strategy, which holds that a dike can only be planned on the programme when the safety standards are exceeded, indicating dike reinforcement is needed shortly. The second,

third and fourth item is varied as provided in Table 4.3 because these appeared to be important in elaborative calculations. For the other items a single starting point is taken, see Table 4.4.

Table 4.3.: *Overview of varied aspects of the tactical plans implemented in the model.*

Metric for prioritisation	**Budget**	**Priority condition**
Based on safety level, see equation (2.13)	Proportional budget for case study area wrt to the national budget, in 2015 50 M€	No further planning restriction
Based on individual risk on victims, see equation (2.14) (also applicable for economic risk effect)	Double budget for case study area: In 2015 100 M€	Top 3 rank first, postponing other measures
Based on benefit-cost ratio, see equation (2.15)		

Table 4.4.: *Overview of starting points for parameters in the tactical plans implemented in the model.*

Parameter	**Used in this study**
Planning criterion	The probability of failure of the dike segment exceeding the standards, and the probability of failure of the dike section exceeding its length-proportional value calculated with equation (4.17).
Minimal risk reduction rate	0 (which means: no)
Planning window	12 years
Reinforcement	Standard level at design horizon
Design horizon	50 years
Overplanning	Allowed for the preparation years of a reinforcement
Intangible aspects	No

These variations together lead to $3 \times 2 \times 2 = 12$ different tactical plans. Two other variants are calculated which are in fact no realistic tactical plans: the 'do nothing' option representing the growing risk over time, and the option with infinite budget leading to reinforcement of all dikes at once after the 7-year preparation period. All tactical plans are presented in Table 4.5. In Table 4.6 the results of all tactical plans are provided.

Figure 4.18 summarizes the results for all tactical plans except 13 and 14. The horizontal axis represents the expected number of victims in the simulation period of 100 years. The vertical axis contains the discounted value of the sum of costs and economic risks in the same period.

The difference between the total present value of costs and risks for the 'do nothing' option (tactical plan 13) and plans 1-12 reflect the effect of the flood risk strategy to ensafe the area, on an average about

Table 4.5.: *Overview of tactical plans implemented in the model, composed of the different decision rules in Table 4.3.*

Tactical plan	Metric for prioritisation	Budget	Priority condition
1	safety level	Proportional	no
2	safety level	Proportional	top 3
3	safety level	Doubled	no
4	safety level	Doubled	top 3
5	individual risk level	Proportional	no
6	individual risk level	Proportional	top 3
7	individual risk level	Doubled	no
8	individual risk level	Doubled	top 3
9	benefit-cost ratio	Proportional	no
10	benefit-cost ratio	Proportional	top 3
11	benefit-cost ratio	Doubled	no
12	benefit-cost ratio	Doubled	top 3
13	economic risk level	0	top 3
14	economic risk level	∞	top 3

Table 4.6.: *Overview of results for all tactical plans in Table 4.5.*

Tactical plan	Present value risk (billion €)	Present value cost (billion €)	Total present value (cost & risk, billion €)	Individual risk (victims)
1	4.27	1.47	5.74	226
2	3.38	1.47	4.85	159
3	2.12	1.86	3.98	86
4	1.95	1.88	3.83	81
5	3.18	1.47	4.64	180
6	2.73	1.46	4.18	126
7	1.84	1.87	3.71	78
8	1.80	1.88	3.68	76
9	3.44	1.47	4.91	184
10	2.59	1.48	4.07	125
11	1.80	1.87	3.67	79
12	1.78	1.88	3.66	77
13	8.15	0.00	8.15	972
14	1.36	2.05	3.42	59

50%. The individual risk is reduced by on an average about 85%. The differences between the tactical plans 1-12 are up to 40% for the total present value and up to 70% for individual risk, which is the same order of magnitude as the effect of the flood risk strategy. Especially the differences caused by the prioritisation metric and priority condition. Figure

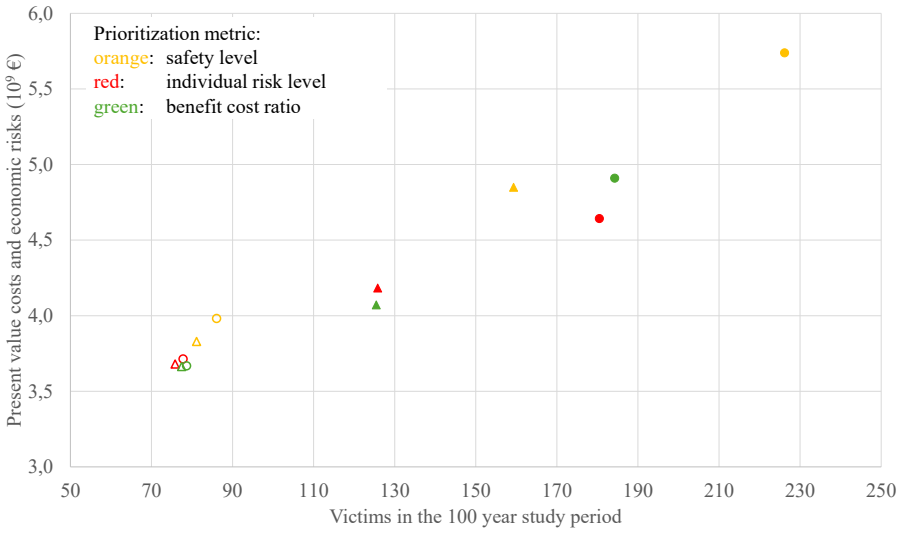

Figure 4.18.: *Model result for tactical plans 1-12, with the budget denoted by filled (proportional budget) or open marker (doubled budget), the prioritisation metric denoted by color, and the priority condition denoted by marker shape (dot: no; triangle: top 3 first)*

4.19 shows that a risk based prioritisation metric in combination with a priority condition for the top 3 ranked dikes (the two most right orange bars) has about the same effect on cost and risk as doubling the budget in combination with a safety-level based metric (left yellow and grey bar).

4.6. DISCUSSION

In this section consecutively are discussed critical assumptions, extensibility, application and practical implications with respect to the presented methodology and application.

4.6.1. ASSUMPTIONS

The type of flood risk intervention considered in this chapter is dike reinforcement. During the simulation the probability of failure is assessed with fragility curves on a yearly basis. A prerequisite for the application of the methodology is the availability of existing actual fragility curves or actual failure probabilities per dike subsection. In countries where these quantities are used to meet design standards, such as the UK, Germany and the Netherlands, these are assumed to be available, because

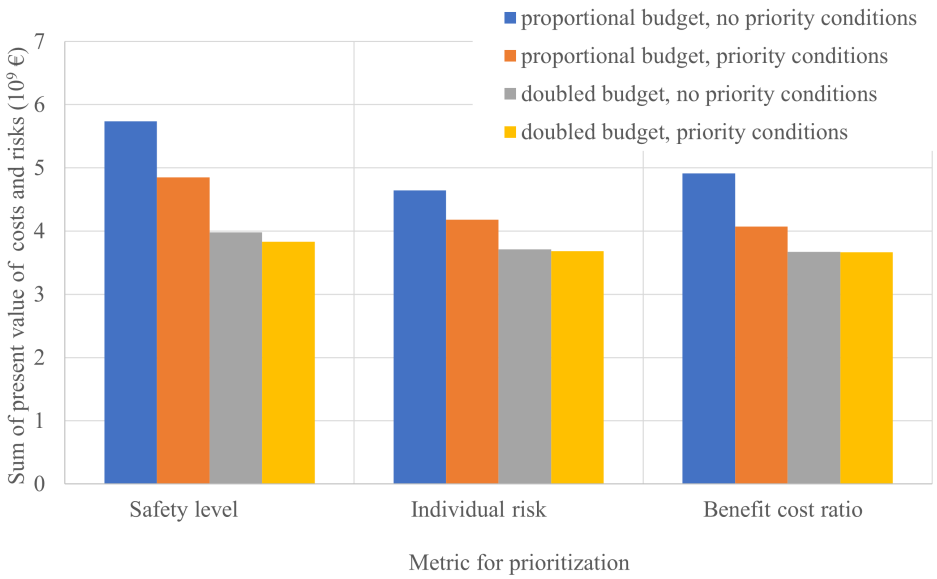

Figure 4.19.: *Overview of present values of cost and risk for tactical plans 1-12*

prior to the planning process, these are part of the dike condition examination. The same prerequisite holds for a hydraulic model to translate system loads to local loads, and consequence calculations for representative breach locations. In the case study, the actual fragility curves at the start of the analysis are tuned in a way the probabilities per dike section are aligned with VNK [33].

The fragility curves for to-be-reinforced dikes can be determined in several ways. In this chapter, the shape of the fragility curves in the actual situation is used, shifted based on climate change and subsidence to get a provisional fragility curve for a future situation, solving the equations (4.4), (4.3) and (4.2). An alternative approach would be to pro-forma-design conform design standards and derive a fragility curve, which would need detailed information and calculations. Another alternative could be to use a class of standard fragility curves for different typologies of reinforcements, such as adapted dike slopes. These alternative approaches would need a similar approach as used in the present chapter to enable to shift the re-shaped fragility curve until it meets the standard at the design horizon.

For estimations of the effects of breaches on downstream river loads the backwater effect in the polders is neglected. This is sufficiently accurate in case of critical flow through the breach. This holds in the initial phase of the flooding, which phase is assumed to be most important for

the reduction of the event water level maxima downstream. Additional calculations are executed to examine the sensitivity of the downstream water level effect of breach widths on the system risks. They underpinned the low sensitivity for breach widths in the range of most historic observations in the Netherlands, 75-200m [77].

A limitation of this concept is the effect of timing and growth of the breaches on downstream river loads. They are assumed to occur suddenly at the water level maxima of floods. This overestimated the water level reductions downstream the river. Nevertheless, if no system behaviour is taken into account, the downstream water levels are certainly over-estimated. Research is recommended with hydraulic and breach development model simulations, to investigate this time effect on the downstream water level reductions.

4.6.2. APPLICATION AND PRACTICAL IMPLICATIONS

In the case study the probabilities of flooding are based on [33]. Herein, the residual strength, which is defined as the strength of a dike after the occurrence of initial damage due to a failure mechanism, is not taken into account for the geotechnical mechanisms macro stability and piping, which may be important in the river area. Therefore, the probabilities are considered as an upper limit. For development of a method to compare tactical plans, the probabilities are considered to be sufficient.

The different tactical plans lead to different intervention schemes. To illustrate the effect of different prioritisation metrics and the priority condition, Table 4.7 presents the similarities and differences of the interventions in the first 15 years of the analysis for the tactical plans 1, 6 and 10 in Table 4.6. For all plans the length-averaged $\Delta\ h_k$ is similar. The breakdown of the reinforcement surface to branches shows clearly that the attention of the individual risk-driven intervention tactic (plan 6) is almost completely on dikes along the Waal (see Figure 4.5), protecting large and deep polders from flooding. The Waal is the largest river branch of the Rhine River, and may cause flood depths with high risks to victims. The other two tactical plans 1 and 10 show more spread of the interventions over the river branches with a focus on the Nederrijn-Lek. Another difference, shown in the number of sections column, is the focus of plan 6 on the reinforcement of a limited number of important sections and the spread of investments over many sections in the other plans.

4.6.3. EXTENSIBILITY

The methodology to compare tactical plans is developed to be generically applicable. The fragility curves and the intervention's decision rules are crucial elements. In the case study a normal distributed fragility curve per dike section is used. Equation (4.2) is suitable for other shapes, e.g. for a fragility curve composed of different failure mechanisms. The

Table 4.7.: *Overview of reinforcements for tactical plans 1, 6 and 10 (see Table 4.5) for the reinforcements up to and including 2030. NB. The reinforcement surface is the dike length multiplied by the dike height increase.*

	Reinforcements			Reinforcement surface per branch (* 1000 m^2)				
Tactical plan	**Length (km)**	**Length-averaged $\triangle h_k$ (m)**	**Number of sections (-)**	**Rhine**	**Waal**	**Pannerdensch Canal**	**Nederrijn-Lek**	**IJssel**
1	140.1	1.13	26	3	48	14	**75**	19
6	103.6	1.33	10	0	**102**	13	22	0
10	183.0	0.85	24	17	41	13	**71**	14

intervention decisions may be based on different design rules. In the case study compliance with safety standards is required at the end of the design horizon. The methodology is suitable for other intervention rules or intensities as elaborated in [45] or e.g. for a fixed reinforcement step of a factor 10 in safety. Furthermore, this methodology is suitable for a cascade of strategies, e.g. to elaborate adaptive pathways of strategies [43]. Sub-paths in a pathway, can be implemented as different tactical plans being effective in certain periods, translated into additional or changed intervention rules like Table 4.3.

In this study the river discharge is the main stochastic variable determining the local water levels. The MC approach in combination with the physical river discharge model and consequence simulations integrates causal knowledge about a system with probabilistic and risk analysis techniques [145]. This enabled us to take into account breach effects on system loads without additional hydraulic calculations. The application can be extended to e.g. an area near sea, where the local water level is determined by river discharge and sea water level. In the case water levels are determined by multiple stochastic system load variables, additional hydraulic calculations for several different combinations of those variables are required to determine the system effects of a breach event. Since breaches near the sea have a limited effect on water levels at neighbouring locations compared with breaches in riverine areas, the system effects are expected to be smaller.

4.7. CONCLUSIONS

This chapter focuses on the development and application of a methodology for the comparison of tactical plans for interventions in an interdependent system of dikes. Concluding, the developed model-based tactical planning approach is applicable in a riverine area, tactical planning is important for the reduction of flood risks over time, and the methodology is extendable to other water systems.

The methodology is applied to the system of dikes along the Rhine River branches in the Netherlands, taking into account deterioration due to subsidence, climate change and population growth. The case study shows the applicability of the methodology to calculate the portfolio metrics performance, risk and cost, which are key for mature asset management decisions [19, 22].

Tactical planning is important to effectively and efficiently reduce flood risks over time to the compliant level. This is based on the calculation of the costs and risks over time for 12 different tactical plans for different prioritisation and planning considerations and different budgets. The results show the present value of the sum of costs and risks of the plans differ by up to about 40% with respect to that of the plan with the highest present value. For individual risks the differences are up to 70%. An example is that interventions based on a benefit-cost-ratio prioritisation in combination with the condition to reinforce the top 3 ranked dikes first (plan 10), have the same effect on cost and risk as decisions based on a safety level based prioritisation in combination with doubling the budget (plan 3). Furthermore, different plans lead to different patterns and intensity of measures in the system.

The application can be extended to other than riverine areas, which would need additional hydraulic calculations. System effects near the sea are expected to be smaller than the effects along rivers.

This chapter underpins that the application of the presented methodology provides understanding that supports planning discussion and the corresponding tactical decisions. This study contributes to the work on model-based planning of interventions in large portfolios of interdependent assets.

5

FLOOD RISK-BASED UPDATING OF STANDARDS

A disposition to preserve, and an ability to improve, taken together, would be my standard of a statesman.

Edmund Burke (English politician and philosopher, 1729-1797)

Objective of this chapter is to study how reliability standards, expressed as probabilities of dike segment failure, can be applied to improve opportunities for risk based dike designs, and tactical planning of dike reinforcements. First, the approach to assess the economic optimal flood probability, used by the Dutch Delta Committee (1958), is adapted to enable comparison to the probabilities used as input for the recently formalized standards (2017). Therefore, the derivation is adapted to reflect wave overtopping in stead of overflow. Furthermore, the approach is extended to include relative water level rise and reinforcements over time. Second, building on the finding the comparison appeared to be rather good, the failure mechanism piping is added in the derivation, to research the effect of the starting point in the analyses to date which used only wave overtopping. The effect on the optimal flood probabilities appeared to be small. Third, an analytical relation is developed for economic optimal design horizons. Finally, using the adapted Van Dantzig relation, a simple approach has been developed to update the economically optimal failure probability, based on a proposed design and planning. This can serve to check whether the reliability standard is still adequate. Therewith, it is practical possible to keep a dynamic focus on the optimal economic risk.

Parts of this chapter has been published in F. den Heijer, P.H.A.J.M Van Gelder, and M. Kok. "Risk-aware updating of reliability standards for flood defences". Submitted for: Journal of Flood Risk Management (2025).

5.1. RISK-BASED STANDARDS FOR FLOOD DEFENCES

5.1.1. STANDARDS PART OF MATURE RISK MANAGEMENT

The European Union established the Floods Directive 2007/60/EC [34], meant to guide the member states in their flood risk management, and stimulate them to manage their flood risks based on the same rationale: to map risks, plan and take measures, and monitor. Nevertheless, despite the Floods Directive stimulated the application of quantitative approaches, still differences in risk approaches are present [3, 23]. Managing their flood defences, different countries use different approaches for standardization and performance assessment [16, 23, 49].

Risk management is a part of mature strategic asset management, as explained in Section 1.2. Therein, the three dimensions of risk management capabilities as presented in [27] are given: technical, financial and administrative. A part of the administrative capability is the formulation of policies and strategies. A practical utilization of a flood risk management strategy is the definition of a standard, which can be used for performance analyses to decide on interventions.

For interventions on flood defences several organisations cooperate to initiate, budget, design and prepare and to maintain, see Section 1.5.2. Standardization is interpreted as one of the 'bridging mechanisms, ie instruments that remedy fragmentation by enhancing interconnectedness between relevant actors through information transfer, coordination and cooperation' [146]. More practical, standardization delivers the reason for the involved organisations to invest when and where, in a complex portfolio of flood risk reducing assets. This chapter refines and extends to the available methods for standardization of the failure probability of flood defences.

5.1.2. STANDARDS IN THE NETHERLANDS

In the Netherlands the flood risk standards are introduced in 1956 by Van Dantzig [14], after the disaster in the southern part of the country in 1953. It is the first known quantitative risk-based derivation of an economic optimal safety level for flood defences. Herein, the probability of an undesired flood event was based on water level exceedance frequencies and the consequences of flooding were based on complete economic loss in the polder. Being quantitatively derived for the western part of the Netherlands which is prone to sea floods, the standards were qualitatively extended to other parts of the country, depending on the character of the threat (rivers, sea), and the consequences at risk. These water level exceedance frequencies, to be withstand by the flood defences, are established by law in 1996 [147].

Due to sea level rise and economic growth, flood risks are time dependent. In 2017 the standards were updated. They are expressed as acceptability-limits for the probability per year on flooding. To derive economic optimal safety levels, the risks are based on the failure mechanism wave overtopping, and on calculations for the extension of floods and their consequences [51, 52]. The costs for reinforcement took into account a dike shape which was assumed to be sufficient to withstand geotechnical failure mechanisms. Next to the economic optimal safety level, the acceptable individual and group risks on victims are used to choose the standards (see Section 2.4.1). Despite the background of a time-dependent dynamic risk approach, the standards are not dynamic but static in the Dutch law [82].

The Dutch government prescribes the performance assessment methods. The National Flood Protection Program manages the budget for reinforcements. Water Boards are in charge for the actual management of most of the flood defences. They monitor the performance of the flood defences and process the budgets to market to execute reinforcements in case the performance is not compliant to standards.

5.1.3. KNOWLEDGE GAP AND APPROACH

The objective in this thesis is to improve utilization of risk analysis for flood defence systems. Given a standard expressed in the probability of flooding, despite these are risk-based, it is a challenge to keep focus on risk-aware decisions for reinforcements of individual dikes and systems. Especially the measures which focus on reducing consequences are prone to be dropped or even to be not considered, because there is no benefit in the process and budgetting. Nevertheless, benefits are in place, because the optimal safety level differs depending on the construction. The Chapters 3 and 4 provide methods how to compare the effects of the construction and order of reinforcements. However, there is no existing method which value and evaluate reinforcement proposals with standards taking into account their effect on consequences. In fact, the effects are assumed to be 'frozen' at the level used deriving the reliability standard.

The gap addressed in this chapter is to research whether there is a method to use standards for measures with a focus on consequence reduction. Note, this gap still focusses on the flood defences, the prevention layer in the multi layer safety concept [148]. A part of the challenge is to use the standards in a such a way to benefit from consequence reducing measures, which would be a better utilization of risk analysis, but to keep it in the operational context to avoid formal or juridical discussions about protection levels, additional extensive calculations, and other practical problems which would be cumbersome to overcome.

Following these elaborations, the objective of this chapter is to study how standards, expressed as probabilities, can be used risk-aware to obtain better opportunities for risk based dike designs, and tactical planning of dike reinforcements. The hypothesis is that the simple formula of Van Dantzig, adopted by the first Delta Committee (1960, [50]), which is easy to use in an operational context, can be adapted to meet this objective.

The approach consists of several steps. Firstly, a time dynamic component is added to the formula of Van Dantzig and compared with the time-dynamic approach, derived based on the advice of the second Delta Committee (2008, [87]), which has been used for the present Dutch standards (section 5.2). The approach of Van Dantzig and the time-dynamic approach both consider only one failure mechanism (overflow and wave overtopping respectively). In case the design shape is variable, and more specific the probability budgets reflecting the mutual relation between different failure mechanisms, it could be questionable whether the starting point to use only one failure mechanism is accurate enough. Therefore, as a second step this chapter studies the effect of adding the failure mechanism piping in the analysis. Both an analytic and numeric approach are developed and applied on cases studies to validate the derivation (section 5.3). This provides insight whether the method to derive economic optimal standards holds using only overtopping as failure mechanism, which would be much easier. Third, an analytical relation is developed for economic optimal design horizons. Fourth, an approach is developed to enable updating of the economic optimal reliability based on a proposed design and planning (section 5.4).

5.2. ECONOMIC OPTIMAL SAFETY STANDARDS

5.2.1. ORIGIN, DEVELOPMENTS AND REASON TO DIVE IN IT AGAIN

The Delta Committee [14, 50] developed an approach to determine the economically optimal safety standard as the sum of present value of risks and investments:

$$C_{tot} = I + R^{PV} \tag{5.1}$$

In which:

C_{tot}	Total cost of investments and present value of risks	€
I	Investments, given by $I_0 + \Delta h_d \cdot I'$	€
I_0	Initial costs of an reinforcement, independent from the magnitude of the reinforcement	€

I'	Marginal costs of a dike segment reinforcement per meter added dike height	€/m
Δh_d	Dike reinforcement height	m
R^{PV}	Present value of risks	€

In [32] is illustrated that, considering only the failure mechanism overflow and assuming an exponential water level distribution, this leads to a relatively simple equation for the optimal safety standard by minimizing C_{tot}:

$$P_{f_{opt}} = \frac{I'Br}{D} \tag{5.2}$$

In which:

$P_{f_{opt}}$	Economic optimal probability of flooding	per year
B	Scale parameter of the exponential water level distribution $F_h = 1 - exp\left(-\frac{h-A}{B}\right)$ valid for $h \geqslant A$. NB. B is equal to the decimation height by division by ln(10)	m
A	Location parameter of the exponential water level distribution	m
h	Water level	$m + NAP$
r	Discount rate	–
D	Economic damage in the polder caused by flooding due to failure of the dike segment	€

However, the economic growth, climate change and deterioration are not expressed in this equation. Therefore, in [51] the optimal safety standard for a series of dike stretches in a dike segment is modelled as an optimization approach of total costs, summing the series of intervention costs over time and the economic risks of flooding over time with:

$$C_{tot} = \sum_j \sum_i \frac{I_{ij}}{(1+r)^{T_{ij}}} + \sum_{t=0}^{t=z} \frac{D_\delta(t) \cdot P_f(t)}{(1+r)^t} + \frac{D_\delta(z) \cdot P_f(z)}{(1+r)^z} \cdot \frac{1}{ln(1+r)} \tag{5.3}$$

In which:

i	Indicator of successive investment	–
j	Indicator of dike segment	–
I_{ij}	Investment i at dike segment j	€

t	Time indicator: time with respect to the start of the analysis	*year*
T_{ij}	Time of investment i at dike segment j	*year*
z	Time after which system is assumed to remain unchanged [51]	*year*
$P_f(t)$	Probability of flooding at time t, in [51] defined as the maximum over all dike stretches in the dike segment	*peryear*
$D_\delta(t)$ $D_\delta(z)$	Economic damage caused by flooding anywhere along the dike segment, at time t and z respectively, subject to economic growth δ	€
δ	Economic growth rate	–

This equation is solved using AIMMS optimisation software (http://www.aimms.com), considering the failure mechanism overtopping. This resulted in a saw-tooth pattern for the probabilities of flooding in time, presented in Figure 5.1.

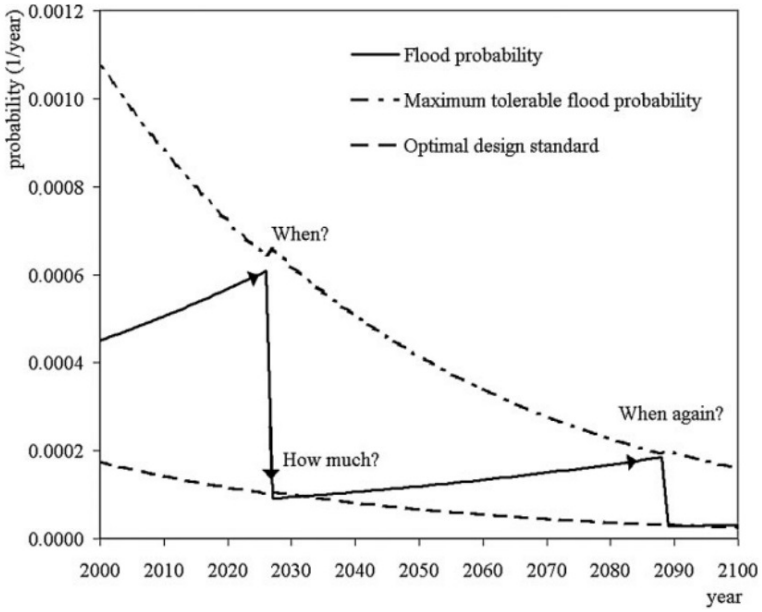

Figure 5.1.: *Saw-tooth pattern for the probabilities of flooding including upper and lower limits (copy of Figure 3 in [51]).*

The sudden reductions of the probabilities reflect the interventions (when, how much, when again) for a dike segment in the Netherlands. The result shows an upper limit curve (determining the time interven-

tion) and a lower limit curve (determining the optimal design probabilities). The middle probability, defined as the average between upper and lower curve, is presented as a representative value for standardization. Kind [51] observed a linear relationship between the middle probabilities and the relative damage, see the greybox below.

Intermezzo:
Optimal probability related to marginal costs and damage.

Based on a fit of results from equation (5.3) in [51] a linear relationship is found between the ratio of damage and the cost to decrease the probability tenfold on the one hand and the reciprocal optimal flood protection standard on the other hand, see Figure 5.2.

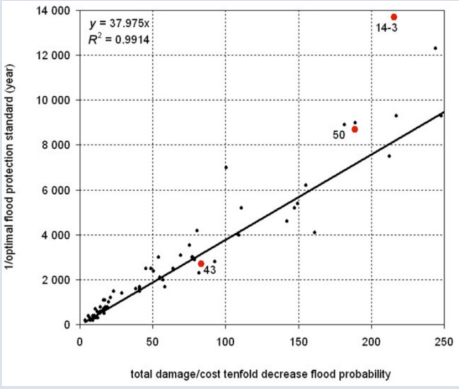

Figure 5.2.: *Relation presented in Figure 7 in [51].*

Let consider the approach developed by the first Delta Committee whether this is understandable. Rewriting equation (5.2) as its reciprocal, it follows:

$$\frac{1}{P_{f_{opt}}} = \frac{D}{I' \cdot B \cdot r} \tag{5.4}$$

Assuming the water levels follow an exponential distribution, the cost to decrease the probability of flooding tenfold $I^{10} = I' \cdot B \cdot ln(10)$, it follows:

$$\frac{1}{P_{f_{opt}}} = \frac{D}{I^{10}} \cdot \frac{ln(10)}{r} \tag{5.5}$$

In which:

I^{10}	Cost to decrease the probability of flooding tenfold	€

Therewith the equation based on the Delta Commissions approach is in the shape of a linear relation of Figure 5.2. This relationship is

not dependent on the location and scale parameters in the exponential distribution, and therewith it is spatially independent, enabling to use it for multiple dike segments as shown in the Figure 5.2. The factor to the damage/cost ratio to obtain the reciprocal optimal flood protection standard is $ln(10)/r$. With the discount equal to 5.5%, as taken in [51], this factor is calculated to be 42, which is quite comparable with the value of 38 found in [51].

The Intermezzo in the greybox above rises the question whether the results of the approaches of the first Delta Committee and the one used for the present standards as presented in [51] are comparable. If the answer on this question would be positive it would not only underpin the numerical implementation of equation (5.3) but it would provide practical benefits for standardization, because it would prevent the extensive model calculations which are needed to solve equation (5.3). To obtain comparability of both approaches, an approximative time dependent approach is developed based on the approach of the first Dutch Delta Committee which led to equation (5.2). In the next subsections first the lower limit is derived, then the upper limit. A comparison is made with available data in [51]. Starting from upper and lower limit the design horizon is derived, for which some special cases are presented.

5.2.2. LOWER LIMIT OF FLOOD PROBABILITIES DETERMINING OPTIMAL DESIGN PROBABILITIES

Searching for a comparison for the lower limit of the floods probabilities in time in [51] the following starting points are taken to adapt the approach of the first Delta Committee [50]:

- Assuming water levels h follow an exponential distribution which shifts over time due to relative deterioration η representing subsidence and climate change effect (which dynamic effects are constant over time just as in [51]):

$$F_h(t) = 1 - exp\left(-\frac{h-(A+\eta\cdot t)}{B}\right) \tag{5.6}$$

In which:

$F_h(t)$	Cumulative distribution function of water level in time	*peryear*
η	Relative deterioration representing subsidence and climate change effect	*m/year*

- Considering the failure mechanism wave overtopping in stead of overflow. The dike height is denoted by h_d and has a probability $P_f(h_d)$ to be overtopped by a discharge with a certain volume of x l/m/s. The probability distribution of dike heights is assumed to follow an exponential distribution, shifting over time just as the water levels. In deviation from equation (5.2) the factors B and η in the exponential distribution refer to the required dike height. Therefore, the parameter B based on water levels is increased with a factor f_{ovx}. The dike height increase over time is assumed to increase proportionate with the water level increase η. Since the theoretical lowest dike height design h_d would be based on the failure mechanism overflow, the lower limit of $f_{ovx} = 1$ which means the dike heights are based on the water level distribution as used to derive equation (5.1). In fact there is no theoretical upper limit for f_{ovx}. Some practical considerations and results based on calculations are provided in the Intermezzo in the greybox below.

Intermezzo: scale parameter for dike height

The scale parameter for dike height considering the failure mechanism wave overtopping is $f_{ovx} \cdot B$, with theoretically $f_{ovx} \geq 1$ as explained in the main text. f_{ovx} is 1 in case only water level would be considered.
The dike height is the sum of water level and freeboard. Therefore, in case of full dependence between water levels and waves in combination with depth limited wave conditions, which could occur in coastal zones, f_{ovx} will be much larger than 1. Depth limited wave heights $H_s \approx 0.5$ to 0.6 times the waterdepth. The freeboard for mild sloped dikes (1:4) is approximately 2 to 2.5 times H_s [149]. Together this leads to a freeboard of about 1 to 1.5 times the water depth. Therefore the scale parameter of dike heigth is larger than B up to a scale parameter factor $f_{ovx} \approx 2$ to 2.5. The more wave attack, especially in case it is combined with water level set-up, the larger the scale parameter for dike height. Locations which are located exposed to wave attack would get higher values of f_{ovx} than locations located lee.
For about 80 locations in the Netherlands f_{ovx} is calculated based on existing results of calculations with HYDRA-NL [144]. This resulted for different areas and coastal environments in different values f_{ovx}, as shown in Figure 5.3. The Figure shows the range of values of f_{ovx}. The more exposed the location, the larger f_{ovx}. All values exceeds 1, except one for which offshore wind directions could cause this below-theoretical value.
Note, the f_{ovx} decreases (theoretically) to the lower limit in case in-

finite large overtopping discharges would be acceptable. Thus, the larger the accepted overtopping discharge the lower f_{ovx}.

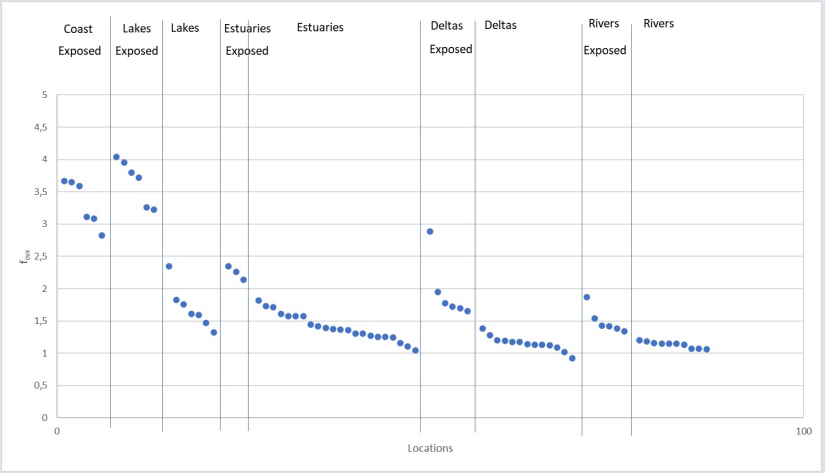

Figure 5.3.: *Determination of f_{ovx} for 78 locations in different areas with different dike profiles, with separate selections for exposed locations and several different water systems.*

The following practical starting points are used to apply the approach of the first Delta Committee [50] for comparison with [51]:

- optimizing per dike segment as a whole, thus neglecting the differences of loads, strength and consequences within a dike segment. The assumption is that, in case the dike and the hydraulic loads do not change that much along the dike segment, this will only effect the result marginally.
- Determine the timing of the first reinforcement to come at $t = \Delta t$ neglecting the changes in the second term in equation (5.3) after the first reinforcement. This means in practice that the dynamic effects on risks (the second term in equation (5.3)) are neglected after $t = \Delta t$, see Figure 5.4. Note, the larger $t = \Delta t$ the more comparable the approaches presented in section 5.2.

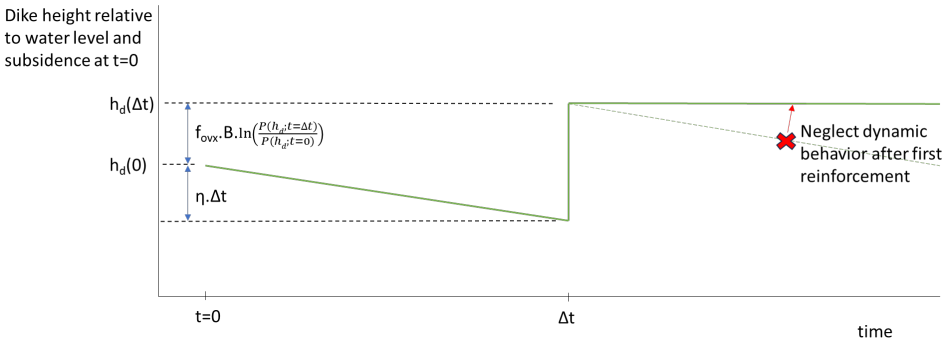

Figure 5.4.: *Schematic representation of the relative dike height h_d in time.*

The following relations are implemented for investments and damage over time, which are based on [51] :

- In [51] the i^{th} investment costs for dike segment j is assessed by:

$$I_{ij} = (I_0 + \Delta h_{d_i} \cdot I') \cdot f_{I_{ij}} \tag{5.7}$$

In which:

Δh_{d_i}	Dike height increase of the i^{th} successive dike height increase.	–
$f_{I_{ij}}$	Parameter indicating the cost of the next dike reinforcements is higher than the earlier ones due to increased dimensions, for dike segment j, in [51] taken as $exp\left(\lambda_j \cdot \sum_i \Delta h_{d_i}\right)$	-
λ_j	Parameter indicating the cost of the next dike increases is higher than the earlier ones, for dike segment j	*per m*

- In [51] the damage over time is assessed based on the assumptions of economic growth and the effects of water level increase and dike height increase, both leading to larger damage in case of a flood event:

$$\begin{aligned} D_\delta(\Delta t^i) &= D(0) \cdot (1+\delta)^{\Delta t} \cdot f_h(\Delta t) \cdot \prod_i f_{\Delta h_{d_i}}(\Delta t) \\ f_h(\Delta t) &= exp(\Psi_j \cdot \eta_j \cdot \Delta t) \\ f_{\Delta h_{d_i}}(\Delta t) &= exp(\zeta_j \cdot \Delta h_{d_i}(\Delta t)) \equiv \frac{D_\delta(\Delta t^i)}{D_\delta(\Delta t^{i-})} \end{aligned} \tag{5.8}$$

In which:

$D(0)$	Flood event damage at t=0	€
$D_\delta(\Delta t^i)$	Damage just after the i^{th} reinforcement. With $D_\delta(\Delta t^{i-})$ The damage just before the i^{th} reinforcement	€
$f_h(\Delta t)$	Factor indicating the flood event damage increase due to effect of water level increase.	–
η_j	Relative deterioration, including climate change effect on water level and subsidence, for dike segment j	$m/year$
$f_{\Delta h_{d_i}}(\Delta t)$	Factor indicating the flood event damage increase due to effect of i successive dike height increases up to Δt.	–
$\Delta h_{d_i}(\Delta t))$	The i^{th} dike height increase at Δt.	–
ζ_j	Increase of damage through dike heightening	$1/m$
Ψ_j	Parameter for additional damage due to gradual and permanent increase of load water levels due to e.g. climate changes	–

With this assumptions and starting points the intervention timing representing the dynamic effect in (5.3) can be included in the approach of the first Dutch Delta Committee. Since the analysis in this thesis is executed per dike segment, and for a single reinforcement, in the following the indicators i and j are omitted. The probabilities before the intervention at Δt and after the intervention are respectively:

$$\begin{aligned} P_f(h_d(t)) &= exp\left(-\frac{h_d(0)-(A+\eta\cdot t)}{f_{ovx}\cdot B}\right) \quad t<\Delta t \\ P_f(h_d(t)) &= exp\left(-\frac{h_d(\Delta t)-(A+\eta\cdot t)}{f_{ovx}\cdot B}\right) \quad t\geqslant\Delta t \end{aligned} \tag{5.9}$$

In which:

$P_f(h_d(t))$	Probability of failure due to overtopping at time t	$peryear$
$h_d(0)$	Dike heigth at $t=0$	$m+SWL$
Δt	Reinforcement time	$year$
$h_d(\Delta t)$	Reinforced dike height at $t=\Delta t$ relative to water level and subsidence at $t=0$	$m+SWL$
A	Location parameter of the exponential water level distribution	$m+SWL$

f_{ovx}	Factor to convert the water level scale parameter B into the dike height scale parameter taking wave overtopping into account, which is the ratio between dike heigth increase and water level increase for equal frequency decrease for both	–

Just as in (5.1) and (5.3) the sum of risks and investments is minimized, however, the timing of the investment I is not necessarily at t=0, thus these cost has to be included as a present value as well:

$$C_{tot}^{PV} = I^{PV} + R^{PV} \tag{5.10}$$

In which:

C_{tot}^{PV}	Present value of total cost of investments and risks	€
I^{PV}	Present value of investments	€
R^{PV}	Present value of Risks R, in which $R = P_f(h_d(t)) \cdot D_\delta(t)$	€

Figure 5.4 shows the schematisation in time, distinguishing the situation before the intervention and after. The dike reinforcement height is assessed by:

$$\Delta h_d = (h_d(\Delta t) - (h_d(0) - \eta \cdot \Delta t)) \tag{5.11}$$

The optimal design dike height is found minimizing the cost, with the intervention timing as a degree of freedom:

$$\frac{\mathrm{d}C_{tot}^{PV}}{\mathrm{d}h_d(\Delta t)} = 0 \tag{5.12}$$

Therewith, in Appendix B.1 the probability of flooding is derived corresponding with the economic optimal design:

$$P_{f_{opt}}(\Delta t) = \frac{I' \cdot B \cdot r}{D(0)} \cdot \frac{f_I \cdot f_{ovx}}{(1+\delta)^{\Delta t}} \tag{5.13}$$

In which:

$P_{f_{opt}}(\Delta t)$	Economic optimal design probability of flooding for a reinforcement at time (Δt)	$per year$
f_I	Parameter indicating the cost of the next dike reinforcement is higher than the last one due to increased dimensions	-

Equation (5.13) looks quite alike equation (5.2) except the factor f_{ovx} to translate the scale parameter for water level B to a scale parameter for dike height, the factor f_I to correct investments for increasing dike dimensions, and the time dependence of the damage D due to economic growth $(1+\delta)^{\Delta t}$. In (5.13) the Δt is the remaining unknown parameter. With $t = \Delta t$ the optimal probability of flooding is time dependent, corresponding with the time dependent optimal design curve, presented as the lower line in Figure 5.1 copied from [51]. Note, I' is no subject to economic growth δ in both approaches.

5.2.3. UPPER LIMIT OF FLOOD PROBABILITIES DETERMINING BENEFICIAL TIME FOR INTERVENTION

For comparison of both approaches assessment of the upper limit of the floods probabilities in time in [51] is needed as well. For this the utility criterion in [32, 50] is used: an intervention at time Δt is economic beneficial if the economic risk reduction transcends the investments:

$$\Delta R^{PV}(\Delta t) - I^{PV}(\Delta t) > 0 \tag{5.14}$$

In which:

$\Delta R^{PV}(\Delta t)$	Present value of risk difference in case of intervention at time Δt	€
$I^{PV}(\Delta t)$	Present value of investment at time Δt	€

The following simplifying starting point is taken, additional to the ones in section 5.2.2:

- The probabilities of flooding are continuously increasing in time, which is quite reasonable regarding subsidence and climate change.
- The dike height after reinforcement meets $P_{standard}$, determining the investment at Δt with equation (5.7) given Δh_d (NB. $P_{standard}$ is the pursued or targeted design probability of flooding at Δt, which in practice is not necessarily equal to $P_{f_{opt}}(\Delta t)$).

Substituting equation (5.11) in (5.9) for $t = \Delta t$ provides the reinforcement height Δh_d, including the relative decrease of dike height due to subsidence and climate change (see as well Figure 5.4):

$$\Delta h_d = \eta \cdot \Delta t + f_{ovx} \cdot B \cdot ln\left(\frac{P_f(0)}{P_{standard}}\right) = \eta \cdot \Delta t + f_{ovx} \cdot B \cdot f_{dp} \tag{5.15}$$

In which:

$P_f(0)$	Probability of flooding at $t = 0$.	$per year$
$P_{standard}$	Targeted design probability of flooding at Δt.	$per year$
f_{dp}	Factor representing the logarithm of the division between the actual probability and the standard, the probability after reinforcement: $f_{dp} = ln\left(\frac{P_f(0)}{P_{standard}}\right)$.	-

Therewith, in Appendix B.2 the probability of flooding just before intervention is derived:

$$P_f(\Delta t^-) = f_{\Delta h_d} \cdot \left(P_{standard} + \frac{r \cdot f_I}{D_\delta(\Delta t)} \cdot \left(I_0 + \left(\eta \cdot \Delta t + f_{ovx} \cdot B \cdot f_{dp}\right) \cdot I'\right)\right) \tag{5.16}$$

In which:

$P_f(\Delta t^-)$	Probability of flooding just before intervention, see equation (5.9).	$per year$

Note, $P_f(\Delta t^-)$ is always larger than $P_{standard}$ in case $P_f(0) > P_{standard}$. This is normally the case since $P_{standard}$ realized at the last reinforcement and the probabilities are increasing in time. With $t = \Delta t$ the optimal intervention probability of flooding is time dependent, corresponding with the time dependent upper lines in Figures 3 and 4 in [51].

5.2.4. DERIVATION OF INTERVENTION TIMING

The upper limit in equation (5.16) in section 5.2.3 can be used to derive the first beneficial time to intervene, see the derivation of equation (B.23) in Appendix B.3:

$$\Delta t = \frac{f_{ovx} \cdot B}{\eta} \cdot ln\left(f_{\Delta h_d} \cdot \frac{P_{f_{opt}}(\Delta t)}{P_f(0)} \cdot \left(\frac{I_0}{I' \cdot f_{ovx} \cdot B} + \frac{\eta \cdot \Delta t}{f_{ovx} \cdot B} + f_{dp} + \frac{P_{standard}}{P_{f_{opt}}(\Delta t)}\right)\right) \tag{5.17}$$

representing the first economic optimal reinforcement time. This is an implicit equation: the parameter Δt is on both sides of the equality sign. Despite the formula is still not completely explicit for Δt it is quickly converging since the Δt at the right side of the equality sign is under the logarithm sign. NB. a first estimate for Δt can be made using 50 years which is usual for dikes. Furthermore, this equation may lead to negative values of Δt in case the first time of beneficial investment is already

passed at $t = 0$.

Equation (5.17) contains parameters which are all needed for traditional dike design, no additional data is required:

- Water level decimation height, related to the scale parameter B
- Ratio between the scale parameter for dike height and for water level f_{ovx}
- Relative water level increase rate (including e.g. climate change and subsidence) η
- Actual probability of flooding $P_f(0)$
- The pursued or targeted design probability of flooding $P_{standard}$
- Investment data I_0 and I'
- Starting points for economic analyses: discount rate r, growth rate δ
- Potential flood damage D at $t = 0$

Some special cases enable to further simplify equation (5.17). A first special case is if the dike is compliant to $P_{standard}$ at $t = 0$, because f_{dp} (which is the logarithm of $P_f(0)/P_{standard}$) becomes zero and will disappear. Equation (5.17) then looks like:

$$\Delta t = \frac{f_{ovx} \cdot B}{\eta} \cdot ln\left(f_{\Delta h_d} \cdot \frac{P_{f_{opt}}(\Delta t)}{P_f(0)} \cdot \left(\frac{I_0}{I' \cdot f_{ovx} \cdot B} + \frac{\eta \cdot \Delta t}{f_{ovx} \cdot B} + \frac{P_{standard}}{P_{f_{opt}}(\Delta t)}\right)\right) \tag{5.18}$$

A second special case emerge as the design probability $P_{standard}$ is defined as the economic optimal probability, because the last term will become equal to 1. Equation (5.17) then looks like:

$$\Delta t = \frac{f_{ovx} \cdot B}{\eta} \cdot ln\left(f_{\Delta h_d} \cdot \frac{P_{f_{opt}}(\Delta t)}{P_f(0)} \cdot \left(\frac{I_0}{I' \cdot f_{ovx} \cdot B} + \frac{\eta \cdot \Delta t}{f_{ovx} \cdot B} + ln\left(\frac{P_f(0)}{P_{f_{opt}}(\Delta t)}\right) + 1\right)\right) \tag{5.19}$$

A third special case is as the dike at $t = 0$ is compliant to the economic optimal probability ($P_{f_{opt}}(0)$), and the design probability $P_{standard}$ at time Δt is defined as the economic optimal probability ($P_{f_{opt}}(\Delta t)$). In Appendix B.3 this special case is figured out resulting in the remarkable handy equation (B.29), which could be simply applied to indicate the economically optimal standard and design horizon:

$$\Delta t = \frac{f_{ovx} \cdot B}{\eta + \delta \cdot f_{ovx} \cdot B} \cdot ln\left(f_{\Delta h_d} \cdot \left(\frac{I_0}{I' \cdot f_{ovx} \cdot B} + \frac{\eta \cdot \Delta t}{f_{ovx} \cdot B} + \delta \cdot \Delta t + 1\right)\right) \quad (5.20)$$

Again, just as equation (5.17) equation (5.20) is not completely explicit, but it quickly converges, since the Δt at the right side of the equality sign is under the logarithm sign. NB. A first estimate for Δt can be made using 50 years which is usual for dikes.

With the result of the economic optimal intervention timing the derivation of the flood probabilities over time in the adapted Delta Commitee approach is ready for comparison in a case.

5.2.5. COMPARISON FOR DUTCH DIKE SEGMENTS

The comparison between the two approaches introduced in the previous sections is performed for the results of the optimal probability of failure as presented in [51], with the following starting points:

- The comparison is carried out for the year 2050, per dike segment, for the practical reason of availability of data in [51]. The economic growth (1.9%) and discount (5.5%) are used as presented in [51]. The listed actual values for I, D and $P_{f_{opt}}$ in [51] were used.
- Additional data used in [51] is needed for η, $P_f(0)$, decimation heights h^{10} and h_d^{10}, and damage increase factors due to dike height and water level increase, here denoted as ζ and Ψ respectively, and data for increase of investments for additional dike heights λ. These data is provided by its author on request. It is available for dike subsegments.
- The comparison with the adapted approach of the first Delta Commission is carried out on dike segment level. Therefore, the data on dike subsegment level is translated to segment level by a length-based average for η, decimation heights h^{10} and h_d^{10}, ζ and Ψ. The actual probability $P_f(0)$ for the dike segment is based on dependent failure of subsegments.
- The optimal probability of failure, the so-called middle probability is calculated as the mean of upper limit in equation (5.13) and the lower limit in equation (5.16)

Due to the weak dependence of the factors in equation (5.8) on the dike height increase, the calculation of the upper and lower limits is slightly implicit, requiring some iterations to obtain a stable solution. Figure 5.5 shows the comparison for the middle probabilities in year 2050, for the case no reinforcements would have been executed by then. To distinguish the data in a part for which the first beneficial intervention timing is before 2050 and a part for which this is after 2050, the optimal

design horizon is estimated with equation (5.17). The comparison for the dots in blue, for which the first beneficial intervention timing is beyond 2050, is rather good, the trend is similar. The samples for the dikes for which reinforcement would be beneficial before 2050 (orange dots) are in less good agreement.

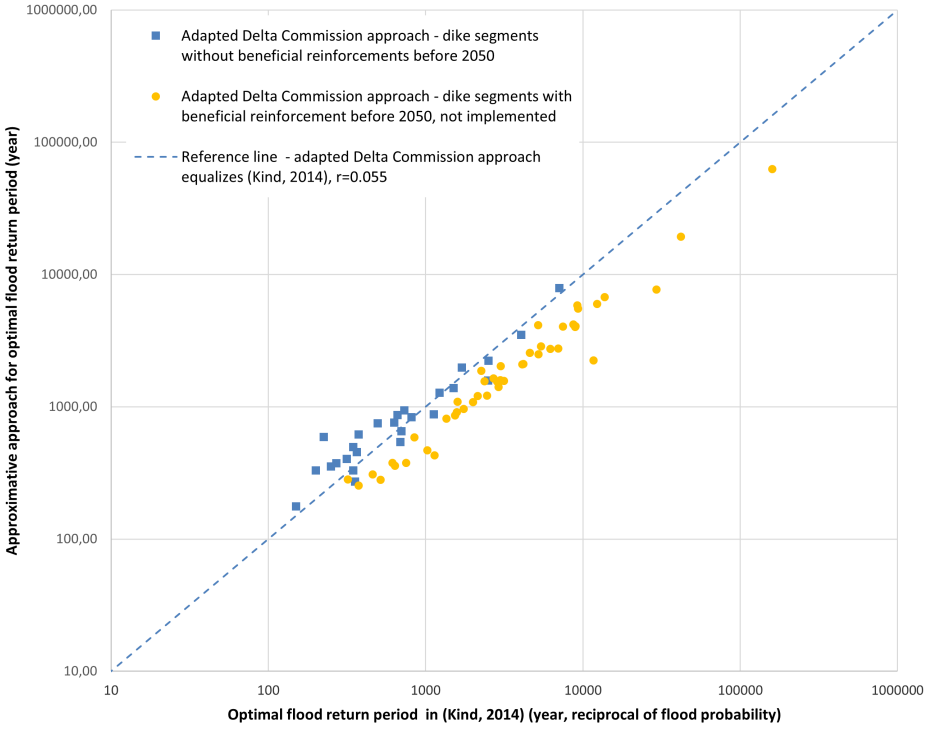

Figure 5.5.: *Comparison of the adapted Delta Commission approach with the results of [51]. The results took no reinforcements into account, despite there are dike segments for which they would be beneficial (orange dots).*

Therefore, some of the data records for dike segments could have been subject for reinforcement between 2011 (the reference of the data records in [51]) and 2050 due to the exceedance of the upper limit before 2050, however, this is not recorded in [51]. The less good agreement of the dike segments for which reinforcement would be beneficial indicates the relevance to include the effect of reinforcements in the present comparison. Figure 5.6, representing the results of the third special case in equation (5.20) in section 5.2.4 using the same data as used for Figure 5.5, indicates the life time of reinforcements. Most of the results are in

the same course: as expected, a higher ratio between fixed and marginal costs will lead to a longer design horizon. Some data points seem to be outliers but these are situated in controlled water systems in small lakes, with very small yearly water level increase η. This is demonstrated in Figure 5.7 in which the dots are divided in classes of $\eta \cdot (f_{ovx} B)^{-1}$, which is the reciprocal of the first term in equation (5.17) determining the intervention time. Despite the average equals about 38 years, there are several dike segments with life times of less than 20 years, because of relatively low fixed costs. Since the comparison is executed for the period 2011 until 2050, almost 40 years, this confirms the proposition that inclusion of reinforcements may improve the comparability of both approaches considered in this section.

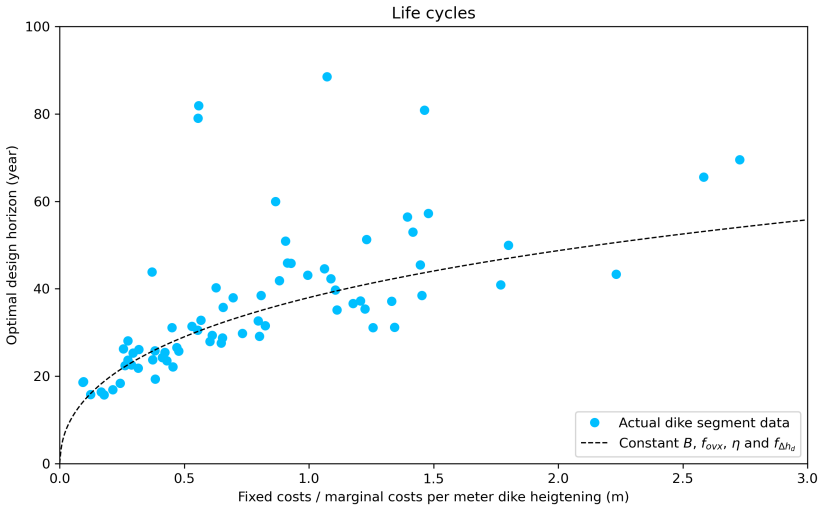

Figure 5.6.: *Optimal intervention interval for the dike segments in [51] (blue dots). The curve is obtained with constant values for B (0.3m) , f_{ovx} (1.5), η (0.01 m/year) and ζ (0.2).*

To include the effect of reinforcements the calculation schedule is used as presented in Figure 5.8. Based on a first estimate to find out whether the first reinforcement would be beneficial before the horizon of interest, it is decided to whether or not enter the right grey reinforcement loop which performs an reinforcement. In case the next reinforcement interval would exceed the horizon of interest the left grey block in the schedule is chosen to estimate the upper and lower limits at the horizon of interest. Note, the loops within both grey boxes contain a minor step for convergence of the factors f_I, f_h, and $f_{\Delta hd}$ which are based on the magnitude of the reinforcement itself.

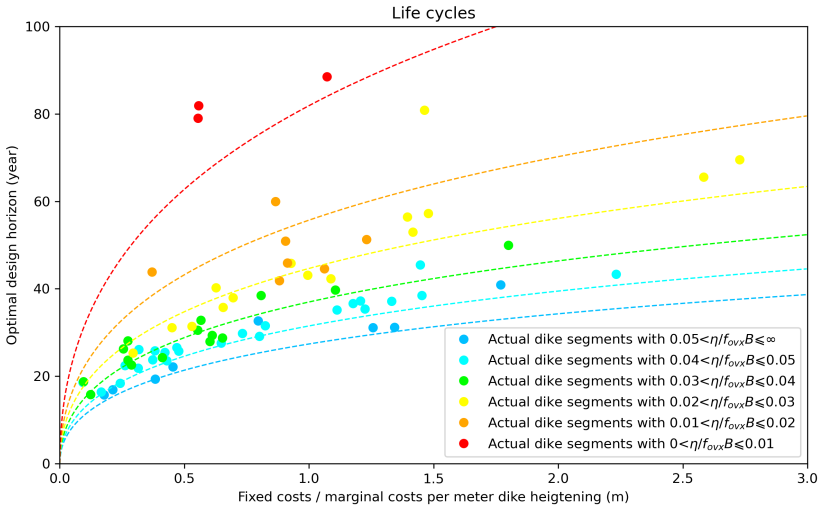

Figure 5.7.: *Optimal intervention interval for the dike segments in [51] divided in classes for $\eta \cdot (f_{ovx} B)^{-1}$ (coloured dots). The coloured curves corresponding to these classes are obtained with constant values per class for B, f_{ovx}, η and ζ. In blue, light-blue, green, yellow, orange and red respectively the following values are used for B (0.38, 0.23, 0.19, 0.17,0.15, 0.14), f_{ovx} (1.05, 1.15, 1.25, 1.35, 1.45, 1.55) η (0.0004, 0.004. 0.006. 0.008, 0.01, 0.012) and ζ (0.2 for all).*

The additional starting points for the calculations including the effect of interventions are:

- The upper limit is taken absolute, starting from the point of view sufficient budget and sufficient execution capacity is available. Therefore, if the probability exceeds the upper limit given by equation (5.17) before t=39 (target year 2050 minus the start-year of analyis 2011), then a reinforcement is executed.
- In case reinforcement appeared to would have been beneficial before 2011 (the start of analysis and the basis of the data records), 2011 is taken as the first reinforcement time.
- The reinforced dike is designed at the safety level of the lower limit for $t = \Delta t$. The probability $P_{f_{opt}}(\Delta t)$ just after reinforcement is taken as the new $P_f(0)$, and the term $\eta \cdot \Delta t$ in equation (5.9) is changed in $\eta \cdot (t - \Delta t)$

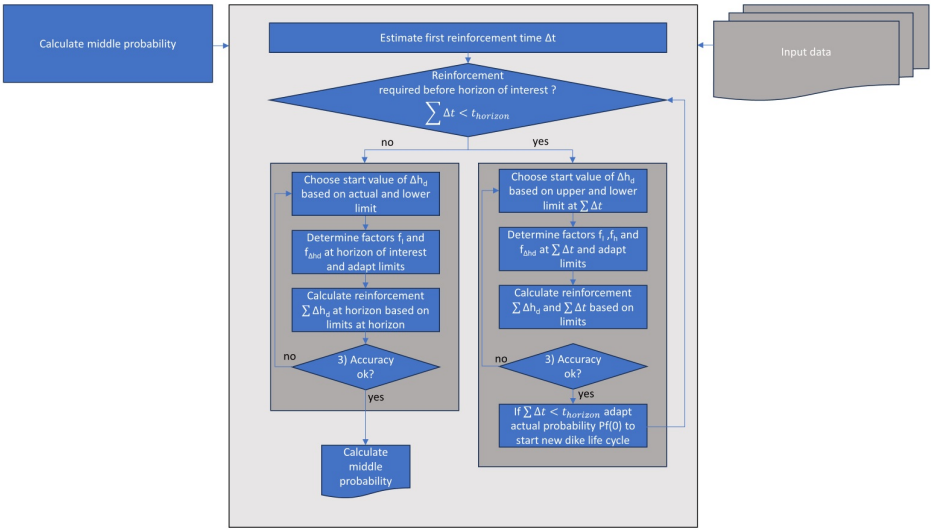

Figure 5.8.: *Flowchart determination of middle probabilities for Adapted Delta Commission approach.*

- Calculating the upper limit with equation (5.16) $P_{standard}$ is taken equal to the economic optimal probability ($P_{f_{opt}}(\Delta t)$).
- For completed reinforcements before the horizon of interest, the factor $f_{\Delta h_d}$ is based on a reinforcement height equal to $f_{ovx} \cdot B \cdot ln\left(p_{upper\ limit}/p_{lower\ limit}\right)$ at the time of the reinforcement. In case of the last dike life cycle, not ending with a reinforcement, it is taken as $f_{ovx} \cdot B \cdot ln\left(p_{actual}(t_{horizon})/p_{lower\ limit}\right)$.
- More than one reinforcement is possible, following the schedule in Figure 5.8 again, using $\sum \Delta t$ in stead of Δt in the second block to evaluate whether another reinforcement would be necessary.
- Iterations has been performed to find a stable value for Δt for a dike segment.

Figure 5.9 shows the comparison for the middle probabilities in year 2050, for the case the beneficial reinforcements are executed. the comparison is much better than in Figure 5.5. The average difference between the return periods based on the Adapted Delta Commission approach and [51] is only about 5% on an average. The comparison is carried out again for results for a discount rate of 3%, see Figure 5.10, for which the average differences with the approach of [51] is about 10% with respect to return periods. Based on these results the analytical approach of the lower and upper limits as well as the estimates of the intervention timing, respectively in sections 5.2.2 and 5.2.3 are considered to

be in the same order of accuracy as the calculations in [51]. Therewith, the approach may be used for standard estimations.

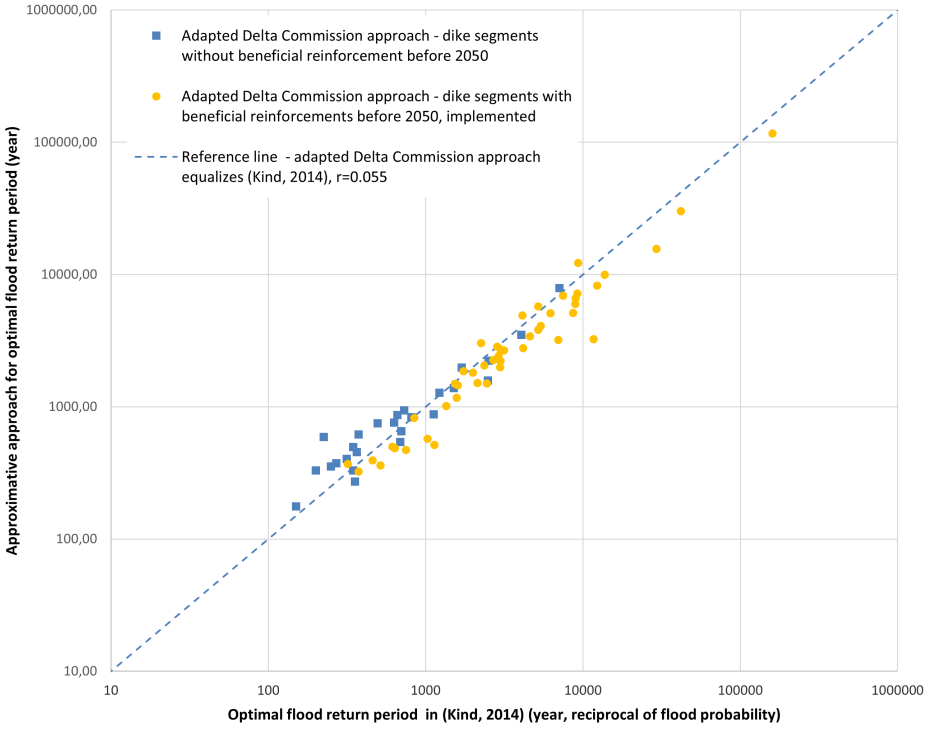

Figure 5.9.: *Comparison of the adapted Delta Commission approach with the results of [51]. The results took the reinforcements into account for dike segments for which that would be beneficial (orange dots).*

To extent the case so far, which concerned only the year 2050 for the reason of availability of results in [51], the course of the flood probabilities over time is figured out to serve as qualitative verification on the adapted Delta Commitiee approach.

The situation without reinforcement steps is straight forward. Equation (5.13) is like the curve for the lower limit in [51], and equation (5.16) is like the upper limit curve in [51], both with Δt substituted by t.

Despite the theory is figured out for the time until and including the first reinforcement, the time beyond the first reinforcement step is assessed like the flow chart presented in Figure 5.8. Therewith, a time dependent safety level and dike height pattern can be developed, starting after each reinforcement with $t = 0$ for calculating the upper limit with

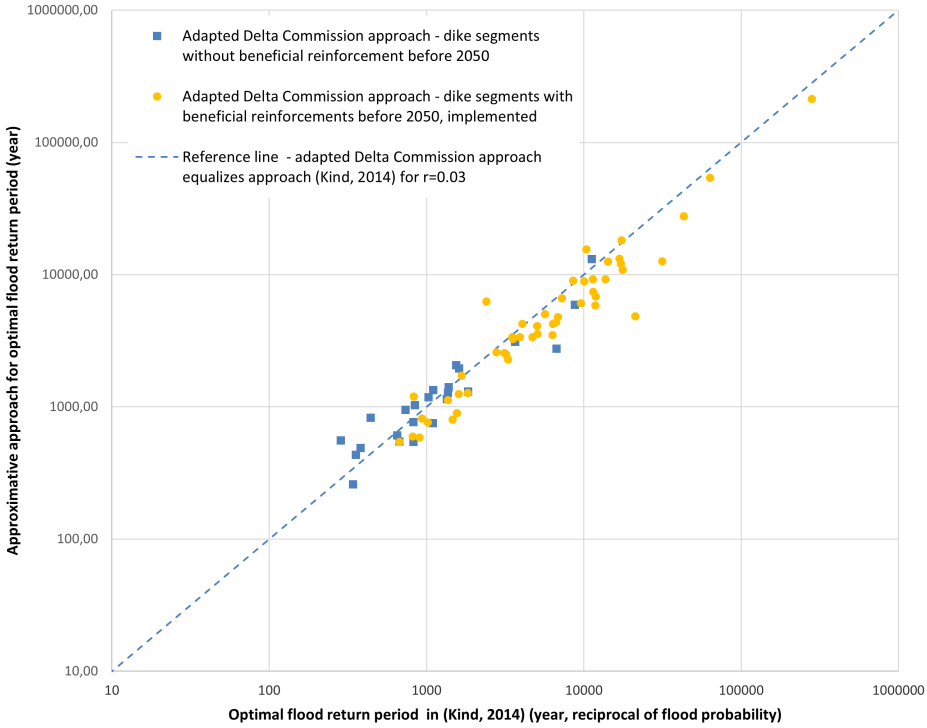

Figure 5.10.: *Comparison of the adapted Delta Commission approach with the results of [51] derived for r=3.0%. The results took the reinforcements into account for dike segments for which that would be beneficial (orange dots).*

equation (5.16) and using $P_f(0)$ equal to the lower limit at the time of the last reinforcement. Dike height over time is found rewriting equation (5.9):

$$h_d(t) - A = f_{ovx} \cdot B \cdot ln(P_f(0)) - \eta \cdot t \qquad \textit{before } 1^{st} \textit{ reinforcement}$$

$$h_d(t) - A = f_{ovx} \cdot B \cdot ln(P_{f_{opt}}(\Delta t)) - \eta \cdot (t - \sum \Delta t) \qquad \textit{after } 1^{st} \textit{ reinforcement} \tag{5.21}$$

In which:

$\sum \Delta t$	Time of most recent intervention	*year*

A case 'safety over time' is figured out for dike segment IJsseldelta (de-

noted with 11-1 in [51]). The data used is given in Table 5.1. Figures 5.11 and 5.12 provide respectively the probability development over time and the dike height differences over time relative to its value at the start of the analysis.

Table 5.1.: *Data for dike segment IJsseldelta (denoted with 11-1 in [51]) for the case 'safety over time'.*

Parameter	**Value**	**Unity**
$P_{f_{actueel}}$	1/1000	*per year*
I	$71 \cdot 10^6$	*€/m*
I_0	$128 \cdot 10^6$	*€*
B	0.12	*m*
r	5.5	*%*
η	0.007	*m/year*
$D(t=0)$	$2477 \cdot 10^6$	*€*
δ	0.019	*per year*
λ	0.16	*per m*
ζ	0.088	*per m*
Ψ	0.0	*per m*

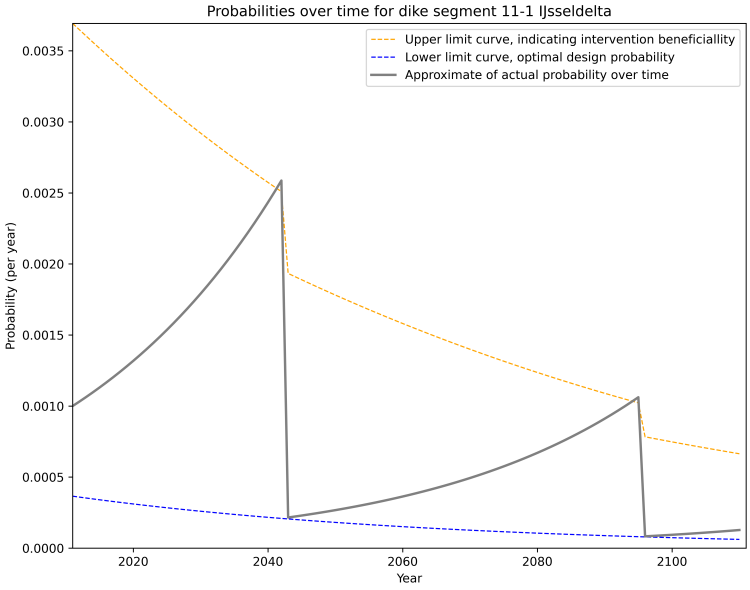

Figure 5.11.: *Probabilities over time, together with its upper and lower limits, for dike segment IJsseldelta, in [51] denoted by 11-1.*

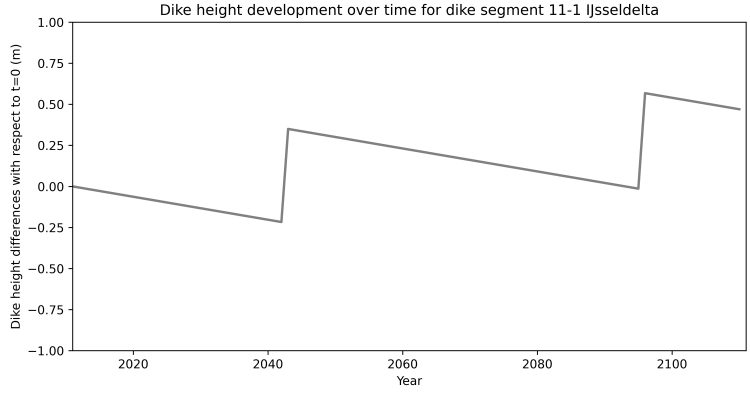

Figure 5.12.: *Dike height over time, relative to parameter A in its exponential dike height distribution, for dike segment IJsseldelta, in [51] denoted by 11-1.*

5.3. RELIABILITY STANDARDS - ANALYSIS FOR TWO FAILURE MECHANISMS

5.3.1. INTRODUCTION AND STARTING POINTS

The approaches determining the economic optimal failure probability in [14, 51] and the developed analytical approach in section 5.2 only involve the failure mechanism overtopping. In this section the effect is eleborated of the potential occurrence of a second failure mechanism, which potentially could cause a second occurrence of damage.

Since the analytical approach in section 5.2 appeared to be sufficient accurate, the Adapted Delta Commission method is assumed to be usable for the analysis of the effect of two failure mechanisms. This is convenient since it enables to use the exponential distribution of water levels as a simplifying starting point in the derivation the optimal failure probabilities (see section 5.2.2). Therefore, the analysis starts from the approach of the first Delta Commission [50]. The following starting points are used to perform an analysis like section 5.2:

- Piping is elaborated as a second failure mechanism. Piping may occur due to the berm is not high enough above polder level, just at the toe of the inner slope, or due to the berm is not long enough, just at the toe of the berm.
- The simple rule of Bligh is used [150]: no piping will occur in case:

$$\Delta H_{cr} < \frac{L}{c_p} \tag{5.22}$$

In which:

ΔH_{cr}	Critical head $h - h_m$ or $h - h_b$ over the dike	m
L	Minimum length to prevent piping, in case of no additional lengths next to the dike this is the minimal required length of the dike footprint	m
h_m	Polder water level	$m + NAP$
h_b	Berm level	$m + NAP$
c_p	Piping factor, with a value of 18 in the rule of Bligh	$-$

- The marginal costs I' are based on the cross sections surface. The failure mechanism overtopping mainly determines dike heights. The failure mechanism piping mainly determines the dimensions of the berm. Both, these failure mechanisms determine the surface of dikes' cross section. Therefore, instead of cost optimization based

on dike height in equation (5.12), the surface of the dike cross section is taken as the basis for cost minimization.

- The requirements in the cross section originating from other failure mechanisms, such as geotechnical stability which may require some additional berm height or some gentler inner slope, are assumed to be less important.
- The time dependency of the optimal flood probability, as illustrated in section 5.2, is not considered. Therefore, the analysis is set up to solve equation (5.1) in stead of (5.10).
- Some dikes are that high and mild sloped that the footprint of the dike is that wide that no berm is required to reduce the piping probability sufficiently. In this situation the berm width is equal to zero. In fact it is a special case of the analysis. Therefore, in this Section these two situations are considered consecutively: with berm and without berm.

Figure 5.13 provides an overview of this sections order. The total costs C_{tot}^{PV}, in practice as well denoted with Total Cost of Ownership (TCO), are derivated in the sections 5.3.2 and 5.3.3 (for the situation with and without berm respectively). Then, in section 5.3.4, a case for some locations in the Netherlands is carried out. A numeric approach had been set-up to check the implementation.

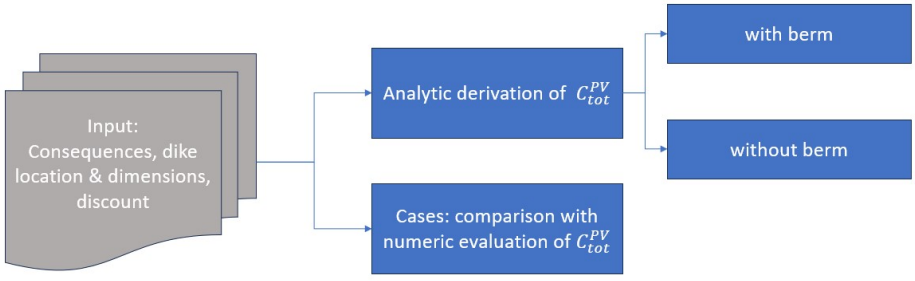

Figure 5.13.: *Flowchart of section 5.3.*

5.3.2. DERIVATION FOR SITUATION WITH BERM

A schematic overview of a dike cross section is given in Figure 5.14. With the parameters defined in the Figure, the surface of dikes' cross section is:

$$S_d = \left(Br_d + (cot\alpha_{bu} + cot\alpha_{bi}) \cdot \frac{h_d - h_m}{2} \right) \cdot (h_d - h_m) + L_b \cdot (h_b - h_m) \quad (5.23)$$

In which:

S_d	Dikes cross sections surface, a volume per meter dike length	m^3/m
Br_d	Dikes crest width	m
$cot\alpha_{bu}$	Cotangent of the outer dike slope	$-$
$cot\alpha_{bi}$	Cotangent of the inner dike slope	$-$
L_b	Length of berm	m
h_b	Height of berm with respect to reference level	$m + NAP$
h_m	Polder water level	$m + NAP$
h	Outside water level	$m + NAP$
h_d	Dike crest heigth level	$m + NAP$

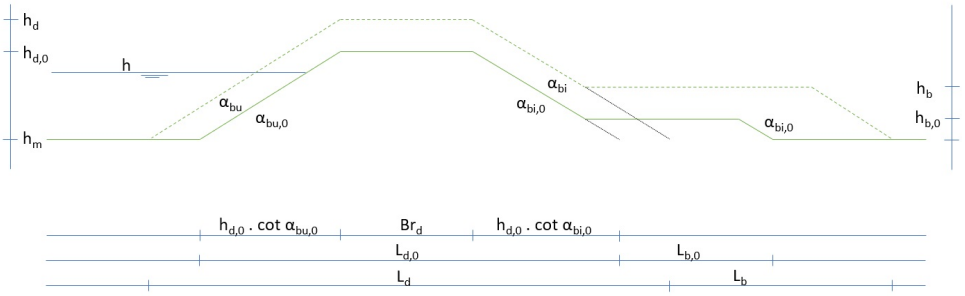

Figure 5.14.: *Schematic overview of a dike cross section. The dimension parameters are added with a '0' to denote the situation before reinforcement. In dashed the cross section includes a reinforcement.*

With the water level distribution $F(h) = 1 - exp\left(-\frac{h-A}{B}\right)$ as in section 5.2.2, the probabilities of failure due to respectively overtopping and piping at inner slope or berm toe are expressed dependent on dike dimensions:

$$
\begin{aligned}
P_{f_{h-d}}(h_d) &= exp\left(-\frac{h_d - A_{h_d}}{f_{ovx} \cdot B}\right) \\
P_{f_{pip-is}}(h_{cr_{is}}) &= exp\left(-\frac{h_{cr_{is}} - A_h}{B}\right) \\
P_{f_{pip-bt}}(h_{cr_{bt}}) &= exp\left(-\frac{h_{cr_{bt}} - A_h}{B}\right)
\end{aligned}
\tag{5.24}
$$

In which:

$h_{cr_{is}}$	Critical water level for piping at inner slope, equal to $h_b + \Delta H_{cr_{is}}$	$m + NAP$
$h_{cr_{bt}}$	Critical water level for piping at berm toe, equal to $h_m + \Delta H_{cr_{bt}}$	$m + NAP$
$\Delta H_{cr_{is}}$	Critical head for piping at inner slope, referring to equation (5.22) equal to $\frac{L_d - (h_b - h_m) \cdot cot\alpha_{bi}}{c_p}$	m
$\Delta H_{cr_{bt}}$	Critical head for piping at berm toe, referring to equation (5.22) equal to $\frac{L_d + L_b}{c_p}$	m
L_b	Length of berm	m
L_d	Virtual footprint of dike excluding the berm	m
$P_{f_{h-d}}(h_d)$	Probability of failure due to overtopping, dependent on h_d	*per year*
$P_{f_{pip-is}}$	Probability of failure due to piping at inner slope, dependent on $(L_d, h_b, h_m, \alpha_{bi})$	*per year*
$P_{f_{pip-bt}}$	Probability of failure due to piping at berm toe, dependent on (L_d, L_b, h_m)	*per year*
A_{h_d}	Parameter in the exponential distribution for required dike crest height. Note, this parameter depends on the overtopping discharge	$m + NAP$
A_h	parameter in the exponential water level distribution	$m + NAP$

which can be rewritten as:

$$
\begin{aligned}
P_{f_{h-d}}(h_d) &= exp\left(-\frac{h_d - A_{h_d}}{f_{ovx} \cdot B}\right) \\
P_{f_{pip-is}}(h_{cr_{is}}) &= exp\left(-\frac{L_d - (h_b - h_m) \cdot cot\alpha_{bi} + c_p \cdot (h_b - A_h)}{c_p \cdot B}\right) \\
P_{f_{pip-bt}}(h_{cr_{bt}}) &= exp\left(-\frac{L_d + L_b + c_p \cdot (h_m - A_h)}{c_p \cdot B}\right)
\end{aligned}
\tag{5.25}
$$

Following the Delta Commissions approach equation (5.1) is elaborated as:

$$
C_{tot}^{PV} = I + \sum P_f \cdot \frac{D}{r} = I + \frac{D}{r} \cdot \left(P_{f_{h-d}}(h_d) + MAX(P_{f_{pip-is}}(h_{cr_{is}}), P_{f_{pip-bt}}(h_{cr_{bt}}))\right) \tag{5.26}
$$

Herein, the term with the product of the both probabilities for overtopping and piping, which is normally distracted to prevent double counting, is neglected because of the small probabilities. Furthermore, the consequences D are assumed to be independent of the type of failure. Furthermore, the two piping mechanisms are assumed to be fully dependent, and both are assumed to be independent from the overtopping mechanism. Which of both piping submechanisms prevails depends on the berm length relative to berm height: equalizing the critical heads for piping at berm toe $h_m + \frac{L_d + L_b}{c_p}$ and for piping at inner slope $\frac{L_d - (h_b - h_m) \cdot cot\alpha_{bi}}{c_p}$ leads to $L_b = (h_b - h_m) \cdot (c_p - cot\alpha_{bi})$. Therewith, it follows whether piping will occur at berm toe or at inner slope:

$$\begin{aligned} P_{f_{pip}} &= P_{f_{pip-is}}(h_{cr_{is}}) \quad L_b > (h_b - h_m) \cdot (c_p - cot\alpha_{bi}) \\ P_{f_{pip}} &= P_{f_{pip-bt}}(h_{cr_{bt}}) \quad L_b \leqslant (h_b - h_m) \cdot (c_p - cot\alpha_{bi}) \end{aligned} \tag{5.27}$$

In which:

$P_{f_{pip}}$	Maximum of probabilities $P_{f_{pip-is}}(h_{cr_{is}})$ and $P_{f_{pip-bt}}(h_{cr_{bt}})$).	m^3/m

Minimizing the total costs is elaborated as in 5.2.2, with the derivative to the dike cross section surface instead of the dike heigth:

$$\frac{dC_{tot}^{PV}}{dS_d} = 0 \tag{5.28}$$

Together with equations (5.27) and (5.26), equation (5.28) is:

$$\begin{aligned} \frac{dC_{tot}^{PV}}{dS_d} &= I'^{\Delta S_d} + \frac{D}{r} \cdot \left(\frac{dP_{f_{h-d}}(h_d)}{dS_d} + \frac{dP_{f_{pip-is}}(h_{cr_{is}})}{dS_d} \right) \quad L_b > (h_b - h_m) \cdot (c_p - cot\alpha_{bi}) \\ \frac{dC_{tot}^{PV}}{dS_d} &= I'^{\Delta S_d} + \frac{D}{r} \cdot \left(\frac{dP_{f_{h-d}}(h_d)}{dS_d} + \frac{dP_{f_{pip-bt}}(h_{cr_{bt}})}{dS_d} \right) \quad L_b \leqslant (h_b - h_m) \cdot (c_p - cot\alpha_{bi}) \end{aligned} \tag{5.29}$$

In which:

$I'^{\Delta S_d}$	Marginal costs per unity of dike cross section surface.	€/ m^3/m

Since the two piping submechanisms are assumed to be fully dependend, the minimization of S_d would use the maximum of the both piping probabilities in equation (5.26). In fact, this determines the relation between berm heigth $h_b - h_m$ and berm length L_b with equation (5.27). A berm height exceeding $L_b/(c_p - cot\alpha_{bi})$ would make no sense for safety, just as a berm length exceeding $(h_b - h_m) \cdot (c_p - cot\alpha_{bi})$. Using this as the condition for berm height, $h_b - h_m$ is equal to $L_b/(c_p - cot\alpha_{bi})$. Therewith, the equation (5.29) simplifies to the first or to the second line.

In Appendix B.4 the derivatives for each dike shape parameter are derived to enable to solve equation (5.29) analytically, substituting (5.25). In Appendix B.5.1 the probability $P_{f_{opt}}$ which belongs to $\frac{dC_{tot}^{PV}}{dS_d} = 0$, corresponding to the minimum of C_{tot}^{PV} in equation (5.28) is figured out for the situation with berm. With the probabilities from equation (5.25), and with the derivatives for each dike shape parameter in equation (B.61), and $cot\alpha_{bu} + cot\alpha_{bi}$ denoted as $cot\alpha's$, it follows:

$$P_{f_{opt}} = \frac{I'^{\Delta S_d} \cdot f_{ovx} \cdot B \cdot L_d \cdot r}{D} \cdot \left(\frac{c_p \cdot (h_b - h_m)}{\gamma_{h_d} \cdot c_p \cdot (h_b - h_m) + \gamma_p \cdot f_{ovx} \cdot (L_d + (h_b - h_m) \cdot cot\alpha's)} \right) \tag{5.30}$$

In which:

γ_{h_d}	Fraction of the total probability to failure mechanism overtopping	-
γ_p	Fraction of the total probability to failure mechanism piping, equal to $1 - \gamma_{h_d}$	-
$cot\alpha's$	Denotion of $cot\alpha_{bu} + cot\alpha_{bi}$	-

Substituting $h_b - h_m = L_b/(c_p - cot\alpha_{bi})$ leads to an equivalent formulation with the berm length L_b in the counter in stead of the berm height $h_b - h_m$:

$$P_{f_{opt}} = \frac{I'^{\Delta S_d} \cdot f_{ovx} \cdot B \cdot L_d \cdot r}{D} \cdot \left(\frac{c_p \cdot L_b}{\gamma_{h_d} \cdot c_p \cdot L_b + \gamma_p \cdot f_{ovx} \cdot \left(L_d \cdot (c_p - cot\alpha_{bi}) + L_b \cdot cot\alpha's\right)} \right) \tag{5.31}$$

Two notes can be made about the shape of this equation. Firstly, in case $\gamma_{h_d} = 1$, which means the probability of piping is neglectible, equation (5.30) the term within the large brackets is equal to 1. It turns into the shape of equation (5.13) for overtopping only. Secondly, with the

geometric translation $I'^{\Delta S_d} = I'/L_d$ the first part of the equations (5.30) and (5.31) is the same as equation (5.13), except the factors f_I and Δt representing the time dependence. This means that the last part of the equation between brackets reflects the effect of taking into account a second failure mechanism.

Equation (5.30) still has γ_{h_d} as a degree of freedom. In fact it can be interpreted as an optimum given a certain value of γ_{h_d}. The global solution is found searching in the domain of γ_{h_d} [0,1] for the lowest societal costs.

Solving the equation (5.30) two checks has to be made.

- In the derivation in this section a berm is assumed to exist. Searching in the domain for γ_{h_d} in [0,1] the smaller its value, the larger the fraction of the probability available for piping, leading to smaller berm dimensions, and the lower the cost. This would lead to a minimum cost for berm dimensions equal to zero which cannot be a valid result, because the equation is clearly not valid for the situation without a berm ($h_b - h_m = 0$, $L_b = 0$) since this would lead to an optimal probability of failure of 0. Therefore, while searching in the domain of γ_{h_d} [0,1] the validity of equation (5.30) is checked for the condition whether the probability $P_{f_{opt}}$ following from equation (5.30) is equal to the sum of the probabilities per failure mechanism $P_{f_{h-d}} + P_{f_{pip}}$ based on equation (5.25). This check limits the berm dimensions would decrease irrealisticly.
- Another check is whether the numerator of the term between brackets is larger than zero. This is mostly the case since c_p (in the range of about 15 to 20 [150]) is larger than $cot\alpha_{bi}$ (for dikes mostly in the range of about 3 to 6).

5.3.3. DERIVATION FOR SITUATION WITHOUT BERM

A dike with a relatively large height (e.g. a dike along sea) may be sufficiently safe with respect to both failure mechanisms, without a berm: the footprint of the dike may be that wide, that it reduces the probability of piping sufficiently, at least to the extent the optimum for societal cost is lower than in the case with berm. The case of no berm needs a slightly adapted approach with respect to the previous Subsection. In the special case of no berm ($L_b = 0$) the probability for piping in (5.25) is:

$$P_{f_{pip-is}}(h_{cr_{is}}) = exp\left(-\frac{L_d + c_p \cdot (h_m - A_h)}{c_p \cdot B}\right) \tag{5.32}$$

The minimum societal costs are found solving:

$$\frac{dC_{tot}^{PV}}{dS_d} = I'^{\Delta S_d} + \frac{D}{r} \cdot \left(\frac{dP_{f_{h-d}}(h_d)}{dS_d} + \frac{dP_{f_{pip-is}}(h_{cr_{is}})}{dS_d}\right) \tag{5.33}$$

With the probability for overtopping from equation (5.25) and for piping from equation (5.32), and with the derivatives for each dike shape parameter in equation (B.61), it follows:

$$\frac{dC_{tot}^{PV}}{dS_d} = I'^{\Delta S_d} + \frac{D}{r} \cdot P_f \cdot \frac{1}{B} \cdot \frac{1}{L_d} \cdot \left(\frac{-\gamma_{h_d}}{f_{ovx}} + \frac{-\gamma_p \cdot cot\alpha' s}{c_p} \right) \tag{5.34}$$

Thus, the probability $P_{f_{opt}}$ which belongs to the minimum of C_{tot} for the situation without berm is:

$$P_{f_{opt}} = \frac{I'^{\Delta S_d} \cdot f_{ovx} \cdot B \cdot L_d \cdot r}{D} \cdot \left(\frac{c_p}{\gamma_{h_d} \cdot c_p + \gamma_p \cdot f_{ovx} \cdot cot\alpha' s} \right) \tag{5.35}$$

With γ_{h_d} and γ_p in the domain [0,1] the denumerator between the brackets is always larger than 0. In this special case the degree of freedom γ_{h_d} can be solved because of the existence of a second relation: the relation between the dike height and the dikes footprint is fixed by the condition no berm is present, see Figure 5.14:

$$L_d = Br_d + cot\alpha' s \cdot (h_d - h_m) \tag{5.36}$$

Therewith, the dike cross section is determined as:

$$\begin{aligned} h_d &= A_{h_d} - f_{ovx} \cdot B \cdot ln(\gamma_{h_d} \cdot P_f) \\ L_{d,\,noberm} &= c_p \cdot (A_h - h_m) - c_p \cdot B \cdot ln(\gamma_p \cdot P_f) \end{aligned} \tag{5.37}$$

In Appendix B.5.2 this is figured out to derive the corresponding probability of failure P_f. With $A_{h_d} - h_m$ denoted as A_{ov} and $A_h - h_m$ denoted as A_p this results in:

$$P_f = exp\left(\frac{c_p \cdot (B \cdot ln(\gamma_p) - A_p) + cot\alpha' s \cdot (A_{ov} - f_{ovx} \cdot B \cdot ln(\gamma_{h_d})) + Br_d}{B \cdot (f_{ovx} \cdot cot\alpha' s - c_p)} \right) \tag{5.38}$$

Equate the resulting probability P_f with $P_{f_{opt}}$ in equation (5.35) provides the result for the value of γ_{h_d} for which the corresponding probability of failure will lead to lowest societal costs, under the condition of no berm exists.

5.3.4. APPLICATION

The analytical relations derived in the previous subsections are applied for several locations in the Netherlands. For the comparison 7 dike segments are investigated, subject to different load systems in the Netherlands: dike segments Schiermonnikoog, Hollandse Kust, Grebbe, South-Flevoland, IJssel-West, Oude Maas, and Western Scheldt.

The total costs are calculated with an adapted shape of equation (5.1), using the marginal cost per unit of the dikes cross sections surface:

$$C_{tot}^{PV} = I + R^{PV} = I_0 + I'^{\Delta S_d} \cdot \Delta S_d + P_{f_{tot}} \cdot \frac{D}{r} \tag{5.39}$$

In which:

ΔS_d	Difference between cross section surfaces of reinforced dike and existing dike	m^3/m

The cost $I'^{\Delta S_d}$ per unity of dike cross sections surface is key-input for determination of the costs. A practical approach can be used to derive $I'^{\Delta S_d}$ from the available I' per dike segment which is used in [51]: assuming a reinforcement would keep the dike shape (slopes and crest width) as the existing dike shape, the marginal investments per meter dike heightening could simply be divided by the dikes footprint L_d to get the marginal investments per squared meter cross sections surface:

$$I'^{\Delta S_d} = \frac{I'}{L_d} \tag{5.40}$$

However, in the analysis in this section the dike shape is a degree of freedom. For a variety of dike shape parameters and corresponding values of S_d the $I'^{\Delta S_d}$ can be derived from I'. Therefore, for each dike shape in the analysis, a virtual reinforcement height $\Delta\tilde{h}_d$ is introduced which is based on existing dike shape (slopes and crest width), with the same additional dike shape surface ΔS_d. Note, since the dike shapes are not recorded in [51], in this application the proxy of the existing dike shape is used. Therewith, the marginal costs per unity of cross section can be derived from I':

$$I'^{\Delta S_d} \cdot \Delta S_d = I' \cdot \Delta\tilde{h}_d \tag{5.41}$$

$$\Rightarrow I'^{\Delta S_d} = I' \cdot \frac{\Delta\tilde{h}_d}{\Delta S_d} \tag{5.42}$$

In which:

$\Delta\tilde{h}_d$	Dikes equivalent reinforcement height, using existing dike slopes and crest width, corresponding to an additional cross section surface ΔS_d.	m

Note, in case the dike shape would be the same as the existing shape $\Delta h_d = \Delta\tilde{h}_d$ and therewith $\Delta S_d = \Delta h_d \cdot L_d$ which translates equation (5.42) in equation (5.40). In Appendix B.6 this equivalent reinforcement height is derived for different dike shapes as:

$$\Delta\tilde{h}_d = -\frac{h_0}{2} - \frac{Br_d}{cot\alpha'_0 s} + \sqrt{\left(\frac{h_0}{2}\right)^2 + \frac{h_0 \cdot Br_d}{cot\alpha'_0 s} + \left(\frac{Br_d}{cot\alpha'_0 s}\right)^2 + \frac{2 \cdot \Delta S_d}{cot\alpha'_0 s}} \tag{5.43}$$

in which ΔS_d is the only variable. Therewith, $I'^{\Delta S_d}$ can be determined from I' with equation (5.42).

In Figure 5.14 six dimensions are degrees of freedom: the slopes of inner and outer slope, the dike height and crest width, and the berm length and berm height. In the cases in this application the outer slope is not varied, since it is related to the factor converting the water level scale parameter B to reflect overtopping f_{ovx}, which is taken as a given in this application. The dike crest width is not varied as well since it mostly will be determined by other functionalities than dike safety. For the remaining 4 dimensional parameters, the berm length and berm width are related by $h_b - h_m = L_b/(c_p - cot\alpha_{bi})$, see equation (5.27). Thus, three dimensions remain to be a variable in the application: dike height h_d, berm length L_b, inner slope $cot\alpha_{bi}$.

Below, first the calculation schemes are explained and illustrated for location Grebbe. Then, the results for all locations are summarized and analyzed. The data used for the locations is provided in Table 5.2. The parameters of the exponential load distributions are based on calculations with HYDRA-NL [144], the dike data is based on global characteristics of the dike segments considered. The discount rate is 0.055 per year.

Table 5.2.: *Data as used for the comparative analysis on locations Schiermonnikoog (Loc 1), Hollandse Kust (Loc 2), Grebbe (Loc 3), South-Flevoland (Loc 4), IJssel-West (Loc 5), Oude Maas (Loc 6), and Western Scheldt (Loc 7).*

Location	**Loc 1**	**Loc 2**	**Loc 3**	**Loc 4**	**Loc 5**	**Loc 6**	**Loc 7**
A_h $(m+NAP)$	2.77	2.11	10.21	0.28	7.48	2.89	3.87
A_{h_d} $(m+NAP)$	3.41	5.97	10.37	0.68	7.52	2.81	4.39
B (m)	0.22	0.226	0.052	0.21	0.12	0.21	0.19
$f_{ovx} \cdot B$ (m)	0.28	0.465	0.161	0.43	0.17	0.24	0.36
$cot\alpha_{bi,0}$ $(-)$	3	3	3	3	3	3	3
$cot\alpha_{bu,0}$ $(-)$	5	5	3	4	3	3	4
$h_{d,0}$ $(m+NAP)$	4	8	11	3	8	4	6
h_m $(m+NAP)$	0.77	0.11	7.21	-1.72	5.48	0.89	0
Br_d (m)	7	4	7	4	7	7	4
I' $(M€/m)$	18	122	18	115	129	251	176
I_0 $(M€)$	4.93	107.46	6.67	1050	143.47	139.09	79.15
$D(0)$ $(M€)$	85	2499	27947	16790	3957	23814	4375

CALCULATION SCHEME FOR THE SITUATION WITH BERM

For the situation of a dike shape with berm the optimal probability of failure is derived solving equation (5.30). It relates to two of the three remaining dimensional parameters and can be interpreted as an optimal probability given a certain value of γ_{h_d}, and given a value for $cot\alpha_{bi}$. The optimal probability can be practically determined with a series of calculations for γ_{h_d} and $cot\alpha_{bi}$, evaluating the total costs, also shown in the flowchart in Figure 5.15:

- Determine a start value of $P_{f_{opt}}$ with $\gamma_{h_d} = 1$, which is the situation leaving no failure room for piping. Therewith, the term between large brackets in equation (5.30) is 1, resulting in equation (5.13) focussing on overtopping only.
- Apply this probability as a proxy for the optimum for γ_{h_d} slightly lower, e.g. 0.999, and calculate the corresponding dike dimensions h_d and L_b with:

$$\begin{aligned} h_d &= A_{h_d} - f_{ovx} \cdot B \cdot ln(\gamma_{h_d} \cdot P_f) \\ L_b &= c_p \cdot (A_h - h_m) - c_p \cdot B \cdot ln(\gamma_p \cdot P_f) \; - \; L_d \end{aligned} \tag{5.44}$$

  Note, the berm length is relatively long in this first estimate since $\gamma_p = 1 - \gamma_{h_d}$ is almost zero, leaving only a very small fraction of the probability for piping.
- Therewith, equation (5.30) can be used to find $P_{f_{opt}}(\gamma_{h_d})$ and therewith the corresponding costs C_{tot}^{PV} can be calculated.
- Decrease γ_{h_d} using $P_{f_{opt}}$ from the last step, and repeat its evaluation of $P_{f_{opt}}(\gamma_{h_d})$ and the corresponding costs C_{tot}^{PV}.
- Repeat decreasing γ_{h_d} as long as the berm dimensions L_b are larger than 0, the denumerator of equation (5.30) is positive, and the condition $P_{f_{opt}} = P_{f_{h-d}} + P_{f_{pip}}$ is met.

The optimum for γ_{h_d} is found at the minimum costs C_{tot}^{PV} in this series of calculations. The corresponding dike height and berm dimensions are determined with equation (5.44). In fact, this calculation scheme simulates for a given inner slope a series of results giving more and more room for the failure mechanism piping, resulting in a smaller berm length and berm height, continued until costs C_{tot}^{PV} are minimal. The series of calculations is repeated for a next value of the inner slope as long as the slopes are in the integration interval.

Figure 5.16 provides an example for location Grebbe, presenting the path of the combinations of the three varied dimensional parameters

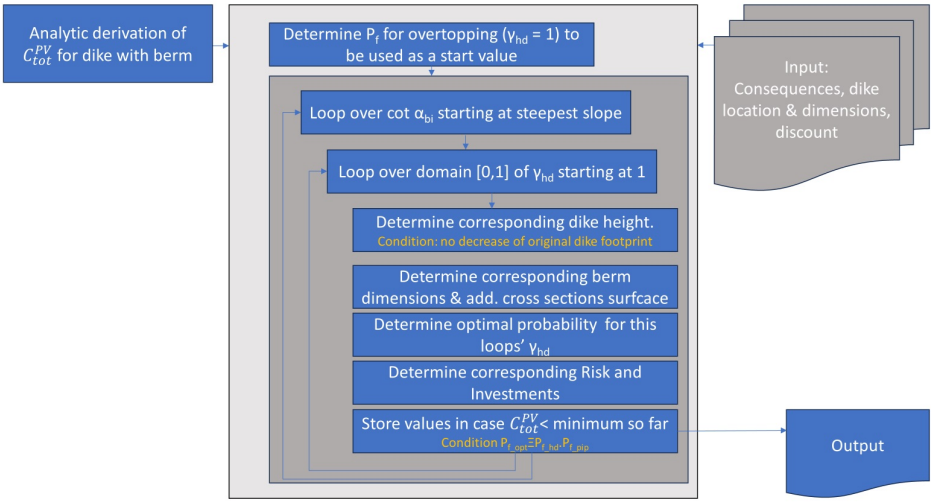

Figure 5.15.: *Flowchart of the approach to solve equation* (5.30).

to the combination with minimum total costs. Dike height is presented on the x-axis, berm length on the y-axis and slope by annotations near the path-curve. Following the scheme in Figure 5.15 the minimum costs are stored during the process per value of inner slope. This resulted in a path of 'sub-minima' walking along the slopes. It started for a steep slope with a dike height of over 13m+NAP, and a berm width of about 30 m. Increasing the cotangent of the slope stepwise causes at first mainly a gradual decrease of dike height and an increase of berm length. At a certain point the cost reduction takes place mainly by gentling the slope in combination with shortening berm. This sharp kink in the curve may seem contra-intuitive, because in the 2 dimensional plot only the berm length seem to decrease from that point on. However, still the probability of failure still decreases since the slope becomes gentler, increasing the total length between the dike toe at river side and the berm toe at the landward side. The red dot marks the combination of dike height and berm length at the end of the path with minimal total costs. Using the data in Table 5.2 the a dike heigth resulted in 12.39 m+NAP and the berm length in 20.75 m and a berm height of 1.54 m, and an inner slope of 4.52. Total costs are 91 M€.

WITHOUT BERM

The equation (5.35) can be interpreted as an optimum probability of failure with a dike shape without berm. The optimal value can practically be solved with a series of calculations which equalize the equations

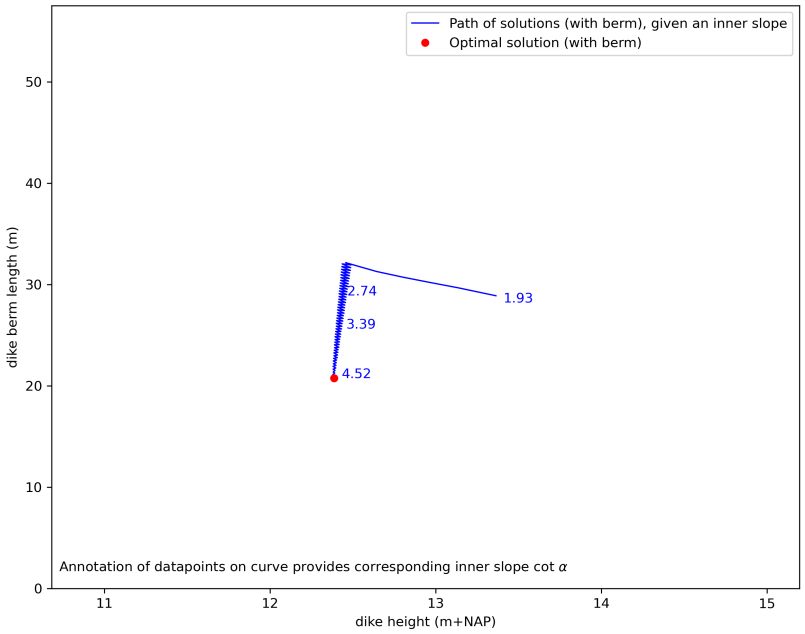

Figure 5.16.: *Overview of optimal combinations of dike height and berm length for location Grebbe, indicating the dimensions belonging at optimal costs.*

(5.35) and (5.38). Per value of the inner slope the domain of γ_{h_d} [0,1] is search to find the value of γ_{h_d} for which both are equal. In a second loop the slope is adapted as long as the costs decrease. The schedule is shown in Figure 5.17.

SEMI-ANALYTICAL ECONOMIC OPTIMUM PROBABILITY OF FAILURE

The result of both costs (for the optima with berm and without berm) are compared. The minimum of both prevails. In the case of location Grebbe, which is along a river, a situation without berm has no realistic solution, because the dikes foot print is too small to prevent piping sufficiently.

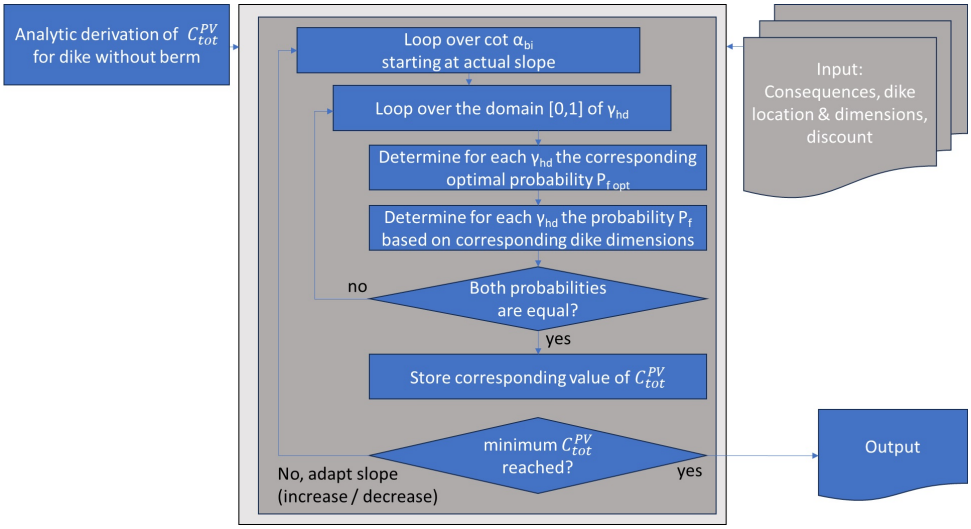

Figure 5.17.: *Flowchart of the approach to solve equation* (5.38).

5

RESULTS AND ANALYSIS

The results for the seven locations in the case are presented in Table 5.3. The columns 2 to 5 represent the found optimal dimensions (dike height, berm lenght and slope) and the corresponding additional surface of the dikes cross section ΔS_d. Column 6 represent the fraction of the optimal probability for the failure mechanism overtopping. Column 7 represents the optimal probability of failure. Column 8 provides $ratio_{p_f}$, the ratio between the probability of failure taking into account both the failure mechanisms overtopping and piping, and the probability of failure in case of taking into account overtopping only. The ratio for this analytical-based method varied in the 7 cases between 0.75 and 1.34 with a factor 0.96 on an average. Taking into account a second fialure mechanism has no significant effect on the optimal probabilities of failure.

To analyse the results in Table 5.3 a numerical model is figured out to find out whether the results based on derivations in this section are plausible. Furthermore, the numerical approach serves as a check on the implementation. The set-up is explained in Appendix B.7. A graphical result presenting the results of both methods for the location Grebbe is given in Figure 5.18. It shows isolines of additional cross sections surface ΔS_d (coloured curves). The black curve shows the path of combinations of dike height (x-axis), berm length (y-axis) and inner slope (annotated along the curve) corresponding to the sub-minimal costs per value of ΔS_d. It clearly shows the berm length and dike height increase gradually with increasing ΔS_d, and the inner slope decreases gradually. The global optimum for the numerical method is marked with a black dot on

Table 5.3.: *Results for analytical-based method for locations Schiermonnikoog (Loc 1), Hollandse Kust (Loc 2), Grebbe (Loc 3), South-Flevoland (Loc 4), IJssel-West (Loc 5), Oude Maas (Loc 6), and Western Scheldt (Loc 7).*

Location	dike height	berm length	slope	$\triangle S_d$	γ_{h_d}	$P_{f_{opt}}$	$ratio_{p_f}$	Total costs
	(m+ NAP)	(m)	(-)	m^3/m	(-)	$\cdot 10^{-5}$ / year	(-)	$\cdot 10^6$€
Loc 1	5.14	18.79	4.20	75.4	0.57	355.9	0.99	72.4
Loc 2	9.06	0	2.64	60.0	0.90	144.0	1.01	534.4
Loc 3	12.39	20.75	4.52	99.4	0.74	0.5	0.76	90.9
Loc 4	4.75	28.65	2.26	111.5	0.56	13.9	0.75	691.2
Loc 5	8.98	11.02	7.66	64.7	0.59	31.6	0.95	635.8
Loc 6	4.96	10.59	10.25	101.6	0.61	21.4	1.34	1599.4
Loc 7	7.14	27.96	5.12	171.6	0.59	81.0	0.93	1206.8

the curve. The path of the analytical based method from Figure 5.16 is provided in this Figure as well in blue with the optimum in red. The global optima are very close.

Figure 5.18 shows the dimensions for the global optima for both approaches are rather comparable. The slightly differences in dike height and berm length resulted in about 4% difference of the additional cross section surface. In Appendix B.7 in Table B.2 the results for the numerical approach is provided. For all locations the dimensions are rather comparable with the analytical based approach. The average difference in additional cross section surface in the columns headed ΔS_d is about 12%. The dikes' dimensions dike height, berm length and inner slope differ on an average respectively 2% (0.09m), 7% (1.2 m) and 5%. The fraction of the failure probability for overtopping, γ_{h_d} is for the analytical based method 0.65 on an average, and for the numerical method 0.52 on an average. The difference in optimal probability is not that small, but not that large either: the analytical based method lead to probabilities which are about 1.7 times lower than the probabilities got with the numerical method. The differences in dike dimension provide a typical reflection to value this difference as not that significant.

The numerical method results in a $ratio_{p_f}$ of 1.75 on an average for the 7 locations in this research. This means that the economic optimal probability derived with the two most relevant failure mechanisms for the dikes cross sections surface, is 75% larger than in case it is derived with overtopping only. The analytical-based method $ratio_{p_f}$ is 0.96. The difference with the numeric-based $ratio_{p_f}$ is in line with the difference in failure probabilities for both methods.

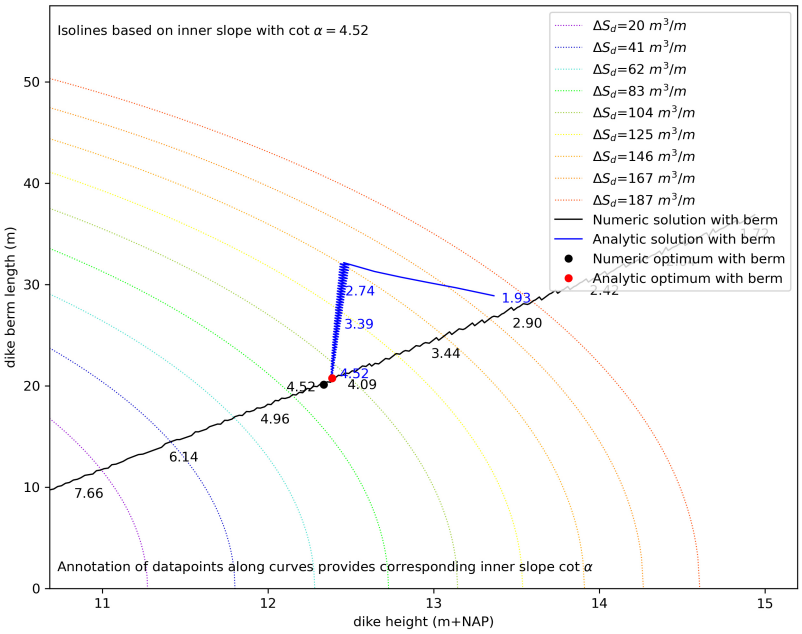

Figure 5.18.: *Overview of the path of optimal combinations of dike height, berm length and inner slope for location Grebbe, indicating the global optimum for both the analytical and the numerical method. NB. The three dike shape dimensions are presented in a 2-D graph. Though, the isolines of ΔS_d depend on the inner slope, see equations* (B.100) *and* (B.101) *in Appendix B.7. Here, the isolines are provided for the inner slope corresponding with the global minimal costs.*

5.4. RISK AWARE UPDATING OF RELIABILITY STANDARDS

5.4.1. NEED AND OPPORTUNITIES OF UPDATING RELIABILITY STANDARDS

THE NEED

Given flood defence management use standardization expressed as probabilities of failure, the need for updating of reliability standards is threefold. Firstly, as figured out in Chapter 3 the type of dike construction affects the risk, and therewith it affects the risk-optimal design. A dike with a clay core causes delay in the breach process and breach dimen-

sions will be reduced with respect to a dike with a sand core. Reduced breach dimensions will reduce the flood volume and consequently the consequences of flooding, and therewith the optimal design probabilities of failure (see equation (5.13). Therewith, given a dike design is aimed to be laid out economic optimal the design and the reliability standard are coupled.

Secondly, new or updated or rectified information may come available, which affect the standards. The present application of the National database of Flood Simulations [54] can serve as an example in the Dutch context. The implementation of the breachgrowth formula of Verheij & van der Knaap [77] for location Grebbedijk in Chapter 3 lead to breach-widths of about 200m for dikes with sand core and 100m for dikes with clay core (see Figure 3.3), which corresponds with the data they used in their derivation. More in general, in the simulations of floodings in the Dutch National database of Flood Simulations [54] the breach-widths most likely correspond with breaches in sand dikes, named as brittle in Chapter 3 (see Appendix C). Therewith, in most of the simulations the consequences are overestimated (see Figure 2.4) leading to reliability standards which are more stringent than the optimal probabilities of failure (see equation (5.13). Referring to the Dutch organisation of flood defence asset management (see Section 1.5.2) this will lead to a too large portion of the dikes qualified for reinforcements.

Third, the economic optimal design reliability is ageing, as demonstrated in Section 5.2. Therewith, in case the planning of an reinforcement shifts considerably with respect to the year for which the standard is derived, e.g. due to availability of resources, the design reliability may need to be updated.

THE OPPORTUNITIES

In case of application of reliability standards, such as the Dutch standards for probability of flood defence failure, the tactic and operational flood defence management turns into the management of dike failure probabilities. The consequences are not involved any more. If the reliability standards are risk-based, the consequences are only explicitly involved during derivation of the standards at strategic decision level.

On the one hand the management of dike failure probabilities supports to ease the flood defence manager. In case the pursued safety level would be a variable, then increased risks due to increased values in a polder would be a reason to update the safety level and therewith to a demand to reinforce the flood defence. This seems unworkable for the Water Boards. On the other hand, with probability-standards (even laid down in Law in the Netherlands) risk-awareness is no inherent part of the flood defence managers work. This could exclude alternative risk aware reinforcement options. There can be incentives which are positive for the flood defence (system) manager which would be enabled by risk aware

use of standards. For instance:

- For the Flood defence manager. In case at a certain location a sheet-pile is to be placed, it can be constructed to be stable after a breach in overflow conditions, reducing the flood volume considerably and therewith reducing the consequences significantly (see Chapter 3). The reduced damage would lead to an economic optimum corresponding with less stringent performance requirements for the flood defence, decreasing the dimensions of the reinforcement.
- Furthermore, again for the Flood defence manager. As figured out in Chapter 4 the planning of a portfolio of reinforcements is affected by the risks due to individual dike segments and their standards. In case system risk reduction is used as a metric for the tactical plan in stead of meeting the reliability standard, a flood defence manager may bring forward the planning of a reinforcement by proposing a more risk averse design.
- For the Flood defence system manager. In case the budget request for programming reinforcements is higher than the available budget (see Chapter 4) it could be beneficial to reduce system risks alternatively, by using a temporarily reduced standard such as conducted along the Eastern Scheldt in the Netherlands before building the Eastern Scheldt Barrier (1985), or solving only specific failure paths [45].
- For the Government, in most countries held responsible in case of flooding. The risk may be less, in case the dike construction on high risk locations is ductile, decimating the risk on victims [88].

The Flood defence manager (e.g. Water Boards) outsource reinforcements. Urged by competition, contractors strive for investment cost optimality given the standard. If the dike construction type is not prescribed, this leads to the use of materials which are cheapest to use in place. Note that investment cost optimality differs from optimization of the Total Cost of Ownership, which includes the flood risk effect of investments as well.

In the Netherlands, the actual management of the flood defences is rather straight forward, because the standards are laid down in the Dutch Law. In some other countries performance requirements are used, however, they are not formalized in Law. Some of them are based on quantitative risk analysis [23]. In all cases, if a performance measure is defined as a probability of flooding or its proxy such as exceedance frequencies of hydraulic loads, the same opportunities are in place with respect to its risk aware updating.

5.4.2. PROPOSAL FOR RISK AWARE UPDATING OF RELIABILITY STANDARDS

The objective of this Section is to elaborate whether it is possible to use reliability standards risk aware. This may come across contra-intuitive since for example the standards in the Netherlands are derived based on risk. However, the present standards in the Netherlands does not provide a relation between construction type and optimal safety level (see Chapter 3. Therefore, a standardized updating of present reliability standards enables to tune the safety level and corresponding dike design.

In case of the Netherlands, a risk based framework of standards is in place. The presented risk aware updating of reliability standards only yields for locations where the economic criterion prevails the criteria for individual risk. Note, the presented standardized updating may be helpful to homogenize the economic optimal flood probabilities used for the present standards to values tailored to the actual construction of the dikes.

The result of Section 5.2 is an approach like Van Dantzig [14] adapted for dynamic effects, which is proven to be comparable with the approach in [51] which is used for the standardization in the Netherlands. The result of Section 5.3 underpins the main starting point in [14] and [51] to use only the failure mechanism overtopping. This does not lead to significantly different economic optimal probabilities of failure. Therewith, it is concluded that the adapted Van Dantzig relation can be used for further elaborations to apply the standards risk-aware. A translation factor f_d is introduced:

$$P_{f_{risk-opt}} = f_d \cdot P_{standard} \equiv f_d \cdot P_{f_{opt}}(\Delta t_{standard}) = f_d \cdot \frac{I' \cdot f_{ovx_{standard}} \cdot B \cdot r}{D(\Delta t_{standard})} \tag{5.45}$$

In which:

$P_{f_{risk-opt}}$	Optimal probability of failure adapted with respect to a specific dike design.	$per year$
f_d	Factor to translate existing flood probability standards to risk optimal probabilities valid for a certain design	$-$
$P_{standard}$	Standard in terms of probability of flooding due to failure of the flood defence	$per year$

$\Delta t_{standard}$	Period starting from present to the year for which the standards are derived. In the Dutch example in this chapter this is equal to 39, since 2011 is the year for which the load, investment and damage data applies in [54], and 2050 is the horizon for the Dutch standards	*year*
$fovx_{standard}$	Factor f_{ovx} converting water level scale parameter B into dike height scale parameter, applied for standardisation	–

The translation factor f_d enables to 'replace' the design-dependent variables in the adapted Van Dantzig relation which the ones corresponding to a dike design or its reinforcement. With $\Delta t = \Delta t_{standard}$ it follows:

$$f_d = \frac{I'_{design} \cdot fovx_{design} \cdot D(\Delta t_{standard})}{I' \cdot fovx_{standard} \cdot D_{design}(\Delta t_{design})} \tag{5.46}$$

In which:

I'_{design}	Marginal investment costs corresponding to a flood defence design, with the same year of price index as I'. Note, since other reinforcements than dike heightening are opportune, a marginal investment resulting in a tenfold flood probability I^{10}_{design} can be used as well, provided it is used in combination with I^{10} in stead of I' in the denumerator of equation (5.46). If I' is based on dike heightening the I^{10} can be calculated with $I' \cdot f_{ovx} \cdot B \cdot ln(10)$.	€/*m*
$D_{design}(\Delta t_{design})$	Economic damage corresponding to a flood defence design, valid for the design horizon with respect to 2011, the year for which the data applies, used for the analysis of the Dutch standards	€
$fovx_{design}$	Factor f_{ovx} converting water level scale parameter B into dike height scale parameter, applied for a design	–

In fact, this proposal uses the existing reliability standard, either formal established by Law or well-underpinned otherwise, and applies a relative adaptation to connect to the values which fit the design under consideration. This requires insight in the investment and damage for the reference situation as well as for the proposed situation. An example

for a dike to be reinforced by a sheetpile, provided the economic criterion prevailed during the standardization: for marginal costs which are 2 times larger than taken into account in the standardization analysis, and a damage which is reduced by a factor 5 due to the reinforcement, the economic optimal probability would be a factor 10 less stringent than the existing standard.

5.5. CONCLUDING DISCUSSION

The analytic approach for the derivation of an optimal economic probability of failure, provided by the first Dutch Delta Commission [50], is extended to reflect dynamic effects such as climate change, subsidence and reinforcement interventions. The approach underpins the linear relationship found in [51] between the ratio of damage and the cost to decrease the probability tenfold D/I^{10} on the one hand and the reciprocal optimal probability of failure $1/P_{f_{opt}}$ on the other hand. A flowchart of the approach is presented in Figure 5.8 and an example of the result for a dike segment is presented in Figure 5.11.

In Chapter 3 the relation is demonstrated between structural robustness and economic optimal design safety level. The present chapter demonstrates this design safety level depends on the design dimensions as well, because the factor converting the scale parameter for water level B into the scale parameter for dike height, $f_{ovx}B$, is partly determined by dikes outer slope shape and roughness and partly by the local wave conditions, see Section 5.2.2.

The derivation of economic optimal probabilities of failure for the first and second Dutch Delta Commission used one failure mechanism which were overflow [14] and overtopping [51] respectively, with the dike height as the physical dimension connected to the probability of failure. In [37] a numeric approach for design is elaborated, with the dike shape (four dimensional parameters) as a degree of freedom considering the failure mechanisms overtopping, piping and inner slope stability, given a target reliability. In this chapter the target reliability is not a given, but the idea to consider more failure mechanism is taken along. The analytic approach for optimal economic probability is developed for two failure mechanisms, overtopping and piping, to research the starting point in [14] to use only overtopping. Dike height, berm dimensions and inner slope are taken as the physical dimensions of the dike shape connected to the probability of failure. Applied for 7 locations, the optimal economic probability appeared to be more or less similar to the results considering only the failure mechanism overtopping. This result underpins the starting point used in the studies up to present using only the failure mechanism overtopping.

The second Dutch Delta Commission used the so-called middle probabilities, introduced in [67]. Comparison of the derived analytic approach

with the numeric approach to derive middle probability as used in [51] shows the quality for over 70 dike segments is satisfying (see Figure 5.9). Especially equation (5.13) of the lower limit curve, reflecting the design safety level, looks quite alike the equation (5.2) provided by the first Dutch Delta Commission. Furthermore, the equation is simple to use, enabling application for all levels of flood defence asset management: in early decision stages for reinforcement (operational), what-if studies (tactical) or policy analysis over larger areas (strategic).

Furthermore, the economic optimal life cycle of flood defences can be estimated analytically with equation (5.20). The exercise in Figure 5.7 provides the insight some of the flood defences have short optimal life cycles, even less than 20 years. Next to the long known dependence on the ratio of fixed and marginal investment costs, the optimal life cycle strongly depends on the ratio of water level increase rate and the dike height scale parameter $\eta \cdot (f_{ovx} B)^{-1}$. This means that in case the relative water level increase rate is low, it is beneficial to use long design horizons.

The middle probabilities and maximum tolerable probabilities are included in the Dutch law. The benefit of the middle probabilities would be to have time to prevent exceedance of the maximum tolerable probabilities. In [51] this time is given as approximately 20 years which 'is well in accordance with actual experiences in the Netherlands for the time it takes to implement large-scale flood prevention projects'. Related to the actual practice for the design horizon for dikes, mostly 50 years, this time comes across as a mid-term warning. This study shows the economic optimal life cycles in the Netherlands are about 40 years on an average. However, for a number of dike segments it is even shorter than 25 year. In case for those dike segments the optimal design horizon is chosen, the middle probability would only be about 10 year before reaching intolerable probabilities which is short to timely reinforce, referring to the Dutch experience, as cited here above. The shorter the design horizon, the more reinforcements should be seen as a semi-continu proces.

Finally, the method determining the economic optimal reliability standard developed in this chapter may serve to consider whether existing standards still fits adequately. This chapter proposes a translation factor to risk aware update the existing standard for reinforcements with the degrees of freedom: time of reinforcement, design horizon, and the consequences due to the structural robustness of the design e.g. by the core material.

6

COMPREHENSIVE FLOOD DEFENCE MANAGEMENT

...competition, we see now, is destructive. It would be better if everyone would work together as a system, with the aim for everybody to win. What we need is cooperation and transformation to a new style of management.

W. E. Deming, in: The New Economics for Industry, Government, Education (second edition, 2000).

Risk analysis is an indispensable element in risk-informed decision making on each of the asset management decision levels used in asset management practices. In this chapter, the risk analyses are combined with this concept of decision levels, and the concept of the Deming circle as an organisational concept for continuous capability improvement. Coherently and dynamicly used, they can bridge the practical disconnections between the decision levels. The decisions are to be taken by different actors due to the fragmented responsibility. Due to the increasing complexity, practical bottlenecks and dilemmas arise that need to be solved. This prompts flood defence asset management to mature. The success of asset management of flood defence systems depends on the practical implementation of cooperation and the ability and agility to choose and change the shape of cooperation dependent on the situation. This is better accommodated by an Agile process than by a Waterfall process. If such a process is continuously related to societal acceptability, the risk perspective focuses on the ALARA risk management principle.

6.1. COHERENCE OF ELABORATED RISK ANALYSES IN THE FRAME OF ASSET MANAGEMENT

Risk management is presented in this thesis as a part of Asset Management, see Section 1.2, which is shortly defined as 'the art of balancing performance cost and risk in the long term' [22]. Risk analysis is an indispensable element in risk-informed decision making on each of the asset management levels [24, 27], see Figure 1.2 as well. Especially for dikes, the EU Floods Directive [34] stimulates to come up with quantitative risk analyses. The main objective of this thesis is: to develop and test methods for coherent utilization of risk analysis in flood defence system management subject to deterioration and climate change. In the previous chapters risk-based methodologies have been developed to enable enhancement of flood risk management.

Chapter 3 answers the question how the flood defence construction contributes to flood risk reduction. An assessment method of risks and investments is presented, valuing structural robustness of a construction type, represented by consequence reduction due to its ductile behaviour during high loads. The results show the total societal costs and the individual risks on victims strongly depend on the construction type. Next to load decrease, strength increase and consequence decrease the structural robustness of the dike construction is a fourth main option for risk reduction.

Chapter 4 shows how tactical planning of interventions contribute to system risk reduction. A method is developed to compare different tactics to prioritize and plan measures in interdependent systems of dikes to reduce risks most effectively and efficiently over time. Therefore time-aggregated risks are introduced. The results of a case on a system of dikes along the Rhine river branches underpins that tactical planning and corresponding decisions are important for reduction of time-aggregated flood risks.

Chapter 5 elaborates an analytical approach deriving economic optimal risk-based probabilities of dike segment failure, their 'ageing' and economic optimal design horizons. It underpinned the approach in earlier studies to only consider the failure mechanism overtopping. It presents a dynamic and simple to use approach enabling to consider regularly whether a safety level still fits adequately, and to plan interventions to come and their accompanying design requirement and horizon.

Although the practical application of the risk analyses used in Chapters 3, 4 and 5 differ, they are consistently based on the risk-neutral concept as presented in Section 2.1. Coherently used, they can bridge the practical disconnections between the decision levels, indicated by the arrows in Figure 1.2. Figure 6.1 shows the coherence between the elaborations in these chapters. Below the interactions shown in this Figure are described:

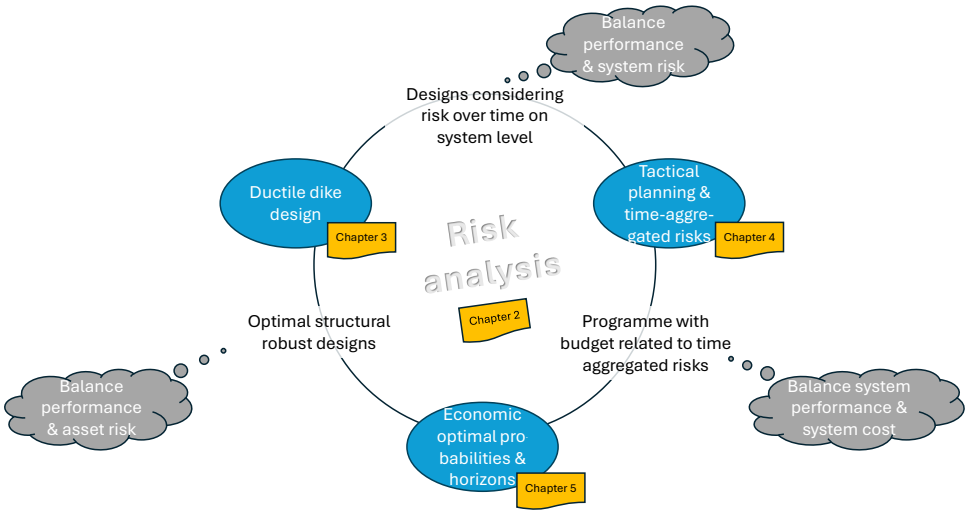

Figure 6.1.: *Overview of the coherence between the risk analysis elaborations performed in this thesis, and their connection to the asset management indicators performance, cost and risk.*

- Safety performance level related to the structural robustness of dikes. The derivation of an economic risk optimization in Chapter 5 delivers the economic optimal intervention timing, the design dike safety level and accompanying design horizon, and a factor to correct for the structural robustness of the design. This can be used to prepare for interventions. Using a design horizon as input, the integrated risk analysis in Chapter 3 delivers the relation between the economic and individual risk. These risk types are presented on the axes of Figures 3.12 and 3.13. These Figures show the relation between these risk types, and that the minimum societal costs depends on the dike design. Together the Chapters 3 and 5 deliver an economic optimal structural design. Furthermore, the relation between economic and individual risk from Chapter 3 delivers the opportunity to evaluate whether non-economic requirements are met (such as the standard for individual risk in the Netherlands) or whether the cost per extra life saved would rise thoughts about the construction type for dike design. Referring to the short definition of the core goal of IAM in [22] this enables balancing asset performance and accompanying risk.

An example of the coherent utilization of the risk analyses for dike design and optimal safety performance requirements: con-

sider a structural robust reinforcement with a sheetpile, which would be very expensive but which would decrease the potential consequences considerably. A coherent coupling between the risk analyses would enable to adapt the performance requirement (see equations (5.45) and (5.46) in Section 5.4.2) and the design horizon (equation (5.17) in Section 5.2.4). Assuming the costs in this case are mostly the marginal costs I' due to high steel prices, this would lead to a less stringent performance requirement and a shorter design horizon, both reducing required dimensions and costs. Note, especially for the reinforcement of a sheetpile the extensibility needs attention. A second reinforcement can be disproportionate more expensive in case there is a sheetpile in place already. The derivation in this thesis starts from a proportionate cost increase factor f_I in equation (5.13), as does the deriviation in [51].

- Prioritisation related to reinforcement alternatives of dikes in system. The tactical planning based on time aggregated system risks in Chapter 4 uses the fragility curves from the individual dikes in the system (Chapter 3) and their safety performance requirements and design horizons (Chapter 5). Despite fragility curves do not represent the time dependent behaviour of a dike during an event (see Figure 4.4 in Section 4.3.1), for structural robust or ductile dikes a fragility curve can be derived from probability analyses, just as for brittle dikes. Therewith, the effect of structural robustness of individual dikes in system can be elaborated since fragility curves can be constructed for different reinforcement alternatives, providing its failure character. Herewith, the system risk analysis for tactical planning can be performed, also based on a set of metrics for risk reduction, planning criteria and budget over time (see Table 4.3 in Section 4.5.3). Referring to the short definition of the core goal of IAM in [22] this enables balancing system performance and accompanying risk.

  An example of the coherent utilization of the risk analyses for dike design and for tactical planning: with the fragility curves corresponding to several reinforcement alternatives their risk reduction effect can be implemented in the time-aggregated system risk analysis. Given a tactical plan, evaluation of all relevant combinations of reinforcement alternatives enable to balance structural robustness of the designs at the dike segments in system, with the time-aggregated system risk reduction, leading to a reinforcement programme.

- Flood defence system assessment related to resources. The optimal performance requirements and the accompanying design horizons

from Chapter 5 are input for the design of individual dike reinforcements of Chapter 3 and for the system risk analysis for tactical planning in Chapter 4. Herewith, the corresponding budget need and accompanying time-aggregated system risk can be generated for several tactical plans and accompanying reinforcement programmes. Referring to the short definition of the core goal of IAM in [22] this enables balancing system cost and accompanying system performance expressed by its time-aggregated system risk.

An example of the coherent utilization of the risk analyses for systems assessment: consider a series of tactical plans and their accompanying programmes, budgets and capacities is confronted with constraints. In case none of them fit, two ultimate options exist: the tactical plan which is most close to the constraint is accepted, resulting in an adapted system performance expressed by its time-aggregated system risk, or the acceptability and accompanying resources come into discussion.

6.2. DYNAMIC CONNECTED RISK ANALYSIS AND PROCESS

In each of the Chapters 3, 4 and 5 it appeared to be important to utilize the risk analyses to connect disciplines, assets in system and to approach physical processes and system development by interventions in a dynamic way. A connective risk analysis is defined in this thesis as to connect the involved disciplines and system effects in the physical domain. A dynamic risk analysis is defined in this thesis as to enable to involve the changes over time on the time scale appropriate for the considered decision level. A dynamic connected risk analysis has several features of both aspects summarized in Table 6.1 per decision level. Appendix D provides an overview of differences between a dynamic and static, and between a connected and disconnected flood risk approach. In Appendix E a case study is performed for location Grebbedijk (see Section 1.5) to assess the magnitude of potential differences between the dynamic connected approach (key topic 1: integrated risk-based optimization of dike design) and the static disconnected approach. It appeared the dynamic connected approach reduces investment costs with about 20% and risk with a factor 3 with respect to the static disconnected approach.

The connection between the decision levels is important as well. As presented in [151] different actors are responsible for the decisions on the different decision levels, such as to take a system measure, prepare the reinforcement programme, or perform a reinforcement. Therewith, different actors are responsible for the risk analyses on the corresponding decision levels. As introduced in Section 6.1, the output of the risk analysis on the one decision level is the input for the risk analysis on the

Table 6.1.: *Overview of connective and dynamic aspects in the risk analyses performed to elaborate the key topics.*

Key topic	**Related decision level & Objective**	**Connective aspects**	**Dynamic aspects**
1. Integrated risk-based optimization of dike design.	Operational. Design of structural robustness and dimensions	Technical disciplines during flood event	Time dependent behaviour of loads and dike during flood event
2. Integrated portfolio prioritisation of measures in system	Tactic. Development of tactical plans to determine programme and order	Relation between individual measures and system effect	Time aggregated system risk, based on effect of present and upcoming measures
3. Performance requirements for comprehensive risk based flood defence management	Strategic. Method for optimal performance requirements & design horizons	Relation between measure and performance requirement	Time dependent requirements, based on design and reinforcement timing

other decision levels. Furthermore, actors on spatial planning, politics or the occurrence of events affect the decisions as well. Therefore, the connection between decision levels has a dynamic character.

To assess this dynamic connection, in the following the elaborated risk analyses in this thesis (summarized in Section 6.1) are combined with the concept of decision levels used in asset management practices [21, 24, 25], and the concept of the Deming circle as an organisational concept for continuous capability improvement [152]. In Figure 6.2 The circle is presented together with the explanation of the four distinguished steps PLAN, DO, CHECK and ACT, following the descriptions in [152].

Starting with the aim of the responsible flood-defence-actors to continuously reduce flood risk against acceptable investments, the process can be presented as a continuous search for an optimal programme of interventions such as reinforcements. The risk management objectives used in this thesis are compliance (operational level), risk reduction over time (tactical level), and economic optimalisation and a societal acceptable limit on victims (strategic level). Note, the risk on victims may lead to even more stringent requirements than economic optimalisation. Following the strategic ALARA/ALARP principle: As Low as Reasonable Achievable/Acceptable/Possible [153], the programme of optimal interventions in system results in an optimal system risk reduction over time on tactical level. On operational level, a single intervention like a reinforcement on a location in the system, the risk objective is compliance. In Figure

6.3 the decision levels are presented together with the corresponding risk management objective, used in the corresponding chapters in this thesis.

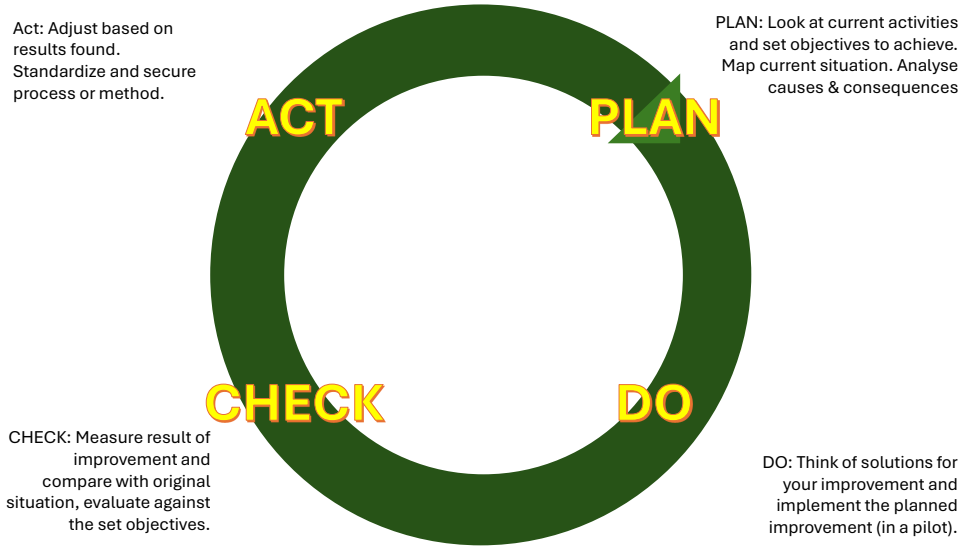

Figure 6.2.: *PDCA-circle including brief explanation of the steps (adapted from [152]).*

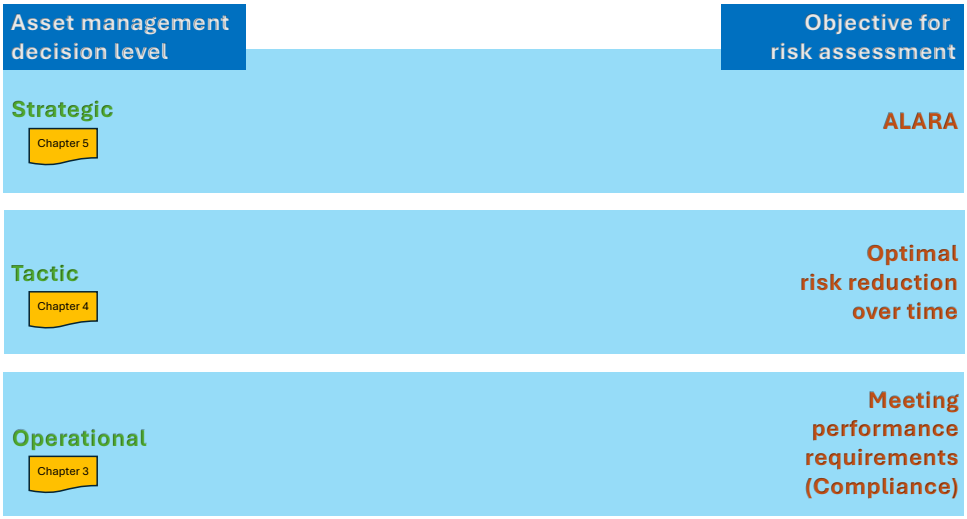

Figure 6.3.: *Schematic overview of asset management decision levels and corresponding risk management objectives.*

Table 6.2 provides an overview of the key-outcome of the risk analyses addressed in the Chapters 3, 4 and 5, connecting the decision levels. They can be divided in impact on asset level and on system level, as described in [24]. The one affects the implementation of interventions. The other affects the elaboration of system measures and programmes. To accommodate two different workflows, the Deming's circle is split in two communicating circles.

Table 6.2.: *Overview of key-output of risk analyses, connecting the decision levels.*

Outcome	**Description**	**Connected decision levels**	**Examples of key-output of Chapters 3, 4 and 5**
Tactical plan	Choose tactical plan and system measure	Strategic to Tactic	Tactical plan, Planning metrics, budget
Prepare reinforcements	Determine programme of interventions, confirm intervention	Tactic to operational	Timing, type, performance requirement and horizon
Execute reinforcements	Design and execution of reinforcements	Operational to Tactic	updated safety level, fragility curve and risk contribution to system
Safety assessments	Determination of actual safety level of flood defences	Tactic to strategic	actual safety level and system risk
Elaborate system state	Calculate system risks in actual situation	Tactic to operational	actual safety level of system components
Elaborate tactical plans & system measures	Calculate risks and investments over time for several combinations of tactical plans and system measures	Operational to tactic	Time aggregated risks for combinations of tactical plans and system measures
Evaluate & propose	Evaluate tactical plans and system measures to determine preferred plan to propose	Tactic to strategic	Preferred tactical plan and corresponding budget

In Figure 6.4 both concepts are combined. The Deming's circle is turned a bit to align it with the decision levels, since PLAN and CHECK best match with the tactic level and DO with the operational level. Consequently ACT is placed on strategic level, stipulating the strategic role

of securing system process, adjustments and communication.

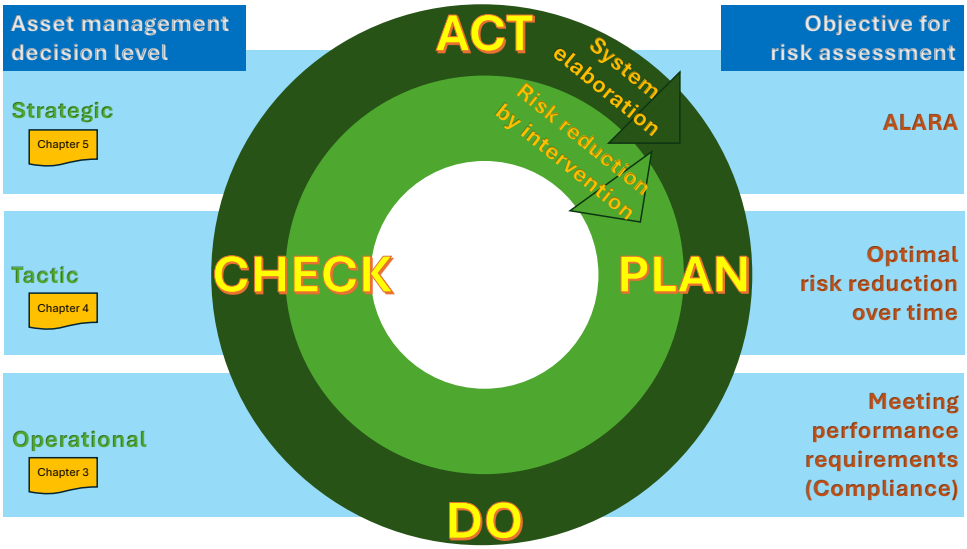

Figure 6.4.: *Schematic overview of the (slightly turned) PDCA circles for system elaboration and intervention, related to the asset management decision levels and risk management objectives.*

Finally, the components from Table 6.2 are put on the ground plate of Figure 6.4, resulting in Figure 6.5. The outer circle consists of continuous system elaborations processing all (dynamic) information due to executed reinforcements, actual assessments, climate change, subsidence, potential system measures such as building storm surge barriers, reinforcement proposals, innovative techniques, management experiences, uptaken knowledge, data, development of potential consequences etc. The inner circle consists of the actual interventions. The connection between the outer and inner circle is straight forward: a tactical plan feeds the inner asset circle, and the performed interventions feed the outer system circle. Based thereon, the strategic choices can be changed. This way the process has a high degree of adaptability.

In fact the dynamic character of the information can lead to a changing perspective on the preferred tactical plan including timing and order of measures. Steegh [154] describes the agile working method as: 'The agile way of working prioritises flexibility, iterative development of projects and a people-centred approach. Agile encourages rapid response to change and continuous improvement'. Ruël [155] describes the Waterfall approach as: 'The Waterfall approach has been the dominant approach for enterprise systems (ES) implementation since the 1970s. It offers ES project managers a simple, step-by-step way to make ES projects man-

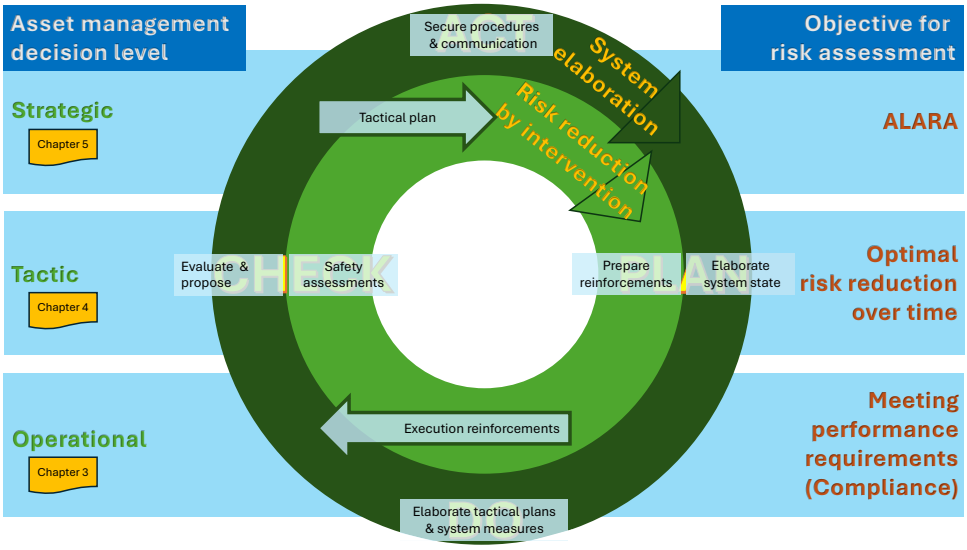

Figure 6.5.: *Schematic overview of dynamic concept for flood defence asset management.*

6

ageable and minimize drawbacks'. Therewith, the dynamic character is better accommodated by an agile process than by a Waterfall-like process [155] in which the different decision levels close with a decision, because these decisions may be aged at the time of implementation of an intervention. In the proposed agile process the only irrevocable decision is to perform an intervention, all other decisions are open unto this final decision. Together this provides a comprehensive perspective for utilization of risk analyses in flood defence system management.

In the concept presented in Figure 6.5 the focus in on continuous improvement of the system safety. Figure 6.6 presents a graph which shows safety progress over time. The system state over time is presented on the axes as used in Figure 4.19. The x-axis reflects the expected number of victims in system in a reference period. The reference period serves to calculate the time aggregated risk, in Chapter 4 a period of 100 year is taken. On the y-axis reflects the societal costs, which is the sum of the present value of investment and risk in system in the reference period. The red line represents the past performance up to present system state. Assuming each intervention in the past has been as well beneficial as reducing the number of victims, the red line starts in the corner right above and moves down left over time, as reflected by the denoted years along the line. Some possible tracks are drawn for future activities (blue arrows). In a system subject to deterioration and climate change, inactivity and maladaptation will lead to an increase of societal costs and

the expected number of victims. An ineffective programme will reduce the expected number of victims, but accompanied with an increase of societal costs. The other two paths are directed left-down. Those can be interpreted as effective programs. They are based on two different tactical plans. In the one for which the metrics determining the tactical plan focus on reduction of victims, interventions may require more budget than in case the focus would be purely on the reduction of societal costs (most left directed track). In the one for which the metrics determining the tactical plan focus on reduction of societal costs (lowest track), interventions may lead to more victims than in case the focus would be purely on the reduction of victims. Following the risk assessment objectives (Figure 6.5, far right) to bring economic and individual risk as low as reasonable achievable or societal acceptable (ALARA), progress can be measured as the distance to the left down corner in Figure 6.6.

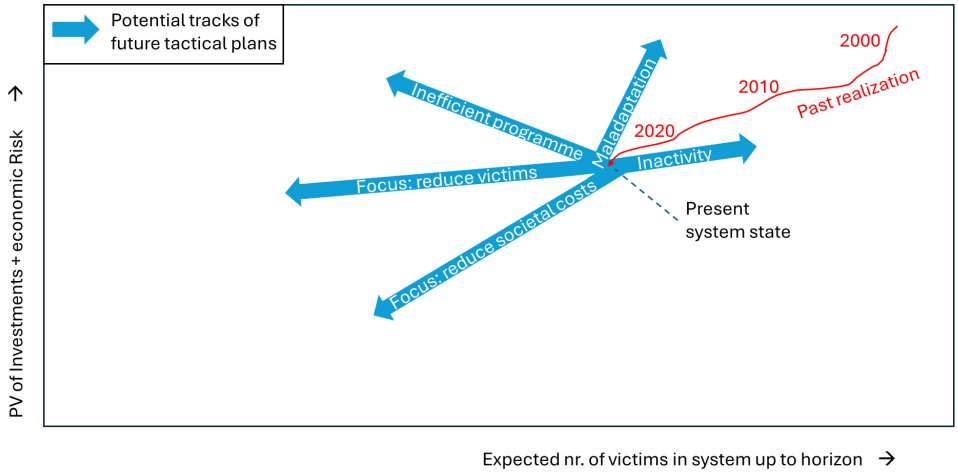

Figure 6.6.: *Overview of economic and individual risk reduction over time. Past performance in red, labels in years, and potential tracks of tactical plans in blue.*

6.3. COMPREHENSIVE FLOOD DEFENCE SYSTEM MANAGEMENT

The concept in the previous section is described below in a storyline how the process could work.

Starting the process in the outer circle in Figure 6.5 at the strategic decision level (ACT), 'Secure procedures' is mainly about providing starting

points for system development on the relevant sectors (e.g. technical, spatial, capacity, capability), as well as about communication of choices and investigating societal acceptability. One of the procedures elaborated in this thesis can be the prescription of the method for derivation of an economic optimal safety level in Chapter 5. Most relevant for utilizing the risk analysis in a dynamic connected way are the starting points for tactical planning providing room for a series of tactical plans like Table 4.5. The starting points may include to consider system measures as well.

The system elaboration process continues with 'elaboration system state' (PLAN), inventorying the present system condition as a starter. For each dike segment a preliminary assessment is performed based on a preliminary safety level as the performance requirement. Further elaboration of interventions can be done without the dikes which reinforcement is certainly out of programme horizon. For the remaining dike segments an inventory of several reinforcement alternatives is made, including alternatives changing the construction type, and including future projections of ageing. The accompanying performance requirement is based on the prescribed method from the strategic decision level (Chapter 5, equations (5.45) and (5.46)).

With 'elaborate tactical plans & system measures' (DO) potential intervention programmes are composed based on a series of tactical plans fitting in the strategic starting points, including potential system measures. For each dike in system reinforcement alternatives are analysed, for several structural robustnesses. For each tactical plan the initial safety level for the dike segments in system is derived based on actual assessments, and the intended safety level is based on the prescribed method from the strategic decision level (Chapter 5) and the reinforcement alternative. Therewith, the time-aggregated risk reductions corresponding to the tactical plans and corresponding interventions can be calculated, see Chapter 4.

With 'Evaluate & propose' (CHECK) these time-aggregated risk reductions are weighed and a proposal is made for a tactical plan, to be decided for at strategic level. At strategic level the proposal is confirmed or rejected.

In case it is confirmed the choice for a tactical plan is the start of the inner intervention circle in Figure 6.5 (ACT). In case it is rejected the argument for the rejection is added to the set of starting points provided to the next step in the outer system elaboration circle. In that case a next iteration in the outer circle may lead to confirmation of a proposed plan, entering the intervention circle.

Following the strategic choice for a tactical plan, with 'preprare reinforcements' (PLAN) the corresponding intervention programme is set-up. The programme is build based on actual assessments and the confirmed tactical plan including the budget. Therewith, the timing, construction

type, safety performance requirement and design horizons are determined.

Following the system programme, the first upcoming reinforcements need a formal decision after which they cannot be withdrawn by programme considerations without loss. Then, the reinforcement can be executed (DO). Note, the formal reinforcement decision contains not only earmarking the dike segments to be reinforced, but the reinforcement plan as well, including construction type and safety level, because of its effect on the system.

Finally, the last step in the intervention circle is to update the 'actual assessments' for all flood defences in system (CHECK) based on the actual system and status of the interventions. These actual assessments are input for 'communication' (ACT) and for the next steps in the system elaboration circle in Figure 6.5 evaluating interventions to continuously find the best coherent tactical plans.

In this way the executed reinforcements are tuned on their direct effects, reducing the risk in polders they protect, and on their system effects, due to the increased loads (e.g. in a river: for downstream located dikes). Individually, the executed reinforcements meet the required safety levels, they are compliant. Due to the thoroughly evaluated tactical plans, the time aggregated flood risk in system is optimal reduced over time, within the strategic boundaries. At strategic level, due to the thoroughly consideration and communication on the progress, the process is related to societal acceptability, meeting the ALARA principle [153].

6.4. ASSET MANAGEMENT OF FLOOD DEFENCES NEEDS COOPERATION

The different steps in the Deming circle in Section 6.2 refer to the asset management decision levels. In case the decisions are to be taken by different actors the responsibility is fragmented, which is the case for flood defence system management in many countries [23]. Therefore, the proposal in Section 6.2 for an agile process for flood defence system management is complex. Due to the increasing complexity, practical bottlenecks and dilemmas arise. Goldratt and Cox [156] point out the role of bottlenecks in a manufacturing process, defining a bottleneck as a constraint resource that creates limitations in the production process. In this thesis this definition is used in the context of cooperation for flood risk management: the constraints are the interests of involved

The majority of Section 6.4 and a part of Section 6.5 has been published in F. den Heijer, J. Rijke, M. Bosch-Rekveldt, A. de Leeuw, and María Barciela-Rial. "Asset management of flood defences as a co-production – An analysis of cooperation in five situations in the Netherlands". In: Journal of Flood Risk Management (2023). doi: 10.1111/jfr3.12909

stakeholders, creating limitations to the asset management process of dikes. In this thesis a dilemma is defined as a situation in which a non-trivial choice has to be made between options to solve the bottleneck. Non-trivial means here that all options may have downsides leading to ambiguous solutions.

This section takes an organizational perspective on flood defence asset management and focuses on the shape of cooperation in different situations of flood defence asset management. The aim of this section is to explore the present practice of cooperation in flood defence asset management since cooperation is an indispensable condition to overcome bottlenecks in the process proposed in the previous section, to get it work in practice.

Practical bottlenecks and dilemmas prompts flood defence asset management to mature [157]. The last decades have witnessed a tendency towards integrated management of resources (e.g. [158–160]). At the same time, aversion to change leads to a preference for traditional approaches within the flood risk management sector [146, 161, 162]. This conservative balance between stability and change is intrinsically given by the importance of the end goal: to protect people and properties against flooding [163]. However, this hampers innovation and fully integrated management [164–166] highlighting the importance of finding the best mix of activities to provide the best life cycle performance and to optimize work delivery programs of the managed assets. Key elements in such an integrated approach would be participation and cooperation [164, 167]. However, establishing cooperation among the main actors involved in flood risk management is a challenge [168].

Presuming that in practice the shape of cooperation depends on ad-hoc responses to bottlenecks and dilemmas, the question is: how do dilemmas and bottlenecks influence the shape of cooperation in the practice of flood defence management?

FIVE SITUATIONS

To explore this question five situations are taken from [169] originating in the Netherlands covering several interfaces between decision levels and the main cluster of flood defence tasks (Section 1.5). The five situations highlight several bottlenecks and dilemmas faced in the practice of integrated asset management. The situations are summarized in Table 6.3 and briefly described in Appendix F. The locations of the situations are shown in Figure 6.7 and the interfaces are shown in Figure 6.8.

For each situation, data were gathered through semi-structured interviews and document analysis. To observe the response of the institutions on the situations, in total 67 interviews were held with respondents holding different roles and responsibilities. A qualitative analysis of the situations points to the response of institutions to changes is reflected in dilemmas and bottlenecks at these interfaces. In Appendix F for each sit-

Table 6.3.: *Overview of the five situations.*

Situation	Description
1. Dike segment approach – Strategy development of dike segment reinforcement	Urged by new legislation the Water Authority has to take up the challenge to adapt to new roles and responsibilities in participative processes in spatial planning for dike reinforcement. The Water Authority lacks a clear vision of the shape and implementation of the required integrated approach.
2. Management agreement liquefaction prevention	The occurrence of macro-instability caused by liquefaction of the foreshore might increase the probability of dike failure. The Ministry is responsible for the maintenance of the estuary adjacent to the dikes, and the Water Authority for the dikes along the Scheldt. Because of the renewed legislation of standards for flood defences in 2017 the old agreements need to be renewed.
3. Innovative dike reinforcement	A project team of the Water Authority selected an innovative cost-friendly reinforcement measure. The maintenance department of the Authority was not involved in this decision. It is not familiar with the monitoring and maintenance for this measure. It hesitates to take over the responsibility after the reinforcement is finalized.
4. Dealing with damage to dikes by beavers	Digging holes, beavers affect flood risk. According to Natural Law, beavers are a protected species. The Water Authority has to trade off whether to take into account the risk of digging beavers in their maintenance and reinforcements, or to strive for a joint policy on the management of the population with nature organisations.
5. Vision on long term monitoring	The existing monitoring is performed on a project basis. A decision for long-term monitoring, which is expected to pay off, need changes in the organization and budgets: the cost of data collection is not eligible for national grants. The Water Authority has to trade off whether to organize the budgets itself or accept project based monitoring.

uation the dilemmas and bottlenecks are extracted, as well as shapes of cooperation to overcome them. Bottlenecks can be categorized at three levels [169]: the lack of clear and supported vision of tasks and long-term developments (strategic level); the lack of a clear and supported view of responsibilities (tactical level), and the lack of clear rules and practices for financial, organizational and technical performance (operational level). The situations show the Water Authorities respond ad-hoc to the bottlenecks, aspiring for a shape of cooperation in which the bottleneck can be solved, summarized in the trade-offs in Table 6.4.

To show the current and desired shape of cooperation, the observed development of the organization is plotted on two dimensions of cooperation. For the first dimension, the intensity levels of cooperation defined

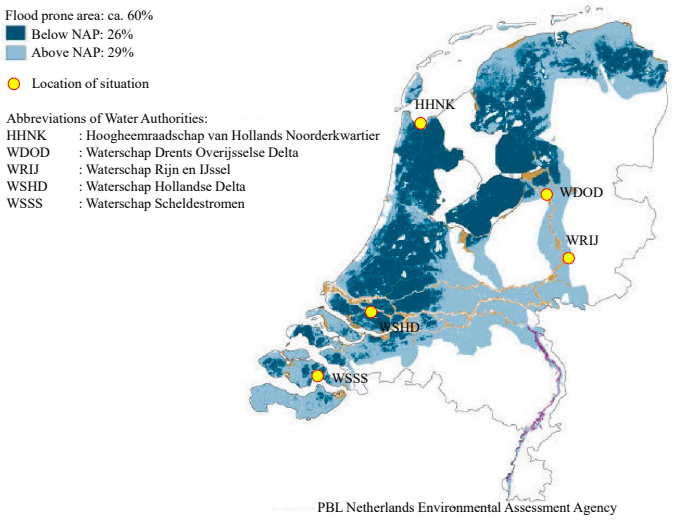

Figure 6.7.: *Locations of the situations. HDSR, HHNK, WDOD, V&V, WSHD, WRIJ, and WSSS are the abbreviations of the Dutch Water Authorities responsible for the flood defences in the selected situations.*

6

Table 6.4.: *Overview of two options for the flood defence manager (Water Board) to approach the trade-offs in the five situations, see Appendix F.*

Situation	**Option 1**	**Option 2**
1. Dike segment approach – Strategy development of dike segment reinforcement	Mandatory contribution to integrative approach	Embrace integrative approach
2. Management agreement liquefaction prevention	Pre-invest at risk of not getting funded	delay critical repairs and accept spacious dike dimensions
3. Innovative dike reinforcement	Embrace innovation without a maintenance track record	Spacious dike dimensions
4. Dealing with damage to dikes by beavers	Spacious dike dimensions	Restrict protected status of beavers
5. Vision on long term monitoring	Allocate budget for monitoring	Accept uncertainty or propose spacious dike dimensions

by Sadoff and Grey [170] have been used (unilateral, coordination, collaboration, and joint action). For the second dimension, a distinction has been made between internal and external cooperation, corresponding

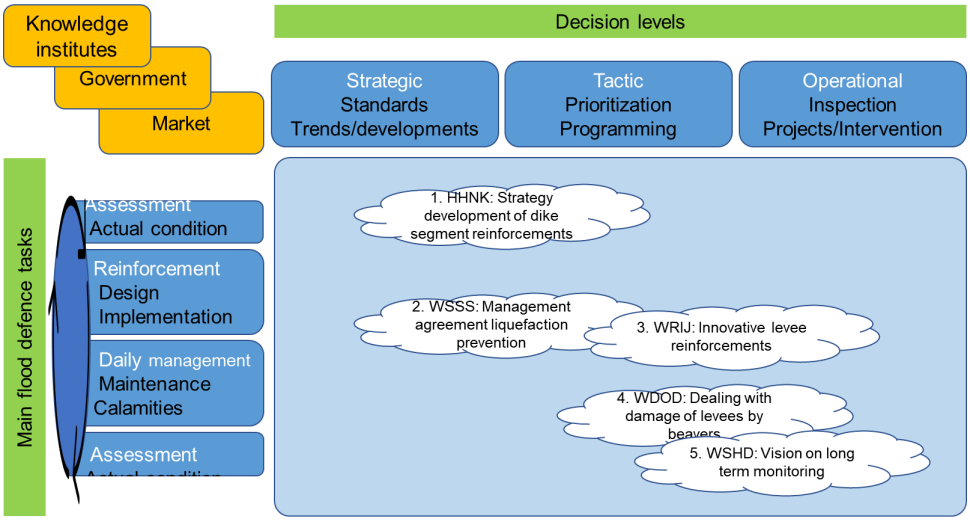

Figure 6.8.: *Overview of situations with respect to decision level and main flood defence task. Note the 'vertical' axis is a 'cylinder' since the three main tasks each interface with the two others. "Assessment" is twice on the vertical axis to visualize this.*

with the Infrastructure Asset Management Maturity Model (IM^3, [157]). Herein, internal cooperation is defined as cooperation within an independent government institution and external cooperation is defined as cooperation between an independent government institution and another actor (public or private).

Although the situations as such are different, there are commonalities. All situations face changing circumstances: legal changes (new Water Act and new Environment and Planning Act), change of rules and protocols (organizational, financial) or change of opportunities (technical, innovations). Such changes could be the catalyst to seek other shapes of cooperation. Seeking a fitting shape for cooperation is in accordance with the principles of adaptive asset management [23]. The aspiration of the Water Authorities to improve cooperation originates from technical or spatial challenges (situation 3), organizational challenges (i.e., responsibilities, tasks and roles; situations 1, 2, 3, 4 and 5) and changing external circumstances (situations 1, 2 and 4). Figure 6.9 plots the aspired change in the shape of cooperation for each situation in a grid of the intensity of cooperation [170] and the asset management dimensions (IM^3, Volker et al., 2013). In Figure 6.9:

- All arrows originate in the left part of the Figure, and most of them

are in the gridcell of internal unilateral action or coordination. This is interpreted as the institution's basic attitude, acting based on its own responsibilities and influence.

- All arrows are directed to the right or upward to external coordination. This is interpreted as the Water Authorities' aspired cooperation.
- Most arrows are short, bridging only one gridcell, and one is longer, the dike segment approach (situation 1).

Note, when cooperation has led to agreements, rules, protocols, clear new responsibilities, decreased content complexity, or when the circumstances become stable, the required intensity of cooperation may decrease.

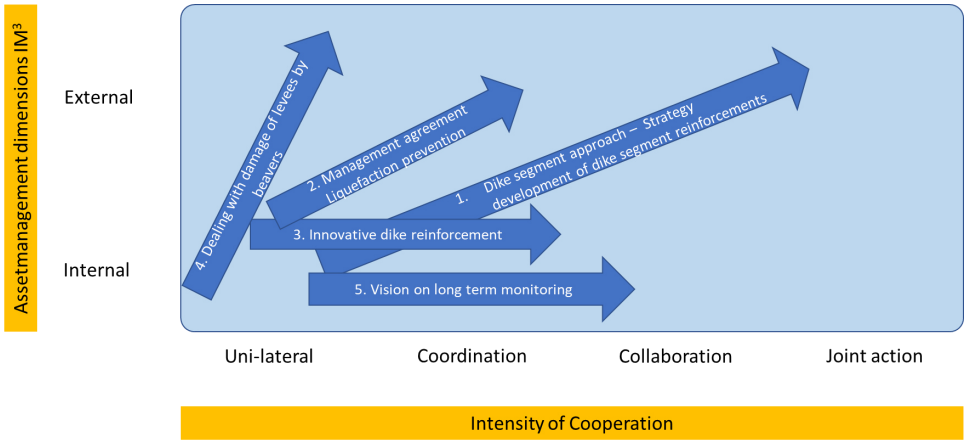

Figure 6.9.: *Overview of the Water Authority's observed change in the shape of cooperation for the situations in the case, in terms of cooperation intensity [170] and two relevant dimensions of the asset management maturity model IM³ [157].*

DISCUSSION

The situations show the need to carefully shape cooperation. Situations in the case were raised by Water Authorities as problems they experience, related to cooperation. The Water Authorities selected the situations after they experienced the practical problems, with the aim to enable research cooperation. The observed (intuitive) responses and

trade-offs made in the situations described, show how this works out in practice: except arrow 1, the arrows in Figure 6.9 are short, pointing to a careful search for intensification of the cooperation: not too ambitious, but steadily. This may be an artefact of the origin of the situations, brought in by the Water Authorities, who have a practical attitude and maybe intuitively look for situations for which the solution is nearby. The most noticeable observed change of cooperation is in the situation of the dike segment approach, suggesting the need to both intensify cooperation and involve more organizations, in this situation on the level of a whole region.

Obviously, there is no universal 'good' shape of cooperation. As cooperation is common in the daily work attitude of the Water Authorities, this opens the discussion of how to gain maximal benefits. The analysis of the situations shows how gaining benefits work in practice. Bottlenecks and dilemmas in cooperation have different characteristics. The bottlenecks are mostly caused by changes in technical or organizational starting points. Bottlenecks do not have a solution at first sight. Typical dilemmas have two sides, both leading to some negative impact. The dilemmas are mostly caused by different interests. Involved parties have different objectives and success indicators, weighing the dilemmas differently. The shape of cooperation between the involved parties depends on the benefits they get in accomplishing their own success indicators. The situations show the necessity to change the shape of cooperation, to overcome the bottlenecks due to change in circumstances as summarized in Figure 6.9, where the arrows vary in length and direction depending on the situation.

When a dilemma occurs *within* an organization, an escalation ladder can be used to solve the problem. In Figure 6.10 a simple solution for a bottleneck between departments in the own organization is illustrated, which could be solved by escalation to a management level exceeding the departments (light blue). When a dilemma is *in between* organizations, however, escalation possibilities are more complicated and the problem is harder to solve. This applies to flood defence projects: at each of the decision levels, an explicit non-juridical possibility to escalate to a central point is missing. Given their multi-managed nature, a central, single authority hardly exists for the management of complex systems. Effective cooperation between actors is therefore vital to flood defence asset management. However, achieving integration in practice is a recurring challenge, especially in flood risk management where multiple actors need to work together across fragmented policy domains [164]. In this regard, cooperation intensities as proposed by Sadoff and Grey [170] are instruments to shape cooperation. In the situations studied, apparently, there was a tendency to change the bottlenecks in dilemmas. The aspired change of cooperation changes the decision context and involvement of stakeholders, re-arranging the bottlenecks in dilem-

mas, for which a trade-off can be made.

This finding shows that the success in asset management of flood defence systems is dependent on the practical implementation of cooperation and the ability and agility to choose and change the shape of cooperation dependent on the situation: *situational cooperation*. Figure 6.10 shows the position of situational cooperation found in the situations: a change (e.g. in law) may introduce a bottleneck (e.g. the change requires a new approach); when the involved stakeholders are able to relate this bottleneck to a dilemma with respect to cooperation, they can search for a shape of cooperation which enables to re-arrange the bottleneck in a dilemma that can be traded-off.

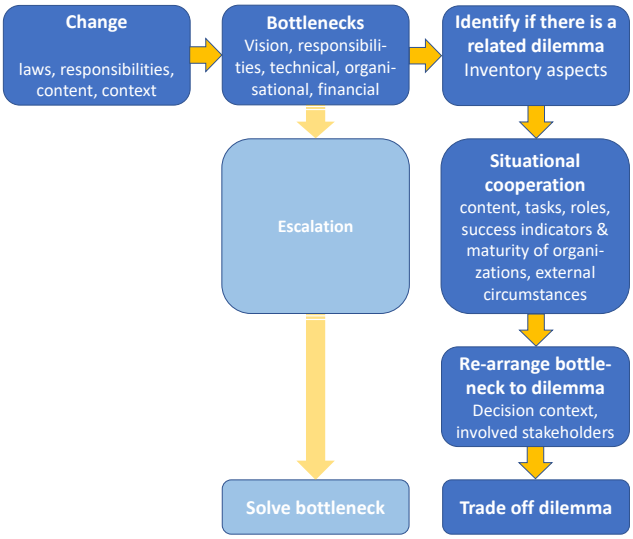

Figure 6.10.: *Schematic overview of observed coherence between change, bottlenecks, and dilemmas, pointing out the role of situational cooperation.*

Based on the situations studied, two aspects seem important for the implementation of situational cooperation. Firstly, it is observed that sharing of knowledge on different decision levels involved in the re-arranged dilemma is important. This supports the findings of [168] who identified local bodies on site, trust with stakeholders, and usage of local knowledge as key factors to strengthen cooperation. Secondly, the adoption capacity of an organization to new procedures and methods seems important. The adoption of new working methods requires change on all levels of the organization. This is a difficult process that can take a long time, especially if certain rules, procedures and working methods have long been institutionalized in the organization [161, 171].

The relevance of cooperation in flood defence management is not lim-

ited to the situations in the Netherlands [172]. The main flood defence tasks and the decision levels are the same in all countries, but the institutional organization and responsibilities differ between countries. In deltaic areas, worldwide cooperation will be important when risk reduction measures interfere with other interests such as space and finance. The effectiveness of management is dependent on the quality of fulfilling roles by the actors involved [173], as well as the enabling context [174]. Successful fulfilment of roles and tasks in multi-actor settings is one of the key aspects in the field of project and programme management (e.g. [174–177]). This section shows that awareness of tasks and roles in the organizations involved is also important for the management of flood defences because bottlenecks that cannot be solved by escalation have to be shifted to a decision context where it appears to be a dilemma. Situational cooperation in flood defence asset management will bring in an intuitively known yet underexposed pillar in the body of literature on Water Governance.

The incentives for cooperation are time-dependent (arrows in Figure 6.9). The five situations investigated were brought in with an actual problem or dilemma, for which intensified cooperation supported a way out. Other situations may benefit from less cooperation, e.g., when a change has led to new accepted working methods it could be efficient to re-shape the cooperation to a less intensive level. Thus, the right-directed arrows in Figure 6.9 do not point out that joint action is always better than unilateral action.

Although the scientific developments on flood defence asset management maturity are mainly technical [23, 24], this study shows that organizational maturity should be developed as well. This confirms the observation in [157] that mature asset management is not only technical but organizational and inter-organizational as well, and that integrated approaches have the potential to enable better outcomes [164]. This is a step further than suggested by Woodhouse [166], who already pointed out the importance of evaluation and optimization of combining technical options and actions. Even technical and organizational changes interfere, as illustrated in situation 3 where a technical innovation requires a shift in the shape of cooperation.

The main conclusion from this section is that the multi-managed practice of flood defence management requires situational cooperation to support re-arranging bottlenecks in dilemmas for which a trade-off can be made. In the presented situations, the Water authorities chose the shape of cooperation dependent on the complexity of content, the complexity of organizational context, and relevant external circumstances. To support organizational maturity to deliberately design fit-for-purpose shapes of cooperation it is recommended to develop and use proper tools to identify and implement situational cooperation in flood defence asset management, such as training, serious games and sharing of best prac-

tices. The role of these tools should include clarification of the starting points of the own organization, decision contexts, creating awareness of the role of effective interface management, and adoption capacity.

6.5. CONCLUSION COMPREHENSIVE RISK PERSPECTIVE

This chapter links the risk analyses in this thesis to coherently support the flood defence asset management on the three decision levels. The circumstances are dynamic on several time scales, requiring a dynamic connected risk analysis and corresponding dynamic decision process. The proposed agile process uses the steps in the Deming circle for continuously improvement, and connects to the appropriate risk management objectives on the several decision levels. In this process the executed reinforcements ensure compliance, meeting the design dependent safety requirements. Due to the thoroughly evaluated tactical plans, the time aggregated flood risk in system is optimal reduced over time, within the strategic boundaries. At strategic level, due to the thoroughly consideration and communication on the progress, the process is related to societal acceptability, meeting the ALARA principle [153]. In the proposed agile process the only irrevocable decision is to perform an intervention, all other decisions are open unto this final decision.

An agile process complicates the decision context, since several actors are responsible for the main clusters of flood defences tasks. The explored five situations in the Netherlands clearly show that different parts in the proposed process in this chapter may ask for a different shape of cooperation, depending on the content, the typology and difference in tasks, roles, success indicators and maturity of the asset management in the involved organizations, and on relevant external circumstances. In other words, the success of asset management of flood defence systems depends on the practical implementation of cooperation and the ability and agility to choose and change the shape of cooperation dependent on the situation. The bottlenecks that are faced in the five situations can be categorized at the three asset management decision levels levels: the availability of a clear and supported vision on tasks and long-term developments (strategic level); the availability of a clear and supported view on responsibilities (tactical level), and the availability of clear rules and practices for financial, organizational and technical performance (operational level).

In the step 'secure procedures' in the proposed agile process its practical implications should be guided. Based on [169] it appeared that bottlenecks and dilemmas are weighed differently by different organizations or departments in organizations, due to different objectives and success indicators. The desired shape of cooperation between the involved parties depends on the benefits they get in accomplishing their own success indicators. In case an escalation step is not opportune, be-

cause a central authority does not exist for the management of complex multi-managed systems in public space, sound cooperation is required for successful re-arranging bottlenecks in dilemmas for which a trade-off can be made.

The comprehensive risk-perspective and the dynamic process enables to report the progress of flood risk reduction to society on system level.

7

CONCLUSIONS AND RECOMMENDATIONS

[Flood risk reduction is a] "tender and important matter [that] had to be handled with caution, after mature deliberation and with the knowledge of all".

Thorbecke's interpretation in 1850 of King Willem I's motive to publish the River Commissions proposal in 1827 to reduce flood risks by river diversions.

Structural robustness is important for flood risk reduction because it affects the optimal dike design. Trade-offs of dike design and corresponding risks and investments can consider the dike construction as an additional and highly relevant alternative main option for risk reduction, next to load decrease, strength increase and consequence decrease. Tactical planning is important to effectively and efficiently reduce system flood risks over time. The time-aggregated risk reduction can be introduced as a decision variable for evaluation of tactical plans. Risk aware updating of flood defence performance requirements enables to keep a dynamic focus on the optimal economic risk, updating the requirements (in the Netherlands: the standard) dependent on the timing of an intervention and the structural robustness of a design. Further steps are recommended to develop and enhance the approach and implementation of these findings and to mature the application, enabling to utilize structural robustness, to set up tactical plans for portfolio planning, and to investigate the effects of risk-based updating of performance requirements. A dynamic process can be introduced to continuously focus on effective and efficient risk reduction, supporting a sound cooperation between actors, tailored to the situation.

7.1. MAIN FINDINGS

The objective in this thesis is to develop and test methods for coherent risk analysis in flood defence system management. In this section the questions introduced in Chapter 1 are answered.

7.1.1. HOW CAN STRUCTURAL ROBUSTNESS CONTRIBUTE TO FLOOD RISK REDUCTION?

To answer this question, in this thesis a new step to an integrated risk assessment has been made. Present practice of flood risk analyses use separate analyses for probability of flooding and consequences of flooding, with the failure mechanism in the flood probability analyses treated separately. In Chapter 3 the whole chain from loads, strength, erosion and dike breach, flooding and consequences is modelled time dependent during a flood event. This enables to relate a flood event directly to consequences. Therewith, probability distributions of flood events can be translated to exceedance curves of water levels in the polder (F_H-curves, Figure 3.4).

Chapter 3 shows different dike construction types lead to significant different exceedance curves of water levels in the polder (see Figure 3.9): the risk appears to be highly dependent on the construction of the dike. Constructing a clay core, a sheetpile or extra dike width affects investments as well. In contrast to most of current risk analyses in which probability and consequences are needed explicitly, the integrated risk analysis includes dike failure, without the need for an explicit probability of dike failure.

The model is applied on the case 'Grebbedijk' in a riverine area in the Netherlands. A graphical representation provides insight in economic and individual risk on victims (Figures 3.12 and 3.13). It shows the large differences in societal costs varying from 10 up to 50 M€ between the different dike construction types, and the corresponding economic optimal probabilities of dike failure vary between $0.03 \cdot 10^{-5}$ and $0.4 \cdot 10^{-5}$ per year, which is significant. The application shows the second optimal construction type costs 5M€ more than the optimal one (which is about 50%), providing a reduction of the individual risk by a factor 15.

Concluding, structural robustness is important for flood risk reduction because it affects the optimal dike design. Applying an integrated risk analysis enable to consider the dike construction as an additional and highly relevant alternative main option for risk reduction, next to the existing ones such as load decrease, strength increase and consequence decrease.

7.1.2. HOW CAN PLANNING OF MEASURES CONTRIBUTE TO SYSTEM RISK REDUCTION?

To answer this question, in this thesis the effect of tactical plans is investigated, which define the prioritisation and planning of consecutive interventions to implement a flood risk reduction strategy. A model-based planning method is developed to enable a risk analysis over time for an interdependent system of dikes, subject to changes in loads, strengths and consequences. The risk reduction effect of an intervention at a time is modelled by reducing the probability of dike failure at that point in time. Chapter 4 shows tactical plans of interventions affects system risk reduction significantly.

The time-aggregated system flood risk is introduced to evaluate the effectivity and efficiency of a tactic. This is the total economic and individual risk in the system over a period of time, taking into account the effect of man-induced changes like dike reinforcements, and the autonomic changes such as climate change, subsidence and population growth. The time-aggregated system flood risk, in this thesis taken over 100 year, is a measure enabling comparison of different tactics, because it identifies the effectivity of the man-induced changes with respect to the risk reduction.

The model-base planning method is applied on a case with a system of about 500 km of dikes along the Dutch Rhine river branches. A riverine area is special with respect to the tactical plan because an upstream dike breach reduce the water levels downstream and therewith the downstream dike performances. The case study calculates the portfolio metrics performance, risk and cost, for 12 different tactical plans for different prioritisation and planning considerations and different budgets. The results show the present value of the sum of costs and risks of the plans differ by up to about 40% with respect to that of the plan with the highest present value (about 6 billion €). For individual risks the differences are up to 70% with respect to the plan with the highest value (about 200 victims). The case underpins that tactical plans and corresponding planning decisions are important for reduction of time-aggregated flood risks.

Next to budget, the prioritisation metric and a planning priority for high risk locations appeared to be important. Furthermore, different plans lead to a different patterns and intensity of measures in the system. For example, the prioritisation metric based on benefit-cost ratio leads to interventions focussing on reinforcements along the Nederrijn-Lek branche, reducing flood probabilities in large polders with a high damage potential. The metric based on individual risk leads to a focus on reinforcements along the Waal branche, reducing the flood probabilities in polders with relatively high potential of victims.

Concluding, tactical planning is important to effectively and efficiently reduce flood risks over time to a compliant level. The application of the presented methodology to develop and compare a number of tactical

plans, provides understanding that supports planning discussions and the corresponding tactical decisions.

7.1.3. HOW CAN RISK-BASED STANDARDS REFLECT THE BENEFITS OF STRUCTURAL ROBUST DESIGNS?

To answer this question, in this thesis a method is developed to enable risk aware updating of standards. The risk is dependent on the construction type (Chapter 3), and the optimal performance requirements are ageing (Chapter 5). Furthermore, the timing of an intervention depends on the tactical plan in the system (Chapter 4). Therefore, it is needed to keep a dynamic focus on optimal risk reduction dependent on the design and on the intervention timing.

Based on the analytic approach of Van Dantzig [14], the existing static economic optimal performance requirement based on overflow is adapted to a time dependent dynamic one based on overtopping. Furthermore, it is extended to contain the effect of piping. It appeared that the effect of considering piping next to overtopping does not lead to significant different optimal performance requirements. Furthermore, an optimal intervention timing and economic optimal life cycles are derived, which appear to be dependent on the ratio of the water level increase rate η and the load rate parameter $f_{ovx} \cdot B$. Finally, a relation is proposed to insert the effect of the construction type in the performance requirement.

For the case of the standards in the Netherlands, the results based on the derived relations are compared with results of the numerical approach used for the preparations for the Dutch Flood Protection Act [51], including more than 70 dike segments. The agreement in the case is good, the return periods differ 5% on an average (see Figures 5.9 and 5.10). Actual practice is to use a design horizon of 50 years. The optimal life cycles of the dike segments in the case are about 40 year on an average, with for most of the dike segments a life cycle between 20 and 60 year.

Concluding, with the adapted analytic approach of Van Dantzig [14] it is practically possible to update the flood defence performance requirement, to keep a dynamic focus on optimal risk reduction, dependent on the timing of an intervention and a design construction type.

7.2. DYNAMIC CONNECTED RISK ANALYSIS

The methods used to research the questions in this thesis in Chapters 3, 4 and 5, and pointed out in the previous section, are set up to connect elements which are distinguished in present practice, and to include dynamic elements. From different perspectives it is beneficial to perform the risk analyses 'connected':

- Risk analysis perspective: connecting the physical models of loads, strength, dike breach and consequences the cut between probabilities and consequences is not needed any more. No subjective choices for scenarios for dike breach and consequences are needed, because flood events are physically connected to the consequences they cause;
- Systems perspective: connecting planned (system-) measures to system effect over time, values the effect of a tactic, supporting prioritisation and planning discussions;
- Design perspective: connecting performance requirements with the dike construction type, values a structural robust design, providing an opportunity to focus on risk reduction rather than meeting a reliability standard.

It is beneficial to perform the risk analyses 'dynamic', on different time scales :

- Flood event: the time dependence of the loads during a flood event enables to assess dike breach timing and character, and (for riverine environments) the downstream water level reduction. Both increase the quality of the assessment of the dike failure probability and the accompanying flood volume, and therewith the assessment of the consequences;
- Design horizon: the optimal design horizon is dependent on the design and location characteristics. Applying a shorter horizon saves budget which can be used for other reinforcements to reduce system risks, and up to that horizon it consumes less space;
- Programme: using a dynamic tactical plan enables to pursue optimal system risk reduction. Reinforcements over time can be selected based on their planned system effects, considering the dependence between risk reduction, priority, location, and design proposal.

Furthermore, to manage a system of flood defences an agile process accommodates connection of the asset management decision levels, with responsible roles for the flood defence manager and the flood defence system manager, see Chapter 6. They provide the information to carry out and synchronize the dynamic connected risk analyses on strategic, tactic and operational decision level, supporting an open decision process. Standards, tactical plans, system measures, reinforcement proposals, knowledge, innovations and assessments affect each other. During the process these may be elaborated or updated. The dynamic character of the information brought in by flood defence managers can lead to a changing perspective of the flood defence system manager on

the preferred tactical plan including timing and order of measures. That in turn affects the work of the flood defence managers. This needs sound and continuous cooperation on all decision levels, tailored to the situation. In the proposed agile process the only irrevocable decision is to perform an intervention, all other decisions are open unto this final decision for an intervention. The major advantage is this keeps attention on optimal risk reduction on all decision levels. Concluding, a dynamic connected risk analysis can be used to enable comprehensive flood risk management, with a focus on continuous improvement of the system risk reduction.

7.3. RECOMMENDATIONS

The recommendations based on the research in this thesis follow the answers on the questions provided in the preceding section. In this section the recommendations are presented consecutively for future research and for engineering, planning and policy practice.

7.3.1. INTEGRATED RISK-BASED OPTIMIZATION OF DIKE DESIGN

RECOMMENDATIONS FOR FUTURE RESEARCH

Further steps are recommended to develop and enhance the implementation of the approach in Chapter 3 to evaluate structural robustness of the dike construction type, and to mature its application:

- The considered initiating dike failure mechanisms can be extended, to achieve a complete dike failure analysis. For example, the failure path starting with the macro-instability mechanism can be implemented. This can be based on the geotechnical dike construction schematization and the time dependent phreatic surface in the dike, and on assessment of remaining profiles after slidings.
- Furthermore, the physics of failure paths can be enhanced, to increase quality of the dike failure analysis. For example, the erosion of a damaged dike profile is modelled by the NRCS derived from spillway research [178], describing a somewhat different physical process than erosion due to overtopping.
- The approach is elaborated for a single dike stretch. For dike segments with considerable lengths, so-called length effects reflect varying load and strength parameters along the length of the dike segment. In past research this effect is taken into account by a mathematical measure adapting the reliability index β. With the presented approach in Chapter 3 the length effect can be assessed based on the physical process of a series of dike cross sections. The approach accommodates that even the development of more than

one damaged cross sections may exist in the same dike segment. This can enhance the modelling and understanding of length effects as modelled mathematically in [179].

RECOMMENDATIONS FOR ENGINEERING PRACTICE

Evaluation of structural robustness can be standard in dike assessment and design. This will further mature the flood risk approach, leading to well-considered reinforcement decisions and designs, with a structural robustness dependent on the potential consequences. Fully implemented, with structural robust dikes at high-risk locations, the consequences are mainly economic damage, which simplify the trade-offs. Therefore, further steps are recommended to utilize structural robustness for application in the dike design in Flood Protection Programs:

- For applications in other than riverine areas, the load regimes can include areas such as the deltaic, sea, estuarine and lake environments. Therefore, the assessment of the flood volume can be extended, which is important because of its direct relation to the risks of flooding in equation (3.12). In the present approach the effect of a breach on the load water levels is implemented for the riverine area, excluding near bifurcation points. Especially for deltaic areas where river discharge and sea level determine local water levels, a numerical hydraulic model is required to reflect the effect of a breach.

- In Chapter 3 the loads and strengths are drawn by a MC-IS procedure. The proxy for the consequences in Figures 2.4 enables to evaluate a series of floods with 'random' circumstances. For areas in which the 0-D approach is not accurate, the consequences of a breach can be modelled, either by a proxy or a full 2D numerical model.

- Above mentioned recommendations require extra calculation time. Two improvements can be considered in the present implementation of the approach. First, the presented heuristic optimization, simply calculating a matrix with as much ribs as degrees of freedom in the design, is too time consuming in cases with large matrices. This will play a larger role in case of extension of the present implementation of the approach to assess a dike segment in stead of a cross section, with different reinforcement solutions for different dike sections. In such cases solutions have to be implemented like a greedy search algorithm such as used in [45]. Second, the use of calculation clusters with multiple cores. However not that complex, this strongly will increase the attractivity to use the benefits of the approach.

7.3.2. INTEGRATED PORTFOLIO PRIORITISATION OF MEASURES

RECOMMENDATIONS FOR FUTURE RESEARCH

Further steps are recommended to develop and enhance the implementation of the approach to evaluate tactical plans for portfolio planning presented in Chapter 4, and to mature its application:

- To assess the probability of failure of the dike stretches in the portfolio in the actual and reinforced situation, fragility curves play a pivoting role. Firstly, it can be studied to what extent decisions depend on the level of detail of the fragility curves. In this thesis integrated fragility curves per dike stretch are used. A more detailed level is to use fragility curves per failure path. Secondly, the fragility curves depend on the construction type and therewith on the structural robustness. It can be studied to what extent the structural robustness of individual dikes affect the portfolio planning decisions. If so, the flood defence managers can influence the importance of reinforcement of their dikes. This requires that fragility curves used in the method of Chapter 4 are aligned with reinforcement plans, in stead of the implementation in this thesis to shift them equally to the dike height increase.
- In this thesis the timing and development of breaches is rudimentary implemented: the breaches occur suddenly at maximum water level of a flood event, and consequently the downstream effect occurs suddenly. Alternative timing of breaches, due to for example postponement of a breach by ductile dikes or by emergency measures, is neglected. Furthermore, the downstream effect of a breach is overestimated by neglecting the backwater effect in the polders. It is questionable to what extent the timing and time development of a breach affect the finding in this thesis.
- The present implementation of the approach can be used in a sea environment, in case the load regime is adapted and the interdependence of dike stretches is neglected. Extensibility of the method for other load regimes, such as in deltaic areas with influence of river discharge and sea water level can be investigated, especially because the downstream risk effect of reinforcements differ from the river load regime.

RECOMMENDATIONS FOR PLANNING PRACTICE

The time-aggregated risk reduction can be introduced as a decision variable for evaluation of tactical plans. This will further mature the flood risk management, leading to well-considered planning decisions to effectively reduce risks in system. Therefore, further steps are recommended to operationalize the implementation of tactical planning for application in Flood Protection Programs:

- The effect of the choice for a tactical plan is considerable, as shown in Table 4.7. A preference for the reduction of damage can result in a focus on reinforcements in another river branche than a preference for the reduction of the number of victims. Therefore, it is recommended to prepare for a preferential tactical metric.
- The reinforcement decision is the only irreversible decision in the process presented in Chapter 6. This will affect the workflow of flood defence managers, because assessments and design propositions are required to acquire that decision. With the propositions tactical plans can be evaluated and tactical variables chosen, such as the metric, planning and priority condition. This urges the flood defence managers to prepare for a continuous workflow including data availability, up to date and high quality assessments, and several design alternatives. This will have the downside requiring resources, and the advantage of maximum time-aggregated risk reduction on a systems scale due to the thoroughly chosen tactical plan. It is recommended to prepare for a workflow in balance with the expected benefits.
- Effect of new climate projections, system measures, innovative reinforcement techniques, and new knowledge affect the evaluation of the tactical plans continuously. It is recommended to develop protocols for maturity of these components before implementation in the tactical evaluation.

7.3.3. OPTIMAL RISK REDUCTION BY UPDATED PERFORMANCE REQUIREMENTS

The recommendations consists of enhancements to elaborate and mature the application of the presented approach to apply dedicated standards in Chapter 5.

RECOMMENDATIONS FOR FUTURE RESEARCH

Further steps are recommended to investigate the effects and practical implications of updating performance requirements based on design and planning in Chapter 5 and to mature the application:

- An unambiguous flood risk management strategy is important. In case the performance requirements depend on design and planning that may come across as unclear by the institutions involved, which are many [151]. This may cause unexpected behaviour with unexpected effects such as passivity. Therefore, the governance aspects of an open and dynamic process with updatable performance requirements can be investigated.

- The effect of structural robustness with respect to the economic optimal probability of failure is demonstrated in Chapter 3. The present Dutch risk-based standards are based on flooding simulations with a variety of brittle and ductile breaches (Chapter 5). A considerable number of the simulations assume a breach occurring suddenly. It can be investigated to what extent the optimal probability of failure will be affected and whether the flooding simulations can be executed in line with the existing or future flood defence design.
- The findings in this thesis about the potential effect of structural robust designs enable to perform a dedicated system design, with a high structural robustness on densely populated locations. It is recommended to compare the costs and risks of policies based on minimization of victims in system, policies based on minimization of societal costs in system, and combinations of both. This enables a policy decision for an explicit choice for a strategy and the corresponding budgets, risk effects and realization requirements.

RECOMMENDATIONS FOR POLICY PRACTICE

Updating of performance requirements (in the Netherlands: standards) can be introduced as a measure to value the structural robustness and planning of interventions. This will further mature the flood risk management, leading to well-considered reinforcement decisions to effectively and efficiently reduce risks in system. Therefore, further steps are recommended to operationalize the application of updating performance requirements in Flood Protection Programs:

- A practical way to build over time an updated database with flooding simulations, corresponding to the actual structural robustness of the dikes in the system, is to require a new set of flooding simulations to be delivered by the flood defence manager as a prerequisite for the reinforcement decision.
- In countries where performance requirements are set in the shape of a standard for the acceptable probability of failure, this works as a first step in a Waterfall-like approach [155]. The next step regarding planning use them as a prerequisite. The final step regarding design use both the performance requirement and the timing as a prerequisite, and design horizons are disconnected from the proposed dike construction. Based on the interconnections within and between the decision levels explained in this thesis an agile development method [154] is recommended, which would give room for iterative development reconsidering relevant starting points in the process until the reinforcement decision has been taken. Countries

without standards can benefit from the agile development method, as well.

- Given an agile method it is recommended to focus on communication about status and developments to all stakeholders in process, and on their role and opportunities to affect the system risk reduction and accompanying planning of interventions.

7.4. CLOSING REMARKS

This thesis combined risk analysis, risk management and the asset management perspectives. Together, this thesis provides a basis for risk based flood defence system management. Furthermore, a dynamic connected risk analysis combined with a dynamic process is adaptive, which is important for the connection with e.g. spatial planning. This thesis did not address the capabilities and behavioural attitude of the institutions involved, as well as data availability and accessibility, which are crucial to let an agile process work. Nevertheless, this thesis contributes to a complete and comprehensive system risk analysis, providing a perspective on the role of tactical asset management in the process. Therewith, this thesis can be summarized as a comprehensive risk-perspective for flood defence system management.

BIBLIOGRAPHY

[1] G. van de Ven. *Man-made lowlands. History of water management and land reclamation in the Netherlands*. Utrecht: Matrijs, 2004, p. 432. isbn: 978-90-5345-191-9.

[2] B. Snyder. “Sea-Level Rise: Re-imagining the Urban Edge A preliminary investigation of the effect of future sea-level rise on the design of our built environment.” PhD thesis. University of California, Berkeley, 2010.

[3] P. Sayers. “Evolution of Strategic Flood Risk Management in Support of Social Justice, Ecosystem Health, and Resilience”. In: *Oxford Research Encyclopedia of Natural Hazard Science* (May 2017). doi: 10.1093/ACREFORE/9780199389407.013.85.

[4] J. Rentschler, M. Salhab, and B. A. Jafino. “Flood exposure and poverty in 188 countries”. In: *Nature communications* (2022). doi: 10.1038/s41467-022-30727-4. url: https://doi.org/10.1038/s41467-022-30727-4.

[5] J. Schanze. “Flood risk management - a basic framework”. In: *Flood risk management : hazards, vulnerability and mitigation measures*. Ed. by J. Schanze, E. Zeman, and J. Marsalek. Springer, 2006, pp. 1–20. isbn: 978-1-4020-4596-7.

[6] P. Samuels, F. Klijn, and J. Dijkman. “AN ANALYSIS OF THE CURRENT PRACTICE OF POLICIES ON RIVER FLOOD RISK MANAGEMENT IN DIFFERENT COUNTRIES”. In: *Irrigation and Drainage* 55 (2006), pp. 141–150. doi: 10.1002/ird.257. url: https://onlinelibrary.wiley.com/doi/10.1002/ird.257.

[7] F. Klijn, H. Kreibich, H. De Moel, E. Penning-Rowsell, F. Klijn, H. Kreibich, H. De Moel, and E. Penning-Rowsell. “Adaptive flood risk management planning based on a comprehensive flood risk conceptualisation”. In: *Mitigation and Adaptation Strategies for Global Change* (2015). doi: 10.1007/s11027-015-9638-z.

[8] M. Gottschalk. *Stormvloeden en rivieroverstromingen in Nederland, Deel I*. Assen, The Netherlands: Van Gorcum, 1971. isbn: 90-232-0717-3.

[9] L. Nagy. *Dike breaches in the Carpathian Basin*. 2006. url: https://www.researchgate.net/publication/237543525%7B%5C_%7DDike%7B%5C_%7Dbreaches%7B%5C_%7Din%7B%5C_%7Dthe%7B%5C_%7DCarpathian%7B%5C_%7DBasin (visited on 02/27/2023).

[10] I. M. van Kempen and S. van Baars. *Official Publication of the European Water Association (EWA)*. Tech. rep. 2009.

[11] A. Vierlingh. *Tracteat van Dyckagie*. 1578.

[12] M. Z. Voorendt. *The development of the Dutch flood safety strategy technical report*. 2016. isbn: 9789074767187.

[13] P. Sayers, Y. Li, G. Galloway, E. Penning-Rowsell, F. Shen, K. Wen, Y. Chen, and T. Le Quesne. *Flood Risk Management: A Strategic Approach | Asian Development Bank*. Asian Development Bank, Manila; China General Institute of Water Resources, Hydropower Planning, and Design, Ministry of Water Resources, Beijing; UNESCO, Paris; WWF International, Gland Switzerland, 2013. isbn: 978-92-3-001159-8. url: https://www.adb.org/publications/flood-risk-management-strategic-approach.

[14] D. van Dantzig. "Economic Decision Problems for Flood Prevention". In: *Econometrica* 24.3 (July 1956), p. 276. issn: 00129682. doi: 10.2307/1911632.

[15] S. Jonkman, H. Voortman, W. Klerk, and S. van Vuren. "Developments in the management of flood defences and hydraulic infrastructure in the Netherlands". In: *Structure and Infrastructure Engineering* 14.7 (2018), pp. 895–910. issn: 17448980. doi: 10.1080/15732479.2018.1441317. url: http://doi.org/10.1080/15732479.2018.1441317.

[16] CIRIA. *International Levee Handbook*. London: CIRIA, Griffin Court, 15 Long Lane, London, EC1A 9PN, UK, 2013. isbn: 978-0-86017-734-0.

[17] Z. W. Kundzewicz, S. Kanae, S. I. Seneviratne, J. Handmer, N. Nicholls, P. Peduzzi, R. Mechler, L. M. Bouwer, N. Arnell, K. Mach, R. Muir-Wood, G. R. Brakenridge, W. Kron, G. Benito, Y. Honda, K. Takahashi, and B. Sherstyukov. "Flood risk and climate change: global and regional perspectives". In: *Hydrological Sciences Journal* 59.1 (2014), pp. 1–28. issn: 21503435. doi: 10.1080/02626667.2013.857411.

[18] IPCC. *Climate Change 2022, Impacts, Adaptation, and Vulnerability*. 2022. url: https://www.ipcc.ch/report/ar6/wg2/downloads/report/IPCC%7B%5C_%7DAR6%7B%5C_%7DWGII%7B%5C_%7DSummaryVolume.pdf (visited on 02/27/2023).

[19] A. Pathirana, F. den Heijer, and P. Sayers. "Water infrastructure asset management is evolving". In: *Infrastructures* 6.6 (2021). issn: 24123811. doi: 10.3390/infrastructures6060090.

[20] ISO. *NEN-ISO 55000: Assetmanagement - Overview, principles and terminology*. ISO55000:2. International Standards Organisation, 2014.

[21] J. Przybyla. *Beste Practices in Asset Management*. Tech. rep. US Army Corps of Engineers, Institute for Water Resources, 2013.

[22] R. E. Brown and B. G. Humphrey. *Asset management for transmission and distribution*. 2005. doi: 10.1109/MPAE.2005.1436499.

[23] B. Vonk, W. J. Klerk, P. Fröhle, B. Gersonius, F. den Heijer, P. Jordan, U. R. Ciocan, J. Rijke, P. Sayers, and R. Ashley. "Adaptive asset management for flood protection: The FAIR framework in action". In: *Infrastructures* 5.12 (2020). issn: 24123811. doi: 10.3390/infrastructures5120109.

[24] F. den Heijer. *ROBAMCI-Eindrapport. Risk and Opportunity Based Asset Management for Critical Infrastructures*. Tech. rep. 11201843-000-ZWS-0017. Deltares, 2020, 2020.

[25] B. Gersonius, B. Vonk, R. M. Ashley, F. den Heijer, W. J. Klerk, N. Manojlovic, J. Rijke, P. Sayers, and A. Pathirana. "Maturity Improvements in Flood Protection Asset Management across the North Sea Region". In: *Infrastructures* 5.12 (2020), p. 112. issn: 2412-3811. doi: 10.3390/INFRASTRUCTURES5120112.

[26] F. den Heijer, J. Rijke, M. Bosch-Rekveldt, A. de Leeuw, and M. Barciela-Rial. "Asset management of flood defences as a co-production – An analysis of cooperation in five situations in the Netherlands". In: *Journal of Flood Risk Management* (2023). doi: 10.1111/jfr3.12909.

[27] K. Poljansek, A. Casajus Valles, M. Marin Ferrer, A. De Jager, F. Dottori, L. Galbusera, B. Garcia Puerta, G. Giannopoulos, S. Girgin, M. Hernandez Ceballos, G. Iurlaro, V. Karlos, E. Krausmann, M. Larcher, A. Lequarre, M. Theocharidou, M. Montero Prieto, G. Naumann, A. Necci, P. Salamon, M. Sangiorgi, M. Raposo De M. Do N. E S. De Sotto Mayor, C. Trueba Alonso, G. Tsionis, J. Vogt, and M. Wood. *Recommendations for National Risk Assessment for Disaster Risk Management in EU*. Tech. rep. Publications Office of

the European Union, Luxembourg, JRC114650, 2019, ISBN 978-92-76-03217-5, 2019. doi: 10.2760/147842.

[28] E. Calle, D. Dillingh, W. Meermans, A. Vrouwenvelder, J. Vrijling, L. de Quelerij, and A. Wubs. *Probabilistisch ontwerpen van waterkeringen, Interimrapport TAW 10*. Tech. rep. Technische Adviescommissie voor de Waterkeringen, 1985.

[29] A. Kortenhaus. "Probabilistische Methoden für Nordseedeiche". PhD thesis. Technischen Universität Braunschweig, 2003.

[30] F. Buijs, P. van Gelder, and J. Hall. "Application of reliability-based flood defence design in the UK". In: *Heron* 49.1 (2004), pp. 33–50.

[31] H. Steenbergen, B. Lassing, A. Vrouwenvelder, and P. . Waarts. "Reliability analysis of flood defence systems". In: *Heron* 49.1 (2004), pp. 51–73.

[32] S. Jonkman, R. D. Steenbergen, O. Morales-Nápoles, A. Vrouwenvelder, and J. Vrijling. "Probabilistic Design: Risk and Reliability Analysis in Civil Enigneering". In: *Collegedictaat CIE4130* (2016).

[33] R. Vergouwe. *De veiligheid van Nederland in kaart: Eindrapportage VNK*. Rijkswaterstaat, projectbureau VNK, 2014. url: https://repository.tudelft.nl/islandora/object/uuid%7B%5C%%7D3A52035faa-43ab-4dd0-a5b0-099119085356.

[34] EU. *DIRECTIVE 2007/60/EC OF THE EUROPEAN PARLIAMENT AND OF THE COUNCIL of 23 October 2007 on the assessment and management of flood risks*. 2007. url: https://eur-lex.europa.eu/legal-content/EN/ALL/?uri=CELEX%7B%5C%%7D3A32007L0060 (visited on 02/27/2023).

[35] J. K. Vrijling, W. van Hengel, and R. J. Houben. "Acceptable risk as a basis for design". In: *Reliability Engineering & System Safety* 59.1 (Jan. 1998), pp. 141–150. issn: 09518320. doi: 10.1016/S0951-8320(97)00135-X.

[36] H. Voortman. *Risk-based design of large-scale flood defence systems*. Tech. rep. 2003. url: https://repository.tudelft.nl/islandora/object/uuid%7B%5C%%7D3A31d3672a-0062-465d-b30a-bacc2ed4b79d.

[37] K. Bischiniotis, W. Kanning, S. N. Jonkman, and M. Kok. "Cost-optimal design of river dikes using probabilistic methods". In: *Flood Risk Management* 11 (2018), S1002–S1014. doi: https://doi.org/10.1111/jfr3.12277.

[38] P. Sayers. *Flood Risk - Planning, design and management of flood defence infrastructure*. ISBN 978-0-7277-5749-4, ICE Publishing, 2012.

[39] A. Kortenhaus and H. Oumeraci. “Flood risk analysis and management in Europe - The way ahead”. In: *ICCE2008*. World Scientific Pub Co Pte Lt, May 2009, pp. 4214–4226. doi: 10.1142/9789814277426_0350.

[40] J. Pol. “Time-dependent development of Backward Erosion Piping”. PhD thesis. Delft University of Technology, ISBN 978-94-6366-622-0, 2022. doi: doi.org/10.4233/uuid.

[41] M. C. Van Mierlo, A. C. Vrouwenvelder, E. O. Calle, J. K. Vrijling, S. N. Jonkman, K. M. De Bruijn, and A. H. Weerts. “Assessment of flood risk accounting for river system behaviour”. In: *International Journal of River Basin Management* 5.2 (2010), pp. 93–104. issn: 18142060. doi: 10.1080/15715124.2007.9635309. url: https://www.tandfonline.com/doi/abs/10.1080/15715124.2007.9635309.

[42] E. J. C. Dupuits, W. J. Klerk, T. Schweckendiek, and K. M. De Bruijn. “Impact of including interdependencies between multiple riverine flood defences on the economically optimal flood safety levels”. In: *Reliability Engineering & System Safety* (2019). doi: 10.1016/j.ress.2019.04.028. url: https://doi.org/10.1016/j.ress.2019.04.028.

[43] M. Haasnoot, J. H. Kwakkel, W. E. Walker, and J. ter Maat. “Dynamic adaptive policy pathways: A method for crafting robust decisions for a deeply uncertain world”. In: *Global Environmental Change* 23.2 (2013). issn: 09593780. doi: 10.1016/j.gloenvcha.2012.12.006.

[44] P. Sayers. “Strategic flood risk management : A systems-based approach”. PhD thesis. TU Delft, ISBN 978-90-73445-51-2, 2023. url: https://ihedelftrepository.contentdm.oclc.org/digital/collection/phd1/id/62769.

[45] W. J. Klerk, W. Kanning, M. Kok, and R. Wolfert. “Optimal planning of flood defence system reinforcements using a greedy search algorithm”. In: *Reliability Engineering & System Safety* 207 (2021), p. 107344. issn: 09518320. doi: 10.1016/j.ress.2020.107344.

[46] D. Y. Yang and D. M. Frangopol. “Risk-based portfolio management of civil infrastructure assets under deep uncertainties associated with climate change: a robust optimisation approach”. In: *Structure and Infrastructure Engineering* 16.4 (2020). issn: 17448980. doi: 10.1080/15732479.2019.1639776.

[47] K. Smet. “Engineering Options: a proactive planning approach for aging water resource infrastructure under uncertainty”. PhD thesis. Harvard University, Graduate School of Arts & Sciences, 2017.

[48] M. Yang, D. Zhang, C. Jiang, F. Wang, and X. Han. “A new solution framework for time-dependent reliability-based design optimization”. In: *Computer Methods in Applied Mechanics and Engineering* 418 (Jan. 2024), p. 116475. issn: 0045-7825. doi: 10.1016/J.CMA.2023.116475.

[49] W. Klerk. “Decisions on life-cycle reliability of flood defence systems”. PhD thesis. 2022.

[50] Deltacommissie. *Rapport Deltacommissie - Eindverslag en interimadviezen*. Staatsdrukkerij- en uitgeversbedrijf, 1960.

[51] J. Kind. “Economically efficient flood protection standards for the Netherlands”. In: *Journal of Flood Risk Management* 7.2 (2014), pp. 103–117. issn: 1753318X. doi: 10.1111/jfr3.12026. url: http://doi.wiley.com/10.1111/jfr3.12026.

[52] C. J. Eijgenraam, R. Brekelmans, D. Den Hertog, and K. Roos. “Optimal strategies for flood prevention”. In: *Management Science* 63.5 (Apr. 2017), pp. 1644–1656. issn: 15265501. doi: 10.1287/mnsc.2015.2395.

[53] A. Driessen, G. van de Ven, and H. Wasser. *Gij beken eeuwigvloeijend. Water in de Streek van Rijn en IJssel*. Matrijs, 2000, p. 288. isbn: 9789053451229.

[54] Helpdesk Water. *National database flood simulations*. 2020. url: https://www.helpdeskwater.nl/onderwerpen/wetgeving-beleid/europese-richtlijn-overstromingsrisico/overstromingsgevaar-overstromingsrisicokaarten/ (visited on 08/27/2020).

[55] M. Kok, R. Jongejan, M. Nieuwjaar, and I. Tanczos. *Fundamentals of flood protection*. ISBN 978-90-8902-160-1. Ministry of Infrastructure and the Environment & Expertise Network for Flood Protection, 2017, p. 143. isbn: 978-90-8902-160-1.

[56] TAW. *Veiligheid van waterkeringen. De nieuwe visie volgens het onderzoeksprogramma TAW Marsroute*. Tech. rep. Technische Adviescommissie voor de Waterkeringen, 1996.

[57] H. van der Most, I. Tánczos, K. de Bruijn, and D. Wagenaar. “New, risk-basis standards for flood protection in the Netherlands”. In: *ICFM6*. 2014.

[58] Ministerie van Infrastructuur en Waterstaat. *Regeling van de Minister van Infrastructuur en Waterstaat, van 12 april 2023, nr. IENW/BSK-2023/94660, houdende vaststelling van regels inzake de beoordeling van de veiligheid van primaire waterkeringen (Regeling veiligheid primaire waterkeringen 2023)*. Tech. rep. 2023. url: https://zoek.

officielebekendmakingen . nl / stcrt - 2023 - 11307.html.

[59] Ministerie van Verkeer en Waterstaat. *Staatscourant 234 - Wijziging regeling bijzondere subsidies waterkeren en waterbeheren, Staatscourant van het Koninkrijk der Nederlanden*. Tech. rep. Ministerie van Verkeer en Waterstaat, 2007.

[60] M. A. U. R. Tariq, R. Farooq, and N. van de Giesen. "A Critical Review of Flood Risk Management and the Selection of Suitable Measures". In: *Applied Sciences* 10.23 (2020), p. 8752. issn: 2076-3417. doi: 10.3390/APP10238752.

[61] K. Thywissen. *Components of Risk - A Comparative Glossary*. Tech. rep. 3-9810582-1-6, United Nations University - Institute for Environment and Human Security, 2006.

[62] P. Samuels and B. Gouldby. *Language of Risk - project definitions (second edition)*. Tech. rep. FLOODsite, 2006.

[63] S. Kaplan and B. J. Garrick. "On The Quantitative Definition of Risk". In: *Risk Analysis* 1.1 (1981), pp. 11–27. issn: 0272-4332. doi: 10.1111/j.1539-6924.1981.tb01350.x.

[64] T. Aven. "Risk assessment and risk management: Review of recent advances on their foundation". In: *European Journal of Operational Research* 253.1 (Aug. 2016), pp. 1–13. issn: 03772217. doi: 10.1016/J.EJOR.2015.12.023.

[65] H. J. Pasman, W. J. Rogers, and M. S. Mannan. "Risk assessment: What is it worth? Shall we just do away with it, or can it do a better job?" In: *Safety Science* 99 (Nov. 2017), pp. 140–155. issn: 0925-7535. doi: 10.1016/J.SSCI.2017.01.011.

[66] P. Sayers, J. W. Hall, and I. C. Meadowcroft. "Towards risk-based flood hazard management in the UK". In: *Proceedings of the Institution of Civil Engineers: Civil Engineering* 150.1 SPECIAL ISSUE (2002), pp. 36–42. issn: 0965089X. doi: 10.1680/cien.2002.150.5.36.

[67] C. J. Eijgenraam. *Optimal safety standards for dike-ring areas*. Tech. rep. ISBN 90-5833-267-5, CPB Netherlands Bureau for Economic Policy Analysis, 2006. url: www.cpb.nl.

[68] F. den Heijer. "Adaptive flood defence management with ductile dikes". In: *Proceedings of the 7th International Symposium on Life-Cycle Civil Engineering (IALCCE 2020)*. Ed. by A. Chen, X. Ruan, and D. Frangopol. Shanghai, China: CRC Press, 2021, pp. 471–478. doi: 10.1201/9780429343292.

[69] L. Van Rijn. *Principles of fluid flow and surface waves in rivers estuaries seas and oceans*. Aqua Publications, 2011. isbn: 978-90-79755-02-8.

[70] E. H. E. Chbab. *Waterstandsverlopen Rijntakken en Maas*. Tech. rep. 1220082-002-HYE-0002, Deltares, 2016. doi: 1220082-002-HYE-0002.

[71] E. H. Chbab. *Basisstochasten WBI-2017 - Statistiek en statistische onzekerheid*. Tech. rep. 1209433-012-HYE-0007 Deltares, 2017.

[72] R. Agtersloot, R. van der Veen, and S. R. van der Veen. *Betrekkingslijnen Rijntakken, versie 2018*. Tech. rep. RURA-Arnhem, 2019. doi: 4500283440.

[73] M. Morris, W. Allsop, F. Buijs, A. Kortenhaus, N. Doorn, and D. Lesniewska. "Failure modes and mechanisms for flood defence structures". In: *Flood Risk Management: Research and Practice* January (2008), pp. 693–701. doi: 10.1201/9780203883020.ch79.

[74] H. Steenbergen and A. Vrouwenvelder. *Theoriehandleiding PC-RING versie 4.0, Deel C: Rekentechnieken*. Tech. rep. 98-CON-R1204, TNO, 1999.

[75] R. Slomp, H. Knoeff, A. Bizzarri, M. Bottema, and W. de Vries. "Probabilistic Flood Defence Assessment Tools". In: *E3S Web of Conferences* 7 (Oct. 2016). Ed. by M. Lang, F. Klijn, and P. Samuels, p. 03015. issn: 2267-1242. doi: 10.1051/e3sconf/20160703015.

[76] M. Van, E. Rosenbrand, R. Tourment, P. Smith, and C. Zwanenburg. *Failure paths for levees*. Tech. rep. International Society of Soil mechanics, Geotechnical Engineering (ISSMGE) – Technical Committee TC201 'Geotechnical aspects of dikes, and levees', 2022, pp. 1–134. doi: doi.org/10.53243/R0006. url: https://doi.org/10.53243/R0006.

[77] H. Verheij. *Aanpassen van het bresgroeimodel in HIS-OM*. Tech. rep. Delft: Q3299, WL|Delft Hydraulics, 2003.

[78] European Committee for Standardization. *Actions on structures - Part 1-7: General actions - Accidental actions*. Tech. rep. Brussels: EN 1991-1-7 Eurocode 1, 2006.

[79] R. Jongejan, H. Stefess, N. Roode, W. ter Horst, and B. Maaskant. "The VNK2 project, a detailed, large scale quantitative flood risk analysis for the Netherlands". In: *ICFM5*. 2011.

[80] K. De Bruijn and M. van der Doef. *Gevolgen van overstromingen - Informatie ten behoeve van het project Waterveiligheid in de 21e eeuw*. Tech. rep. 1204144-004-ZWS-0001, Deltares, 2011, p. 78.

[81] J. Dekker, A. Wolters, F. den Heijer, and S. Fraikin. "Hydraulic Boundary Conditions for Coastal Risk Management - COMRISK Subproject 5". In: *Die Küste 70*. 2005, pp. 57–74.

[82] Ministerie van Infrastructuur en Milieu. *Wet van 2 november 2016 tot wijziging van de Waterwet en enkele andere wetten (Waterwet)*. 2016. url: https://wetten.overheid.nl/BWBR0025458/2021-07-01.

[83] J. K. Vrijling, W. van Hengel, and R. J. Houben. "A framework for risk evaluation". In: *Journal of Hazardous Materials* 43.3 (Oct. 1995), pp. 245–261. issn: 03043894. doi: 10.1016/0304-3894(95)91197-V.

[84] T. Aven and O. Renn. "Risk perspectives". In: *Risk Management and Governance: Concepts, Guidelines and Applications*. Springer Berlin Heidelberg, 2010, pp. 21–48. isbn: 978-3-642-13926-0. doi: 10.1007/978-3-642-13926-0_3. url: https://doi.org/10.1007/978-3-642-13926-0%7B%5C_%7D3.

[85] J. W. Baker, M. Schubert, and M. H. Faber. "On the assessment of robustness". In: *Structural Safety* 30.3 (May 2008), pp. 253–267. issn: 0167-4730. doi: 10.1016/J.STRUSAFE.2006.11.004.

[86] W. Halter, I. Groenouwe, and M. Tonneijck. *Handboek Dijkenbouw, Uitvoering, versterking en nieuwbouw*. Ed. by K. D'Angremond. Hoogwaterbeschermingsprogramma, HWBP, 2018.

[87] Delta Commision. *Samen werken met water - Een land dat leeft, bouwt aan zijn toekomst Bevindingen van de Deltacommissie 2008*. Tech. rep. 2008.

[88] K. de Bruijn and F. Klijn. *Deltadijken: locaties waar deze het meest effectief slachtofferrisico's reduceren*. Tech. rep. 1202628-000-VEB-0005, Deltares, 2011.

[89] H. Knoeff and G. Ellen. *Verkenning deltadijken*. Tech. rep. 1205259-000-ZWS-0004, Deltares, 2012.

[90] J. Breedeveld, Z. Zwanenburg, M. Van, and H. J. Lengkeek. "Impact of the Eemdijk full-scale test programme". In: *Proceedings of the XVII European Conference on Soil Mechanics and Geotechnical Engineering ECSMGE-2019*. International Society for Soil Mechanics and Geotechnical Engineering, 2019. doi: 10.32075/17ECSMGE-2019-0398.

[91] A. van Hoven. *Residual dike strength after macroinstability*. Tech. rep. Deltares, 2014. doi: 1207811-013-HYE-0001-gbh.

[92] A. te Nijenhuis, L. Hüsken, F. Diermanse, A. van der Meer, R. B. Jongejan, and J. Pol. *Faalpaden - Conceptuele analyse van het gebruik van de faalpaden-methodiek voor het bepalen van overstromingskansen in Nederland*. Tech. rep. 2020. doi: 11203719-024-GEO-0016,.

[93] E. Rosenbrand and J. G. Knoeff. *KvK 2019 onderzoek faalpaden en piping*. Tech. rep. Deltares, 2020. doi: 11203719-028-GEO-0009.

[94] G. van den Ham. *Faalpadenanalyse macrostabiliteit binnenwaarts*. Tech. rep. 11203719-027-GEO-0001, Deltares, 2020. doi: 11203719-027-GEO-0001.

[95] C. J. van Westen. *Veiligheid Nederland in Kaart. Hoofdrapport onderzoek overstromingsrisico's*. DWW-2005-081 ISBN 90-369-5604-8, Ministerie van Verkeer en Waterstaat - Rijkswaterstaat, 2005, p. 141. isbn: 90-369-5604-8.

[96] VNK2. *De methode van VNK2 nader verklaard - de technische achtergronden*. Projectbureau VNK2, 2011.

[97] M. J. P. Mens. "System Robustness Analysis in Support of Flood and Drought Risk Management". PhD thesis. TU Delft, 2015. isbn: 9781614994817. doi: 10.3233/978-1-61499-482-4-i.

[98] R. Brinkman. *Probabilistic Toolkit*. 2021. url: https://www.deltares.nl/en/software/probabilistic-toolkit-ptk/.

[99] C. Geerse, R. Slomp, and H. de Waal. *Hydra-Zoet Probabilistic model for the assessment of dike heights : probabilistic model for the assessment of dike heights*. Tech. rep. PR2168, HKV consultants, Ministry of Infrastructure and Environment, Deltares, 2011. url: http://puc.overheid.nl/doc/PUC%7B%5C_%7D143536%7B%5C_%7D31.

[100] E. O. F. Calle. *Dijkdoorbraakprocessen*. Tech. rep. 720201/39, GeoDelft, 2002.

[101] A. J. Smale. *Werkwijzer bepaling Hydraulische Ontwerprandvoorwaarden, Aanvulling OI2014, versie 5 (Hydra-NL 2.4.1)*. Tech. rep. Deltares, 2018. doi: 11202226-009-GEO-0002.

[102] M. Hop. *Technisch ontwerp zeef 2 verkenning Grebbedijk*. Tech. rep. Lievense CSO Infra B.V., 2019. doi: 17M3041-R-015-V02versie2.

[103] B. van den Hurk, A. Klein Tank, G. Lenderink, A. van Ulden, G. van Oldenborgh, C. Katsman, H. van den Brink, F. Keller, J. Bessembinder, G. Burgers, G. Komen, W. Hazeleger, and S. Drijfhout. *KNMI Climate Change Scenarios 2006 for the Netherlands*. Tech. rep. WR2006-01, KNMI, 2006.

[104] Ministerie van Verkeer en Waterstaat and ENW. *Technisch Rapport Ontwerpbelastingen voor het rivierengebied*. Ministerie van Verkeer en Waterstaat. Expertise Netwerk Waterkeren, 2007. isbn: 978-90-369-1409-3.

[105] P. de Grave and G. Baarse. *Kosten van maatregelen, informatie ten behoeve van het project Waterveiligheid 21e eeuw*. Tech. rep. 1204144-003-ZWS-001, Deltares, 2011.

[106] IAM. “Asset Management – An Anatomy”. In: *Asset Management - an Anatomy* (2015).

[107] S. Carpitella, I. Mzougui, J. Benítez, F. Carpitella, A. Certa, J. Izquierdo, and M. L. Cascia. “A risk evaluation framework for the best maintenance strategy: The case of a marine salt manufacture firm”. In: *Reliability Engineering & System Safety* (2020). doi: 10.1016/j.ress.2020.107265. url: https://doi.org/10.1016/j.ress.2020.107265.

[108] G. H. Fuchs, I. Keuning, B. R. Mante, and J. D. Bakker. “A business case of the estimated profit of Life Cycle Management principles”. In: *Life-Cycle of Structural Systems: Design, Assessment, Maintenance and Management - Proceedings of the 4th International Symposium on Life-Cycle Civil Engineering, IALCCE 2014*. 2015. doi: 10.1201/b17618-233.

[109] W. Courage, T. Vrouwenvelder, T. van Mierlo, and T. Schweckendiek. “System behaviour in flood risk calculations”. In: *Georisk: Assessment and Management of Risk for Engineered Systems and Geohazards* 7.2 (2013), pp. 62–76. issn: 17499518. doi: 10.1080/17499518.2013.790732.

[110] N. Sharma, F. Nocera, and P. Gardoni. “Classification and mathematical modeling of infrastructure interdependencies”. In: *Sustainable and Resilient Infrastructure* (2020).

[111] J. Wang, H. Liu, and T. Lin. “Optimal rearrangement and preventive maintenance policies for heterogeneous balanced systems with three failure modes”. In: *Reliability Engineering & System Safety* 238 (Oct. 2023), p. 109429. issn: 0951-8320. doi: 10.1016/J.RESS.2023.109429.

[112] P. Sayers, G. Galloway, E. Penning-Rowsell, L. Yuanyuan, S. Fuxin, C. Yiwei, W. Kang, T. Le Quesne, L. Wang, and Y. Guan. “Strategic flood management: ten ’golden rules’ to guide a sound approach”. In: *International Journal of River Basin Management* (2015). issn: 1814-2060. doi: 10.1080/15715124.2014.902378. url: https://www.tandfonline.com/action/journalInformation?journalCode=trbm20.

[113] S. Vorogushyn. “Analysis of flood hazard under consideration of dike breaches”. PhD thesis. Potsdam, 2008. url: http://opus.kobv.de/ubp/volltexte/2009/2764/.

[114] A. Domeneghetti, S. Vorogushyn, A. Castellarin, B. Merz, and A. Brath. “Probabilistic flood hazard mapping: effects of uncertain boundary conditions”. In: *Hydrology and Earth System Sciences* 17.8 (Aug. 2013), pp. 3127–3140. issn: 1607-7938. doi: 10.5194/hess-17-3127-2013. url: https://hess.copernicus.org/articles/17/3127/2013/.

[115] D. Bachmann. “Beitrag zur Entwicklung eines Entscheidungsunterstützungssystems zur Bewertung und Planung von Hochwasserschutzmaßnahmen”. PhD thesis. RWTH Aachen, 2012. url: http://publications.rwth-aachen.de/record/64633/files/4043.pdf.

[116] D. Bachmann and H. Schüttrumpf. “Integrating the reliability of flood protection structures into catchment-based flood risk analysis”. In: *Hydrologie und Wasserbewirtschaftung* 58.3 (2014), pp. 168–177. url: ISSN%201439-1783.

[117] A. Curran. “FLOOD RISK ANALYSIS OF EMBANKED RIVER SYSTEMS - PROBABILISTIC SYSTEMS APPROACHES FOR THE RHINE AND PO RIVERS”. PhD thesis. Delft University of Technology, 2020. url: ISBN%20978-94-6421-121-4.

[118] Q. Liu, A. Tang, D. Huang, Z. Huang, B. Zhang, and X. Xu. “Total probabilistic measure for the potential risk of regional roads exposed to landslides”. In: *Reliability Engineering & System Safety* 228 (Dec. 2022), p. 108822. issn: 0951-8320. doi: 10.1016/J.RESS.2022.108822.

[119] F. Buijs, J. Hall, P. Sayers, and P. Van Gelder. “Time-dependent reliability analysis of flood defences”. In: *Reliability Engineering & System Safety* 94.12 (2009), pp. 1942–1953. issn: 09518320. doi: 10.1016/j.ress.2009.06.012. url: http://dx.doi.org/10.1016/j.ress.2009.06.012.

[120] A. A. Roubos, D. L. Allaix, T. Schweckendiek, R. D. J. M. Steenbergen, and S. N. Jonkman. “Time-dependent reliability analysis of service-proven quay walls subject to corrosion-induced degradation”. In: *Reliability Engineering & System Safety* (2020). doi: 10.1016/j.ress.2020.107085. url: https://doi.org/10.1016/j.ress.2020.107085.

[121] M. J. P. Mens. *Analyse van systeemrobuustheid*. Tech. rep. ISBN/EAN: 978-94-90070-55-7, Deltares, 2012.

[122] N. Manocha and V. Babovic. “Development and valuation of adaptation pathways for storm water management infrastructure”. In: *Environmental Science & Policy* 77 (Nov. 2017), pp. 86–97. issn: 1462-9011. doi: 10.1016/J.ENVSCI.2017.08.001.

[123] A. Toimil, I. J. Losada, J. Hinkel, and R. J. Nicholls. “Using quantitative dynamic adaptive policy pathways to manage climate change-induced coastal erosion”. In: *Climate Risk Management* 33 (Jan. 2021), p. 100342. issn: 2212-0963. doi: 10.1016/J.CRM.2021.100342.

[124] K. Young and J. W. Hall. “Introducing system interdependency into infrastructure appraisal: from projects to portfolios to pathways”. In: *Infrastructure Complexity* 2.2 (May 2015), pp. 1–18. issn: 2196-3258. doi: 10.1186/s40551-015-0005-8. url: https://infrastructure-complexity.springeropen.com/articles/10.1186/s40551-015-0005-8.

[125] M. van den Boomen. “Replacement optimization of ageing infrastructure under differential inflation”. PhD thesis. Technical University of Delft, 2020. isbn: 978-94-028-1965-6.

[126] J. Fluixá-Sanmartín, I. Escuder-Bueno, A. Morales-Torres, and J. T. Castillo-Rodríguez. “Comprehensive decision-making approach for managing time dependent dam risks”. In: *Reliability Engineering & System Safety* 203 (2020). doi: 10.1016/j.ress.2020.107100. url: https://doi.org/10.1016/j.ress.2020.107100.

[127] T. Xiahou, Y. X. Zheng, Y. Liu, and H. Chen. “Reliability modeling of modular k-out-of-n systems with functional dependency: A case study of radar transmitter systems”. In: *Reliability Engineering & System Safety* 233 (May 2023), p. 109120. issn: 0951-8320. doi: 10.1016/J.RESS.2023.109120.

[128] Z. Pang, T. Li, H. Pei, and X. Si. “A condition-based prognostic approach for age- and state-dependent partially observable nonlinear degrading system”. In: *Reliability Engineering & System Safety* 230 (Feb. 2023), p. 108854. issn: 0951-8320. doi: 10.1016/J.RESS.2022.108854.

[129] Y. Hu, Q. Peng, Q. Ni, X. Wu, and D. Ye. “Event-based safety and reliability analysis integration in model-based space mission design”. In: *Reliability Engineering & System Safety* 229 (Jan. 2023), p. 108866. issn: 0951-8320. doi: 10.1016/J.RESS.2022.108866.

[130] E. Mühlhofer, E. E. Koks, C. M. Kropf, G. Sansavini, and D. N. Bresch. “A generalized natural hazard risk modelling framework for infrastructure failure cascades”. In: *Reliability Engineering & System Safety* 234 (2023), p. 109194. doi: 10.1016/j.ress.2023.109194. url: http://creativecommons.org/licenses/by/4.0/.

[131] L. Zhuang, A. Xu, and X. L. Wang. “A prognostic driven predictive maintenance framework based on Bayesian deep learning”. In: *Reliability Engineering & System Safety* 234 (June 2023), p. 109181. issn: 0951-8320. doi: 10.1016/J.RESS.2023.109181.

[132] X. Guan, H. Sun, R. Hou, Y. Xu, Y. Bao, and H. Li. “A deep reinforcement learning method for structural dominant failure modes searching based on self-play strategy”. In: *Reliability Engineering & System Safety* 233 (May 2023), p. 109093. issn: 0951-8320. doi: 10.1016/J.RESS.2023.109093.

[133] M. Schultz, B. Gouldby, J. Simm, and J. Wibowo. *Beyond the Factor of Safety:Developing Fragility Curves to Characterize System Reliability*. Tech. rep. Geotechnical and Structural Laboratory, ERDC SR-10-1, 2010.

[134] H. Apel, A. H. Thieken, B. Merz, and G. Blöschl. “Flood risk assessment and associated uncertainty”. In: *Natural Hazards and Earth System Science* 4.2 (2004), pp. 295–308. issn: 15618633. doi: 10.5194/NHESS-4-295-2004.

[135] S. Vorogushyn, B. Merz, and H. Apel. “Development of dike fragility curves for piping and micro-instability breach mechanisms”. In: *Natural Hazards and Earth System Science* 9.4 (2009), pp. 1383–1401. issn: 16849981. doi: 10.5194/NHESS-9-1383-2009.

[136] D. Bachmann, N. P. Huber, G. Johann,
bibinitperiod H. Schüttrumpf, and H. Schüttrumpf. “Georisk: Assessment and Management of Risk for Engineered Systems and Geohazards Fragility curves in operational dike reliability assessment”. In: *Assessment and Management of Risk for Engineered Systems and Geohazards* 7.1 (2013), pp. 49–60. doi: 10.1080/17499518.2013.767664. url: http://www.tandfonline.com/loi/ngrk20.

[137] K. Wojciechowska, G. Pleijter, M. Zethof, F. J. Havinga, D. H. Van Haaren, and W. L. A. Ter Horst. “Application of Fragility Curves in Operational Flood Risk Assessment”. In: *Geotechnical Safety and Risk V*. 2015, pp. 528–534. doi: 10.3233/978-1-61499-580-7-528.

[138] J. W. Van Der Meer, W. L. A. Ter Horst, and E. H. Van Velzen. “Calculation of fragility curves for flood defence assets”. In: *Flood Risk Management: Research and Practice* (2009). Ed. by P. Samuals.

[139] C. Kindsvater and R. Carter. “Discharge characteristics of rectangular thin-plate weirs”. In: *Transactions, American Society of Civil Engineers*. Vol. 24. Paper no. 3001, 1959.

[140] ISO. *Water flow measurement in open channels using weirs and venturi flumes - Part 1: Thin plate weirs*. International Organization of Standards 1438/1-1980(E)., 1980.

[141] Hoogwaterbeschermingsprogramma. *HWBP-projecten, Samen Innoveren, 2023*. 2022. url: https://drive.google.com/file/d/1PzV0-26u3lxvZIdzjJVmAbOhSGEX12MV/view (visited on 02/13/2023).

[142] E. H. Vanmarcke. "Matrix formulation of reliability analysis and reliability-based design". In: *Computers and Structures* 3.4 (July 1973), pp. 757–770. issn: 00457949. doi: 10.1016/0045-7949(73)90056-4.

[143] N. Slootjes and D. Wagenaar. *Factsheets normering primaire waterkeringen (factsheets standardization primary flood defences)*. Tech. rep. Ministerie van Infrastructuur en Milieu, DG Ruimte en Water, Directie Algemeen Waterbeleid en Veiligheid, 2016.

[144] M. Duits. *HYDRA-NL gebruikershandleiding, versie 2.7*. Tech. rep. PR4022.10, HKV lijn in water, 2019.

[145] A. Ruiz-Tagle, E. Lopez-Droguett, and K. M. Groth. "A novel probabilistic approach to counterfactual reasoning in system safety". In: *Reliability Engineering & System Safety* 228 (Dec. 2022), p. 108785. issn: 0951-8320. doi: 10.1016/J.RESS.2022.108785.

[146] H. Gilissen, M. Alexander, J. Beyers, P. Chmielewski, P. Matczak, T. Schellenberger, and C. Suykens. "Bridges over Troubled Waters: An Interdisciplinary Framework for Evaluating the Interconnectedness within Fragmented Domestic Flood Risk Management Systems". In: *Journal of Water Law* 25.1 (2016), pp. 12–26. url: https://www.researchgate.net/publication/305770522%7B%5C_%7DBridges%7B%5C_%7Dover%7B%5C_%7DTroubled%7B%5C_%7DWaters%7B%5C_%7DAn%7B%5C_%7DInterdisciplinary%7B%5C_%7DFramework%7B%5C_%7Dfor%7B%5C_%7DEvaluating%7B%5C_%7Dthe%7B%5C_%7DInterconnectedness%7B%5C_%7Dwithin%7B%5C_%7DFragmented%7B%5C_%7DDomestic%7B%5C_%7DFlood%7B%5C_%7DRisk%7B%5C_%7DManagement%7B%5C_%7DSystems.

[147] Ministerie van Verkeer en Waterstaat. *Flood defence Act: Wet van 21 december 1995, houdende algemene regels ter verzekering van de beveiliging door waterkeringen tegen overstromingen door het buitenwater en regeling van enkele daarmee verband houdende aangelegenheden (Wet op de waterkering)*. 1996.

[148] J. Vrijling. “Multi layer safety, a generally efficient solution or work for all”. In: *Safety, Reliability and Risk Analysis: Beyond the Horizon*. Ed. by R. Steenbergen, P. van Gelder, S. Miraglia, and A. Vrouwenvelder. London: Taylor & Francis Group, 2014, pp. 37–43.

[149] J. W. van der Meer. *Technisch Rapport Golfoploop en Golfoverslag bij Dijken*. Tech. rep. Delft: Technische Adviescommissie voor de Waterkeringen (TAW), 2002.

[150] U. Förster, G. van den Ham, E. Calle, and G. Kruse. *Zandmeevoerende wellen*. Tech. rep. Delft: 1202123-003, Deltares, 2012.

[151] C. Dieperink, D. L. T. Hegger, and P. P. J. Driessen. “Towards a diversification of flood risk management in Europe: A reflection on meta-governance challenges”. In: *6th International Conference on Flood Management*. Brazilian Water Resource Association, 2014.

[152] W. Deming. *Out of the crisis*. Ed. by C. f. A. E. S. Massachusetts Institute of Technology. 1986. isbn: 978-0911379013.

[153] TEES. *Risk Acceptance Criteria: Overview of ALARP and Similar Methodologies as Practiced Worldwide - White paper*. Tech. rep. Mary Kay O’Connor Process Safety Center, 2020.

[154] R. Steegh. “Adaptiveness in Action: Exploring the Processes and Outcomes of the Agile Way of Working”. PhD thesis. Tilburg University, 2024. url: https://doi.org/10.26116/tsb.29534433.

[155] H. J. Ruël, T. Bondarouk, and S. Smink. “The Waterfall Approach and Requirement Uncertainty: An In-Depth Case Study of an Enterprise Systems Implementation at a Major Airline Company”. In: *International Journal of Information Technology Project Management* 1.2 (Jan. 2010), pp. 43–60. issn: 1938-0232. doi: 10.4018/JITPM.2010040103. url: https://www.igi-global.com/article/waterfall-approach-requirement-uncertainty/42124.

[156] E. Goldratt and J. Cox. *The goal : a process of ongoing improvement*. North River Press, 1986. isbn: 0-88427-061-0.

[157] L. Volker, A. Ligtvoet, M. van den Boomen, P. Wessels, J. van der Velde, T. van der Lei, and P. Herder. “Asset Management Maturity in Public Infrastructure: the case of Rijkswaterstaat”. In: *International Journal of Strategic Engineering Asset Management* 1.4 (2013), pp. 439–453. doi: 10.1504/IJSEAM.2013.060469.

[158] A. Correljé and B. Broekhans. “Flood risk management in the Netherlands after the 1953 flood: A competition between the public value(s) of water”. In: *Journal of Flood Risk Management* 8.2 (June 2015), pp. 99–115. issn: 1753318X. doi: 10.1111/JFR3.12087.

[159] P. Bubeck, H. Kreibich, E. C. Penning-Rowsell, W. J. Botzen, H. de Moel, and F. Klijn. “Explaining differences in flood management approaches in Europe and in the USA – a comparative analysis”. In: *Journal of Flood Risk Management* 10.4 (Dec. 2017), pp. 436–445. issn: 1753318X. doi: 10.1111/JFR3.12151.

[160] G. N. Dinh and B. S. McIntosh. “An application of Integrated Water Resource Management principles to flood risk mitigation in Mossman, North Queensland, Australia”. In: *World Water Policy* 5.2 (Nov. 2019), pp. 138–160. issn: 2639-541X. doi: 10.1002/WWP2.12011. url: https://onlinelibrary.wiley.com/doi/full/10.1002/wwp2.12011%20https://onlinelibrary.wiley.com/doi/abs/10.1002/wwp2.12011%20https://onlinelibrary.wiley.com/doi/10.1002/wwp2.12011.

[161] E. B. Dent and S. G. Goldberg. “Challenging "resistance to change"”. In: *Journal of Applied Behavioral Science* 35.1 (1999), pp. 25–41. issn: 00218863. doi: 10.1177/0021886399351003. url: https://www.researchgate.net/publication/248815676%7B%5C_%7DChallenging%7B%5C_%7DResistance%7B%5C_%7Dto%7B%5C_%7DChange.

[162] Deltares. *ROBAMCI – Eindrapport ROBAMCI (WP4) – Business estimate and synthese*. Tech. rep. Deltares2019ROB: Deltares, report 11201843 (in Dutch), 2019.

[163] M. Wiering, D. Liefferink, and A. Crabbé. “Stability and change in flood risk governance: on path dependencies and change agents”. In: *Journal of Flood Risk Management* 11.3 (Sept. 2018), pp. 230–238. issn: 1753318X. doi: 10.1111/jfr3.12295. url: http://doi.wiley.com/10.1111/jfr3.12295.

[164] L. Cumiskey, S. J. Priest, F. Klijn, and M. Juntti. “A framework to assess integration in flood risk management: Implications for governance, policy, and practice”. In: *Ecology and Society* 24.4 (2019). issn: 17083087. doi: 10.5751/ES-11298-240417. url: https://doi.org/10.5751/ES-11298-240417.

[165] E. Avoyan and S. Meijerink. “Cross-sector collaboration within Dutch flood risk governance: historical analysis of external triggers”. In: *International Journal of Water Resources Development* 37.1 (Jan. 2021), pp. 24–47. issn: 13600648. doi: 10.

1080/07900627.2019.1707070. url: https://www.tandfonline.com/doi/abs/10.1080/07900627.2019.1707070.

[166] J. Woodhouse. *Asset management decision-making: The SALVO process. Strategic assets: life-cycle value optimization*. Woodhouse Partnership Limited, The Institute of Asset Management, Decision Support Tools Ltd, 2014.

[167] A. Almoradie, V. J. Cortes, and A. Jonoski. "Web-based stakeholder collaboration in flood risk management". In: *Journal of Flood Risk Management* 8.1 (Mar. 2015), pp. 19–38. issn: 1753318X. doi: 10.1111/JFR3.12076.

[168] M. Ishiwatari. "Flood risk governance: Establishing collaborative mechanism for integrated approach". In: *Progress in Disaster Science* 2 (July 2019), p. 100014. issn: 2590-0617. doi: 10.1016/J.PDISAS.2019.100014.

[169] A. de Leeuw. *PROMETHEUS – RAPPORTAGE WP1. Knelpunten, dilemma's en best practices*. Tech. rep. HAN University of Applied Sciences, 2021.

[170] C. W. Sadoff and D. Grey. "Cooperation on International Rivers, Water International". In: *Water International* 30.4 (2005), pp. 420–427. issn: 1941-1707. doi: 10.1080/02508060508691886. url: https://www.tandfonline.com/action/journalInformation?journalCode=rwin20.

[171] A. Van Buuren, J. Lawrence, K. Potter, and J. F. Warner. "Introducing Adaptive Flood Risk Management in England, New Zealand, and the Netherlands: The Impact of Administrative Traditions". In: *Review of Policy Research* 35.6 (2018), pp. 907–929. doi: doi.org/10.1111/ropr.12300.

[172] P. Sayers, B. Gersonius, F. den Heijer, W. J. Klerk, P. Fröhle, P. Jordan, U. Radu Ciocan, J. Rijke, B. Vonk, and R. Ashley. "Towards adaptive asset management in flood risk management: A policy framework". In: *Water Security* 12 (Apr. 2021), p. 100085. issn: 24683124. doi: 10.1016/j.wasec.2021.100085.

[173] D. Jonas. "Empowering project portfolio managers: How management involvement impacts project portfolio management performance". In: *International Journal of Project Management* 28.8 (2010), pp. 818–831. doi: 10.1016/j.ijproman.2010.07.002.

[174] J. Shao and R. Müller. “The development of constructs of program context and program success: A qualitative study”. In: *International Journal of Project Management* 29.8 (Dec. 2011), pp. 947–959. issn: 0263-7863. doi: 10.1016/J.IJPROMAN.2011.02.003.

[175] Y. Hu, A. Chan, and Y. Le. “CONCEPTUAL FRAMEWORK OF PROGRAM ORGANIZATION FOR MANAGING CONSTRUCTION MEGAPROJECTS - CHINESE CLIENT’S PERSPECTIVE”. In: *Engineering Project Organizations Conference* (2012).

[176] J. Shao, R. Müller, and J. Rodney Turner. “Measuring program success”. In: *Project Management Journal* 43.1 (2012), pp. 37–49. doi: doi.org/10.1002/pmj.20286.

[177] Z. Shehu and A. Akintoye. “Construction programme management theory and practice: Contextual and pragmatic approach”. In: *International Journal of Project Management* 27.7 (Oct. 2009), pp. 703–716. issn: 02637863. doi: 10.1016/J.IJPROMAN.2009.02.005. url: https://www.researchgate.net/publication/229379364%7B%5C_%7DConstruction%7B%5C_%7Dprogramme%7B%5C_%7Dmanagement%7B%5C_%7Dtheory%7B%5C_%7Dand%7B%5C_%7Dpractice%7B%5C_%7DContextual%7B%5C_%7Dand%7B%5C_%7Dpragmatic%7B%5C_%7Dapproach.

[178] NRCS. “Field Procedures Guide for the Headcut Erodibility Index”. In: *National Engineering Handbook, Part 628 Dams*. Natural Resources Conservation Service, 1997. Chap. 52.

[179] F. Diermanse, K. Roscoe, J. Lopez de la Cruz, H. Steenbergen, and A. Vrouwenvelder. *Hydra Ring Scientific Documentation*. Tech. rep. Deltares, 2013. doi: 1206006-004.

[180] H. Schüttrumpf, J. Möller, H. Oumeraci, J. Grüne, and R. Weissmann. “Effects of natural sea states on wave overtopping of seadikes”. In: *4th int symposium on waves 2001, Ocean wave measurement and analysis, American Society of Civil Engineers (ASCE)*. New York, 2001, pp. 1565–1574.

[181] S. A. Hughes and N. C. Nadal. “Laboratory study of combined wave overtopping and storm surge overflow of a levee”. In: *Coastal Engineering* 56.3 (2008), pp. 244–259.

[182] J. Pol, V. van Beek, W. Kanning, and S. Jonkman. “Progression rate of backward erosion piping in laboratory experiments and reliability analysis”. In: *7th International Symposium on Geotechnical Safety and Risk (ISGSR 2019)*. Taipei, Taiwan, 2019.

[183] S. K. Mishra and S. M. Seth. “Utilisation de l’hystérésis pour définir la nature de la propagation des ondes de crue dans des canaux naturels”. In: *Hydrological Sciences Journal* 41.2 (1996), pp. 153–170. issn: 21503435. doi: 10.1080/02626669609491489. url: https://www.tandfonline.com/action/journalInformation?journalCode=thsj20.

[184] A. Vrouwenvelder, M. Mierlo, E. Calle, A. Markus, T. Schweckendiek, and W. Courage. *Risk analysis for flood protection systems*. Tech. rep. 1202140.008, Deltares, 034.67189 TNO, DC04.30 Delft Cluster, 2010.

[185] G. Hoffmans and H. Verheij. *Scour Manual*. Rotterdam: ISBN 90 5410 673 5, A.A. Balkema Rotterdam, 1997. isbn: 90 5410 673 5.

[186] S. Caires. *Extreme wind statistics for the Hydraulic Boundary Conditions for the Dutch primary water defences. SBW-Belastingen: Phase 2 of subproject* "*Wind Modelling*". Tech. rep. 1200264-005, Deltares, 2009, p. 314.

[187] F. den Heijer and M. Kok. “Assessment of ductile dike behavior as a novel flood risk reduction measure”. In: *Risk Analysis* (2022), pp. 1–16. doi: 10.1111/risa.14071.

[188] Staatsblad. *Wet van 2 november 2016 tot wijziging van de Waterwet en enkele andere wetten (nieuwe normering primaire waterkeringen)*. Tech. rep. Staatsblad van het Konikrijk der Nederlanden 2016, 431, 2016.

APPENDICES

A

DIKE DUCTILITY MODEL AND PARAMETERS USED IN CHAPTER 3

A.1. INTRODUCTION

The risk analysis in Chapter 3 uses the physical relation between loads $S(t)$, strength $R(t)$, breach growth $S(t)$, all dependent on the time, the bathymetry of the flooded area, and the resulting water depth h in time at location a in a polder with surface A_b:

$$h_{\vec{X},a}(t) = f(S(t), R(t), B(t), A_b) \tag{A.1}$$

In which:

$h_{\vec{X},a}(t)$	Water level at time t on a certain location a in a flood prone area	$m + NAP$
$\vec{X}$	Set of physical and statistical parameters determining loads, strength and breach growth.	
$S(t), R(t), B(t)$	Respectively loads, strength and breach width in time	
A_b	Surface of area protected by a dike, with bathymetry b	m^2

The majority of this appendix has been published in F. den Heijer and M. Kok. "Assessment of ductile dike behavior as a novel flood risk reduction measure". In: Risk Analysis (2023). doi: 10.1111/risa.14071

Note that the value of $h_{\vec{X},a}(t)$ is defined as the water level at time t on a certain location a in a flood prone area. Nevertheless, the loads, strength and breach growth refer to the circumstances on, in and below the dike, as this terminology is commonly used in flood risk studies.

This appendix describes the physical relationships to be substituted in equation (A.1), the probabilistic model, and the investment model, which is together with the damage model in Section 2.3.2 the input for the case study in Chapter 3 of this thesis:

- the load model for a riverine area, including the river discharge over time, the translation form discharges to local water levels, and the storm wind, wind set-up, and wave growth.
- the strength model: overtopping [149] including the near-crest effects [180, 181], revetment erosion [16] over time, and core erosion [178]; piping [150] including the growth over time [182], and an educated estimation for the situation with a sheetpile based on the relation between Bligh and Lane
- the breach model [77], including the width growth in time and a solid layer limiting growth in depth. The breach model includes the mutual effect of river discharge and breach discharge on local river water level
- additional exercise for the damage model included in this thesis in Chapter 2
- climate change and subsidence model, also included in this thesis in Chapter 3, since the loads on the dike in equation (A.1) will change over its lifetime.
- the investment model, to enable assessment of change of construction type, or change of design dimensions, developed starting from [105] and [45]
- the details of the calculations: the flowcharts of the comparative analysis, the evaluation of the reliability function and the calculation of probabilities, and a numerical scheme for the calculation of the breach discharge in time.
- statistics of discharge and wind in the probabilistic model
- elaborations with the probabilistic model
- Finally, this appendix provides a set of tables with the values of the parameters used in the case presented in this thesis.

A.2. LOAD MODEL

A.2.1. RIVER DISCHARGE AND STORM WIND

The loads on the dike consists of water levels and waves. The water levels in a riverine are based on the occurrence of a flood wave. The waves are based on the occurrence of storm wind.

The river flood wave is taken far upstream of the possible breach locations to prevent being influenced by the hydraulic effects of the breach, see equation (A.2) and an example of a flood wave in Figure A.1. For the upstream system border the national border has been taken in the case study.

$$Q_u(t) = \begin{cases} \bar{Q}_u & t < T_{st} \cap t > T_{std} + T \\ \bar{Q}_u + 0.5(\hat{Q}_u - \bar{Q}_u)\cdot & \\ \quad \left(1 - \cos\left(\pi \frac{t - T_{std}}{T_{inc}}\right)\right) & T_{st} < t < T_{inc} \\ \bar{Q}_u + 0.5(\hat{Q}_u - \bar{Q}_u)\cdot & \\ \quad \left(1 - \cos\left(\pi \frac{t - T_{std} - (T_{inc} - T_{dec})}{T_{dec}}\right)\right) & T_{inc} < t < T_{inc} + T_{dec} \end{cases} \tag{A.2}$$

In which:

$Q_u(t)$	Upstream river discharge in time	m^3/s
$\bar{Q}_u$	Mean upstream river discharge	m^3/s
$\hat{Q}_u$	Event maximum river discharge, maximized by $\hat{Q}_{u,max}$	m^3/s
$\hat{Q}_{u,max}$	Limit on event maximum river discharge entering the upstream system border	m^3/s
t	Time	*hour*
T	Duration of river discharge event, $T_{inc}+T_{dec}$	*hour*
T_{std}	Start of river discharge event with respect to start time, here taken as 0 hours	*hour*
T_{inc}	Duration of discharge increase	*hour*
T_{dec}	Duration of discharge decrease	*hour*

Storm winds cause waves which cause overtopping and erosion of inner slope. Wind has a very changeable nature. For this study we defined only one wind direction and one storm per flood wave. The storm wind is defined in time as given in equation (A.3), with a minimum to reflect the mean windspeed for the time there is no storm.

$$U_w(t) = MAX\left(0.5 \cdot \hat{U}_w\left(1 - \cos\left(2 \cdot \pi \frac{t - T_{sts}}{T_{storm}}\right)\right), 0.5 \cdot \hat{U}_w\right) \tag{A.3}$$

In which:

$U_w(t)$	Windspeed in time at 10m above ground level	*m/s*
$\hat{U}_w$	Event maximum windspeed	*m/s*
T_{storm}	Duration of storm event	*hour*
T_{sts}	Start of storm event with respect to start time, here taken as 0 hours	*hour*

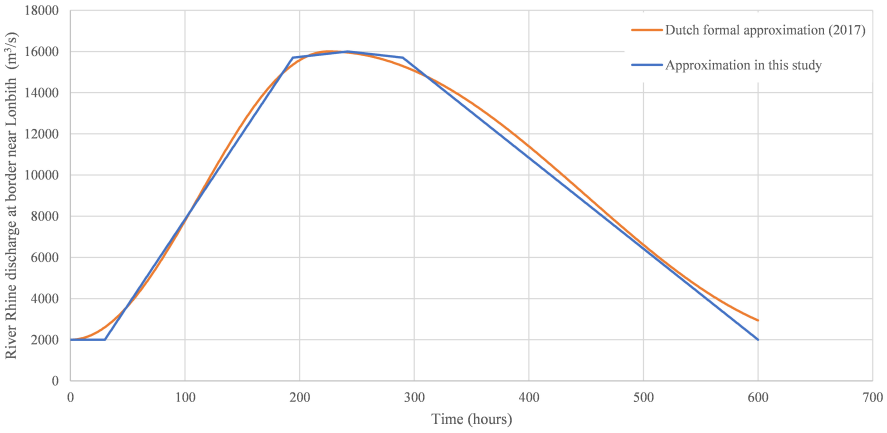

Figure A.1.: *Discharge in time for a river flood wave with a maximum discharge of 16000 m^3/s, comparing the formal approximation based on [70] with the approximation of equation (A.2), which fits well with T_{inc}=225 hours and T_{dec}=450 hours.*

A.2.2. WATER LEVELS

Based on the occurrence of a flood wave at a certain upstream system border, the water levels in a riverine area are dependent on the river characteristics and local effects. The river characteristics determine the translation of this wave along a river to the location of interest. Both river characteristics and local effects are described below. Note that the definition of the load model in time is the specific point in equation (A.1).

The relation between the river discharge upstream and a location anywhere in the river area, given no breach, is given by [72] as a polynomial function, relative to the water levels at the upstream system border:

$$h_{L_x}(t) = c_6 \cdot h_u^6(t) + c_5 \cdot h_u^5(t) + c_4 \cdot h_u^4(t) + c_3 \cdot h_u^3(t) + c_2 \cdot h_u^2(t) + c_1 \cdot h_u(t) + c_0 \tag{A.4}$$

In which:

$h_{L_x}(t)$	Local water level at location L_x in time	$m+NAP$
$c_0..c_6$	Coefficients determining the relation between local and upstream water level, based on calculations with a numerical hydraulic model	-
$h_u(t)$	Upstream water level in time	$m+NAP$

The coefficients in equation (A.4) are assumed to be independent of time, each discharge at the upstream system border is assumed to relate at the same moment with a water level anywhere in the river area. Thus, these relations do not reproduce the hysteresis characteristics of the flood wave [183]. For flood waves with very high discharges the water levels are extrapolated based on water levels derivative for an event discharge maximum $\hat{Q}_u = 16000 m^3/s$.

In [72] a table is provided with water levels h_u for a range of discharges at the upstream border, to be used in equation (A.4). To obtain the upstream river water level at the Dutch border (Lobith) as a function of the discharge, a relation is fitted, see equation (A.5). In Figure A.2 the comparison between the fit and the table in [72] is shown.

$$h_u(t) = \begin{cases} 3.1 + 0.0653 \cdot \sqrt{4.11 \cdot Q_u(t)} & Q_u(t) < 8000 \\ h_{u,8e3} + (h_{u,10e3} - h_{u,8e3}\left(\frac{Q_u(t)-8e3}{10e3-8e3}\right) & 8000 < Q_u(t) < 10000 \\ 8.47 + 0.0298 \cdot \sqrt{6.11 \cdot Q_u(t)} & 10000 < Q_u(t) < 16000 \\ h_{u,16e3} + h'_{u,16e3} \cdot (Q_u(t) - 16e3) & Q_u(t) > 16000 \end{cases} \tag{A.5}$$

In which:

$h_{u,8e3}$, $h_{u,10e3}$, $h_{u,16e3}$	Upstream water level for discharges with return periods of 8000, 10000, 16000 years respectively	$m+NAP$
$h'_{u,16e3}$	Derivative of water level for a discharge of 16000 or more $0.5 \cdot 0.0298 \cdot \sqrt{6.11} \cdot Q_{u,16e3}^{-0.5}$	$m+NAP$

Since [72] provides the coefficients $c_0..c_6$ for a limited number of locations in the river area, the local water level on a random location has been derived by linear interpolation depending on the river kilometrage:

$$h_{ele}(t) = m_h + (h_{L1}(t) - h_{L2}(t)) \cdot \frac{rkm_L - rkm_{L2}}{rkm_{L1} - rkm_{L2}} \tag{A.6}$$

In which:

$h_{ele}(t)$	Local water level in time excluding local effects such as a breach	$m + NAP$
$h_{L1}(t)$, $h_{L2}(t)$	Local water level at L1 resp. L2 in time	$m + NAP$
rkm_L, rkm_{L1}, rkm_{L2}	River kilometrage at locations L, L1 and L2 respectively, where L1 is upstream and L2 downstream from L	km
m_h	Model uncertainty of water level, in fact the uncertainty in equations (A.4) and (A.5) and the linear interpolation in equation (A.6) together	m

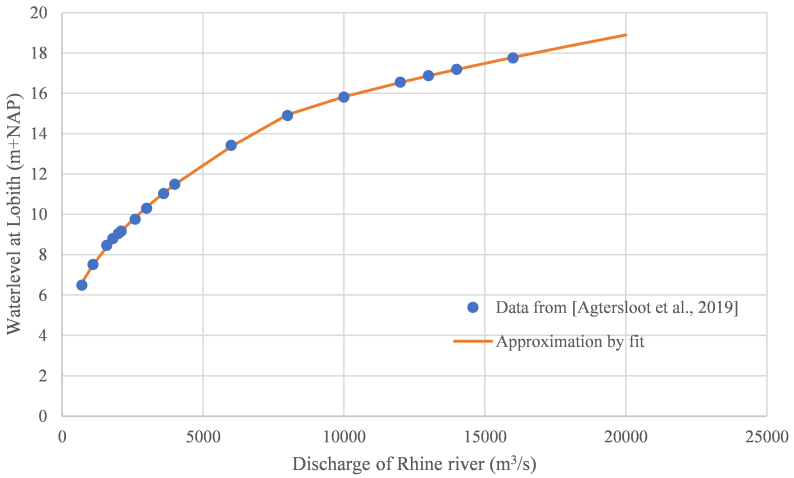

Figure A.2.: *Relation between discharge and water level at Lobith near the Dutch border, in which the approximation reflects equation* (A.5).

Second element of the local water level comprises local effects. The water level directly in front of the dike is increased by wind direction and windspeed. Although this is a secondary effect, it is included in the model by:

$$\Delta h_{setup}(t) = \frac{0,35 \cdot 10^{-6} \cdot U_w^2(t) \cdot F \cdot cos\theta_w}{depth_{su}} \tag{A.7}$$

In which:

$\Delta h_{setup}(t)$	Local water level difference over the river in wind direction	m
F_{su}	Fetch for set-up in wind direction	m
θ_w	Angle between dike normal and wind direction	°
$depth_{su}$	Mean water depth for wind set-up, assessed by the difference between dike height and river side dike toe	m

Thus, without a breach the local water level is:

$$h(t) = h_{ele}(t) + \Delta h_{setup}(t) \tag{A.8}$$

However, an important local effect is the effect of the occurrence of a breach. The discharge through the breach depends on the interaction between breach growth and the water levels in time. The numerical scheme to calculate the interdependence is given in section A.7. The equations for breach growth in time are given in section A.4. In this section the effect of breach width in time on water levels in time is given.

For inflow in the polder the discharge in time is given by:

$$Q_{breach}(t) = MIN \begin{cases} m_{Q_{breach}} \cdot B(t) \cdot (h_{polder}(t) - d_{bres}) \cdot \\ \qquad \sqrt{2g \cdot (h(t) - h_{polder}(t))} \\ m_{Q_{breach}} \cdot B(t) \cdot \frac{2}{3}\sqrt{\frac{2}{3}g} \cdot (h(t) - d_{bres})^{\frac{3}{2}} \end{cases} \tag{A.9}$$

In which:

$h(t)$	Local water level in time	$m + NAP$
$B(t)$	Breach width in time	m
$m_{Q_{breach}}$	Model uncertainty on breach width $B(t)$	-
$h_{polder}(t)$	Water level in de polder in time	$m + NAP$
d_{bres}	Minimum threshold level in breach, the maximum of polder level, foreland level, or a unerodible height (e.g. sheetpile)	$m + NAP$
$Q_{breach}(t)$	Discharge through dike breach into the polder	m^3/s

Since the law of preservation of discharge the upstream volumes should equal the sum of the discharge downstream the river and the discharge flowing into the polder through the breach. Since secondary time effects are neglected this should be the case at any point in time:

$$Q_u(t) = Q_{downs}(t) + Q_{breach}(t) \tag{A.10}$$

In which:

$Q_{downs}(t)$	Discharge downstream of breach in the river in time. Note, in case of a breach this discharge is dependent on the local water level, to be iteratively determined together with equation (A.9), see section A.7	m^3/s

This simple rule is complicated in a delta river, where the main branch upstream a location could bifurcate in several branches. Thus, the upstream river discharge at the border may be chosen upstream from bifurcation points, because of data availability or other reasons. When a breach could occur in one of the branches, the branch discharge is the upstream discharge. This branch discharge is a fraction of the discharge upstream of the bifurcation point. Equation (A.10) change in:

$$Q_u(t) \cdot b_Q = Q_{b,\,downs}(t) + Q_{breach}(t) \tag{A.11}$$

In which:

b_Q	Fraction of discharge Q_u flowing into branch b	-
$Q_{b,\,downs}(t)$	Discharge downstream of breach in branch b in time. Note, in case of a breach this discharge is dependent on the local water level, to be iteratively determined together with equation (A.9), see section A.7	m^3/s

N.B. When a breach location is near an upstream bifurcation point equation (A.11) is not valid without a doubt, because the upstream water levels will be influenced by the breach effect

A.2.3. WAVES AND WAVE IMPACT

The waves are modelled dependent on windspeed and fetch, based on the equations of Brettschneider [104].

$$\tilde{H} = 0.283 \cdot \tanh(0.53 \cdot \tilde{d}^{0.75}) \cdot \tanh\left(\frac{0.0125 \cdot \tilde{F}^{0.42}}{\tanh(0.53 \cdot \tilde{d}^{0.75})}\right) \tag{A.12}$$

$$\tilde{T} = 2.4\pi \cdot \tanh(0.833 \cdot \tilde{d}^{0.375}) \cdot \tanh\left(\frac{0.077 \cdot \tilde{F}^{0.25}}{\tanh(0.833 \cdot \tilde{d}^{0.375})}\right) \tag{A.13}$$

In which:

$\tilde{H}$	Dimensionless wave height in time, $\frac{H_{1/3} \cdot g}{U_w^2(t)}$	-
$\tilde{d}$	Dimensionless water depth in time, $\frac{d \cdot g}{U_w^2(t)}$	-
$\tilde{F}$	Dimensionless fetch in time, $\frac{F \cdot g}{U_w^2(t)}$	-
$\tilde{T}$	Dimensionless wave period in time, $\frac{T_{1/3} \cdot g}{U_w(t)}$	-
g	Gravitational acceleration	m/s^2
d_{wg}	Representative water depth for wave growth, here approximated by the difference between water level and dike toe level	m
F	Representative fetch for wave growth, calculated as F_{eff} times the actual fetch in a wind direction	m
F_{eff}	Factor on the measured fetch lengths to represent effective fetch length according to [104]	-
$H_{1/3}$	Significant wave height in time, assumed to be equal to H_s or H_{m0}	m
$T_{1/3}$	Significant wave period in time, assumed to be equal to T_s	s

The resulting wave height and wave period are assumed to represent the significant wave height and significant wave period respectively [104]. Input variables for the calculation of these wave parameters are: wind speed, representative fetch in wind direction, and water depth.

Wind speed and wind direction are directly sampled, as explained in the section A.8. Providing waves are not depth limited, water depth in riverine circumstances is not that important for wave growth. High river discharges are a prerequisite for loads on a river dike. Since wind speed and river discharge are independent, wind speeds are usually not that high during extreme discharges. That is why waves heights are mostly not that large and not depth limited. Therefore, water depth is tentatively chosen as the difference between dike crest level and dike toe level.

The wave growth model is not perfect. Model uncertainty is represented as:

$$H_s(t) = m_{H_s} \cdot \tilde{H} \frac{\cdot U_w^2(t)}{g} \tag{A.14}$$

$$T_s(t) = m_{T_s} \cdot \tilde{T} \frac{\cdot U_w(t)}{g} \tag{A.15}$$

In which:

$H_s(t)$	Significant wave height, assumed to be equal to $H_{1/3}(t)$	m
m_{H_s}	Model uncertainty on significant wave height	$-$
m_{T_s}	Model uncertainty on significant wave period	$-$
$T_s(t)$	Significant wave period, assumed to be equal to $T_{1/3}(t)$	s

The significant wave period T_s from equations A.12 and A.12 [104] has to be transformed to a spectral wave period $T_{m_{-1,0}}$, the input for the wave overtopping formula. In [144] this translation is given via the peak period T_p as:

$$\begin{cases} T_p = 1.08 \cdot T_s \\ T_{m_{-1,0}} = T_p / 1.1 \end{cases} \tag{A.16}$$

In which:

T_p	Wave peak period	s
$T_{m_{-1,0}}$	Spectral wave period	s

Wave overtopping over the dike is modelled conform [149]:

$$\frac{q_{vdM1}(t)}{\sqrt{gH_{m_0}^3}} = \frac{0.067}{\sqrt{\tan\alpha}} \cdot \gamma_b \cdot \xi_0 \cdot \exp\left(m_{qvdM1} \cdot \frac{h_{crest} - h(t)}{H_{m_0}(t)} \cdot \frac{1}{\xi_0 \cdot \gamma_b \gamma_f \gamma_\beta \gamma_v} \right) \tag{A.17}$$

$$\frac{q_{vdM2}(t)}{\sqrt{gH_{m_0}^3}} = 0.2 \cdot \exp\left(m_{qvdM2} \cdot \frac{h_{crest} - h(t)}{H_{m_0}(t)} \cdot \frac{1}{\gamma_f \cdot \gamma_\beta} \right) \tag{A.18}$$

$$q_{vdM}(t) = MIN(q_{vdM1}(t), q_{vdM2}(t)) \tag{A.19}$$

In which:

$q_{vdM1}(t)$	Overtopping discharge for breaking waves	$m^3/s/m$
$q_{vdM2}(t)$	Overtopping discharge for non-breaking waves	$m^3/s/m$

m_{qvdM1}	Model uncertainty of parameter q_{vdM1} representing overtopping discharge for breaking waves,distributed as a truncated normal with mean, standard deviation, under bound, upper bound (-4.75;0.5; -5.75;-3.75)	–
m_{qvdM2}	Model uncertainty of parameter q_{vdM2} representing overtopping discharge for breaking waves,distributed as a truncated normal with mean, standard deviation, under bound, upper bound (-2.6;0.35; -3.3;-1.9)	–
$H_{m_0}(t)$	Significant wave height, assumed to be equal to $H_s(t)$	m
$\tan\alpha$	Slope of river side of dike	–
$\gamma_b, \gamma_f,$ γ_β, γ_v	Reduction factors for respectively the effect of berm, roughness, angle of wave attack, and shallow foreshore	–
ξ_0	Irribarren parameter, $\frac{\tan\alpha}{\sqrt{s_0}}$	–
h_{crest}	Dike crest height	m
s_0	Wave steepness, $\frac{2\pi \cdot H_{m_0}}{g \cdot T^2_{m-1,0}}$	–

Only the influence factor due to angle of short-crested wave attack is modelled. The other influence factors, for e.g. berm or roughness, are assumed to be 1, reflecting no reduction.

$$\gamma_\beta = 1 - 0.0033 \cdot |\beta| \tag{A.20}$$

In which:

β	Angle of wave attack between wave propagation direction and dike normal perpendicular	*degrees*

For water levels near and above crest equations (A.17), (A.18) and (A.19) are not validated. In [16] different formulas are given for this domain. In this study we use a combination of the formulas of [181] for water levels near and above the crest, with a minimum determined by the first term, which is equal to the formula of [180] for water levels at the crest.

$$q_{wo}(t) = \begin{cases} q_w(t) + q_o(t) = \\ \quad 0.0537 \cdot \xi_{m-1,0} \cdot \sqrt{g H^3_{m_0}} + 0.5443 \cdot \sqrt{g\,|-R_c^3|} & h(t) > h_{crest} \\ q_w(t) = 0.0537 \cdot \xi_{m-1,0} \cdot \sqrt{g H^3_{m_0}} & h(t) \leq h_{crest} \end{cases}$$

(A.21)

In which:

$q_{wo}(t)$	Overtopping discharge for waves and overflow	$m^3/s/m$
$q_w(t)$	Overtopping discharge for waves	$m^3/s/m$
$q_o(t)$	Overtopping discharge for overflow	$m^3/s/m$
$\xi_{m-1,0}$	Irribarren parameter, $\frac{\tan\alpha}{\sqrt{s_0}}$ with s_0 based on $T_{m-1,0}$	$-$
R_c	Negative relative crest height, $h(t)-h_{crest}$	m

Combining the equations for water levels below and above the crest the following formula is used, mainly using [149] for water levels below the crest, [180] for water levels near the crest, and [181] for water levels above the crest. An example is given in Figure A.3.

$$q(t) = \begin{cases} MIN(q_{vdM}(t), q_{wo}(t)) & h(t) \le h_{crest} \\ q_{wo}(t) & h(t) > h_{crest} \end{cases} \quad \text{(A.22)}$$

In which:

$q(t)$	Overtopping discharge	$m^3/s/m$

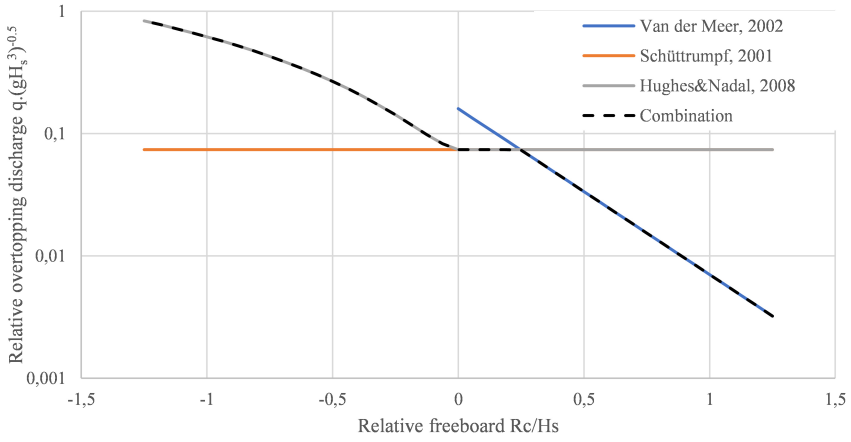

Figure A.3.: *Overtopping discharge as a function of relative crest height. Example based on crest height R_c = 12 m+NAP; $\tan\alpha$ = 0.33; wave parameters based on windspeed U_w = 13 m/s; Fetch = 2500m; resulting in $H_s = 0.4m; T_p = 2.3s$;*

A.3. STRENGTH MODEL

Figure A.4 shows a schematic overview of the dike cross section. The strength of the dike during the flood wave as described in section A.2 is described by mainly 2 erosion mechanisms. Firstly, the erosion of the grass cover on the landside of the dike due to overtopping and overflow, followed by cliff-erosion of the damaged grass cover. Secondly, the development of one or more pipes below the dike, with and without a sheetpile. These erosion mechanisms are described in the following sections.

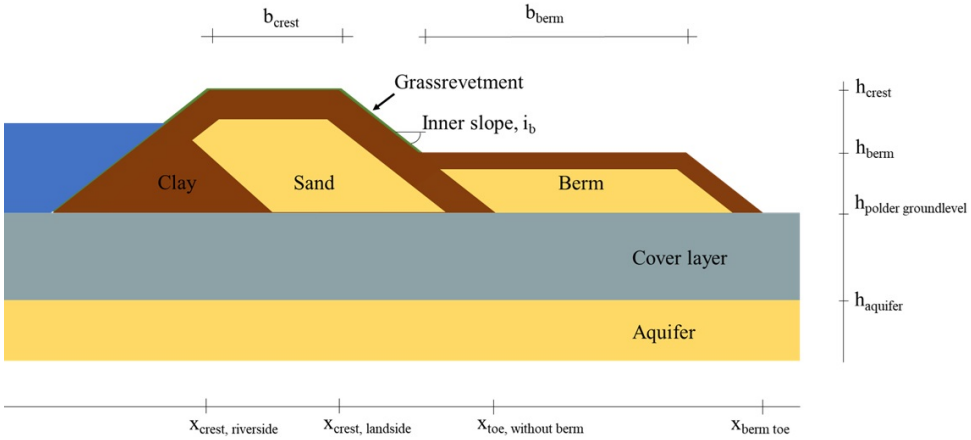

Figure A.4.: *Schematic overview of a dike cross section.*

A.3.1. EROSION LANDWARD SLOPE GRASS COVER

The basis of the erosion of the inner slope grass cover is the formula in [184], given equation (A.23). This formula is a simple and rather accurate approximation of the basic relations in [16], as shown in Figure A.5.

$$u_{c,grass} = f_g \cdot \frac{3.8}{1 + 0.8 \cdot \log t_e} \tag{A.23}$$

In which:

$u_{c,grass}$	Critical flow velocity on grass cover	*m/s*
f_g	Factor for grass quality (bad: 0.7; medium: 1.0; good: 1.4)	-
t_e	Length of time grass cover is resistant to withstand flow velocity u_c	-

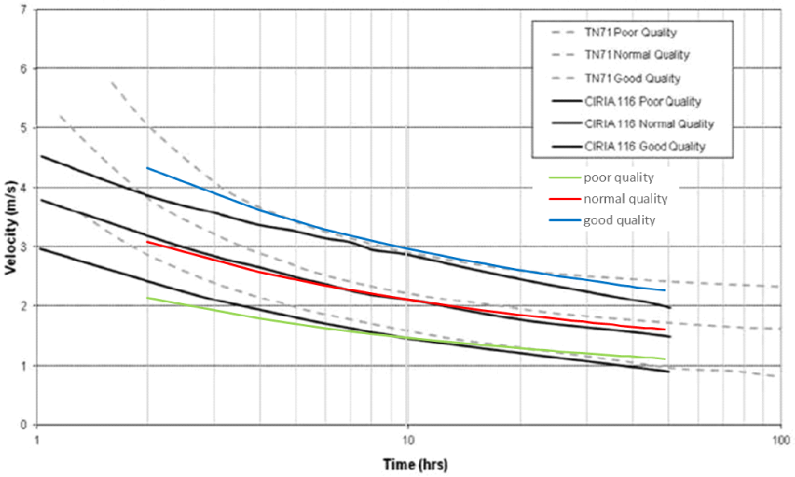

Figure A.5.: *Grass performance curves (Figure 8.49, p.813 in [16]), providing critical velocities as function of load time, here added with the colored approximations by [184].*

Equation (A.23) is meant for uniform non-fluctuating flow over a grass cover. However, it is used to estimate an erosion fraction per unit of time to simulate the erosion during a time variable flow velocity, occurring during a flood wave. Equation (A.23) is rewritten to estimate the time a grass cover is able to withstand a certain flow velocity on the inner slope u_i at time t.

$$t_e(t \in t, t + \Delta t) = 10^{\frac{1}{0.8} \cdot \left(\frac{3.8 \cdot fg}{u_i(t)} - 1 \right)} \tag{A.24}$$

In which:

Δt	Timestep	s
$u_i(t)$	Flow velocity on inner slope in time	-
$t_e(t)$	Length of time during which the grass cover is resistant to withstand flow velocity u on time t	-

Each timestep Δt the grass cover erodes with a fraction $\Delta t / t_e$. Integration over time leads to equation (A.25):

$$fr_g = \int_0^T \frac{1}{t_e(t)} dt \tag{A.25}$$

In which:

fr_g	Eroded fraction of grass cover	m/s

At the moment fr_g exceeds 1 the grass cover is assumed to be damaged, indicated by the time $t_{d,grass}$. To solve equation (A.25) the flow velocities are required at each moment in time during the flood wave. The overtopping discharges are known from equation (A.22). However, overtopping due to a combination of waves and overflow will not lead to a uniform load on the grass cover, nevertheless the wind wave averaged overtopping discharges are used to estimate the flow velocities during the flood wave with the formula of Manning [16].

$$u_b = \frac{h_b^{1/6}}{n} \cdot \sqrt{h_b \cdot i_b} \tag{A.26}$$

In which:

u_b	Flow velocity on inner slope	m/s
h_b	Water depth on inner slope	m
i_b	Slope of inner (landward) side of dike	-
n	Manning roughness coefficient	-

In [16] the roughness coefficient is given for several lopes. Using these, the roughness coefficient is estimated by:

$$n = \frac{0.00125}{i_b} + 0.0225 \tag{A.27}$$

Rewrite of equation (A.26) with $u_i(t)$ instead of u_b leads to an explicit formulation of the flow velocity, which is based on the time dependent wind wave averaged overtopping discharge.

$$u_i(t) = \frac{q^{0.4}(t) \cdot i_b^{0.3}}{n^{0.6}} \tag{A.28}$$

By using the result of equation (A.28) in equation (A.24) now the integration in equation (A.25) can be solved.

A.3.2. EROSION OF LANDWARD SLOPE WITHOUT GRASS COVER

When the grass cover on the inner slope is damaged the erosion of underlying material starts. The model of NRCS [178] is used, schematic shown in Figure A.6.

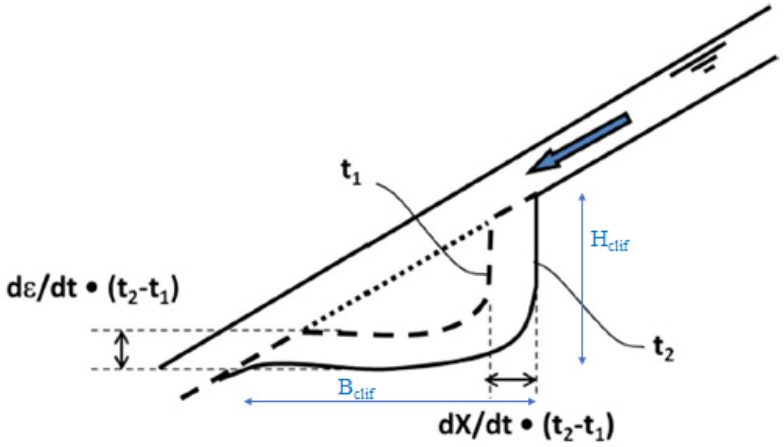

Figure A.6.: *Schematic overview of cliff erosion H_{clif} and B_{clif} between $t = t_1$ and $t = t_2$ at the land side cover of the dike.*

The gradient for the horizontal growth of the cliff is given in equation (A.29):

$$\frac{dx}{dt} = C_x \cdot (A(t) - A_0) \tag{A.29}$$

In which:

$\frac{dx}{dt}$	Horizontal cliff growth rate	$m/hour$
C_x	Horizontal growth rate coefficient, translates unity s in $A(t)$ and A_0 to hours as well	$s^{2/3}/hour$
$A(t)$	Cliff load parameter	$m/s^{1/3}$
A_0	Load threshold for cliff growth	$m/s^{1/3}$

The gradient for vertical growth of the cliff is given in equation (A.30):

$$\frac{d\epsilon}{dt} = k_d \cdot (\tau_e - \tau_c) \tag{A.30}$$

In which:

$\frac{d\epsilon}{dt}$	Vertical cliff growth rate	$m/hour$
k_d	Vertical growth rate coefficient	$m/hour/Pa$
τ_e	Actual sheer stress	$Pa\ (= kg/ms^2)$
τ_c	Critical sheer stress	$Pa\ (= kg/ms^2)$

Respectively, the parameters C_x, $A(t)$ and A_0 in equation (A.29) are figured out below.

$$C_x = \begin{cases} 3.04 - 0.79 \cdot \ln(K_h) & K_h \leq 18.2 \\ 0.75 & K_h > 18.2 \end{cases} \tag{A.31}$$

In which:

K_h	Erodibility index, in [178] given as $M_s \cdot K_b \cdot K_d \cdot J_s$. With a residual friction angle for sand of 33.7° results $K_h = 0.01$ based on $(M_s;K_b;K_d;J_s) = (0.015;1;0.65;1)$. With a residual friction angle for clay of 22° results $K_h = 0.03$ based on $(M_s;K_b;K_d;J_s) = (0.075;1;0.4;1)$. This order of magnitude has been found also in [91].	-
M_s	Material Strength number	-
K_b	Particle size number	-
K_d	Interparticle bond shear stress, $\tan\phi'_r$, with ϕ'_r the residual friction angle	-
J_s	Relative ground structure number	-

$$A(t) = (q(t) \cdot H_{clif}(t))^{1/3} \tag{A.32}$$

In which:

$H_{clif}(t)$	Height of cliff in time	m

$$A_0 = C_{ftm} \cdot \left(189 \cdot \sqrt{K_h} \cdot \exp\left(\frac{-3.23}{\ln(101 \cdot K_h)}\right)\right)^{1/3} \tag{A.33}$$

In which:

C_{ftm}	Conversion factor of ft to m: 0.3048	m/ft

The parameters in equation (A.30) are figured out below. Important parameters are: the permeability, depending on the clay-fraction, the estimation of the actual flow velocities on the cliff bottom, and the critical flow velocities. Note that the load parameters h_{clif} and u_{clif} are time dependent, as well as the critical velocity on the cliff bottom, due to its dependency on the actual water level.

$$k_d = \frac{0.036 \cdot \gamma_w}{\gamma_s} \cdot \exp\left(-0.121 \cdot c_{\%}^{0.406} \cdot \left(\frac{\gamma_s}{\gamma_w}\right)^{3.1}\right) \tag{A.34}$$

In which:

γ_w	Specific weight of water	kN/m^3
γ_s	Specific weight of soil, a mix of sand and clay	kN/m^3
$c_{\%}$	Fraction of clay	-

$$\tau_e = \rho g \left(\frac{u_{clif}(t)}{C_{clif}(t)}\right)^2 \tag{A.35}$$

In which:

ρ	Mass density of water	kg/m^3
$u_{clif}(t)$	Horizontal flow velocity at cliff bottom in time, based on the overtopping discharge, averaged over the wave period: $\frac{q(t)}{h_{clif}(t)}$	m/s
$C_{clif}(t)$	Coefficient of Chezy, $\frac{h_{clif}(t)^{1/6}}{n}$, dependent of time because of time dependency of water level h_{clif}	$m^{1/2}/s$
$h_{clif}(t)$	Water depth at cliff bottom in time, based on the overtopping discharge and assumed critical flow at inner slope below the cliff: $\left(\frac{q(t)}{2/3 \cdot \sqrt{2/3 \cdot g}}\right)^{2/3}$	m/s

$$\tau_c = \rho g \left(\frac{u_{c,clif}(t)}{C_{clif}(t)}\right)^2 \tag{A.36}$$

In which:

$u_{c,clif}(t)$	Critical flow velocity at cliff bottom in time	m/s

The critical flow velocity at cliff bottom is based on Mirtkhoulava's relations [185]:

$$u_{c,clif} = MAX\left(\log\left(\frac{8.8 \cdot h_{clif}(t)}{d_\alpha}\right)\sqrt{\frac{0.4}{\rho}\cdot\left((\rho_s-\rho)\cdot g\cdot d_\alpha + 0.6\cdot C_f\right)}; U_{c,min}\right) \tag{A.37}$$

In which:

d_α	Size of detaching aggregates. Typical values are 0.001m (sand) and 0.004 m (clay)	m
ρ_s	Mass density of soil at cliff bottom	kg/m^3
C_f	Fatigue rupture strength of clay, $C_f = 0.035 \cdot C_0$, with C_0 the cohesion [185]	-
$u_{c,min}$	Minimal critical flow velocity at cliff bottom, depending on material	m/s

The cliff will grow in horizontal and vertical directions. The cliff will grow vertically until the cliff height is large enough to start growth horizontally, when $A(t)$ exceeds A_0. In the phase the cliff only grows vertically the cliff width is increasing as well, in landward direction with $\frac{d\epsilon}{dt}/i_b$. It is assumed that the vertical growth will end when the erosion of the cliff bottom reaches ground level or berm level, in case of presence of a berm. The horizontal growth will propagate until erosion reaches the riverside of the dike. The cliff width is defined as the integral over time, starting when an initial damage of the grass cover occurs on a location at the inner slope:

$$B_{clif}(t) = \int_{t_{d,grass}}^{T}\left(C_x(A-A_0) + MAX\left(\frac{k_d(\tau_e-\tau_c)}{i_b}; x_{d,\,initial} - x_{ecg}\right)\right)dt \tag{A.38}$$

In which:

B_{clif}	Width of cliff in dike cross section	m
$x_{d,\,initial}$	Location of initial damage on inner slope with respect to x_{crest}, see Figure A.4	m
x_{ecg}	Horizontal position where vertical cliff growth ends, assumed at inner slope toe (at the maximum of berm level and ground level)	m

Note, $(A(t)-A_0)$ is defined as 0 in case $A(t) < A_0$ to prevent negative cliff growth. Note, τ_c depends on the thickness of the clay layer in case of a sand core: as long as $H_{clif} < clay layer\, thickness/\cos(i_b)$ the value of τ_c is based on the critical flow velocity of clay, otherwise the value of τ_c is based on the critical flow velocity of sand. The height of initial damage on the inner slope is uncertain. However, when a berm is present the damage is assumed to occur above the berm:

$$h_{d,\,initial} = h_{ecg} + m_{init.\,dam.} \cdot (h_{crest} - h_{ecg}) \tag{A.39}$$

In which:

$h_{d,\,initial}$	Height where initial damage occurs, and where vertical cliff growth starts	$m + NAP$
$m_{init.\,dam.}$	Stochastic model parameter to reflect uncertainty for height of initial damage (> 0 ; < 1)	-
h_{ecg}	Vertical position where vertical cliff growth ends, assumed at inner slope toe (at the maximum of berm level and ground level)	$m + NAP$

Based on the initial damage height, the initial horizontal position of the cliff is determined by:

$$x_{d,\,initial} = x_{crest} + \frac{(h_{crest} - h_{d,\,initial})}{i_b} - \frac{H_{clif,\,intitial}}{i_b} \tag{A.40}$$

In which:

$H_{clif,\,intitial}$	Height of initial damage	m

The horizontal growth propagates, depending on the loads, until erosion reaches the riverside of the dike. The ultimate horizontal position of the

riverside of the cliff, in which the remaining profile is able to withstand the actual river loads, is assumed to be the river side of crest. Note that when stability would be involved this assumption could need a change. The maximal cliff width is defined as the distance between the river side of the crest and the most landward location which is assumed to be possibly reached by the growing cliff: the inner toe (or in case of a berm the point where inner slope connects with the berm). The fraction of cliff erosion is the actual cliff width relative to the maximal cliff width:

$$fr_{clif}(t) = \frac{B_{clif}}{B_{clif,max}} \tag{A.41}$$

In which:

$fr_{clif}(t)$	Eroded fraction of dike width at time t	-
$B_{clif,max}$	Maximum width of cliff in dike cross section, defined as the horizontal distance between the river side of crest and inner toe (or in case of a berm the point where inner slope connects with berm)	m

The time $t_{breach_{clif}}$ is determined at the moment fr_{clif} exceeds 1. When no other dike failure mechanism reaches an erosion fraction of 1, at this time breach growth will start, see section A.4.

A.3.3. PIPING

For the development of pipes below the dike mainly 3 partial mechanisms are considered:

- uplift and bursting of impermeable layer at the landward side of the dike
- heave of erodible material (sand) through the bursted impermeable layer
- pipe growth towards riverside

In [150] bursting and heave are defined as conditions for the occurrence of unlimited pipe growth. Only when these conditions are fulfilled, will they enable the development of a pipe. Due to the time dependent approach, these conditions may be fulfilled for only a part of duration of the flood wave. The condition of bursting, once occurred during a flood wave, is assumed to stay fulfilled even when the water level decreased.

In fact, there are numerous possible pipe locations. In this study we choose 2 of them. At the land side of the berm in the toe ditch, and

on the berm located just next to the upper part of the inner slope. The condition for bursting is given in equation (A.42):

$$\begin{cases} (h(t) - h_{landside}) \cdot r_{head\,drop} \cdot \gamma_{s,burst} > D_{cl} \cdot \frac{\gamma_s - \gamma_w}{\gamma_w} & bursting \\ (h(t) - h_{landside}) \cdot r_{head\,drop} \cdot \gamma_{s,burst} \leq D_{cl} \cdot \frac{\gamma_s - \gamma_w}{\gamma_w} & no\,bursting \end{cases} \tag{A.42}$$

In which:

$h_{landside}$	Ground level at landside of the dike	$m + NAP$
$r_{head\,drop}$	Response factor for head. Decreases from riverside to landside. Here referring to the head at landward pipe exit point	-
$\gamma_{s,burst}$	Factor to schematize the uncertainty of the subsurface with respect to burst	-
D_{cl}	Thickness of cover layer at the land side of the dike	m

The condition for heave is given in equation (A.43):

$$\begin{cases} \frac{(h(t) - h_{landside}) \cdot r_{head\,drop}}{D_{cl}} \cdot \gamma_{s,heave} > i_{crit} & heave \\ \frac{(h(t) - h_{landside}) \cdot r_{head\,drop}}{D_{cl}} \cdot \gamma_{s,heave} \leq i_{crit} & no\,heave \end{cases} \tag{A.43}$$

In which:

$\gamma_{s,heave}$	Factor to schematize the uncertainty of the subsurface with respect to heave	-
i_{crit}	Critical head with respect to heave	-

When both conditions are fulfilled pipe growth is possible. Equation (A.44) gives the critical head. If exceeded, unlimited pipe growth is expected to take place.

$$\begin{cases} \Delta H_{crit} > \gamma_{s,pip} \cdot (h(t) - h_{landside} - r_{exit} \cdot D_{cl}) & unlimited\,pipegrowth \\ \Delta H_{crit} \leq \gamma_{s,pip} \cdot (h(t) - h_{landside} - r_{exit} \cdot D_{cl}) & no\,unlimited\,pipegrowth \end{cases} \tag{A.44}$$

In which:

ΔH_{crit}	Critical relative head in formula of Sellmeier [150]	m
$\gamma_{s,pip}$	Factor to schematize the uncertainty of critical head for unlimited pipe growth	-
r_{exit}	Factor to schematize resistance at pipe exit point. Common practice in the Netherlands to use 0.3 (the so-called 0.3D rule) based on [150]	-

The critical head in [150], known as well as Sellmeier's rule, is defined as:

$$\Delta H_{crit} = L \cdot F_{resistance} \cdot F_{scale} \cdot F_{geometry} \tag{A.45}$$

With:

$$F_{resistance} = \frac{\gamma'_p}{\gamma_w} \cdot \eta \cdot \tan\theta \cdot \left(\frac{RD}{RDm}\right)^{0.35} \tag{A.46}$$

$$F_{scale} = \frac{d_{70m}}{\sqrt[3]{\kappa \cdot L}} \left(\frac{m_{d70} \cdot d_{70}}{d_{70m}}\right)^{0.40} \tag{A.47}$$

$$F_{geometry} = 0.91 \cdot \left(\frac{D}{L}\right)^{\frac{0.28}{\left(\frac{D}{L}\right)^{-1}} + 0.04} \tag{A.48}$$

In which:

$F_{resistance}$	Factor representing resistance	-
F_{scale}	Factor representing effect of scale	-
$F_{geometry}$	Factor representing effect of geometry	-
γ_p	Submerged weight of sand	kN/m^3
η	Coefficient of White	kN/m^3
θ	Roll resistance of sand particles	°
RD/RDm	Relative density of sand below dike with respect to model, here assumed to be 1	-
m_{d70}	Uncertainty of 70-percentile of particle size	m
d_{70_m}	Mean d_{70} in scale model tests	m
d_{70}	70-percentile of particle size	m
L	Horizontal distance of leakage path	m
D	Thickness of sand layer	m

The time t_{pip} is determined at the moment the conditions of equation (A.42) equation (A.43) and equation (A.44) are met. In this concept more than one piping path and corresponding value for L can be evaluated, e.g. dependent on the presence of a berm, or a toe ditch. Each path is given a code j.

Starting from time t_{pip_j} the pipe will grow towards the riverside. The velocity depends on the ration between head and remaining pipelength [182]:

$$v_{pipe}(t,j) = \frac{c \cdot k \cdot (h(t) - h_{landside})}{0.5 \cdot (L_j - l(t)) \cdot n_p} \tag{A.49}$$

In which:

$v_{pipe}(t,j)$	Velocity of pipe length increase in time for piping path j	m/s
c	Proportionality constant pipe growth	-
k	Permeability	m/s
$l(t)$	Length of pipe at time t	m

The fraction of erosion due to piping is defined as the ratio of the distance of pipe erosion and maximal pipe length L. Based on [150] it is assumed the pipe has grown until 50% of the length L in case the criterion of equation (A.45) has been met. Since this is an uncertain assumption, a stochastic model parameter m_{pip} is introduced. This leads to equation (A.50):

$$\forall j \in (1,\ n_{pp}) : fr_{piping_j} = m_{pip} \cdot 0.5 + \frac{1}{L_j} \int_{t_{pip_j}}^{T} v_{pipe}(t,j)dt \tag{A.50}$$

In which:

fr_{piping}	Eroded fraction of maximal pipe length	-
t_{pip}	Time critical head ΔH_{crit} is exceeded	s
j	index for leakage paths j	-
L_j	Horizontal distance of leakage path j	m
m_{pip}	Model uncertainty on pipe length when critical head is exceeded	-
n_{pp}	Number of considered piping paths j	-

The time $t_{breach_{pip}}$ is determined at the moment fr_{piping} for one of the considered piping paths exceeds 1. The minimum of the corresponding times $t_{breach_{pip}}$ is the one representative for start breaching by piping.

$$t_{breach_{pip}} = MIN\left(t_{breach_{pip_1}}..t_{breach_{pip_j}}..t_{breach_{pip_n}}\right) \tag{A.51}$$

In which:

$t_{breach_{pip_j}}$	Moment in time the pipe has grown over the total available leakage length L for piping path j	s

A.3.4. PIPING FOR DIKES WITH A SHEETPILE

A sheetpile has two effects in this concept: it lengthens the leakage lengths for pipe growth and it reduces the breach discharge, provided it is stable after breaching, see Figures A.7 and A.8. In this paragraph only the first function is relevant. An assumption has been made for the lengths of the sheetpile, to be stable in case of dike breach, see Figures A.7 and A.8 and equation (A.52):

$$L_{sp} = f_{spl} \cdot (h_{sp} - h_{landside}) \tag{A.52}$$

In which:

L_{sh}	Length of sheetpile	m
h_{sp}	Height of sheetpile with respect to reference level	$m + NAP$
f_{spl}	Factor reflecting the depth of the toe of sheetpile below ground level with respect to the part exceeding ground level, here taken as 5	-

The length of the leakage path increases, due to the presence of a sheetpile. The critical head increases consequently. The critical head of Sellmeier's rule, given in equation (A.45) is not available for the presence of a sheetpile. For design, the formula of Lane is used [150] which is derived in the same period of time as the formula of Bligh for situations without a sheetpile[150]. In this thesis, the effect of a sheetpile on the critical head based on Sellmeier's rule is assumed to be the same as the ratio between the equations of Lane and Bligh, provided the ratio exceeds 1:

$$\Delta H_{crit\,sp} = \Delta H_{crit} \cdot MAX\left(\frac{\Delta H_{Lane}}{\Delta H_{Bligh}}; 1\right) \tag{A.53}$$

In which:

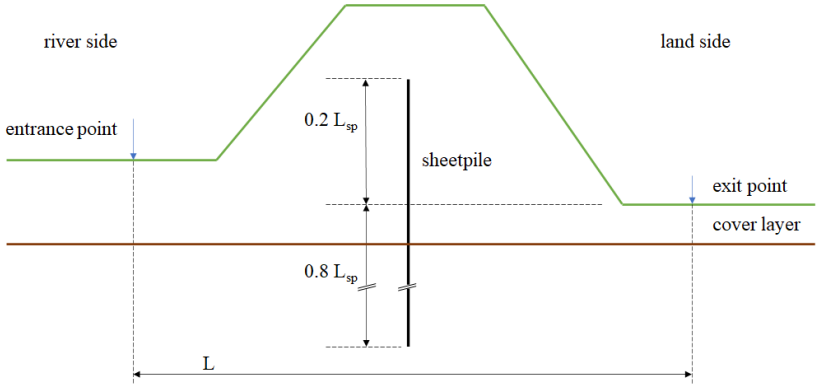

Figure A.7.: *Schematic overview of sheetpile in dike.*

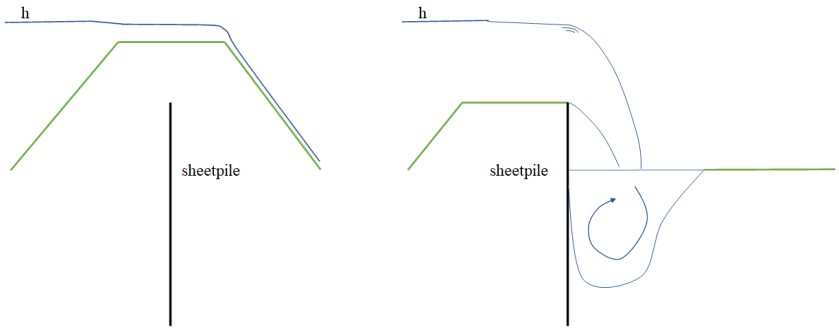

Figure A.8.: *Schematic overview of effect of sheetpile after a breach.*

$\Delta H_{crit\,sp}$	Critical head in case of presence of a sheetpile	m
ΔH_{Lane}	Critical head in case of presence of a sheetpile, formula of Lane [150]	m
ΔH_{Bligh}	Critical head, in formula of Bligh [150]	m

The ratio between the formulas of Lane and Bligh is:

$$\frac{\Delta H_{Lane}}{\Delta H_{Bligh}} = \frac{\frac{\frac{L_h}{3}+2L_v}{C_w}}{\frac{L_h}{18}} = \frac{6+36\cdot\frac{L_v}{L_h}}{C_w} \tag{A.54}$$

In which:

L_h	Horizontal leakage path	m
L_v	Vertical leakage path	m
C_w	Creep factor, characterizing the material in the aquifer	m

With the adaption of the critical head in case of a sheetpile in equation (A.53) the equations (A.49) and (A.50) can be used to determine the time of dike breach during a flood wave.

A.4. BREACH GROWTH MODEL

During a flood wave different several mechanisms cause erosion or reduce strength. When one of these mechanisms t_{breach} occurs, an initial breach is assumed to be present and breach growth starts. In this study this is the moment in time when at least one of the erosion fractions exceeds 1, see equations (A.41) and (A.50).

$$t_{breach} = MIN\left(t_{breach_{pip}}..t_{breach_{mechanism_i}}..t_{breach_{clif}}\right) \tag{A.55}$$

In which:

$t_{breach_{pip}}$	Moment in time the pipe has grown over the total available leakage length L	s
$t_{breach_{mechanism_i}}$	Moment in time the resistance of mechanism i reduced to nihil	s
$t_{breach_{clif}}$	Moment in time the cliff has grown over the total available width	s

In [77] an equation is given to relate the head over an initial breach to the breach width in time:

$$B_0(t) = f_1 \cdot \frac{g^{0.5} \cdot \Delta H^{1.5}}{u_c} \log\left(1 + \frac{f_2 \cdot g}{u_c} \cdot t\right) \tag{A.56}$$

In which:

$B_0(t)$	Breach width in time, for time-independent head	m
f_1	Coefficient breach growth	m
f_2	Coefficient breach growth	m
ΔH	Head over the breach	m
u_c	Critical flow velocity depending on the material	m/s

Since the loads are time dependent the breach width in time has to be assessed by:

$$B(t) = \int_{t_{breach}}^{T} \frac{dB(t)}{dt} dt \tag{A.57}$$

In which:

$B(t)$	Breach width in time	m
$\frac{dB(t)}{dt}$	Growth velocity of breach width	m

$$\frac{dB(t)}{dt} = \frac{f_1 \cdot f_2}{\ln(10)} \cdot \frac{(g \cdot (h(t) - h_{polder}(t)))^{1.5}}{u_c^2} \left(\frac{1}{1 + \frac{f_2 \cdot g}{u_c} \cdot (t - t_{breach})} \right) \tag{A.58}$$

However, for small values of $t - t_{breach}$ equation (A.56) is used to calculate $B_0(t)$, due to unstable values of $\frac{dB(t)}{dt}$. For these values of t the head at time t is determined as the average head from the start of breach growth t_{breach} until t:

$$\Delta H(t) = \frac{(h(t_{breach}) - h_{threshold}) + (h(t) - h_{threshold})}{2} \tag{A.59}$$

In which:

$h(t_{breach})$	Water level in the river at start of breach growth	$m + NAP$
$h_{threshold}$	Reference height, chosen as height of threshold in breach	$m + NAP$

Thus, the equation to assess breach width in time used in this study is:

$$B(t) = B_0(t_{sbg} - t_{breach}) + \int_{t_{sbg}}^{T} \frac{dB(t)}{dt} dt \tag{A.60}$$

In which:

t_{sbg}	Time after dike breach from which equation (A.58) is used	s

A.5. DAMAGE MODEL

The damage model is described section 2.3.2. The relation between consequences and flood volume is shown in Figures 2.4. The assumption of a linear relation is supported by an additional excercise. The result is presented in Figure A.9 which show the moving average of 10 datapoints for economic damage and victims.

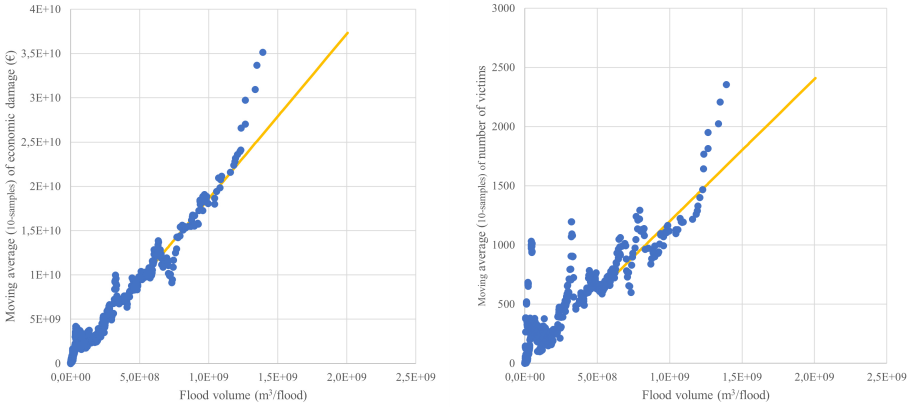

(a) *Damage* (b) *Victims*

Figure A.9.: *Overview of moving averaged data, taking the average of 10 samples.*

A.6. COST MODEL

A.6.1. INVESTMENT COSTS

The investment costs for dike reinforcement are based on the model KOSWAT [105] and experience of waterboards [45], resulting in reinforcement costs of about 7 M€ per km. To get a proper difference with respect to reinforcement costs of different cross sections, the costs are related to

volumes (supply, replace or remove), material (clay or sand), construction (sheetpile, thickness of clay layer), renewal of pavement on the dike, acquisition of the room for dike reinforcement, and initial costs (e.g. for design). Equation (A.61) gives the composition of these costs:

$$I = L_{dijk} \cdot (I_0 + V_{add-sand} \cdot C_{V,sand} + V_{add-clay} \cdot C_{V,clay} + V_{replace} \cdot C_{replace} + V_{remove} \cdot C_{remove} + A_{add-room} \cdot C_A + L_{sheetpile} \cdot C_{sp} + I_p \cdot C_{pavement}) \quad \text{(A.61)}$$

In which:

I	Investments for total reinforcement	€
I_0	Marginal initial costs for dike reinforcement	€/m
I_p	Indicator for renewal of the pavement on the dike, 0 for no dike heightening and 1 for dike heightening	-
L_{dijk}	Length of dike stretch to be reinforced	m
$V_{add-sand}$	Marginal volume of sand to be added	m^3/m
$V_{add-clay}$	Marginal volume of clay to be added	m^3/m
$V_{replace}$	Marginal volume of sand or clay to be replaced locally	m^3/m
V_{remove}	Marginal volume of sand or clay to be removed	m^3/m
$A_{add-room}$	Marginal room to be acquired for dike reinforcement	m^2/m
C_{V-sand}	Marginal costs to acquire sand and put in place	$€/m^3$
C_{V-clay}	Marginal costs to acquire sand and put in place	$€/m^3$
$C_{replace}$	Marginal costs to replace sand or clay locally	$€/m^3$
C_{remove}	Marginal costs to remove sand or clay	$€/m^3$
$C_{add-room}$	Marginal costs to acquire room	$€/m^2/m$
C_{sp}	Marginal costs to put in place a sheetpile	$€/m^2/m$
$C_{pavement}$	Marginal costs to remove and renew the pavement	€/m

A.6.2. SOCIETAL COSTS

Societal costs are calculated as the sum of investment costs and present value of risks.

$$SC = I + \frac{R}{r} \quad \text{(A.62)}$$

In which:

SC	Present value of societal costs	€
R	Economic risk per year	€ per year
r	Interest rate	per year

A.7. FLOWCHARTS OF CALCULATIONS

In this section the flowcharts are presented for the calculations. The main flowchart consists of the risks as well as the investments, see Figure A.10. Detail A provides the flowchart for the determination of the F_H-curve, see Figure A.11. Detail B provides the flowchart of the reliability function, see Figure A.12. Detail C provides the flowchart of the iterative determination of flood level at breach in time, see Figure A.13.

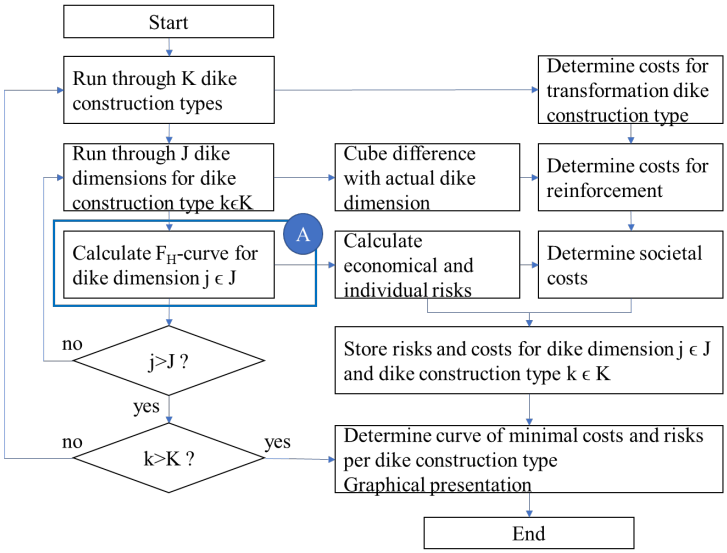

Figure A.10.: *Main overview of calculation scheme.*

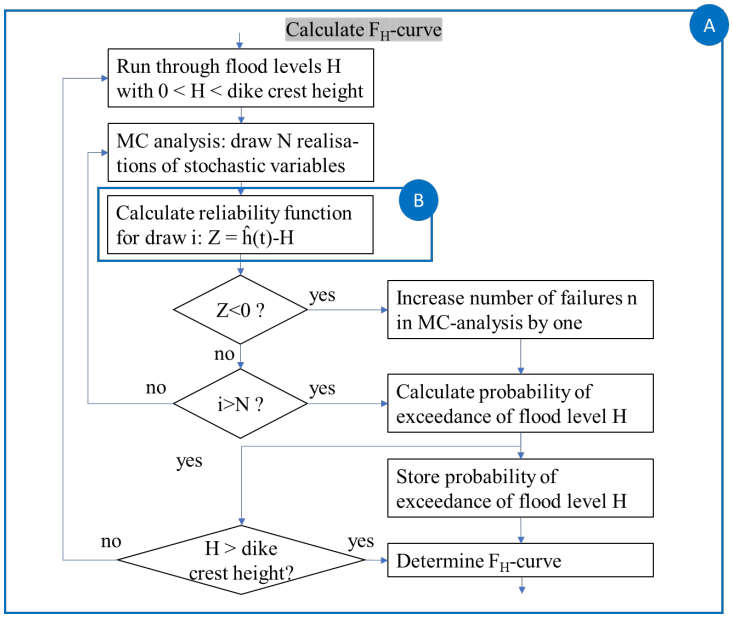

Figure A.11.: *Detail A of calculation scheme.*

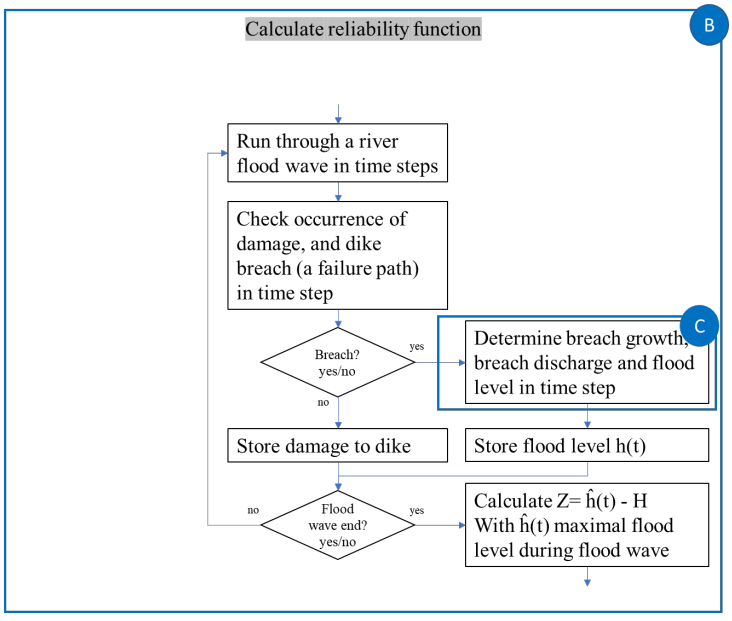

Figure A.12.: *Detail B of calculation scheme.*

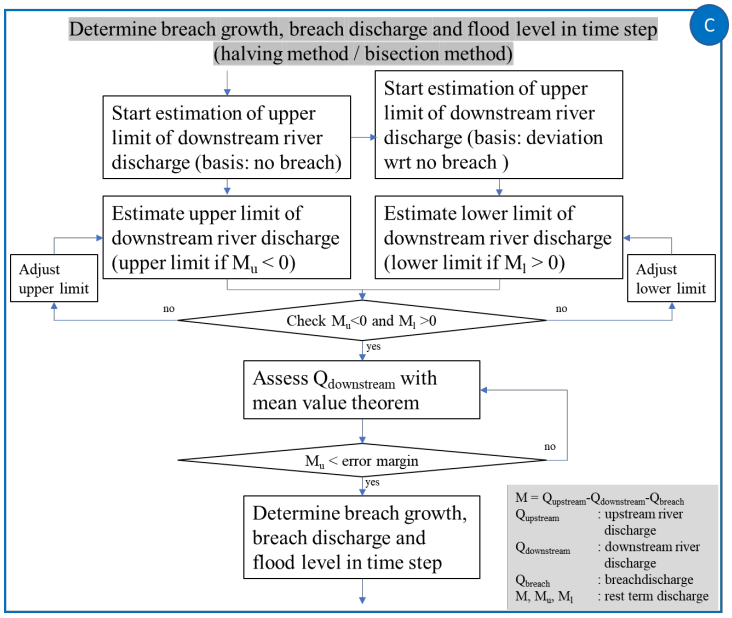

Figure A.13.: *Detail C of calculation scheme.*

A.8. PROBABILISTIC APPROACH

The probabilistic approach is a Monte Carlo draw, with Important Sampling (MC-IS). This paragraph adds to the main article some specifics about the application of the probabilistic approach. First some transformations for wind and river discharge to meet the realistic distributions. Second some specifics for the use of MC-IS.

A.8.1. WIND DIRECTION AND WIND SPEED

Each MC-draw the characteristics of one storm have been drawn, respectively the wind direction, the maximum wind speed per flood wave conditional on wind direction, the storm duration and the moment during a flood wave where the storm occurs. Starting point is the occurrence of only one storm per flood wave, and one wind direction per storm.

The probability of occurrence of a wind direction is based on [104], transformed to wind sectors of 30 degrees. The statistical distribution of wind speed and direction is given in [186] per wind sector of 30 degrees. For the river area, the station Herwijnen is chosen as most representative. Since the time base of a flood wave is about a month, the distributions are transformed to a monthly basis, conditional on the wind direction. In this study the wind speeds are modelled as Gumbel distributions. The transformation from the original distribution in [186] is:

$$F_{U|R_m} = \frac{F_{U,R_{yr}}}{N_{month} \cdot p_R} \tag{A.63}$$

In which:

$F_{U\|R_m}$	Wind speed frequency of exceedance, conditional on wind sector	*per month*
$F_{U,R_{yr}}$	Wind speed frequency of exceedance, for a wind sector	*per year*
N_{month}	Number of the (for dike safety) relevant months in a year. Mostly taken as 6 in the Netherlands	-
p_R	Probability of occurrence of wind from a wind sector	-

A.8.2. TRANSFORMATION RIVER DISCHARGE

In a riverine area the maximal river discharge during a flood wave is the most important stochastic variable to assess flood risks. Four transformations are made, to represent respectively a sound statistical distribution, statistical uncertainty, climate change and a physical maximum discharge.

First, the transformation to represent the statistical distribution, given for the Rhine river in [70]. The river discharge $\hat{Q}_u$ is represented by a Gumbel distribution, fitting very well for the discharges above about 14500 m^3/s. For lower discharges, a transformation is used as given in Table A.1, based on the difference between the return periods of both distributions. In between the values a linear interpolation is used.

Table A.1.: *Base for transformation of Monte Carlo draw of discharge from a Gumbel distribution to the reference in [70].*

Discharge from MC draw	Transformed discharge
< 9981	$\hat{Q}_u = \hat{Q}_u \cdot 3500/9981$
10479	5000
10764	5940
11470	7979
11938	9130
12644	10910
13402	12770
14089	14000
> 14480	$\hat{Q}_u = \hat{Q}_u$

Secondly, the transformation to represent the statistical uncertainty. In [70] a table has been given with the 95% reliability of the event maximum river discharge per return period. Based hereon, in this study a continuous relationship is used. Especially for the extreme discharges this relation fits the table very well.

$$\hat{Q}_u = \hat{Q}_u + m_Q \cdot \left(201 + \exp\left(\frac{3226 + \hat{Q}_u}{2967} \right) \right) \tag{A.64}$$

In which:

m_Q	Model factor representing statistical uncertainty of maximum discharge	m^3/s

Third, the transformation to represent climate change. For this equation (3.14) is used.

Fourth, the transformation to represent the physical maximum discharge. When the drawn event maximum discharge after these three transformations exceeds the physical maximum value, the drawn event is assumed to be equal to the physical maximum discharge.

A.8.3. MONTE CARLO IMPORTANT SAMPLING DRAWS

The technique Monte Carlo Important sampling (MC-IS) is used in the Probabilistic ToolKit (PTK) with optimized sample center [98]. This paragraph provides the application.

A Monte Carlo Important Sampling draw requires the definition of a sample center for all stochastic variables. Four of the variables are assumed to be important in the case of a riverine area: the river discharge, the statistical uncertainty of the river discharge, the uncertainty in the model to calculate a local water level based on the river discharge, and the start time of a storm. Values for these variables deviate from the mean value, see Table A.2.

The option 'optimal sample centre' is used to further optimize the sample centre for a series of calculations for a given set of dike dimensions. To find the optimal sample center, the calculations are preceded by two loops of 30% of the sample series length to locate the failure region for the given set of dike dimensions and a flooding with a water level in the polder >=0.1m. The gravity centre of the samples in this loop defines the magnitude of the shift for each stochastic parameter to reach a sample centre just on the limit state function. This procedure has been carried out for each individual combination of dike dimensions and construction type.

Table A.2.: *Overview of calculation parameters for using the technique MC-IS optimized sample center.*

Variable	Description	Value	Unity
m_h	Model uncertainty of water level, in fact the uncertainty in equations (A.4) and (A.5) and the linear interpolation in equation (A.6) together	0.075	–
m_Q	Model factor representing statistical uncertainty of maximum discharge	0.5	–
$\hat{Q}_u$	Event maximum river discharge, maximized by $\hat{Q}_{u,max}$	18000	m^3/s
T_{sts}	Start of storm event with respect to start time river flood event	200	*hour*
$N_{realizations}$	Number of realizations	10000	–

Furthermore, the tool requires a certain number of samples. To derive a sound number of samples for one set of dike dimensions 10 random sample series has been drawn. The results are shown in Figure A.14.

In Figure A.14a the development of the reliability index as a function of the number of samples is shown for the sample series. In Figure A.14b the development of the mean and standard deviation for the sample series is shown as a function of the number of samples. The mean is stable at 10000 samples, the standard deviation at 30000 samples. In this thesis 10000 samples is chosen. Note, due to the uncertain location of the reliability function in the multidimensional space of stochastic variables, the value representing the relative spread in samples with respect to the sample centre, is chosen rather high at 1.5 (default 1), which requires an increased number of samples to reach the same accuracy.

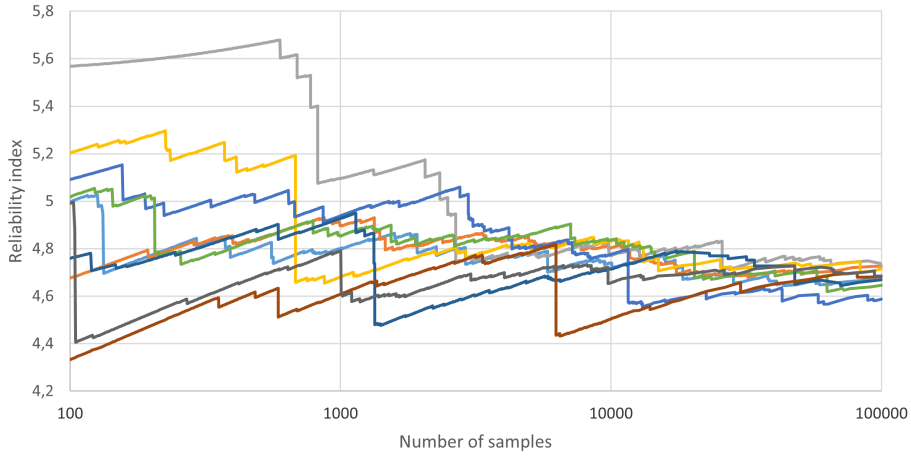

(a) *Overview of development of reliability index for 10 different random sample series*

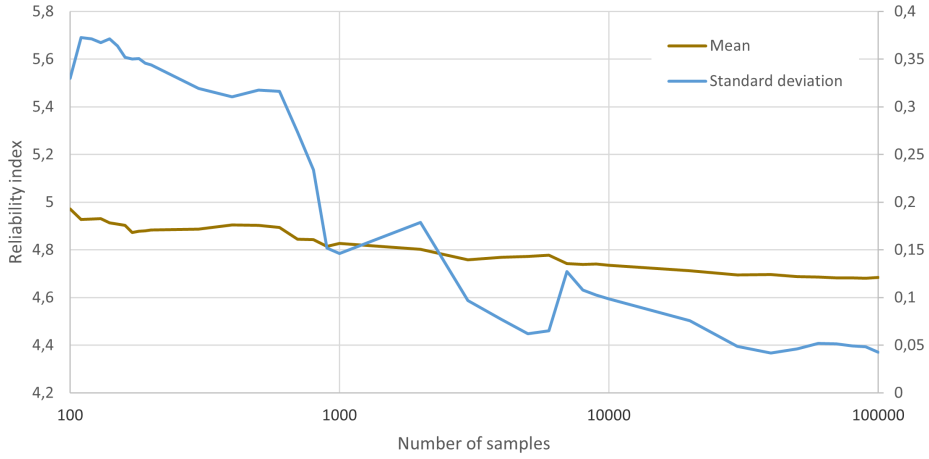

(b) *Development of mean and standard deviation of reliability index for 10 different random sample series*

Figure A.14.: *Derivation of required number of samples based on development of reliability index for 10 different random sample series.*

A.9. CASE STUDY GREBBE

This paragraph provides the values of the parameters used in the calculations for the case on location along the 'Grebbedijk'. In Figure A.15 a

cross section of the case location has been given. The calculations have been made for six construction types:

- Sand dike, a dike with a sand core
- Clay dike, a dike with a clay core
- Sand dike with sheetpile, a dike with a sand core and a flood resistant sheetpile
- Clay dike with sheetpile, a dike with a clay core and a flood resistant sheetpile
- Sand dike with extra width, a wide dike with a sand core
- Clay dike with extra width, a wide dike with a clay core

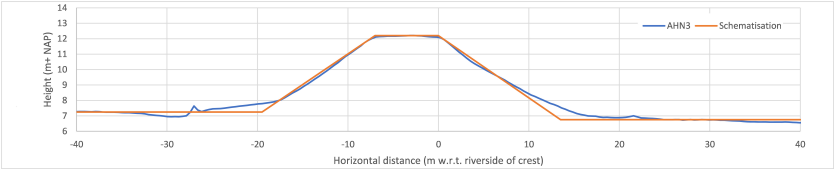

Figure A.15.: *Cross section of dike at case location, measured (AHN3, a digital terrain model, blue line) and schematized for this study (orange line).*

Tables A.3 and A.4 provide an overview of the characteristics of the stochastic variables.

Tables A.5, A.6, A.7, A.8 and A.9 provide an overview of the values of the deterministic variables. In these tables some parameters have the value 'variable'. These parameters provide the dike dimensions which are varied to heuristically optimize the reinforcement (see the calculation scheme in Figure A.10 in section A.7 'Run through J dike dimensions for dike construction $k \in K$').

Tables A.10, A.11, A.12, A.13, A.14 and A.15 provide the values of the geometric parameters, as input for the optimization of the six construction types.

The optimization approach is rather straight forward. Since optimization is not the core of this thesis, the optimization is heuristic: define the lowest values of the geometric parameters equal to the existing situation and increase them stepwise. When the existing situation is obviously far from the optimum, the lowest value is chosen larger than the existing situation. This is the case for berm width because piping occurs in the existing situation relative frequently. The highest value in the matrix is chosen high enough to ensure the optimum is included in the matrix. For the meaning of the variables, see Figure A.4. The results in Chapter 3 prove the optimum has been found.

Table A.3.: *Stochastic variables representing loads and strength of dike.*

Variable	Description	Type	μ	σ	Unity	Remark
D_{cl}	Thickness of cover layer at the land side of the dike	Normal	1.5	0.1	m	
h_{crest}	Dike crest height	Normal	variable	0.04	m	
m_{d70}	Uncertainty of 70-percentile of particle size	Normal	1	0.15	–	
$m_{init.dam.}$	Model uncertainty for location of initial damage	uniform	0.33	0.19	–	> 0 ; $< 2/3$
m_h	Model uncertainty of water level in equations (A.4), (A.5) and (A.6) together	Normal	0	0.15	m	
m_{pip}	Model uncertainty on pipe length when critical head is exceeded	normal	1	0.1	–	
m_Q	Model factor representing statistical uncertainty of maximum discharge	normal	0	1	–	
m_{H_s}	Model uncertainty on significant wave height	Lognormal	0.96	0.27	–	
m_{T_s}	Model uncertainty on significant wave period	Lognormal	1.03	0.13	–	
m_b	Model uncertainty of breach width	truncated normal	1	0.2	–	domain [0.4;100]
m_{qvdM1}	Model uncertainty of parameter in equation (A.17) representing overtopping discharge for breaking waves	truncated normal	-4.75	0.5	–	domain [-5.75;-3.75]
m_{qvdM2}	Model uncertainty of parameter in equation (A.18) representing overtopping discharge for non-breaking waves	truncated normal	-2.6	0.35	–	domain [-3.3;-1.9]
$\hat{Q}_u$	Event maximum river discharge	Gumbel	9778	799	m^3/s	per month $\leq \hat{Q}_{u,max}$
T_{dec}	Duration of discharge decrease	Normal	450	112.5	hour	
T_{storm}	Duration of storm event	Normal	50	10	hour	
T_{sts}	Start of storm event with respect to start time river flood event	Uniform	337.5		*hour*	min.: 0 max.: 675
$\hat{U}_{w,R}$	$> 345°; < 15°$ $> 15°; < 45°$ $> 45°; < 75°$ $> 75°; < 105°$ $> 105°; < 135°$ $> 135°; < 165°$ $> 165°; < 195°$ $> 195°; < 225°$ $> 225°; < 255°$ $> 255°; < 285°$ $> 285°; < 315°$ $> 315°; < 345°$	Gumbel	11.98 12.00 12.56 11.81 11.00 10.74 13.57 15.80 18.73 18.38 17.08 14.47	1.61 1.67 1.53 1.67 1.53 1.53 1.81 1.72 2.50 2.78 2.78 2.08	*m/s*	Wind speed maximum per month

Table A.4.: *Table for stochastic variable R_{wind} providing the fraction of storms from each wind direction.*

Variable	**Description**	**Type**	**Fraction of storms** %	**Unity**	**Remark**
R_{wind}	Probability distribution over wind directions: $> 0°; < 15°$ $> 15°; < 45°$ $> 45°; < 75°$ $> 75°; < 105°$ $> 105°; < 135°$ $> 135°; < 165°$ $> 165°; < 195°$ $> 195°; < 225°$ $> 225°; < 255°$ $> 255°; < 285°$ $> 285°; < 315°$ $> 315°; < 345°$ $> 345°; < 360°$	Table	 0.03111 0.065565 0.081544 0.075169 0.056759 0.070741 0.099321 0.12356 0.12372 0.10064 0.073355 0.066697 0.031826	/sector	

Table A.5.: *Deterministic variables characters A-C.*

Variable	Description	μ	Unity	Remark
A_b	Surface of area protected by a dike, with bathymetry b	$351 \cdot 10^6$	m^2	
b	Climate coefficient G+ climate coefficient W+	0.1 0.25	-	[103]
b_Q	Fraction of discharge Q_u flowing into branche b	0.21	-	
c	Proportionality constant pipe growth	1.6	-	[182]
c_{cl}	Coefficient climate change effect on discharge	0.00168	-	
c_d	Coefficient for marginal consequences, dependent on type	18.6 $1.2 \cdot 10^{-6}$	€/m^3 victims/m^3	
$C_{add-room}$	Marginal costs to acquire room	40	€/m^2/m	
C_f	Fatigue rupture strength of clay, $0.035 \cdot C_0$, with C_0 the cohesion	sand: 0 clay: 1225	m/s	[185]
C_{ftm}	Conversion factor of ft to m	0.3048	m/ft	
$C_{pavement}$	Marginal costs to remove and renew the pavement	600	€/m	
$C_{replace}$	Marginal costs to replace sand or clay locally	10	€/m^3	
C_{remove}	Marginal costs to remove sand or clay	15	€/m^3	
C_{sp}	Marginal costs to put in place a sheetpile	350	€/m^2/m	
C_{V-clay}	Marginal costs to acquire sand and put in place	47	€/m^3	
C_{V-sand}	Marginal costs to acquire sand and put in place	40	€/m^3	
C_w	Creep factor, characterizing the material in the aquifer	6	m	
$c_{\%}$	Fraction of clay	sandcore: 0 claycore: 1	-	
$c_0..c_6$	Coefficients determining the relation between local and upstream water level, based on calculations with a numerical hydraulic model		-	[72]

Table A.6.: *Deterministic variables characters D-F.*

Variable	Description	μ	Unity	Remark
d_α	Size of detaching aggregates	sand: 0.001 clay: 0.004	m	
d_{70_m}	Mean d_{70} in scale model tests	$2.08 \cdot 10^{-4}$	m	
d_{70}	70-percentile of particle size	$3.07 \cdot 10^{-4}$	m	
d_{bres}	Minimum threshold level in breach	variable	m+NAP	
D	Thickness of sand layer	50	m	
f_g	Factor for grass quality	bad: 0.7 medium:1.0 good: 1.4	-	[16]
f_1	Coefficient breach growth	sand: 1.2 clay: 1.4	m	
f_2	Coefficient breach growth	0.04	m	
f_{spl}	Factor reflecting the depth of the toe of sheetpile below ground level with respect to the part exceeding ground level	5	-	
F_{su}	Fetch for set-up in wind direction		m	
F	Representative fetch for wave growth	150 ° :1500 180 °: 1250 210 °: 1200 240 °: 1450 270 °: 1300 300 °: 500	m	

Table A.7.: *Deterministic variables characters G-L.*

Variable	Description	μ	Unity	Remark
g	Gravitational acceleration	9.81	m/s^2	
$h_{landside}$	Ground level at landside of the dike	7.25	m+NAP	
h_{sp}	Height of sheetpile with respect to reference level	variable	m+NAP	
$H_{clif,\,intitial}$	Height of initial damage	0.15	m	
i_{crit}	Critical head w.r.t. heave	0.3	-	
i_b	Slope of inner (landward) side of dike	variable	-	
I_p	Indicator for renewal of the pavement on the dike, respectively for no dike heightening and dike heightening	0 ; 1	-	
I_0	Marginal initial costs for dike reinforcement	200	$€/m$	
k	Permeability	$5.4 \cdot 10^{-4}$	m/s	[102]: 47m/day
L_{dijk}	Length of dike stretch to be reinforced	5500	m	

Table A.8.: *Deterministic variables characters M-Z.*

Variable	Description	μ	Unity	Remark
$m_{Q_{breach}}$	Model uncertainty on breach width $B(t)$	1	-	
n_{pp}	Number of considered piping paths j	2	-	
$\bar{Q}_u$	Mean upstream river discharge	2000	m^3/s	
$\hat{Q}_{u,max}$	Limit on event maximum river discharge entering the upstream system border	18000	m^3/s	
r	Interest rate	0.03	$per\,year$	
$r_{head\,drop}$	Response factor for head. Decreases from riverside to landside. Here referring to the head at landward pipe exit point	0,81	-	based on head drop data in [102]
r_{exit}	Factor to schematize resistance at pipe exit point	0.3	-	[150]
RD/RDm	Relative density of sand below dike with respect to model	1	-	
Δt	Timestep	3600	s	
$\tan\alpha$	Slope of river side of dike	1:2.5	-	
T_{inc}	Duration of discharge increase	225	hour	
T_{std}	Start of river discharge event with respect to start	0	hour	
u_c	Critical flow velocity depending on the material	sand:0.2 clay: 0.5	m/s	
$u_{c,min}$	Minimal critical flow velocity at cliff bottom, depending on material	sand:0.2 clay: 0.5	m/s	

Table A.9.: *Deterministic variables Greek characters.*

Variable	Description	μ	Unity	Remark
γ_b	Reduction factor for the effect of berm on overtopping	1	-	
γ_f	Reduction factor for the effect of roughness on overtopping	1	-	
γ_p	Submerged weight of sand	16.9	kN/m^3	
γ_s	Specific weight of soil, a mix of sand and clay	16.9	kN/m^3	
$\gamma_{s,burst}$	Factor to schematize the uncertainty of the subsurface with respect to burst	1.25	-	
$\gamma_{s,heave}$	Factor to schematize the uncertainty of the subsurface with respect to heave	1.05	-	
$\gamma_{s,pip}$	Factor to schematize the uncertainty of critical head for unlimited pipe growth	1.05	-	
γ_v	Reduction factor for the effect of shallow foreshore on overtopping	1	-	
γ_w	Specific weight of water	10	kN/m^3	
η	Coefficient of White	0.25	kN/m^3	
θ	Roll resistance of sand particles	37	°	
ρ	Mass density of water	1000	kg/m^3	
ρ_s	Mass density of soil at cliff bottom	1690	kg/m^3	

Table A.10.: *Dimension - variations for construction type Sand dike.*

Variable	Description	Lowest value	Highest value	Step size	Unity
h_{crest}	Dike crest height w.r.t. reference level	12.2	12.8	0.1	m+NAP
b_{berm}	Berm width	9	21	3	m
h_{berm}	Berm height w.r.t. reference level	7.5	8.25	0.25	m+NAP
i_b	Cotangent of inner slope	2.5	3.0	0.25	-
b_{crest}	Crest width	7			m
d_{bres}	Minimum threshold level in breach	7.25			m+NAP

Table A.11.: *Dimension - variations for construction type Sand dike with extra width.*

Variable	Description	Lowest value	Highest value	Step size	Unity
h_{crest}	Dike crest height w.r.t. reference level	12.2	12.5	0.1	m+NAP
b_{berm}	Berm width	0	18	3	m
h_{berm}	Berm height w.r.t. reference level	7.5	8.0	0.25	m+NAP
i_b	Cotangent of inner slope	2.5	3.5	0.25	-
b_{crest}	Crest width	17			m
d_{bres}	Minimum threshold level in breach	7.25			m+NAP

Table A.12.: *Dimension - variations for construction type Sand dike with sheetpile.*

Variable	Description	Lowest value	Highest value	Step size	Unity
h_{crest}	Dike crest height w.r.t. reference level	12.2	12.5	0.1	m+NAP
b_{berm}	Berm width	0	6	3	m
h_{berm}	Berm height w.r.t. reference level	7.25	8.00	0.25	m+NAP
i_b	Cotangent of inner slope	2.5	3.0	0.25	-
b_{crest}	Crest width	7			m
d_{bres}	Minimum threshold level in breach	8.75			m+NAP

Table A.13.: *Dimension - variations for construction type Clay dike.*

Variable	Description	Lowest value	Highest value	Step size	Unity
h_{crest}	Dike crest height w.r.t. reference level	12.2	12.6	0.1	m+NAP
b_{berm}	Berm width	9	21	3	m
h_{berm}	Berm height w.r.t. reference level	7.5	8.25	0.25	m+NAP
i_b	Cotangent of inner slope	2.5	3.0	0.25	-
b_{crest}	Crest width	7			m
d_{bres}	Minimum threshold level in breach	7.25			m+NAP

Table A.14.: *Dimension - variations for construction type Clay dike with extra width.*

Variable	Description	Lowest value	Highest value	Step size	Unity
h_{crest}	Dike crest height w.r.t. reference level	12.2	12.3	0.1	m+NAP
b_{berm}	Berm width	0	18	3	m
h_{berm}	Berm height w.r.t. reference level	7.5	8.0	0.25	m+NAP
i_b	Cotangent of inner slope	2.5	3.25	0.25	-
b_{crest}	Crest width	17			m
d_{bres}	Minimum threshold level in breach	7.25			m+NAP

Table A.15.: *Dimension - variations for construction type Clay dike with sheetpile.*

Variable	Description	Lowest value	Highest value	Step size	Unity
h_{crest}	Dike crest height w.r.t. reference level	12.2	12.4	0.1	m+NAP
b_{berm}	Berm width	0	6	3	m
h_{berm}	Berm height w.r.t. reference level	7.25	7.75	0.25	m+NAP
i_b	Cotangent of inner slope	2.5	3.0	0.25	-
b_{crest}	Crest width	7			m
d_{bres}	Minimum threshold level in breach	8.75			m+NAP

A.10. PARAMETERS

In section A.9 the stochastic and independent deterministic variables are defined. In this paragraph all other (dependent) parameters used in the equations in this appendix are given in alphabetical order in Tables A.16, A.17, A.18, A.19 and A.20.

Table A.16.: *Parameters characters A-F.*

Variable	Description	Unity
A	Cliff load parameter	$m/s^{1/3}$
$A_{add-room}$	Marginal room to be acquired for dike reinforcement	m^2/m
A_0	Load threshold for cliff growth	$m/s^{1/3}$
b_d	Exponent for consequences	-
B_{clif}	Width of cliff in dike cross section	m
$B_{clif,max}$	Maximum width of cliff in dike cross section, defined as the horizontal distance between the river side of crest and inner toe (or in case of a berm the point where inner slope connects with berm)	m
$B(t)$	Breach width in time	m
$\frac{dB(t)}{dt}$	Growth velocity of breach width	m
$B_0(t)$	Breach width in time, for time-independent head	m
$C_{clif}(t)$	Coefficient of Chezy, $\frac{h_{clif}(t)^{1/6}}{n}$, dependent of time because of time dependency of water level h_{clif}	$m^{1/2}/s$
C_x	Horizontal growth rate coefficient, translates unity s in A and A_0 to hours as well	$s^{2/3}/hour$
d	Consequences, e.g. €or victims due to a flooding	€, victims
$depth_{su}$	Mean water depth for wind set-up, assessed by the difference between dike height and river side dike toe	m
d_{wg}	Representative water depth for wave growth, here approximated by the difference between water level and dike toe level	m
$\tilde{d}$	Dimensionless water depth in time, $\frac{d \cdot g}{U_w^2(t)}$	-
$fr_{clif}(t)$	Eroded fraction of dike width at time t	-
fr_g	Eroded fraction of grass cover	m/s
fr_{piping}	Eroded fraction of maximal pipe length	-
$\tilde{F}$	Dimensionless fetch in time, $\frac{F \cdot g}{U_w^2(t)}$	-
$F_{geometry}$	Factor representing effect of geometry	-
$F_{resistance}$	Factor representing resistance	-
F_{scale}	Factor representing effect of scale	-

A

Table A.17.: *Parameters characters H-J.*

Variable	Description	Unity
h_b	Water depth on inner slope	-
$h_{clif}(t)$	Water depth at cliff bottom in time, based on the overtopping discharge and assumed critical flow at inner slope below the cliff: $\left(\frac{q(t)}{2/3 \cdot \sqrt{2/3 \cdot g}}\right)^{2/3}$	m/s
$h_{d,\,initial}$	Height where initial damage occurs, and where vertical cliff growth starts	m+NAP
h_{ecg}	Vertical position where vertical cliff growth ends, assumed at inner slope toe (at the maximum of berm level and ground level)	m+NAP
$h_{ele}(t)$	Local water level in time excluding local effects such as a breach	m+NAP
$h(t)$	Local water level in time	m+NAP
$h_{Lx}(t)$	Local water level at location L_x in time	m+NAP
$h_{L1}(t)$,$h_{L2}(t)$	Local water level at L1 resp. L2 in time	m+NAP
$horizon$	Year of interest	year
h_{polder}	Water level in de polder	m+NAP
$h(t_{breach})$	Water level in the river at start of breach growth	m+NAP
$h_{threshold}$	Reference height, chosen as height of threshold in breach	m+NAP
$h_u(t)$	Upstream water level in time	m+NAP
$h_{u,8e3}$, $h_{u,10e3}$, $h_{u,16e3}$	Upstream water level for discharges 8000, 10000, 16000 respectively	m+NAP
$h'_{u,16e3}$	Derivative of water level for a discharge of 16000 or more: $0.5 \cdot 0.0298 \cdot \sqrt{6.11} \cdot Q_{u,16000}^{-0.5}$	m/m^3
h_x	Height for location x in dike cross section	m+NAP
$h_{x,2015}$	Height in 2015 for location x in dike cross section	m+NAP
$h_{\vec{x},a}(t)$	Water level at time t on a certain location a in a flood prone area	m+NAP
$\frac{dh_x}{dt}$	Velocity of subsidence	m/year
$\Delta h_{setup}(t)$	Local water level difference over the river in wind direction in time	m
$\tilde{H}$	Dimensionless wave height in time, $\frac{H_{1/3} \cdot g}{U_w^2(t)}$	-
$H_{clif}(t)$	Height of cliff in time	m
ΔH	Head over the breach	m
ΔH_{crit}	Critical relative head in formula of Sellmeier [150]	m
$\Delta H_{crit\,sp}$	Critical head in case of presence of a sheetpile	m
ΔH_{Bligh}	Critical head, in formula of Bligh [150]	m
ΔH_{Lane}	Critical head in case of presence of a sheetpile, formula of Lane [150]	m
H_{m0}	Significant wave height	m
$H_{1/3}$	Significant wave height, assumed to be equal to H_s or H_{m0}	m
I	Investments for total reinforcement	€
j	Index for leakage paths j	-
J_s	Relative ground structure number	-

Table A.18.: *Parameters characters K-S.*

Variable	Description	Unity
k_d	Vertical growth rate coefficient	$m/hour/Pa$
K_b	Particle size number	-
K_d	Interparticle bond shear stress, $\tan\phi_r'$, with ϕ_r' the residual friction angle	-
K_h	Erodibility index, in [178] given as $M_s \cdot K_b \cdot K_d \cdot J_s$. With a residual friction angle for sand of 33.7° results $K_h = 0.01$ based on $(M_s;K_b;K_d;J_s) = (0.015;1;0.65;1)$. With a residual friction angle for clay of 22° results $K_h = 0.03$ based on $(M_s;K_b;K_d;J_s) = (0.075;1;0.4;1)$. This order of magnitude has been found also in [91].	-
$l(t)$	Length of pipe at time t	m
L	Horizontal distance of leakage path	m
L_h	Horizontal leakage path	m
L_j	Horizontal distance of leakage path j	m
L_{sh}	Length of sheetpile	
L_v	Vertical leakage path	m
M_s	Material Strength number	-
n	Manning roughness coefficient	-
q	Overtopping discharge	$m^3/s/m$
q_o	Overtopping discharge for overflow	$m^3/s/m$
q_{vdM1}	Overtopping discharge for breaking waves	$m^3/s/m$
q_{vdM2}	Overtopping discharge for non-breaking waves	$m^3/s/m$
q_w	Overtopping discharge for waves	$m^3/s/m$
q_{wo}	Overtopping discharge for waves and overflow	$m^3/s/m$
$Q_{b,downs}(t)$	Discharge downstream of breach in branch b in time. Note, in case of a breach this discharge is dependent on the local water level, to be iteratively determined together with equation (A.9), see section A.7	m^3/s
$Q_{breach}(t)$	Discharge through dike breach into the polder	m^3/s
$Q_{downs}(t)$	Discharge downstream of breach in the river. Note, in case of a breach this discharge is dependent on the local water level, to be iteratively determined together with equation (A.9), see section A.7	m^3/s
$Q_u(t)$	Upstream river discharge in time	m^3/s
$Q_{u,2015}$	Upstream discharge base value in 2015	m^3/s
rkm_L, rkm_{L1}, rkm_{L2}	River kilometrage at locations L, L1 and L2 respectively, where L1 is upstream and L2 downstream from L	km
R	Economic risk per year	$€ per year$
$R(t)$	Strength in time	
R_c	Negative relative crest height, $h - h_{crest}$	m
s_0	Wave steepness, $\frac{2\pi \cdot H_{m_0}}{g \cdot T^2_{m-1,0}}$	-
$S(t)$	Loads in time	
SC	Present value of societal costs	€

A

Table A.19.: *Parameters characters T-Z.*

Variable	Description	Unity
t	Time	hour
$t_{breach_{mechanism_i}}$	Moment in time the resistence mechanism i reduced to nihil	s
$t_{breach_{clif}}$	Moment in time the cliff has grown over the total available width	s
$t_{breach_{pip}}$	Moment in time the pipe has grown over the total available leakage length L	s
$t_{breach_{pip_j}}$	Moment in time the pipe has grown over the total available leakage length L for piping path j	s
t_e	Length of time grass cover is resistant to withstand flow velocity u_c	-
$t_e(t)$	Length of time grass cover is resistant to withstand flow velocity u on time t	-
t_{pip}	Time critical head ΔH_{crit} is exceeded	s
t_{sbg}	Time after dike breach from which equation (A.58) is used	s
T	Duration of river discharge event, T_{inc}+T_{dec}	hour
$T_{m_{-1,0}}$	Spectral wave period	s
T_p	Wave peak period	s
T_s	Significant wave period, assumed to be equal to $T_{1/3}$	s
$\tilde{T}$	Dimensionless wave period in time, $\frac{T_{1/3} \cdot g}{U_w(t)}$	-
$T_{1/3}$	Significant wave period, assumed to be equal to T_s	s
u_b	Flow velocity on inner slope	-
$u_{clif}(t)$	Horizontal flow velocity at cliff bottom in time, based on the overtopping discharge, averaged over the wave period: $\frac{q(t)}{h_{clif}(t)}$	m/s
$u_{c,clif}(t)$	Critical flow velocity at cliff bottom in time	m/s
$u_{c,grass}$	Critical flow velocity on grass cover	m/s
$u_i(t)$	Flow velocity on inner slope in time	-
U_w	Wind speed	m/s
$v_{pipe}(t,j)$	Velocity of pipe length increase in time for piping path j	m/s
V	Flood volume	m^3
$V_{add-clay}$	Marginal volume of clay to be added	m^3/m
$V_{add-sand}$	Marginal volume of sand to be added	m^3/m
V_{remove}	Marginal volume of sand or clay to be removed	m^3/m
$V_{replace}$	Marginal volume of sand or clay to be replaced locally	m^3/m
x_{ecg}	Horizontal position where vertical cliff growth ends, assumed at inner slope toe (at the maximum of berm level and ground level)	m
$x_{d,\,initial}$	Location of initial damage on inner slope with respect to x_{crest}, see Figure A.4	m
$\frac{dx}{dt}$	Horizontal cliff growth rate	m/hour
$\vec{X}$	Set of physical and statistical parameters determining loads, strength and breach growth.	

Table A.20.: *Parameters Greek characters.*

Variable	Description	Unity
β	Angle of wave attack between wave propagation direction and dike normal perpendicular	$m^3/s/m$
γ_β	Reduction factor for the effect of angle of wave attack on overtopping	-
$\frac{d\epsilon}{dt}$	Vertical cliff growth rate	m/hour
θ_w	Angle between dike normal and wind direction	°
τ_c	Critical sheer stress	$Pa = kg/ms^2$
τ_e	Actual sheer stress	$Pa = kg/ms^2$
ξ_0	Irribarren parameter, $\frac{\tan\alpha}{\sqrt{s_0}}$	-
$\xi_{m-1,0}$	Irribarren parameter, $\frac{\tan\alpha}{\sqrt{s_0}}$ with s_0 based on $T_{m-1,0}$	-

A.11. ADAPTED PARAMETERS

Some of the parameters and numerical parameters in the MC-IS approach in this thesis in Chapter 3 are chosen slightly different with respect to [187] to get a more stable and smooth result. Additional, the calculations are extended with a few parameters: the breach width and the parameters in the overtopping formula are taken stochastic, and a factor on the fetch length is taken to represent the effective fetch calculation in [104]. The climate parameters are taken representing climate scenario G+ in [103]. All values which deviate form the application in the supplementary material of [187] are presented in Table A.21.

Table A.21.: *Overview of calculation parameters used, adapted with respect to the supplementary material of [187].*

Variable	Description	Value	Unity
b	Parameter depending on climate scenario	0.1	–
c_{cl}	Parameter depending on climate scenario	0.00168	–
m_b	Model uncertainty of breach width, distributed as a truncated normal with mean, standard deviation, under bound, upper bound	(1;0.2; 0.4;100)	–
m_{qvdM1}	Model uncertainty of parameter q_{vdM1} representing overtopping discharge for breaking waves,distributed as a truncated normal with mean, standard deviation, under bound, upper bound	(-4.75;0.5; -5.75;-3.75)	–
m_{qvdM2}	Model uncertainty of parameter q_{vdM2} representing overtopping discharge for breaking waves,distributed as a truncated normal with mean, standard deviation, under bound, upper bound	(-2.6;0.35; -3.3;-1.9)	–
F_{eff}	Factor on the measured Fetch lengths to represent effective fetch length according to [104]	0.6	–
m_h	Sample centre for model uncertainty of water level	0.075	–
m_Q	Sample centre for model factor representing statistical uncertainty of maximum discharge	0.5	–
$\hat{Q}_u$	Sample centre for event maximum river discharge, maximized by $\hat{Q}_{u,max}$	18000	m^3/s
T_{sts}	Sample centre for start-time of storm-event (Note, the time of discharge event maximum is 225 hours), and relative standard deviation	200; 0.25 (≈ 50 hour)	*hour*

B

DERIVATIONS IN CHAPTER 5 - FLOOD RISK-BASED UPDATING OF STANDARDS

B.1. DERIVATION OF LOWER LIMIT

With the assumptions and starting points in the main text in Section 5.2.2 the intervention timing representing the dynamic effect in equation (5.3) can be included in the approach of the first Dutch Delta Committee. The expected value of economic risk $E(D) = P_f(h_d(t)) \cdot D$, in which the economic damage D at time t=0 is taken independent of water level, corresponding with [51].

The probabilities before the intervention at Δt and after the intervention are respectively:

$$\begin{aligned} P_f(h_d(t)) &= exp\left(-\frac{h_d(0)-(A+\eta\cdot t)}{f_{ovx}\cdot B}\right) \quad t<\Delta t \\ P_f(h_d(t)) &= exp\left(-\frac{h_d(\Delta t)-(A+\eta\cdot t)}{f_{ovx}\cdot B}\right) \quad t\geqslant\Delta t \end{aligned} \tag{B.1}$$

In which:

$P_f(h_d(t))$	Probability of failure due to overtopping at time t	$per year$
$h_d(0)$	Dike heigth at $t=0$	$m+SWL$
η	Relative deterioration representing subsidence and climate change effect	$m/year$
t	Time indicator: time with respect to the start of the analysis	$year$

Δt	Reinforcement time	*year*
$h_d(\Delta t)$	Reinforced dike height at $t = \Delta t$ relative to water level and subsidence at $t = 0$	$m+SWL$
A	Location parameter of the exponential water level distribution	$m+SWL$
B	Scale parameter of the exponential water level distribution	m
f_{ovx}	Factor to convert the water level scale parameter B into the dike height scale parameter taking wave overtopping into account, which is the ratio between dike heigth increase and water level increase for equal frequency decrease for both	$-$

The sum of risks and investments is minimized. The timing of the investment I is not necessarily at t=0, thus these cost has to be included as a present value:

$$C_{tot}^{PV} = I^{PV} + R^{PV} \tag{B.2}$$

In which:

C_{tot}^{PV}	Present value of total cost of investments and risks	€
I^{PV}	Present value of investments	€
R^{PV}	Present value of risks, in which $R = P_f(h_d(t)) \cdot D_\delta(t)$	€
$D_\delta(t)$	Economic damage caused by flooding anywhere along the dike segment, at time t, subject to economic growth δ	€
δ	economic growth rate	$-$

The dike reinforcement height is assessed by:

$$\Delta h_d = (h_d(\Delta t) - (h_d(0) - \eta \cdot \Delta t)) \tag{B.3}$$

In which:

Δh_d	Dike reinforcement height	m

In [51] the i^{th} investment costs to reinforce a dike segment with a height Δh_{d_i} is assessed by:

$$I_i = (I_0 + \Delta h_{d_i} \cdot I') \cdot f_{I_i} \tag{B.4}$$

In which:

I_0	Initial costs of an reinforcement, independent from the magnitude of the reinforcement	€
Δh_{d_i}	Dike height increase of the i^{th} successive dike height increase.	–
f_{I_i}	Parameter indicating the cost of the next dike reinforcements is higher than the earlier ones due to increased dimensions, in [51] taken as $exp\left(\lambda \cdot \sum_i \Delta h_{d_i}\right)$	-
λ	Parameter indicating the cost of the next dike increases is higher than the earlier ones	*perm*

In the following the subscript i is omitted because in the analysis only the first reinforcement is subjected. Using equations (B.1) and (B.3), the total costs in equation (B.2) are:

$$\begin{aligned} C_{tot}^{PV} = & \frac{1}{(1+r)^{\Delta t}} \cdot f_I \cdot (I_0 + (h_d(\Delta t) - (h_d(0) - f_{ovx} \cdot \eta \cdot \Delta t)) \cdot I') \quad + \\ & \sum_{t=0}^{t=\Delta t} \frac{D_\delta(t)}{(1+r)^t} \cdot exp\left(-\frac{h_d(0) - (A + \eta \cdot t)}{f_{ovx} \cdot B}\right) \quad + \\ & \sum_{t=\Delta t}^{t=\infty} \frac{D_\delta(t)}{(1+r)^t} \cdot exp\left(-\frac{h_d(\Delta t) - (A + \eta \cdot t)}{f_{ovx} \cdot B}\right) \end{aligned} \tag{B.5}$$

The optimal design dike height is found minimizing the cost, with the intervention timing as a degree of freedom:

$$\frac{dC_{tot}^{PV}}{dh_d(\Delta t)} = 0 \tag{B.6}$$

Since the second term in equation (B.5) is not dependent on dike height $h_d(\Delta t)$ it disappears in the derivative. Referring to Figure 5.4 the schematisation in time distinguish the situation before the intervention and after. Therefore, because of the starting point that the dynamic effects due to subsidence and climate change are neglected after the first reinforcement, the third term in equation (B.5) can be simplified. With $\frac{1}{ln(1+r)} = \frac{1}{r}$ (valid for small r), the sum of expected risks after $t = \Delta t$ is estimated by :

$$\sum_{t=\Delta t}^{t=\infty} \frac{D_\delta(t) \cdot P_f(h_d(t))}{(1+r)^t} = \frac{D_\delta(\Delta t) \cdot P_f(h_d(\Delta t))}{(1+r)^{\Delta t}} \cdot \frac{1}{r} \tag{B.7}$$

In which:

$D_\delta(\Delta t)$	Economic damage at reinforcement time Δt	€

In equation (5.3) the risks for time $t > z$ are approximated in the same way, with z=300 year [51]. In fact, for Δt is z in equation (5.3) the here presented adapted approach of the first Delta Committee is comparable with [51]. With $P_f(\Delta t)$ written for $P_f(h_d(\Delta t))$ in equation (B.1), the derivative of $P_f(\Delta t)$ with respect to $h_d(\Delta t)$ is $\frac{-1}{f_{ovx} \cdot B} \cdot P_f(\Delta t)$. Substituting equation (B.5) in equation (B.6), with equation (B.7) as the third term in equation (B.5), and with $P_{f_{opt}}(\Delta t)$ is $P_f(\Delta t)$ for the case equation (B.6) is met, leads to:

$$\frac{\mathrm{d}C_{tot}^{PV}}{\mathrm{d}h_d(\Delta t)} = \frac{f_I \cdot I'}{(1+r)^{\Delta t}} - \frac{D_\delta(\Delta t)}{(1+r)^{\Delta t}} \cdot \frac{1}{f_{ovx} \cdot B \cdot r} \cdot P_{f_{opt}}(\Delta t) = 0 \tag{B.8}$$

This leads to:

$$P_{f_{opt}}(\Delta t) = \frac{f_I \cdot I' \cdot f_{ovx} \cdot B \cdot r}{D_\delta(\Delta t)} = \frac{I' \cdot B \cdot r}{D(0)} \cdot \frac{f_I \cdot f_{ovx}}{(1+\delta)^{\Delta t}} \tag{B.9}$$

In which:

$P_{f_{opt}}(\Delta t)$	Economic optimal design probability of flooding for a reinforcement at time (Δt)	*peryear*

B.2. DERIVATION OF UPPER LIMIT

The utility criterion to determine the time Δt of an economic beneficial intervention is the time at which the economic risk reduction transcends the investments [32, 50]:

$$\Delta R^{PV}(\Delta t) - I^{PV}(\Delta t) > 0 \tag{B.10}$$

In which:

$\Delta R^{PV}(\Delta t)$	Present value of risk difference in case of intervention at time Δt	€
$I^{PV}(\Delta t)$	Present value of investment at time Δt	€

The present value of the risk difference due to an intervention at Δt, assessed with equation (B.7) before and after reinforcement, is:

$$\Delta R^{PV}(\Delta t) = \frac{1}{(1+r)^{\Delta t}} \cdot \frac{D_\delta(\Delta t)}{r} \cdot \left(\frac{P_f(\Delta t^-)}{f_{\Delta h_d}} - P_{standard} \right) \tag{B.11}$$

In which:

$P_{standard}$	Targeted design probability of flooding at Δt.	*peryear*
$P_f(\Delta t^-)$	probability of flooding just before intervention, see equation (B.1).	*peryear*
$f_{\Delta h_d}$	Factor indicating the flood event damage increase due to effect of dike height increases at Δt.	–

Note, the potential damage at $t = \Delta t^-$ is a factor $f_{\Delta h_d}$ smaller than the damage at $t = \Delta t$, see equation (5.8). Therefore, the risk at $t = \Delta t^-$ is divided by $f_{\Delta h_d}$. Substituting equation (5.15) and the present value of an investment I at Δt from equation (B.4), the utility criterion in equation (B.10) shows as:

$$\begin{aligned} &\frac{1}{(1+r)^{\Delta t}} \cdot \frac{D_\delta(\Delta t)}{r} \cdot \left(\frac{P_f(\Delta t^-)}{f_{\Delta h_d}} - P_{standard} \right) - \\ &\frac{1}{(1+r)^{\Delta t}} \cdot f_I \cdot \left(I_0 + \left(\eta \cdot \Delta t + f_{ovx} \cdot B \cdot ln\left(\frac{P_f(0)}{P_{standard}} \right) \right) \cdot I' \right) > 0 \end{aligned} \tag{B.12}$$

Since the probabilities of flooding are continuously increasing in time we can find the first point in time for which it is beneficial to intervene with:

$$\begin{aligned} &\frac{D_\delta(\Delta t)}{r} \cdot \left(\frac{P_f(\Delta t^-)}{f_{\Delta h_d}} - P_{standard} \right) - \\ &f_I \cdot \left(I_0 + \left(\eta \cdot \Delta t + f_{ovx} \cdot B \cdot ln\left(\frac{P_f(0)}{P_{standard}} \right) \right) \cdot I' \right) = 0 \end{aligned} \tag{B.13}$$

Rewriting leads to:

$$\begin{aligned} &P_f(\Delta t^-) = f_{\Delta h_d} \cdot \\ &\left(P_{standard} + \frac{r \cdot f_I}{D_\delta(\Delta t)} \cdot \left(I_0 + \left(\eta \cdot \Delta t + f_{ovx} \cdot B \cdot ln\left(\frac{P_f(0)}{P_{standard}} \right) \right) \cdot I' \right) \right) \end{aligned} \tag{B.14}$$

B.3. DERIVATION OF INTERVENTION TIMING

The upper limit in the sections 5.2.3 and B.2 can be used to derive the first beneficial time to intervene. Switching both sides of equation (B.14), and substituting $P_f(\Delta t^-)$ with (B.1) leads to:

$$f_{\Delta h_d} \cdot \left(\frac{r \cdot f_I}{D_\delta(\Delta t)} \cdot \left(I_0 + \left(\eta \cdot \Delta t + f_{ovx} \cdot B \cdot f_{dp}\right) \cdot I'\right) + P_{standard} \right) = exp\left(- \frac{h_d(0) - (A + \eta \cdot \Delta t)}{f_{ovx} \cdot B} \right) \tag{B.15}$$

In which:

f_{dp}	Factor representing the logarithm of the division between the actual probability and the standard, the probability after reinforcement: $f_{dp} = ln\left(\frac{P_f(0)}{P_{standard}}\right)$.	-
$P_f(0)$	Probability of flooding at $t = 0$.	$peryear$

Processing dike height $h_d(0) = A - f_{ovx} \cdot B \cdot ln\left(P_f(0)\right)$ at t=0 in the term right of the equality sign lead to disappearance of $h_d(0)$, A and the factor f_{ovx}. It follows:

$$ln\left(f_{\Delta h_d} \cdot \left(\frac{r \cdot f_I}{D_\delta(\Delta t)} \cdot \left(I_0 + \left(\eta \cdot \Delta t + f_{ovx} \cdot B \cdot f_{dp}\right) \cdot I'\right) + P_{standard} \right)\right) = \frac{B \cdot ln\left(P_f(0)\right) + \frac{\eta \cdot \Delta t}{f_{ovx}}}{B} \tag{B.16}$$

Rewriting leads to:

$$B \cdot ln\left(\frac{P_f(0)}{f_{\Delta h_d}}\right) + \frac{\eta \cdot \Delta t}{f_{ovx}} = B \cdot ln\left(\frac{r \cdot f_I}{D_\delta(\Delta t)} \cdot \left(I_0 + \left(\eta \cdot \Delta t + f_{ovx} \cdot B \cdot f_{dp}\right) \cdot I'\right) + P_{standard} \right) \tag{B.17}$$

Rewriting leads to:

$$\Delta t = \frac{f_{ovx} \cdot B}{\eta} \cdot \left(ln\left(\frac{r \cdot f_I}{D_\delta(\Delta t)} \cdot \left(I_0 + \left(\eta \cdot \Delta t + f_{ovx} \cdot B \cdot f_{dp}\right) \cdot I'\right) + P_{standard} \right) - ln\left(\frac{P_f(0)}{f_{\Delta h_d}}\right)\right) \tag{B.18}$$

Which is equal to:

$$\Delta t = \frac{f_{ovx} \cdot B}{\eta} \cdot ln \left(\frac{\frac{r \cdot f_I}{D_\delta(\Delta t)} \cdot \left(I_0 + \left(\eta \cdot \Delta t + f_{ovx} \cdot B \cdot f_{dp}\right) \cdot I'\right) + P_{standard}}{\frac{P_f(0)}{f_{\Delta h_d}}} \right) \tag{B.19}$$

Rewriting leads to:

$$\Delta t = \frac{f_{ovx} \cdot B}{\eta} \cdot ln \left(\frac{r \cdot f_I \cdot f_{\Delta h_d}}{D_\delta(\Delta t) \cdot P_f(0)} \cdot \left(I_0 + \left(\eta \cdot \Delta t + f_{ovx} \cdot B \cdot f_{dp}\right) \cdot I'\right) + f_{\Delta h_d} \cdot \frac{P_{standard}}{P_f(0)} \right) \tag{B.20}$$

The equation (B.20) is further simplified multiplying some parts of it by an equivalent counter and denominator:

$$\frac{r}{D_\delta(\Delta t) \cdot P_f(0)} = \frac{r}{D_\delta(\Delta t) \cdot P_{f_{opt}}(0)} \cdot \frac{P_{f_{opt}}(\Delta t) \cdot D_\delta(\Delta t)}{f_I \cdot I' \cdot f_{ovx} \cdot B \cdot r} = \frac{P_{f_{opt}}(\Delta t)}{P_f(0)} \cdot \frac{1}{f_I \cdot I' \cdot B \cdot f_{ovx}}$$
$$\frac{P_{standard}}{P_f(0)} = \frac{P_{f_{opt}}(\Delta t)}{P_f(0)} \cdot \frac{P_{standard}}{P_{f_{opt}}(\Delta t)} \tag{B.21}$$

which transforms equation (B.20) in:

$$\Delta t = \frac{f_{ovx} \cdot B}{\eta} \cdot ln \left(f_{\Delta h_d} \cdot \frac{P_{f_{opt}}(\Delta t)}{P_f(0)} \cdot \left(\frac{I_0 + \left(\eta \cdot \Delta t + f_{ovx} \cdot B \cdot f_{dp}\right) \cdot I'}{I' \cdot B \cdot f_{ovx}} + \frac{P_{standard}}{P_{f_{opt}}(\Delta t)} \right) \right) \tag{B.22}$$

Substituting $f_{dp} = ln\left(\frac{P_f(0)}{P_{standard}}\right)$ and rewriting results in:

$$\Delta t = \frac{f_{ovx} \cdot B}{\eta} \cdot ln \left(f_{\Delta h_d} \cdot \frac{P_{f_{opt}}(\Delta t)}{P_f(0)} \cdot \left(\frac{I_0}{I' \cdot f_{ovx} \cdot B} + \frac{\eta \cdot \Delta t}{f_{ovx} \cdot B} + ln\left(\frac{P_f(0)}{P_{standard}}\right) + \frac{P_{standard}}{P_{f_{opt}}(\Delta t)} \right) \right) \tag{B.23}$$

This is equation (B.23) in the main text. One of the special cases distinguished in the main text, addressed to as the 'third', represents the situation in case the dike is compliant to the economic optimal probability $P_{f_{opt}}(0)$ at $t = 0$, and the design probability $P_{standard}$ at time Δt is defined as the economic optimal probability $P_{f_{opt}}(\Delta t)$. In this case equation (B.23) can be further rewritten with:

- rewriting $\frac{P_{f_{opt}}(\Delta t)}{P_f(0)}$ with equation (5.13) or (B.9) as $1/(1+\delta)^{\Delta t}$ which enables to further simplification of the formula.
- rewrite the term $\frac{P_f(0)}{P_{standard}}$ as $\frac{P_f(0)}{P_{f_{opt}}(\Delta t)}$. With equation (5.13) or (B.9) it becomes $(1+\delta)^{\Delta t}$
- just as in the second special case the last term of equation (B.23) will become equal to 1

This leads to:

$$\Delta t = \frac{f_{ovx} \cdot B}{\eta} \cdot \left(ln\left(f_{\Delta h_d}\right) + ln\left(\frac{1}{(1+\delta)^{\Delta t}}\right) + ln\left(\frac{I_0}{I' \cdot f_{ovx} \cdot B} + \frac{\eta \cdot \Delta t}{f_{ovx} \cdot B} + ln\left((1+\delta)^{\Delta t}\right) + 1\right)\right) \tag{B.24}$$

With $1/(1+\delta)^{\Delta t} \approx exp(-\delta \, \Delta \, t)$ and $(1+\delta)^{\Delta t} \approx exp(\delta \, \Delta \, t)$ follows:

$$\Delta t = \frac{f_{ovx} \cdot B}{\eta} \cdot \left(ln\left(f_{\Delta h_d}\right) - \delta \cdot \Delta t + ln\left(\frac{I_0}{I' \cdot f_{ovx} \cdot B} + \frac{\eta \cdot \Delta t}{f_{ovx} \cdot B} + \delta \cdot \Delta t + 1\right)\right) \tag{B.25}$$

This can be rewritten as follows:

$$\Delta t + \frac{f_{ovx} \cdot B}{\eta} \cdot \delta \Delta t = \frac{f_{ovx} \cdot B}{\eta} \cdot \left(ln\left(f_{\Delta h_d}\right) + ln\left(\frac{I_0}{I' \cdot f_{ovx} \cdot B} + \frac{\eta \cdot \Delta t}{f_{ovx} \cdot B} + \delta \cdot \Delta t + 1\right)\right) \tag{B.26}$$

$$\Delta t = \frac{\frac{f_{ovx} \cdot B}{\eta} \cdot \left(ln\left(f_{\Delta h_d}\right) + ln\left(\frac{I_0}{I' \cdot f_{ovx} \cdot B} + \frac{\eta \cdot \Delta t}{f_{ovx} \cdot B} + \delta \cdot \Delta t + 1\right)\right)}{1 + \frac{\delta \cdot f_{ovx} \cdot B}{\eta}} \tag{B.27}$$

With:

$$\frac{\frac{f_{ovx} \cdot B}{\eta}}{1 + \frac{\delta \cdot f_{ovx} \cdot B}{\eta}} = \frac{f_{ovx} \cdot B}{\eta} \cdot \frac{\eta}{\eta + \delta \cdot f_{ovx} \cdot B} = \frac{f_{ovx} \cdot B}{\eta + \delta \cdot f_{ovx} \cdot B} \tag{B.28}$$

this results in a remarkable handy formula, which could be simply applied to indicate the economically optimal standard and design horizon:

$$\Delta t = \frac{f_{ovx} \cdot B}{\eta + \delta \cdot f_{ovx} \cdot B} \cdot ln\left(f_{\Delta h_d} \cdot \left(\frac{I_0}{I' \cdot f_{ovx} \cdot B} + \frac{\eta \cdot \Delta t}{f_{ovx} \cdot B} + \delta \cdot \Delta t + 1\right)\right) \quad \text{(B.29)}$$

Note, the reinforcement height Δh_d, is needed to calculate factor $f_{\Delta h_d}$ at $t = \Delta t$ with equation (5.8). It can be derived using equation (B.1) which rewritten results in $h_d(t) = A - f_{ovx} \cdot B \cdot ln\left(P_f(t)\right)$:

$$\Delta h_d = h_d(\Delta t) - h_d(0) = f_{ovx} \cdot B \cdot ln\left(\frac{P_f(\Delta t^-)}{P_{f_{opt}}(\Delta t)}\right) \quad \text{(B.30)}$$

This leads to a simple relation:

$$\Delta h_d = f_{ovx} \cdot B \cdot ln\left(\frac{P_f(0) \cdot exp\left(\frac{\eta \cdot \Delta t}{f_{ovx} \cdot B}\right)}{P_{f_{opt}}(0) \cdot exp(-\delta\, \Delta\, t)}\right) = \eta \cdot \Delta t + f_{ovx} \cdot B \cdot \delta \cdot \Delta t \quad \text{(B.31)}$$

B.4. DIKE PARAMETER DERIVATIVES TO DIKES CROSS SECTIONS SURFACE

Referring to the parameter definitions in the main text and in the Figure B.1, dikes cross sections surface is:

$$S_d = \left(Br_d + (cot\alpha_{bu} + cot\alpha_{bi}) \cdot \frac{h_d - h_m}{2}\right) \cdot (h_d - h_m) + L_b \cdot (h_b - h_m) \quad \text{(B.32)}$$

In which:

S_d	Dikes cross sections surface, a volume per meter dike length	m^3/m
Br_d	Dikes crest width	m
$cot\alpha_{bu}$	Cotangent of the outer dike slope	$-$
$cot\alpha_{bi}$	Cotangent of the inner dike slope	$-$
L_b	Length of berm	m
h_b	Height of berm with respect to reference level	$m + NAP$
h_m	Polder water level	$m + NAP$
h	Outside water level	$m + NAP$
h_d	Dike crest heigth level	$m + NAP$

To determine the derivatives for each parameter to S_d this equation is rewritten to obtain each cross section shape parameter as a function of S_d. In Figure B.1 the derivative for dike height is schematically showed as $\Delta h_d / \Delta S_d$ which visually can be interpreted as $1/L_d$. Below, the mathematical derivations are presented for dike height h_d, dike berm length

L_b, dike berm width h_b, dike bodies foot print L_d, and slope of inner talud $cot\alpha_{bi}$ respectively.

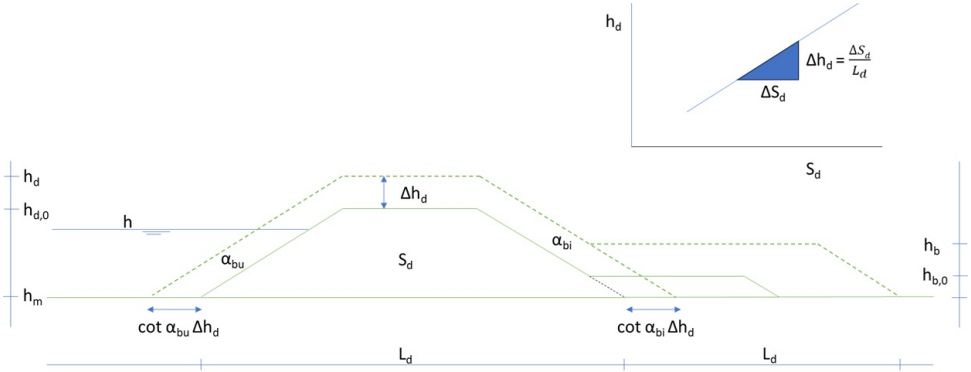

Figure B.1.: *Schematic overview of a dike cross section, and of the derivative for dike height h_d to dike cross sections surface S_d. In dashed the cross section in case of a reinforcement.*

First, the derivative of dike height to S_d. In the derivation the berm can be neglected in equation (B.32) since this will not affect the derivative:

$$S_d = \left(Br_d + (cot\alpha_{bu} + cot\alpha_{bi}) \cdot \frac{h_d - h_m}{2}\right) \cdot (h_d - h_m) \tag{B.33}$$

$$\Rightarrow \frac{(cot\alpha_{bu} + cot\alpha_{bi})}{2} \cdot (h_d - h_m)^2 + Br_d \cdot (h_d - h_m) - S_d = 0 \tag{B.34}$$

$$\Rightarrow h_d - h_m = \frac{-Br_d \pm \sqrt{Br_d^2 - 4 \cdot \frac{(cot\alpha_{bu} + cot\alpha_{bi})}{2} \cdot -S_d}}{(cot\alpha_{bu} + cot\alpha_{bi}} \tag{B.35}$$

Since dike height with respect to ground level is positive, only be positive solution can exist. Taking the derivative of equation (B.35):

$$\frac{\mathrm{d}(h_d - h_m)}{\mathrm{d}S_d} = \frac{1}{(cot\alpha_{bu} + cot\alpha_{bi})} \cdot \frac{2 \cdot (cot\alpha_{bu} + cot\alpha_{bi})}{2 \cdot \sqrt{Br_d^2 + 2 \cdot (cot\alpha_{bu} + cot\alpha_{bi}) \cdot S_d}} \tag{B.36}$$

Substituting equation (B.33) and writing $cot\alpha's$ for $cot\alpha_{bu} + cot\alpha_{bi}$:

$$\frac{\mathrm{d}(h_d - h_m)}{\mathrm{d}S_d} = \frac{1}{\sqrt{Br_d^2 + 2 \cdot cot\alpha's \cdot \left(Br_d \cdot (h_d - h_m) + cot\alpha's \cdot \frac{(h_d - h_m)^2}{2}\right)}}$$

(B.37)

With $cot\alpha$'s replaced with the original denotion $cot\alpha_{bu} + cot\alpha_{bi}$ follows:

$$\frac{\mathrm{d}(h_d - h_m)}{\mathrm{d}S_d} = \frac{\mathrm{d}(h_d)}{\mathrm{d}S_d} = \frac{1}{\sqrt{(Br_d + (cot\alpha_{bu} + cot\alpha_{bi}) \cdot (h_d - h_m))^2}} = \frac{1}{L_d} \tag{B.38}$$

Second, the derivative of dike berm length to S_d. In the derivation the dike body can be neglected in equation (B.32) since this does not affect the derivative:

$$S_d = L_b \cdot (h_b - h_m) \tag{B.39}$$

$$\Rightarrow L_b = \frac{S_d}{(h_b - h_m)} \tag{B.40}$$

Therewith the derivative is:

$$\frac{\mathrm{d}L_b}{\mathrm{d}S_d} = \frac{1}{(h_b - h_m)} \tag{B.41}$$

Third, the derivative of berm height to S_d. In the derivation the dike body can be neglected in equation (B.32) since this does not affect the derivative:

$$S_d = L_b \cdot (h_b - h_m) \tag{B.42}$$

$$\Rightarrow (h_b - h_m) = \frac{S_d}{L_b} \tag{B.43}$$

Therewith the derivative is:

$$\frac{\mathrm{d}(h_b - h_m)}{\mathrm{d}S_d} = \frac{\mathrm{d}(h_b)}{\mathrm{d}S_d} = \frac{1}{L_b} \tag{B.44}$$

Fourth, the derivative of the dikes inner slope to S_d, again starting from equation (B.33) :

$$S_d = Br_d \cdot (h_d - h_m) + \cdot \frac{cot\alpha_{bu} + cot\alpha_{bi}}{2} \cdot (h_d - h_m)^2 \tag{B.45}$$

$$\frac{cot\alpha_{bu} + cot\alpha_{bi}}{2} \cdot (h_d - h_m)^2 = -Br_d \cdot (h_d - h_m) + S_d \tag{B.46}$$

$$cot\alpha_{bi} = 2 \cdot \frac{S_d - Br_d \cdot (h_d - h_m)}{(h_d - h_m)^2} - cot\alpha_{bu} \tag{B.47}$$

Therewith, the derivative is:

$$\frac{\mathrm{d}cot\alpha_{bi}}{\mathrm{d}S_d} = \frac{2}{(h_d - h_m)^2} \tag{B.48}$$

Fifth, the derivative of dike bodies foot print L_d to S_d. In the derivation the berm can be neglected in equation (B.32) since this will not affect the derivative. Therefore, equation (B.33) is used. With $L_d = Br_d + (cot\alpha_{bu} + cot\alpha_{bi}) \cdot (h_d - h_m)$ the dike height is rewritten as follows:

$$(h_d - h_m) = \frac{L_d - Br_d}{(cot\alpha_{bu} + cot\alpha_{bi})} \tag{B.49}$$

Substituting this in equation (B.33) provides:

$$S_d = Br_d \cdot \frac{L_d - Br_d}{(cot\alpha_{bu} + cot\alpha_{bi})} + \frac{(cot\alpha_{bu} + cot\alpha_{bi})}{2} \cdot \left(\frac{L_d - Br_d}{(cot\alpha_{bu} + cot\alpha_{bi})} \right)^2 \tag{B.50}$$

$$\Rightarrow \frac{(cot\alpha_{bu} + cot\alpha_{bi})}{2} (L_d - Br_d)^2 + \frac{Br_d}{(cot\alpha_{bu} + cot\alpha_{bi})} \cdot (L_d - Br_d) - S_d = 0 \tag{B.51}$$

Solutions for this quadratic equation:

$$(L_d - Br_d) = \frac{\frac{-Br_d}{cot\alpha_{bu} + cot\alpha_{bi}} \pm \sqrt{\left(\frac{Br_d}{cot\alpha_{bu} + cot\alpha_{bi}} \right)^2 - \frac{4 \cdot 1 \cdot -S_d}{2 \cdot (cot\alpha_{bu} + cot\alpha_{bi})}}}{\frac{1}{cot\alpha_{bu} + cot\alpha_{bi}}} \tag{B.52}$$

Which can be rewritten as:

$$(L_d - Br_d) = -Br_d \pm (cot\alpha_{bu} + cot\alpha_{bi}) \cdot \sqrt{\frac{Br_d^2 + 2 \cdot (cot\alpha_{bu} + cot\alpha_{bi}) \cdot S_d}{(cot\alpha_{bu} + cot\alpha_{bi})^2}} \tag{B.53}$$

Since L_d is positive, only the positive solution make sense:

$$L_d = \sqrt{Br_d^2 + 2 \cdot (cot\alpha_{bu} + cot\alpha_{bi}) \cdot S_d} \tag{B.54}$$

Therewith, the derivative is:

$$\frac{dL_d}{dS_d} = \frac{1}{2 \cdot \sqrt{Br_d^2 + 2 \cdot (cot\alpha_{bu} + cot\alpha_{bi}) \cdot S_d}} \cdot 2 \cdot (cot\alpha_{bu} + cot\alpha_{bi}) \tag{B.55}$$

Substituting S_d with equation (B.33) and rewriting with $cot\alpha's$ for $cot\alpha_{bu}$+ $cot\alpha_{bi}$:

$$\frac{dL_d}{dS_d} = \frac{cot\alpha's}{\sqrt{Br_d^2 + 2 \cdot cot\alpha's \cdot Br_d \cdot (h_d - h_m) + (cot\alpha's)^2 \cdot (h_d - h_m)^2}} \tag{B.56}$$

This leads to the result, with $cot\alpha's$ replaced with the original denotion $cot\alpha_{bu} + cot\alpha_{bi}$:

$$\frac{dL_d}{dS_d} = \frac{cot\alpha_{bu} + cot\alpha_{bi}}{Br_d + (cot\alpha_{bu} + cot\alpha_{bi}) \cdot (h_d - h_m)} = \frac{cot\alpha_{bu} + cot\alpha_{bi}}{L_d} \tag{B.57}$$

NB. An alternative derivative can be derived with $L_d = Br_d + (cot\alpha_{bu} + cot\alpha_{bi}) \cdot (h_d - h_m)$. Then, the derivative of L_d follows from:

$$\frac{dL_d}{dS_d} = \frac{d\left(Br_d + (cot\alpha_{bu} + cot\alpha_{bi}) \cdot (h_d - h_m)\right)}{dS_d} \tag{B.58}$$

With constants for the outer slope $cot\alpha_{bu}$ and the dike crest width Br_d, and the derivatives for $cot\alpha_{bi}$ (from equation (B.48) and h_d (from equation (B.38) follows:

$$\frac{dL_d}{dS_d} = \frac{d\left(cot\alpha_{bi} \cdot (h_d - h_m)\right)}{dS_d} = \frac{2}{(h_d - h_m)^2} \cdot (h_d - h_m) + \frac{cot\alpha_{bi}}{L_d} \tag{B.59}$$

$$\frac{dL_d}{dS_d} = \frac{2 \cdot L_d + cot\alpha_{bi} \cdot (h_d - h_m)}{h_d \cdot L_d} \tag{B.60}$$

Therewith, the derivatives of all dike parameters to dike cross sections surface are available, which are relevant for this study:

$$\begin{aligned}
\frac{dh_d}{dS_d} &= \frac{1}{L_d} \\
\frac{dh_b}{dS_d} &= \frac{1}{L_b} \\
\frac{dL_b}{dS_d} &= \frac{1}{h_b - h_m} \\
\frac{dcot\alpha_{bi}}{dS_d} &= \frac{2}{(h_d - h_m)^2} \\
\frac{dL_d}{dS_d} &= \frac{cot\alpha_{bi} + cot\alpha_{bu}}{L_d}
\end{aligned} \tag{B.61}$$

B.5. DERIVATION OF LOWER LIMIT FOR TWO FAILURE MECHANISMS

B.5.1. WITH BERM

With the water level distribution $F(h) = 1 - exp\left(-\frac{h-A}{B}\right)$ as in section 5.2.2, the probabilities of failure due to respectively overtopping and piping at inner slope or berm toe are expressed dependent on dike dimensions:

$$\begin{aligned}
P_{f_{h-d}}(h_d) &= exp\left(-\frac{h_d - A_{h_{d-ovx}}}{f_{ovx} \cdot B}\right) \\
P_{f_{pip-is}}(h_{cr_{is}}) &= exp\left(-\frac{h_{cr_{is}} - A_h}{B}\right) \\
P_{f_{pip-bt}}(h_{cr_{bt}}) &= exp\left(-\frac{h_{cr_{bt}} - A_h}{B}\right)
\end{aligned} \tag{B.62}$$

In which:

$h_{cr_{is}}$	Critical water level for piping at inner slope, equal to $h_b + \Delta H_{cr_{is}}$	$m + NAP$
$h_{cr_{bt}}$	Critical water level for piping at berm toe, equal to $h_m + \Delta H_{cr_{bt}}$	$m + NAP$
$\Delta H_{cr_{is}}$	Critical head for piping at inner slope, referring to equation (5.22) equal to $\frac{L_d - (h_b - h_m) \cdot cot\alpha_{bi}}{c_p}$	m
$\Delta H_{cr_{bt}}$	Critical head for piping at berm toe, referring to equation (5.22) equal to $\frac{L_d + L_b}{c_p}$	m

L_b	length of berm	m
L_d	virtual footprint of dike excluding the berm	m
$P_{f_{h-d}}(h_d)$	Probability of failure due to overtopping, dependent on h_d	$per\ year$
$P_{f_{pip-is}}$	Probability of failure due to piping at inner slope, dependent on $(L_d, h_b, h_m, \alpha_{bi})$	$per\ year$
$P_{f_{pip-bt}}$	Probability of failure due to piping at berm toe, dependent on (L_d, L_b, h_m)	$per\ year$
$A_{h_{d-ovx}}$	parameter in the exponential distribution for required dike crest heigth, given an acceptable overtopping discharge ovx	$m + NAP$
A_h	parameter in the exponential water level distribution	$m + NAP$

which can be rewritten as:

$$\begin{aligned} P_{f_{h-d}}(h_d) &= exp\left(-\frac{h_d - A_{h_{d-ovx}}}{f_{ovx} \cdot B}\right) \\ P_{f_{pip-is}}(h_{cr_{is}}) &= exp\left(-\frac{\frac{L_d - (h_b - h_m) \cdot cot\alpha_{bi}}{c_p} + h_b - A_h}{B}\right) \\ P_{f_{pip-bt}}(h_{cr_{bt}}) &= exp\left(-\frac{\frac{L_d + L_b}{c_p} + h_m - A_h}{B}\right) \end{aligned} \tag{B.63}$$

which can be rewritten as:

$$\begin{aligned} P_{f_{h-d}}(h_d) &= exp\left(-\frac{h_d - A_{h_{d-ovx}}}{f_{ovx} \cdot B}\right) \\ P_{f_{pip-is}}(h_{cr_{is}}) &= exp\left(-\frac{L_d - (h_b - h_m) \cdot cot\alpha_{bi} + c_p \cdot (h_b - A_h)}{c_p \cdot B}\right) \\ P_{f_{pip-bt}}(h_{cr_{bt}}) &= exp\left(-\frac{L_d + L_b + c_p \cdot (h_m - A_h)}{c_p \cdot B}\right) \end{aligned} \tag{B.64}$$

To enable to follow the Delta Committees approach, equation (5.1) is elaborated as:

$$C_{tot}^{PV} = I + \sum P_f \cdot \frac{D}{r} = I + \frac{D}{r} \cdot \left(P_{f_{h-d}}(h_d) + MAX(P_{f_{pip-is}}(h_{cr_{is}}), P_{f_{pip-bt}}(h_{cr_{bt}}))\right) \tag{B.65}$$

Herein, the term with the product of the probabilities for both failure mechanisms, which is normally distracted to preventing double counting, is neglected because of the small probabilities. Furthermore, the consequences D are assumed to be equal for each type of failure. The two piping mechanisms are assumed to be fully dependent, and both are assumed to be independent of the overtopping mechanism. Which of both piping submechanisms prevails depends on the berm length relative to berm height: equalizing the critical heads for piping at berm toe $h_m + \frac{L_d + L_b}{c_p}$ and for piping at inner slope $\frac{L_d - (h_b - h_m) \cdot cot\alpha_{bi}}{c_p}$ leads to $L_{b_{eq}} = (h_b - h_m) \cdot (c_p - cot\alpha_{bi})$. Therewith, it follows whether piping will occur at berm toe or at inner slope:

$$\begin{aligned} P_{f_{pip}} &= P_{f_{pip-is}}(h_{cr_{is}}) \quad L_b > L_{b_{eq}} \\ P_{f_{pip}} &= P_{f_{pip-bt}}(h_{cr_{bt}}) \quad L_b \leqslant L_{b_{eq}} \end{aligned} \tag{B.66}$$

In which:

$P_{f_{pip}}$	The maximum of probabilities $P_{f_{pip-is}}(h_{cr_{is}})$ and $P_{f_{pip-bt}}(h_{cr_{bt}})$).	m^3/m

Minimizing the total costs is elaborated as in 5.2.2, with the derivative to the dike cross section surface instead of the dike heigth:

$$\frac{\mathrm{d}C_{tot}^{PV}}{\mathrm{d}S_d} = 0 \tag{B.67}$$

Together with equations (B.66) and (B.65), equation (B.67) is:

$$\begin{aligned} \frac{\mathrm{d}C_{tot}^{PV}}{\mathrm{d}S_d} &= I'^{\Delta S_d} + \frac{D}{r} \cdot \left(\frac{\mathrm{d}P_{f_{h-d}}(h_d)}{\mathrm{d}S_d} + \frac{\mathrm{d}P_{f_{pip-is}}(h_{cr_{is}})}{\mathrm{d}S_d} \right) \quad L_b > L_{b_{eq}} \\ \frac{\mathrm{d}C_{tot}^{PV}}{\mathrm{d}S_d} &= I'^{\Delta S_d} + \frac{D}{r} \cdot \left(\frac{\mathrm{d}P_{f_{h-d}}(h_d)}{\mathrm{d}S_d} + \frac{\mathrm{d}P_{f_{pip-bt}}(h_{cr_{bt}})}{\mathrm{d}S_d} \right) \quad L_b \leqslant L_{b_{eq}} \end{aligned} \tag{B.68}$$

In which:

$I'^{\Delta S_d}$	Marginal costs per unity of dike cross section surface.	€/ m^3/m

Since the two piping submechanisms are assumed to be fully dependend, minimizing S_d using the maximum of the both piping probabilities in equation (B.65) determines the relation between berm heigth $h_b - h_m$ and berm length L_b with equation (B.66). A berm height exceeding $L_b/(c_p - cot\alpha_{bi})$ would make no sense for safety, just as a berm length

exceeding $L_{b_{eq}}$. Using this as the condition for berm height, $h_b - h_m$ is equal to $L_b/(c_p - cot\alpha_{bi})$. Therewith, the equation (B.68) simplifies to the first or the second line.

In Appendix B.4 the derivatives for all relevant dike dimension parameters are derived mathematically, see equation (B.61). Therewith, the derivatives of the probabilities in equation (B.68) are as follows, writing $cot\alpha's$ for $cot\alpha_{bi} + cot\alpha_{bu}$:

$$
\begin{aligned}
\frac{\mathrm{d}P_{f_{h-d}}(h_d)}{\mathrm{d}S_d} &= P_{f_{h-d}}(h_d) \cdot \frac{-1}{f_{ovx} \cdot B} \cdot \frac{1}{L_d} \\
\frac{\mathrm{d}P_{f_{pip-is}}(h_{cr_{is}})}{\mathrm{d}S_d} &= P_{f_{pip-is}}(h_{cr_{is}}) \cdot \frac{\mathrm{d}\left(-\dfrac{L_d - (h_b - h_m) \cdot cot\alpha_{bi} + c_p \cdot h_b}{c_p \cdot B}\right)}{\mathrm{d}S_d} \\
&= P_{f_{pip-is}}(h_{cr_{is}}) \cdot \frac{-1}{c_p \cdot B} \cdot \left(\frac{cot\alpha's}{L_d} - \left(\frac{cot\alpha_{bi}}{L_b} + \frac{2 \cdot (h_b - h_m)}{(h_d - h_m)^2}\right) + \frac{c_p}{L_b}\right) \\
&= P_{f_{pip-is}}(h_{cr_{is}}) \cdot \frac{-1}{c_p \cdot B \cdot L_d} \cdot \\
&\quad \left(cot\alpha's + \frac{L_d(c_p - cot\alpha_{bi})}{L_b} + \frac{2L_d(h_b - h_m)}{(h_d - h_m)^2}\right) \\
\frac{\mathrm{d}P_{f_{pip-bt}}(h_{cr_{bt}})}{\mathrm{d}S_d} &= P_{f_{pip-bt}}(h_{cr_{bt}}) \cdot \frac{\mathrm{d}\left(-\dfrac{L_d + L_b}{c_p \cdot B}\right)}{\mathrm{d}S_d} \\
&= P_{f_{pip-bt}}(h_{cr_{bt}}) \cdot \frac{-1}{c_p \cdot B} \cdot \left(\frac{cot\alpha's}{L_d} + \frac{1}{h_b - h_m}\right) \\
&= P_{f_{pip-bt}}(h_{cr_{bt}}) \cdot \frac{-1}{c_p \cdot B \cdot L_d} \cdot \left(\frac{(h_b - h_m) \cdot cot\alpha's + L_d}{(h_b - h_m)}\right)
\end{aligned}
\tag{B.69}
$$

Substituting the derivatives in equation (B.69) in the second line of equation (B.68), it can be rewritten as:

$$
\frac{\mathrm{d}C_{tot}^{PV}}{\mathrm{d}S_d} = I'^{\Delta S_d} + \frac{D}{r} \cdot \left(\frac{-P_{f_{h-d}}}{f_{ovx} \cdot B \cdot L_d} + \frac{-P_{f_{pip-is}}}{c_p \cdot B \cdot L_d} \cdot \left(\frac{(h_b - h_m) \cdot cot\alpha's + L_d}{(h_b - h_m)}\right)\right) \tag{B.70}
$$

Appointing a failure budget γ_{h_d} as a part of the total probability to failure mechanism overtopping, and consequently $\gamma_p = 1 - \gamma_{h_d}$ to piping, it follows:

$$
\frac{\mathrm{d}C_{tot}^{PV}}{\mathrm{d}S_d} = I'^{\Delta S_d} + \frac{D}{r} \cdot \left(\frac{-\gamma_{h_d} \cdot P_f}{f_{ovx} \cdot B \cdot L_d} + \frac{-\gamma_p \cdot P_f}{c_p \cdot B \cdot L_d} \cdot \left(\frac{L_d + (h_b - h_m) \cdot cot\alpha's}{(h_b - h_m)}\right)\right)
$$

(B.71)

Leading to:

$$\frac{dC_{tot}^{PV}}{dS_d} = I'^{\Delta S_d} - \frac{D \cdot P_f}{r \cdot f_{ovx} \cdot B \cdot L_d} \cdot \left(\gamma_{h_d} + \frac{f_{ovx} \cdot \gamma_p}{c_p} \cdot \left(\frac{L_d + (h_b - h_m) \cdot cot\alpha' s}{(h_b - h_m)} \right) \right) \tag{B.72}$$

Rewriting, it follows:

$$\frac{dC_{tot}^{PV}}{dS_d} = I'^{\Delta S_d} - \frac{D \cdot P_f}{r \cdot f_{ovx} \cdot B \cdot L_d} \cdot \left(\frac{\gamma_{h_d} \cdot c_p \cdot (h_b - h_m) + \gamma_p \cdot f_{ovx} \cdot (L_d + (h_b - h_m) \cdot cot\alpha' s)}{c_p \cdot (h_b - h_m)} \right) \tag{B.73}$$

Thus, the probability $P_{f_{opt}}$ which belongs to $\frac{dC_{tot}^{PV}}{dS_d} = 0$, corresponding to the minimum of C_{tot}^{PV} is:

$$P_{f_{opt}} = \frac{I'^{\Delta S_d} \cdot f_{ovx} \cdot B \cdot L_d \cdot r}{D} \cdot \left(\frac{c_p \cdot (h_b - h_m)}{\gamma_{h_d} \cdot c_p \cdot (h_b - h_m) + \gamma_p \cdot f_{ovx} \cdot (L_d + (h_b - h_m) \cdot cot\alpha' s)} \right) \tag{B.74}$$

Substituting $h_b - h_m = L_b/(c_p - cot\alpha_{bi})$ leads to an equivalent formulation with the bermlength L_b in stead of the berm height $h_b - h_m$:

$$P_{f_{opt}} = \frac{I'^{\Delta S_d} \cdot f_{ovx} \cdot B \cdot L_d \cdot r}{D} \cdot \left(\frac{c_p \cdot L_b}{\gamma_{h_d} \cdot c_p \cdot L_b + \gamma_p \cdot f_{ovx} \cdot \left(L_d \cdot (c_p - cot\alpha_{bi}) + L_b \cdot cot\alpha' s \right)} \right) \tag{B.75}$$

Note, with the geometric translation $I'^{\Delta S_d} = I'/L_d$ the first part of the equations (B.74) and (B.75) is the same as equation (5.13) (except the factors f_I and Δt representing the time dependence, which is excluded in the derivation for two failure mechanisms). This means that the last part of the equation between brackets reflects the effect of taking into account a second failure mechanism.

B.5.2. WITHOUT BERM

Starting point for the derivation in the last section is the presence of a berm. In case of sea dikes the footprint of the dike may be that wide, that it reduces the probability of piping sufficiently, at least to the extent the optimum for societal cost is lower than in the case with berm. In this special case of no berm ($L_b = 0$) the probability for piping in (B.63) is:

$$P_{f_{pip-is}}(h_{cr_{is}}) = exp\left(\frac{-\frac{L_d}{c_p} + h_m - A_h}{B}\right) = exp\left(-\frac{L_d + c_p \cdot (h_m - A_h)}{c_p \cdot B}\right) \tag{B.76}$$

The minimum societal costs are found solving:

$$\frac{dC_{tot}^{PV}}{dS_d} = I'^{\Delta S_d} + \frac{D}{r} \cdot \left(\frac{dP_{f_{h-d}}(h_d)}{dS_d} + \frac{dP_{f_{pip-is}}(h_{cr_{is}})}{dS_d}\right) \tag{B.77}$$

Just as in last section the failure budget γ_{h_d} is defined as the part of the total probability to failure mechanism overtopping, and consequently $\gamma_p = 1 - \gamma_{h_d}$ to piping. With the derivatives from equation (B.61), it follows:

$$\frac{dC_{tot}^{PV}}{dS_d} = I'^{\Delta S_d} + \frac{D}{r} \cdot P_f \cdot \frac{1}{B} \cdot \frac{1}{L_d} \cdot \left(\frac{-\gamma_{h_d}}{f_{ovx}} + \frac{-\gamma_p \cdot (cot\alpha_{bu} + cot\alpha_{bi})}{c_p}\right) \tag{B.78}$$

Thus, the probability $P_{f_{opt}}$ which belongs to the minimum of C_{tot} for the situation without berm is:

$$P_{f_{opt}} = \frac{I'^{\Delta S_d} \cdot f_{ovx} \cdot B \cdot L_d \cdot r}{D} \cdot \left(\frac{c_p}{\gamma_{h_d} \cdot c_p + \gamma_p \cdot f_{ovx} \cdot (cot\alpha_{bu} + cot\alpha_{bi})}\right) \tag{B.79}$$

Herein, again the degree of freedom left is γ_{h_d}. This relation is valid, since the denumerator between the brackets is positive in the whole domain of γ_{h_d} [0,1].

In this special case without berm the degree of freedom can be solved because of a second relation for γ_{h_d}: the relation between the dike height and the dikes footprint is fixed by the condition no berm is present, see Figure B.1:

$$L_d = Br_d + (cot\alpha_{bu} + cot\alpha_{bi}) \cdot (h_d - h_m) \tag{B.80}$$

Therewith, the dike cross section is determined as:

$$\begin{aligned} h_d &= A_{h_d} - f_{ovx} \cdot B \cdot ln(\gamma_{h_d} \cdot P_f) \\ L_d &= c_p \cdot (A_h - h_m) - c_p \cdot B \cdot ln(\gamma_p \cdot P_f) \end{aligned} \tag{B.81}$$

Substituting these dimensions in equation (B.80), it follows:

$$\begin{aligned} &c_p \cdot (A_h - h_m) - c_p \cdot B \cdot ln\left((\gamma_p) \cdot P_f\right) = \\ &\quad Br_d + (cot\alpha_{bu} + cot\alpha_{bi}) \cdot \left(A_{h_d} - f_{ovx} \cdot B \cdot ln\left(\gamma_{h_d} \cdot P_f\right) - h_m\right) \end{aligned} \tag{B.82}$$

Move parts with P_f to the left and the other parts to the right of the equal-sign, and writing $cot\alpha's$ for $cot\alpha_{bi} + cot\alpha_{bu}$:

$$\begin{aligned} &- c_p \cdot B \cdot ln\left((\gamma_p) \cdot P_f\right) + cot\alpha's \cdot f_{ovx} \cdot B \cdot ln\left(\gamma_{h_d} \cdot P_f\right) = \\ &\quad Br_d - c_p \cdot (A_h - h_m) + cot\alpha's \cdot \left(A_{h_d} - h_m\right) \end{aligned} \tag{B.83}$$

Since $ln\left(\gamma_{h_d} \cdot P_f\right) = ln\left(\gamma_{h_d}\right) + ln\left(P_f\right)$ and $ln\left(\gamma_p \cdot P_f\right) = ln\left(\gamma_p\right) + ln\left(P_f\right)$, it follows:

$$\begin{aligned} &- c_p \cdot B \cdot \left(ln\left(\gamma_p\right) + ln\left(P_f\right)\right) + cot\alpha's \cdot f_{ovx} \cdot B \cdot \left(ln\left(\gamma_{h_d}\right) + ln\left(P_f\right)\right) = \\ &\quad Br_d - c_p \cdot (A_h - h_m) + cot\alpha's \cdot \left(A_{h_d} - h_m\right) \end{aligned} \tag{B.84}$$

$$\begin{aligned} &ln\left(P_f\right) \cdot \left(-c_p \cdot B + f_{ovx} \cdot B \cdot cot\alpha's\right) - c_p \cdot B \cdot \left(ln\left(\gamma_p\right)\right) + \\ &\quad cot\alpha's \cdot f_{ovx} \cdot B \cdot \left(ln\left(\gamma_{h_d}\right)\right) = \\ &\quad Br_d - c_p \cdot (A_h - h_m) + cot\alpha's \cdot \left(A_{h_d} - h_m\right) \end{aligned} \tag{B.85}$$

$$\begin{aligned} &ln\left(P_f\right) \cdot \left(-c_p \cdot B + f_{ovx} \cdot B \cdot cot\alpha's\right) = \\ &\quad c_p \cdot B \cdot \left(ln\left(\gamma_p\right)\right) - cot\alpha's \cdot f_{ovx} \cdot B \cdot \left(ln\left(\gamma_{h_d}\right)\right) + \\ &\quad Br_d - c_p \cdot (A_h - h_m) + cot\alpha's \cdot \left(A_{h_d} - h_m\right) \end{aligned} \tag{B.86}$$

$$\begin{aligned} &ln\left(P_f\right) \cdot \left(-c_p \cdot B + f_{ovx} \cdot B \cdot \left(cot\alpha's\right)\right) = \\ &\quad c_p \cdot \left(B \cdot ln\left(\gamma_p\right) - (A_h - h_m)\right) + \\ &\quad cot\alpha's \cdot \left(\left(A_{h_d} - h_m\right) - f_{ovx} \cdot B \cdot ln\left(\gamma_{h_d}\right)\right) + Br_d \end{aligned} \tag{B.87}$$

With $A_{h_d} - h_m$ denoted as A_{ov} and $A_h - h_m$ denoted as A_p, and $cot\alpha_{bu} + cot\alpha_{bi}$ denoted as $cot\alpha's$ this results in:

$$P_f = exp\left(\frac{c_p \cdot \left(B \cdot ln\left(\gamma_p\right) - A_p\right) + cot\alpha's \cdot \left(A_{ov} - f_{ovx} \cdot B \cdot ln\left(\gamma_{h_d}\right)\right) + Br_d}{B \cdot \left(f_{ovx} \cdot cot\alpha's - c_p\right)}\right) \tag{B.88}$$

Equate the resulting probability P_f with $P_{f_{opt}}$ in equation (B.79) provides the result for the value of γ_{h_d} for which the corresponding probability of failure will lead to lowest societal costs, under the condition of no berm exists.

B.6. EQUIVALENT REINFORCEMENT HEIGHT

This appendix determines the relation between the equivalent reinforcement height $\Delta\tilde{h}_d$, defined as the virtual dike heightening for a dike shape with slopes $cot\alpha_{bi,0}$ and $cot\alpha_{bu,0}$ (see Figure B.1) which belongs to an additional cross sections surface ΔS_d. In the following $cot\alpha'_0 s$ is written for $cot\alpha_{bi,0} + cot\alpha_{bu,0}$, and h_0 is written for $(h_{d,0} - h_m)$.

The additional budget is the dike shapes surface volume after reinforcement subtracted with the existing dike shapes surface.

$$\Delta S_d = (h_0 + \Delta\tilde{h}_d) \cdot \left(cot\alpha'_0 s \cdot \frac{(h_0 + \Delta\tilde{h}_d)}{2} + Br_d \right) - h_0 \cdot \left(cot\alpha'_0 s \cdot \frac{h_0}{2} + Br_d \right) \tag{B.89}$$

$$\Delta S_d = \left(\frac{(h_0 + \Delta\tilde{h}_d)^2}{2} \cdot cot\alpha'_0 s + (h_0 + \Delta\tilde{h}_d) \cdot Br_d \right) - \left(\frac{h_0}{2} \cdot cot\alpha'_0 s + h_0 \cdot Br_d \right) \tag{B.90}$$

$$\Delta S_d = \frac{{h_0}^2 + 2 \cdot h_0 \cdot \Delta\tilde{h}_d + {\Delta\tilde{h}_d}^2}{2} \cdot cot\alpha'_0 s + \Delta\tilde{h}_d \cdot Br_d - \frac{{h_0}^2}{2} \cdot cot\alpha'_0 s \tag{B.91}$$

$$\Delta S_d = \frac{h_0 \cdot \Delta\tilde{h}_d + {\Delta\tilde{h}_d}^2}{2} \cdot cot\alpha'_0 s + \Delta\tilde{h}_d \cdot Br_d \tag{B.92}$$

leading to:

$${\Delta\tilde{h}_d}^2 \cdot \frac{cot\alpha'_0 s}{2} + \Delta\tilde{h}_d \cdot \left(h_0 \cdot \frac{cot\alpha'_0 s}{2} + Br_d \right) - \Delta S_d = 0 \tag{B.93}$$

In this quadratic formula the unique value for $\Delta\tilde{h}_d$ can be solved:

$$\Delta\tilde{h}_d = \frac{-\left(h_0 \cdot \frac{cot\alpha'_0 s}{2} + Br_d \right) \pm \sqrt{\left(h_0 \cdot \frac{cot\alpha'_0 s}{2} + Br_d \right)^2 - 4 \cdot \frac{cot\alpha'_0 s}{2} \cdot -\Delta S_d}}{cot\alpha'_0 s} \tag{B.94}$$

$$\Delta\tilde{h}_d = -\frac{h_0}{2} - \frac{Br_d}{cot\alpha'_0 s} \pm \sqrt{\left(\frac{1}{cot\alpha'_0 s} \right)^2 \cdot \left(\left(\frac{h_0 \cdot cot\alpha'_0 s}{2} \right)^2 + h_0 \cdot cot\alpha'_0 s \cdot Br_d + {Br_d}^2 + 2 \cdot cot\alpha'_0 s \cdot \Delta S_d \right)}$$

(B.95)

Since $\Delta\tilde{h}_d$ can only be positive, only the positive solution makes sense. Therewith, equivalent reinforcement height is:

$$\Delta\tilde{h}_d = -\frac{h_0}{2} - \frac{Br_d}{cot\alpha'_0 s} + \sqrt{\left(\frac{h_0}{2}\right)^2 + \frac{h_0 \cdot Br_d}{cot\alpha'_0 s} + \left(\frac{Br_d}{cot\alpha'_0 s}\right)^2 + \frac{2 \cdot \Delta S_d}{cot\alpha'_0 s}} \tag{B.96}$$

This equation shows clearly the logic that the value of $\Delta\tilde{h}_d$ is positive in case ΔS_d is positive, because the first and third term under the square root cancel the first negative terms in this equation. The equivalent reinforcement height reflects a reinforcement height based on existing dike shape with the an additional cross section surface ΔS_d which may be based on a different dike shape.

B.7. NUMERICAL METHOD

A numerical method has been developed to enable comparison with results obtained with the analytical-based method in the main text in Section 5.3.4. The numerical method is based on calculation of combinations of dike height increase, berm length increase and inner slope gentling. The optimal solution is the combination of dimensions which result in minimal cost in this series.

The integration scheme is based on two loops: a stepwise gentling of inner slope and a stepwise increase of the dikes cross sections surface. In the second loop, for each step investments and risk for all combinations of the dike height increase, berm length increase is calculated. Figure B.2 shows the flow chart of the calculation. Per step of the dikes cross sections surface increase, the added surface is divided in a part used to add the dike bodies surface (excluding the surface berm length times berm height) and a part used for the berm (berm length times berm height):

$$\begin{aligned} S_d &= S_{dike\,body} + S_{berm} \\ S_{dike\,body} &= \left(Br_d + (cot\alpha_{bu} + cot\alpha_{bi}) \cdot \frac{h_d - h_m}{2}\right) \cdot (h_d - h_m) \\ S_{berm} &= L_b \cdot (h_b - h_m) \end{aligned} \tag{B.97}$$

The ratio between the two parts is varied stepwise between 0 and 1. For each ratio the dike height corresponding with the surface in the dike body is found rewriting the second line in equation (B.97):

$$\frac{cot\alpha_{bu} + cot\alpha_{bi}}{2} \cdot (h_d - h_m)^2 + Br_d \cdot (h_d - h_m) - S_{dike\,body} = 0 \tag{B.98}$$

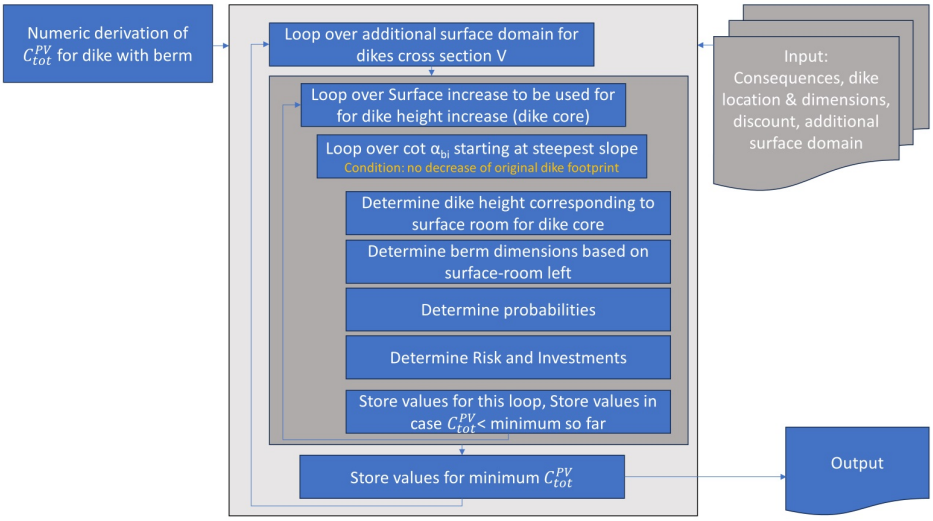

Figure B.2.: *Flowchart of the approach to solve equation (5.30) numeric.*

This leads to:

$$h_d - h_m = \frac{-Br_d \pm \sqrt{Br_d^2 - 4 \cdot \frac{cot\alpha_{bu} + cot\alpha_{bi}}{2} \cdot -S_{dike\,body}}}{cot\alpha_{bu} + cot\alpha_{bi}} \tag{B.99}$$

Since a negative dike height makes no sense, only the positive variant in equation (B.99) is taken into account:

$$h_d - h_m = \frac{-Br_d + \sqrt{Br_d^2 + 2 \cdot cot\alpha_{bu} + cot\alpha_{bi} \cdot S_{dike\,body}}}{cot\alpha_{bu} + cot\alpha_{bi}} \tag{B.100}$$

Note, $h_d - h_m$ is positive for each positive value of $S_{dike\,body}$ and positive values for the slopes $cot\alpha_{bu}$ and $cot\alpha_{bi}$. To find the berm height and berm length corresponding to the surface in the dike berm the third line in equation (B.97) is rewritten with $L_b = (c_p - cot\alpha_{bi}) \cdot (h_b - h_m)$, which corresponds with the minimum berm dimensions (leading to failure due to piping at both inner slope and berm toe, see equation (5.27)):

$$S_{berm} = L_b \cdot (h_b - h_m) = (c_p - cot\alpha_{bi}) \cdot (h_b - h_m) \cdot (h_b - h_m) \tag{B.101}$$

$$(h_b - h_m) = \sqrt{\frac{S_{berm}}{c_p - cot\alpha_{bi}}} \tag{B.102}$$

With equations (B.80), (B.100), (B.102) the dike shape is determined. Therewith, in the second loop in Figure B.2 (the inner loop) the probabilities for the failure mechanisms are known with equation (5.25). To find

the total probability of failure the probabilities per failure mechanism are combined with:

$$P_{f_{tot}} = 1 - (1 - P_{f_{h-d}}) \cdot (1 - P_{f_{pip}}) \tag{B.103}$$

The fraction of the probability of failure corresponding with the failure mechanism overtopping γh_d is calculated with :

$$\gamma h_d = \frac{P_{f_{h-d}}}{P_{f_{tot}}} \tag{B.104}$$

Herewith, the same equation (5.39) as used in the analytical-based method can be calculated for a series of inner slope $cot\alpha_{bi}$, providing for each ΔS_d, a combination of Investment, Risk and total Costs, see Figure B.3. Note, this Figure provides ΔS_d on the x-axis because this is an important decision variable in equation (5.39). In similar graphical representations the value on the x-axis is dike height or probability of failure, see by example Figure 2 in [51] and Figure 5 in [68]. In Figure B.3 per value of ΔS_d on the x-axis, from all combinations of dimensions leading to that value of ΔS_d only the data is presented corresponding with the minimum total costs. Thus, along the curve the inner slope $cot\alpha_{bi}$, berm length and dike height may vary.

Using the data in Table 5.2 the result for minimum costs are a dike height of 12.34 m+NAP and a berm length of 20.14 m and a berm height of 1.49 m, and an inner slope of 4.52. Total minimum costs are 90.1 M€. The numerical parameters used are provided in Table B.1. The results for all locations are provided in Table B.2.

Table B.1.: *Numerical and economical data used for the comparison. *An extra condition is that the optimal dike dimensions are in the domain of the dike bodies footprint L_d equal to or larger than the actual dike bodies footprint $L_{d,0}$.*

Parameter	Description	Value	Unity
ϵ	Accuracy level of iterations	0.02	–
f_{S_d-max}	Factor between maximum and actual dike cross sections surface, used to determine the maximum surface in the calculations	4	–
$f_{\alpha-max}$	Factor between maximum and actual cotangent of the inner slope, used to determine the maximum slope in the calculations	5	–
n	Number of integration steps	250	–
$min\ cot\alpha_{bi}$	Minimum slope *	1.5	–

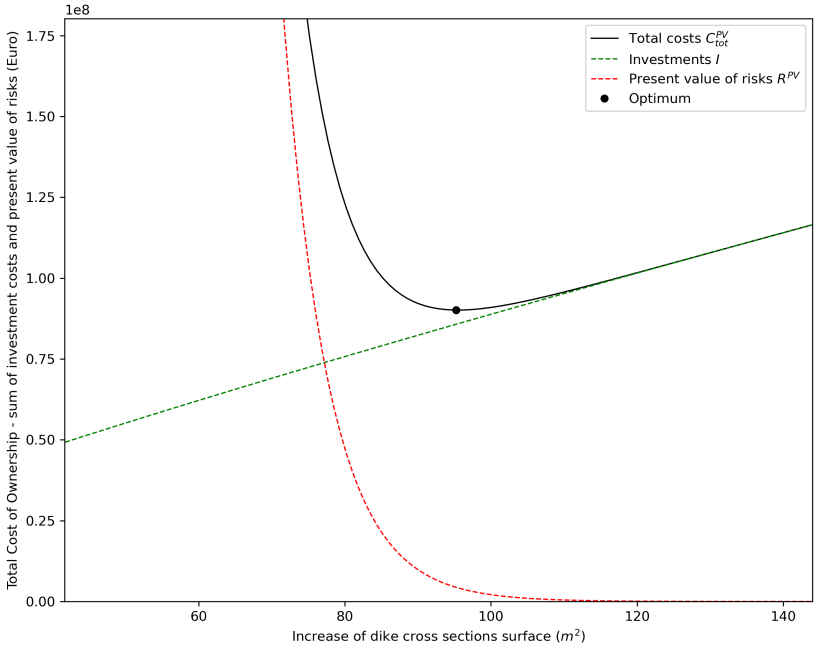

Figure B.3.: *Overview of optimal combinations of dike height, berm length and inner slope for location Grebbe, indicating the global optimum, for both the analytical and the numerical method.*

Table B.2.: *Results for numerical method for locations Schiermonnikoog (Loc 1), Hollandse Kust (Loc 2), Grebbe (Loc 3), South-Flevoland (Loc 4), IJssel-West (Loc 5), Oude Maas (Loc 6), and Western Scheldt (Loc 7).*

Location	**dike height**	**berm length**	**slope**	**ΔS_d**	**γ_{h_d}**	**$P_{f_{opt}}$**	**p_{ratio}**	**Total costs**
	(m+ NAP)	**(m)**	**(-)**	**m^3/m**	(-)	**$\cdot 10^{-5}$ / year**	(-)	**$\cdot 10^6$€**
Loc 1	5.10	18.50	3.44	64,6	0.37	648.3	1.81	70.1
Loc 2	8.93	2.57	2.69	53,9	0.96	181.6	1.28	533.5
Loc 3	12.34	20.14	4.52	95,2	0.57	0.9	1.34	90.1
Loc 4	4.58	26.22	2.26	95,8	0.42	26.9	1.45	674.0
Loc 5	8.90	10.69	7.39	58,6	0.46	66.1	1.99	625.5
Loc 6	4.88	9.57	9.76	89.6	0.43	42.8	2.69	1551.5
Loc 7	7.03	26.81	4.96	154.8	0.43	150.4	1.72	1182.9

C

FLOOD SIMULATIONS IN THE RIVERINE AREA IN THE NETHERLANDS

The starting points for dike breach character in the data of flood simulations and consequences in the Dutch National database of Flood Simulations [54], in Dutch abbreviated as LIWO, are for riverine breaches summarized in Table 2.1. The following points are noticeable in the LIWO-data:

- The flood simulations were executed over a time span of about 20-30 years with varying starting points for the hydraulic forcing and breach characteristics. Especially the older calculations are executed with chosen breach widths.
- The simulations with chosen breach widths use widths of about 200m on an average, which is about 4 times larger than the simulations with calculated widths (about 50m). Especially the few simulations with chosen breach-widths for dikes with clay core used widths of 210m, which is very large with respect to the simulations for dikes with clay core with calculated breach-widths (30m on an average, see Table 2.1).
- Only 112 (25%) of the simulations for which breach widths were available intended to calculate breaches taking a clay core (or a substantial part of clay in the cross section) into account. This is in contradiction with the common assumption that most dikes in the river area consists of clay, or at least for a considerable part of the cross section [100].
- The calculated breach-widths are based on the relation derived in Verheij & van der Knaap [77]. They based their derivation on several events occurred in the last centuries, and on model simula-

tions. In the list of events, only three events were breaches in river dikes (sand). The widths of these breaches were between 150m and 200m, considerably larger than the calculated widths used in the simulations (58m on an average, see Table 2.1). NB. This rises a reasonable doubt about the application of the relation in Verheij & van der Knaap [77] in this simulations. However, the standards in the Netherlands are based on the flood simulations with breach width based on this relation.

- A large part of the simulations no breach-widths are registered (319 simulations, 42%). They are mostly carried out before the relation of Verheij & van der Knaap was available. It may be logic to assume these simulations are carried out with large breach-widths, since by then only the real events in the river areas with large breach-widths were available which were later described in [77].
- Together with the 170 simulations with large wide breaches (column 'chosen breach-width, except the row 'sand') the majority of the simulations is carried out with are with large breaches (61%).
- A considerable part of the simulations are carried out with small breaches, but with the denotion having a sand core (first row). Combined with the above statements, there is reasonable doubt as to whether the breach widths used, correspond to the actual core material. In case the real dikes material is clay and the calculations took relatively wide breaches corresponding with a dike with sand core, the flood volume is overestimated. In that case the flood calculations lead to an overestimation of the actual damages. If used to derive standards for interventions, this will lead to more stringent design standards (see equation (5.13)), and consequently to intervene early and overestimate reinforcements, which both lead to overspending. The other way around, in case the real dikes material is sand and the calculations took relatively small breaches corresponding with a dike with clay core, the flood volume is underestimated. In that case the flood calculations lead to an underestimation of the actual damages. If used to derive standards for interventions, this will lead to less stringent standards and consequently to intervene late and underestimate reinforcements. Both will lead to a hinterland which is more at risk than it should have been in case the dikes material would have been corresponding to the simulations.

Summarizing, the application of the relation in Verheij & van der Knaap [77] in LIWO led to doubtful breach-widths, probably for a significant number of simulations assuming a clay core in case of a present sand core and the other way around. For a lot of the simulations breach-widths are not registered. Reasonably assuming most of these simulations have

been carried out with large breach-widths, before the adoption of the relation in Verheij & van der Knaap (2003), most simulations simulate breaches in sand dikes, named as brittle in Chapter 3. Therewith, in most of the simulations the consequences are overestimated (see Figure 2.4).

D

DYNAMIC CONNECTED VERSUS STATIC DISCONNECTED RISK APPROACH

Each of the key topics presented in Section 1.4 are discussed below consecutively, to stipulate the character of the dynamic connected risk analysis. The topics cover more or less the three decision levels in the framework of asset management.

D.1. KEY TOPIC 1 - OPERATIONAL DECISION LEVEL

Key topic 1 concerns the integrated risk-based optimization of dike design. Chapter 3 delivers an risk optimal combination of design and dimensions given the structural robustness of the design. It enables to compare several design proposals with varying structural robustness. The technical disciplines involved are physically coupled, such as hydraulic and geotechnical engineering, breach growth and consequence analysis, see Chapter 3. The dynamic connection between these disciplines is carried out by an integrated risk analysis, without cuts between the disciplines in the model which would complicate to correctly reflect the time-dependent behaviour during a flood event:

- The occurrence of an initial failure mechanism is checked every time step during an event. After its occurrence the erosion propagates every time step until a breach occurs. The initial failure mechanism and its subsequent erosion up to breaching are denoted as a failure path. The model enables parallel development of several failure paths. The model concept is even suitable for interaction between failure paths, such as would be the case in practice: macro instability may lead to erosion due to overtopping or piping.

- After occurrence of a breach its growth interacts with the hydraulic loads, the breach volume and the polder water level, see equation (3.5) and the physical relations presented in Appendix A. The consequences of flooding are connected to the total volume of the flooding, see Figure 2.4. Therewith, assuming a bath-tube polder, the polder water level determines the consequences.

This way each load event is connected to a consequence (or no consequences in case the dike does not breach). Drawing numerous load events and strength realizations in an probabilistic Monte Carlo analysis the relation between costs and victims is determined, graphical represented in Figures 3.12 and 3.13. An economic optimal design, for which the measure with minimal societal costs is directly related to both dike dimensions and dike construction type, appeared to be comparable with the static optimalisation graphs at the strategic level als presented in [14, 51].

In a static and less connected or disconnected risk approach the technical disciplines are treated consecutively or parallel. A clear disconnection in a risk analysis is if the probability of failure of the dike is calculated disconnected from the calculations to determine the consequences of failure, see equation (2.1). Two examples are:

- Disconnection by consecutive treatment of disciplines: the intermediate results are summarized in starting points for the next discipline in the chain the result of hydraulic analyses lead to a water level as input for geotechnical, breachgrowth and consequence analyses. The consequence analyses and the probability of failure, which is the result of hydraulic and geotechnical analysis, is input for the risk analysis. Failure mechanisms and paths are treated without physical interaction with the dynamics of the loads.
- Disconnection by parallel treatment of failure mechanisms: the probability of failure is based on a Failure Tree approach, in which the initial failure mechanisms are physically distinguished. In most approaches independence is assumed between them, such as in [29, 75]. Some involve dependency in the probabilistic model [74].

Starting points bridge the gap

In present practice of a static disconnected risk analysis, starting points bridge the gap to reflect the dynamic reality:

- The hydraulic starting points used for the consequence calculations are connected to the circumstances due to failure. In the Dutch case [54] the input for flooding model is a chosen

time for dike breach during the flood, which is the practice in other countries as well [23]. Chapter 3 and [117] shows that especially in the river area the time of occurrence of a breach is very important for the total volume of water entering a polder (the integrated positive breach discharge in Figure 3.3 – last subfigure), and therewith the time of occurrence of a breach is important for the consequences, see Figure 2.4.

- The hydraulic starting points used for the analysis of initial failure mechanisms: mostly taken at maximum water level during an event, corresponding to the objected safety level.
- The geotechnical starting points reflecting the process after occurrence of an initial failure mechanism: the failure paths. Each initial failure mechanism may initiate a different follow-up mechanism, and therewith a different additional time to failure [91]. Therefore, depending on the initial failure mechanism the dike may breach on a different time during a flood, consequently leaving different time for breach growth and flooding. Nevertheless, mostly the maximum load water level during an event is taken to assess consequences, corresponding with the objected safety level.
- The starting points for breachgrowth after the breach occurrence time are the growth character (widening) and the final breach dimensions (width and depth). Table 2.1 shows a summary for the Dutch database of calculations for river floods. It clearly shows the majority of the simulations has no registered connection to the hydraulic circumstances during a flood. Only the ‘calculated breach width’ use registered flood characteristics to estimate breachwidth, however, the time of breaching is not registered. Next to the breach occurrence time, the growth characteristics are very important for the total flood volume, referring again to the Figure 3.3 (last two subfigures): the breach width majorly affects the total volume of breach discharge into the polder.

In Appendix E a case study is performed for location Grebbedijk (see Section 1.5) to assess the magnitude of potential differences between the dynamic connected approach (key topic 1: integrated risk-based optimization of dike design) and the static disconnected approach. It appeared the dynamic connected approach reduces investment costs with about 20% and risk with a factor 3 with respect to the static disconnected approach.

D.2. KEY TOPIC 2 - TACTICAL DECISION LEVEL

Key topic 2 concerns the integrated portfolio prioritisation of measures in system. Chapter 4 delivers a method to assess the time aggregated risks in a system. It enables comparison of tactical plans by its accompanying time-aggregated risks. It enables to evaluate a tactical plan based on a quantitative analysis. Each tactical plan consists of starting points for the determination of order and planning of interventions in system, such as the metric, the priority condition and the budget over time. The dynamic connected risk analysis calculates the system risks associated with the tactical plan over time, including the effect of interventions, see Chapter 4. The motive for the interventions in the model is to optimize risk reduction over time. Therewith, the approach delivers the spatial and temporal coherence of upcoming measures by their system effects. The connective character of the approach is reflected the contributions of the interventions to dike segments to the system risk reduction. Therewith, the structural robustness of the design for an intervention on a dike segment effects the system risk. The dynamic character is reflected by inclusion of the changing relative system effects of the measures over time, potentially changing the order. Figure 4.19 is a graphical representation of the differences in risk due to tactical decisions.

In actual practice of applications for flood risk, the risk is considered per unit of time, and the use of system risk considerations for order and planning are no mainstream [27]. A static and less connected or disconnected risk approach is in case the spatial and temporal coherence is neglected. Three examples are:

- Disconnection from design. The order and planning of a dike reinforcement is determined based on the risk reduction corresponding with a standard-design.
- Spatial disconnection. The system effect is neglected. Therewith, the loads are derived based on the assumption that breaches in the neighbourhood do not influence the hydraulic loads. In case of a riverine system this means that the probability of failure of dikes upstream is assumed to be zero.
- Disconnection from developments over time. This is the case if a tactic is not based on changes in the system during the planning period. This neglects the risk effects of the order of reinforcements on adjacent polders.

D.3. KEY TOPIC 3 - STRATEGIC DECISION LEVEL

Key topic 3 concerns the relation between the design and the reliability standard. To apply risk based flood risk management, a lot of countries use a safety level represented by the probability of dike failure [16]. In

Chapters 3 and 5 has been shown the economic optimal safety levels interact with the design and the design horizon.

Chapter 5 presents a method to risk aware update a reliability standard dependent on the costs and consequences of a design. It enables to take into account the risk reduction of structural robust designs. The key parameters in the design with which the economic optimal risk based probability standard can be assessed, are the marginal costs and the damage. The marginal investment is proportionate to the optimal probability of failure, and the economic damage is proportionate to the reciprocal of the optimal probability of failure. With the procedure in Chapter 5 can be derived whether it is beneficial to intervene, and which probability of failure corresponds to the upcoming measure. Therewith, in the dynamic connected risk analysis the economic optimal safety level can be updated dependent on the design, the design horizon, or consequence information. Figure 5.11 is a graphical representation of the dynamics of the performance requirement.

The Dutch economic optimal performance requirements are not time-dependent despite the dynamics over time of the loads (e.g. climate change) strength (e.g. subsidence) and consequences (e.g. economic growth, population). In a static and less connected or disconnected risk approach the pursued safety level is independent of the type of construction and independent of time. Three examples are:

- Less connected to risk. The actual practice of applying performance requirements in some countries is to use load frequencies in combination with design rules (Romania). Other countries use probabilities of dike failure, such as Germany, Belgium [23]. Mostly a probability of 1/100 or 1/1000 per year is used, which are loosely based on risk exercises [23]. In the Netherlands more stringent standards are present, based on extensive risk analyses [51]. All of them are time-independent.
- Disconnected in time: in the Netherlands, the time dependence of economic optimal performance requirements is applied in a practical way, as shown in Chapter 5 and [51]: the standards are considered to be valid up to a certain date (2050). Note, in practice they are used for designs with horizons far beyond.
- Disconnected from design. In a disconnected approach the operational level is disconnected from the strategic level. In a first step a risk based performance requirement is chosen (or derived, as in the Dutch case) and in a second step the dike will be designed to meet that requirement.

E

EXAMPLE OF REDUCED COSTS & RISKS DUE TO CONNECTED RISK APPROACH

A comparison has been made to value the differences in societal costs (present value and investments) between a connected and a disconnected risk analysis. The comparison is made for the location Grebbedijk, used in Chapter 3 as well, considering a semi-existing sand core. Two failure paths are considered, incepted by the failure mechanisms overtopping and piping, see Chapter 3 and A. The Grebbedijk has a length of 5.5 km.

In a disconnected approach the probability of flooding is calculated first, see equation (2.5), multiplied by consequences in a second step, in which the consequences are assumed to be representative for all load events leading to flooding. A characteristic of a connected risk analysis is that load events, duration of the erosion process, time of breaching and breachwidth have effect on consequences, see equation (2.16). To obtain a comparable and analysible result, the application of the two approaches is stepwise aligned.

- Disconnected approach variant 0, tight to current practice. The construction dimension combination (CDC) is based on the failure definition following current practice. Herein the dike is considered to be failed in case a dike is damaged due to the occurrence of a failure mechanism. Following the Dutch standardization exercise, the economic optimal probability of failure is used as the design safety level [51], equally distributed over the two considered failure mechanisms. The consequences are taken from the Dutch national database of flood simulations [54].
- Disconnected approach variant 1. In this variant the CDC still is based on the failure definition following current practice, like vari-

ant 0. The corresponding probability and consequences include the effect of the failure paths until dike breach occurs, taken from Appendix A. This will cause the probability of dike failure drops with respect to the probability of failure used in variant 0.

- Disconnected approach variant 2. In this variant the CDC is based the failure definition according to failure paths, considering the dike to be failed in case a breach, see Appendix A. Following the Dutch standardization exercise, the economic optimal probability of failure is used as the design safety level [51], equally distributed over the two considered failure paths. This will cause the dimensions drop with respect to variant 1. The corresponding consequences are from Appendix A.
- Connected approach. In this variant the CDC is based the failure definition according to failure paths, considering the dike to be failed in case a breach, see Appendix A. The optimal CDC is chosen based on the minimum societal costs (risk and investments). No predefined failure rooms per failure paths are required. This may cause a non-equal distribution of the failure probability over the failure mechanisms, and corresponding dike dimensions with a focus on preventing the failure path responsible for the highest consequences.

The starting points for the comparison are:

- The economic consequences are based on equation (2.9).
- The dike dimensions are taken from basic collection of calculations for a raster of dike dimensions, with dike heigths per 0.1m, berm width per 3m, berm heights per 0.25 m. and inner slope 1:2.5 / 1:2.75 / 1:3.
- The individual risk is calculated in the unity as used in Chapter 3: the average number of victims per ha per year (Note: in the Netherlands the unity of victims per postal code area is used). The surface of the polder protected by the Grebbedijk is 351 km^2.
- No evacuation is taken into account.
- The discount rate and the value of a human life is taken from Appendix A.

Specific for the disconnected approach variant 0 the following starting points are taken :

- The optimal failure probability is based on the economic optimization in [51] of 1/160000 per year for a failure definition based on an overtopping discharge limit.

- Failure of the dike is assessed with the probabilistic model in Chapter 3 using the physical model in Appendix A. However, an adapted failure definition is used to simulate that failure occurs in case the wave overtopping discharge exceeds 1 l/s/m (variant 0): the model is used with an infinite strength of the inner slope revetment and an infinite thickness of the cover layer, D_{cl}.
- The economic consequences are based on [51] and the scenario 11122 / LIWO-1689 in [54] providing for victims: 1396, and for economic damage: 17,9 Billion Euro. These values are presented [51] to be valid for the year 2011. They can be used for the year 2075 since economic growth and inflation are not considered in this comparison.

The results of the comparison are presented in Table E.1. The second column reflects the dike dimensions and corresponding risk effects for the current practice, with a failure definition in which dike damage due to the occurrence of a failure mechanism is assumed to virtually cause failure. Due to the approach in this thesis to include the effect of the failure path (Chapter 3 and Appendix A), the probability of failure corresponding with these dimensions is significantly lower, see the results for variant 1 in the third column. In case of variant 2, the fourth column, the design is based on failure paths, and the dike dimensions are searched corresponding to the probability of failure in variant 0. The dimensions of the dike drop considerably with respect to variant 1. In the last step, column five, the connected approach is applied. The dike dimensions show some more focus on the prevention of overtopping (dike height increase) and less on piping (smaller and lower berm). The needed investments are more or less the same as for variant 2, however, the risks reduce considerably by about a factor 3.

Table E.1.: *Overview of differences between the connected and disconnected risk approach.*

Parameter	**Disconnected variant 0**	**Disconnected variant 1**	**Disconnected variant 2**	**Connected (= first row of Table 3.3)**
Dike height (m+NAP)	12.80	12.80	12.40	12.50
Tangent of inner slope (-)	2.5	2.5	2.5	2.75
Berm width (m)	18	18	18	15
Berm height (m)	0.75	0.75	0.75	0.5
Investments (M€)	15.7	15.7	13.4	13.3
PV of economic risk (M€)	5.7	1.2	5.5	1.7
Probability of failure ($\cdot 10^{-5}/yr$)	0.63	0.15	0.76	0.20
Indiv. risk ($\cdot 10^{-5}/ha/yr$)	0.025	0.005	0.021	0.006
PV of risk and costs (M€)	21.4	16.9	18.9	15

Summarizing, inclusion of the failure paths results in a reduced dike dimensions reducing the investments to be compliant, and application of a connected approach leads to a slightly higher dike with a smaller berm reducing the risk. Therewith, with respect to current practice (variant 0) the connected approach leads to a less extensive reinforcement requiring an investment which is significant smaller: 2.4M€, which is about 20%, and the accompanying risks are about 3 times smaller.

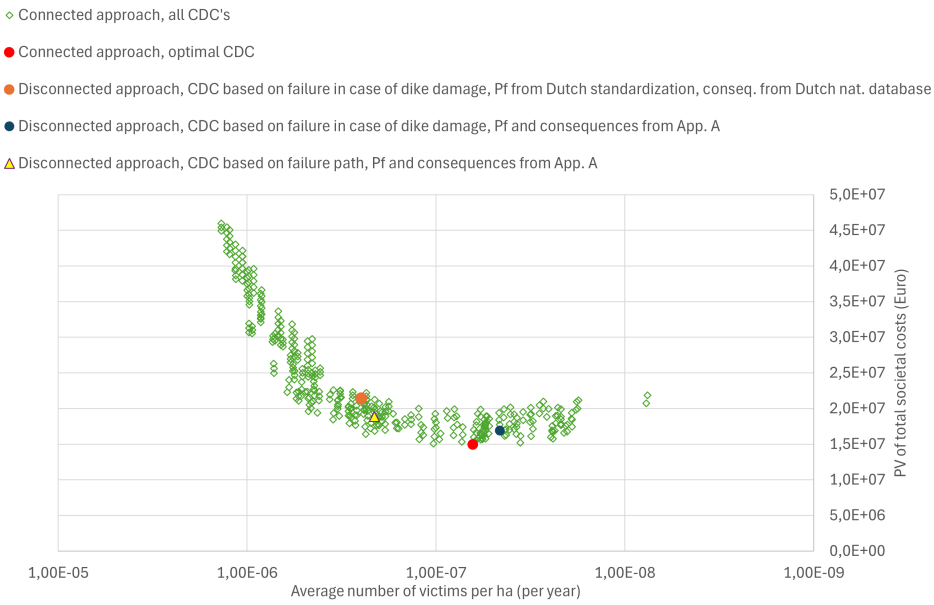

Figure E.1.: *Comparison of the total societal costs for a semi-existing dike with sand core at location Grebbedijk, for the connected risk approach with the results of the disconnected risk approaches for variants 0, 1 and 2.*

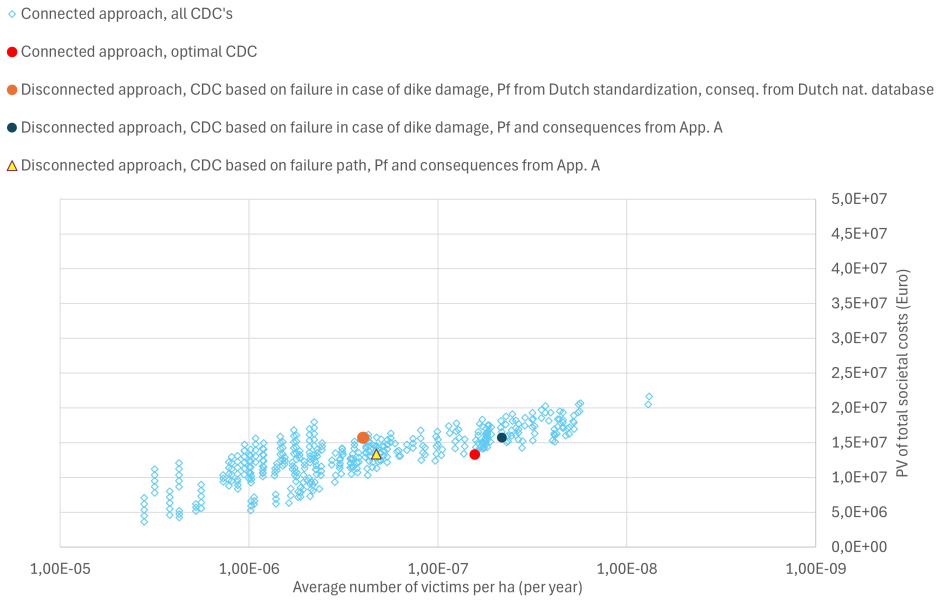

Figure E.2.: *Comparison of the investments for a semi-existing dike with sand core at location Grebbedijk, for the connected risk approach with the results of the disconnected risk approaches for variants 0, 1 and 2.*

F

RESPONSE OF ORGANISATIONS TO BOTTLENECKS AND DILEMMAS

The five situations quoted in the main text of this thesis are briefly described. For more details, we refer to [169].

1. DIKE SEGMENT APPROACH - STRATEGY DEVELOPMENT OF DIKE SEGMENT REINFORCEMENTS

Water Authority: Hoogheemraadschap Hollands Noorderkwartier (In Dutch abbreviated with HHNK)
Urged by new legislation the Water Authority has to take up the challenge to adapt to new roles and responsibilities in participative processes in spatial planning for dike reinforcement. In the existing unilateral action, the narrowly defined project would not hold, because of the required integrated approach. However, the Water Authority lacks a clear vision of the shape and implementation of such an approach: corresponding responsibilities and grants are not clear, and the staff is not familiar with adaptive working processes. The management of the Water Authority approached these practical bottlenecks as a dilemma: choosing between a mandatory step to an integrated approach, keeping a rather disciplinary and project-like approach on the one hand, and embracing a complex fully integrated approach on the other hand. The Water Authority responded to this situation by intensifying its cooperation with regional partners and widening its scope, as a preparation for the fully integrated approach. It is therefore moving from unilateral action to collaborative action or even joint action.

2. MANAGEMENT AGREEMENT LIQUEFACTION PREVENTION

Water Authority: Waterschap Scheldestromen (In Dutch abbreviated with WSSS)

The occurrence of macro-instability caused by liquefaction of the foreshore might increase the probability of dike failure. In the Scheldt River basin, Rijkswaterstaat (part of the Ministry) is responsible for the maintenance of the estuary adjacent to the dikes, and the Water Authority for the dikes along the Scheldt. In practice, the cooperation became unilateral because of the change of responsibilities within Rijkswaterstaat connected to the legislation of standards for flood defences in 2017. The old agreements (establishing responsibilities for actions and costs of the two involved institutions, referred to as external cooperation) between the public authorities need to be renewed, fitting to the renewed Water Act [188] and the protection scheme [141]. Activities to prevent liquefaction are eligible for a subsidy from the HWBP, provided there is 'good management'. However, neither has this practice been defined yet, nor has a framework agreement for funding been concluded. Furthermore, there is not yet a specification of the extent of an acceptable level of erosion beyond which action is required. The Water Authority has to trade-off between performing and financing foreshore repairs in expectation of reimbursement, at risk of not getting funded, or only starting repairs when funds are granted, at risk of delaying critical repairs which can lead to more extensive or spacious repair work. Agreements about the specification of responsibilities regarding the financing of maintenance of the foreshore are necessary to enable the Water Authority to weigh the risks. Therefore, the Water Authority intends to change cooperation from unilateral to external coordination.

3. INNOVATIVE DIKE REINFORCEMENTS

Water Authority: Waterschap Rijn en IJssel (In Dutch abbreviated with WRIJ)

The Water Authority is responsible for dike reinforcement projects. Different departments have a unilateral task to assess dike performance, implement reinforcements and maintain the dike. A project team of the Water Authority selected an innovative measure for the cost-friendly reduction of piping probability over the life cycle of their dikes. The maintenance department of the Authority was not involved in this decision. It is not familiar with the monitoring and maintenance of this measure. Due to this bottleneck, the department hesitates to take over the responsibility after the reinforcement is finalized. The Water Authority has to the trade-off between acceptance of performance uncertainties of innovative solutions or acceptance of the use of extra cost and space for dike reinforcement using standard methods. The observed response of the Water Authority points out they accept the performance uncertainties

and take organizational measures to manage the corresponding risks. The design department has to develop knowledge as a preparation for design and implementation. This knowledge is also required to develop a fit-for-purpose life cycle monitoring and maintenance scheme. Therefore, coordination of the knowledge transfer between departments is key for the willingness to take over the responsibility. The Water Authority strives to improve the yet unilateral cooperation between the departments towards coordinated cooperation, by giving appropriate mandate and power to an innovation manager to fulfill this task.

4. DEALING WITH DAMAGE OF DIKES BY BEAVERS

Water Authority: Waterschap Drents Overijsselse Delta (In Dutch abbreviated with WDOD)

Since the reintegration of the beaver in the Netherlands, beaver populations along the rivers are increasing. During high water, beavers retract to dikes where they dig holes underneath the water surface, affecting flood risk. According to Natural Law, beavers are a protected species, and their preservation extends from provincial to European policy. The province is responsible for nature conservation policy. Nature management organizations are responsible for the actual management of Natura2000 areas. The Water Authority, however, must guarantee flood safety and therefore take action. These organizations cooperate unilaterally on their own task. The water authority has to trade off whether to take into account the risk of digging beavers in their maintenance and reinforcements, or to strive for a coordinated protocol to seek a joint policy on the management of the population with an eye on flood risk management. The observed response was to move towards an increase of awareness about the risk of burrowing species and an increase of mutual understanding of unilateral responsibilities between all the stakeholders involved (Province, Water Authorities and nature conservation managers and stakeholders). Knowledge sharing and an increase in mutual understanding led to a joint policy established in a beaver-protocol. The Water Authority moves from the internal and unilateral decision-making towards external and more coordinated actions. This is a shift from internal to external, though still unilateral cooperation (every authority kept its own responsibility and tasks).

5. VISION ON LONG TERM MONITORING

Water Authority: Waterschap Hollandse Delta (In Dutch abbreviated with WSHD)

The existing monitoring scheme is performed on a project basis and focuses on specific actions. The Water Authority expects the assessment and reinforcement of flood defences based on long-lasting monitoring to pay off. However, a decision for long-lasting monitoring would lead

to changes in the organization and budgets: although HWBP takes benefits from monitoring as well, the cost of data collection is not eligible for grants by HWBP, thus, the Water Authority should organize the budgets itself. The Water Authority has to trade-off the dilemma between acceptance of life cycle monitoring efforts on its own account, combined with an organizational effort for sound internal cooperation, or acceptance of uncertainty or too costly and space-consuming dike designs, mainly paid by HWBP. The Water Authority is investigating how a broad, accepted vision and sustainable support can be acquired in its own organization, to implement monitoring as a continuous source of information for long-term life cycle dike management. This leads to innovation of the workflow because the monitoring is organized in different departments. To break through without financial consequences the Water Authority strives to improve the yet unilateral cooperation between the departments towards coordinated cooperation between the maintenance, assessment and design departments.

LIST OF FIGURES

LIST OF TABLES

CURRICULUM VITæ

Frank den Heijer

10-09-1970	Born in Voorburg, the Netherlands

EDUCATION

1982–1988	Pre-university Secondary Education (Atheneum/VWO) Driestar, Gouda
1988–1992	MSc. Civil Engineering (specialization Hydraulic engineering) Delft University of Technology

EXPERIENCE

1992	Graduation Waterloopkundig Laboratorium, Vollenhove
1993–1997	Project engineer, research manager Road and Hydraulic Engineering division, Delft Ministry of Transport, Public Works and Water Management, Directorate general of Public Works and Water Management
1997–2001	Researcher Marine and Coastal Infrastructure Delft Hydraulics, Delft
2001–2007	Programme manager, department manager National Institute for Coastal and Marine Management, Ministry of Transport, Public Works and Water Management, Directorate general of Public Works and Water Management, The Hague
2007–2010	Project engineer, programme manager Centre for Public Works, Division of Hydraulic and Environmental engineering, Ministry of Transport, Public Works and Water Management,

	Directorate general of Public Works and Water Management, Utrecht
2010–2019	Research programme manager Flood risk management Deltares, Delft
2019–2025	PhD-researcher Section of Hydraulic Structures and Flood Risk Faculty of Civil Engineering and Geosciences Delft University of Technology, Delft
2019–present	Researcher, lecturer Built Environment, Sustainable river management HAN University of applied sciences, Arnhem
2019–present	Consultant, owner Waterinfraworks, Harskamp
2022–2023	Short-Term Consultant, team leader technical team Water Europe and Central Asia World Bank group, Washington
2025–present	Journal of Flood Risk Management, Editor John Wiley & Sons Ltd and The Chartered Institution of Water and Environmental Management (CIWEM)

LIST OF PUBLICATIONS

PEER REVIEWED JOURNAL PUBLICATIONS

RELATED TO THIS THESIS

B. Vonk, W. J. Klerk, P. Fröhle, B. Gersonius, **F. den Heijer**, P. Jordan, U. R. Ciocan, J. Rijke, P. Sayers, and R. Ashley. "Adaptive asset management for flood protection: The FAIR framework in action". In: *Infrastructures* 5.12 (2020). issn: 24123811. doi: 10.3390/infrastructures5120109

B. Gersonius, B. Vonk, R. M. Ashley, **F. den Heijer**, W. J. Klerk, N. Manojlovic, J. Rijke, P. Sayers, and A. Pathirana. "Maturity Improvements in Flood Protection Asset Management across the North Sea Region". In: *Infrastructures* 5.12 (2020), p. 112. issn: 2412-3811. doi: 10.3390/INFRASTRUCTURES5120112

P. Sayers, B. Gersonius, **F. den Heijer**, W. J. Klerk, P. Fröhle, P. Jordan, U. Radu Ciocan, J. Rijke, B. Vonk, and R. Ashley. "Towards adaptive asset management in flood risk management: A policy framework". In: *Water Security* 12 (Apr. 2021), p. 100085. issn: 24683124. doi: 10.1016/j.wasec.2021.100085

A. Pathirana, **F. den Heijer**, and P. Sayers. "Water infrastructure asset management is evolving". In: *Infrastructures* 6.6 (2021). issn: 24123811. doi: 10.3390/infrastructures6060090

F. den Heijer and M. Kok. "Assessment of ductile dike behavior as a novel flood risk reduction measure". In: *Risk Analysis* (2022), pp. 1–16. doi: 10.1111/risa.14071

F. den Heijer, J. Rijke, M. Bosch-Rekveldt, A. de Leeuw, and M. Barciela-Rial. "Asset management of flood defences as a co-production – An analysis of cooperation in five situations in the Netherlands". In: *Journal of Flood Risk Management* (2023). doi: 10.1111/jfr3.12909

F. den Heijer and M. Kok. "Risk-based portfolio planning of dike reinforcements". In: *Reliability Engineering & System Safety* 242 (Feb. 2024), p. 109737. issn: 0951-8320. doi: 10.1016/J.RESS.2023.109737

OTHER

W. J. Klerk, T. Schweckendiek, **F. den Heijer**, and M. Kok. "Value of Information of Structural Health Monitoring in Asset Management of Flood Defences". In: *Infrastructures* 4.3 (2019), p. 56. issn: 2412-3811. doi: 10.3390/infrastructures4030056

F. den Heijer, M. Podt, M. Bosch-Rekveldt, A. de Leeuw, and J. Rijke. "Serious gaming for better cooperation in flood defence asset management". In: *Journal of Flood Risk Management* (2023). doi: 10.1111/jfr3.12910

CONFERENCE PUBLICATIONS

RELATED TO THIS THESIS

A. Van Agthoven, **F. den Heijer**, and A. Kraak. "The way to a floodrisk-based safety concept. Three case studies". In: *RIBAMOD, First international workshop: Current Policy and Practice*. Delft, 1997

A. Roos, **F. den Heijer**, and P. Van Gelder. "A system approach to the optimal safety level of connecting water barriers in a sea-lake environment. Case study: the Afsluitdijk dam, the Netherlands". In: *Risk based decision making in water resources VIII*. Santa Barbara: American Society of Civil Engineers, ASCE, 1997

F. den Heijer and A. de Looff. "Assessment of flood risks in polders along the Dutch Lakes. Computer simulation in risk analysis and hazard mitigation". In: *First international conference on computer simulation in risk analysis and hazard mitigation*. Ed. by J. Rubio, C. Brebbia, and J. Uso. Valencia: ISBN: 1 85312 2 6047. WIT press,Computational Mechanics Publications, 1998

F. den Heijer, R. Vos, and C. Gautier. "Probabilistic approach for safety assessment of waterdefences along the Dutch coast; model and verification". In: *Proceedings of the 31th conference Coastal Engineering*. Ed. by J. McKee Smith. World Scientific Publishing Co. Pte. Ltd, 2008, pp. 4180–4192

F. den Heijer and F. Diermanse. "Towards risk-based assessment of flood defences in The Netherlands". In: *Proceedings of FLOODrisk2012: Comprehensive Flood Risk Management - Research for Policy and Practice* (2012). doi: 10.1201/B13715-146

B. Gersonius, R. Ashley, **F. den Heijer**, W. Klerk, P. Sayers, and J. Rijke. "Asset management maturity for flood protection infrastruc-

ture: A baseline across the North Sea region". In: *Proceedings of the Sixth International Symposium on Life-Cycle Civil Engineering: Life Cycle Analysis and Assessment in Civil Engineering: Towards an Integrated Vision*. Ed. by R. Caspeele, L. Taerwe, and D. M. Frangopol. CRC Press, 2018, pp. 651–658. isbn: 9781315228914. doi: 10.1201/9781315228914-80

F. den Heijer. "Adaptive flood defence management with ductile dikes". In: *Proceedings of the 7th International Symposium on Life-Cycle Civil Engineering (IALCCE 2020)*. Ed. by A. Chen, X. Ruan, and D. Frangopol. Shanghai, China: CRC Press, 2021, pp. 471–478. doi: 10.1201/9780429343292

A. W. Van Der Meer, W. Kanning, T. Schweckendiek, N. J. Van Veen, **F. den Heijer**, and R. Jongejan. "INTERNATIONAL SOCIETY FOR SOIL MECHANICS AND GEOTECHNICAL ENGINEERING A design approach for levees considering the failure path of inner slope instability Une méthode de design des digues considérant les événements qui suivent l'instabilité initiale du ta". In: (2022). url: https://www.issmge.org/publications/online-library

OTHER

J. W. van der Meer, J. W. Langenberg, M. Klein Breteler, D. P. Hurdle, and **F. den Heijer**. "WAVE BOUNDARY CONDITIONS AND OVERTOPPING IN COMPLEX AREAS". in: *Proceedings of the 28th International conference Coastal Engineering 2002 - Solving Coastal Conodrums*. Ed. by J. McKee Smith. World Scientific Publishing Co. Pte. Ltd, 2002, pp. 2092–2104

F. Diermanse, G. Prinsen, H. van den Boogaard, **F. den Heijer**, and C. Geerse. "Application of various techniques to determine exceedence probabilities of water levels of the IJssel Lake". In: *Proceedings of ESREL 2003, Europpean safety and reliability conference*. Ed. by T. Bedrford and P. van Gelder. Maastricht: A.A. Balkema Publishers, ISBN 90 5809 551 7, 2003, pp. 495–502

F. den Heijer, F. Diermanse, and P. van Gelder. "Extreme wave statistics using Regional Frequency Analyses". In: *Proceedings of International Symposium on Stochastic Hydraulics*. Ed. by J. Vrijling, E. Ruijgh, B. Stalenberg, P. Van Gelder, M. Verlaan, A. Zijderveld, and P. Waarts. Nijmegen: IAHR, Paseo Bajo Virgen del Puerto 3, 28005 Madrid, Spain. ISBN: 90-805649-9-0, First published in 2005, 2005

J. Dekker, A. Wolters, **F. den Heijer**, and S. Fraikin. "Hydraulic Boundary Conditions for Coastal Risk Management - COMRISK Subproject 5". In:

Die Küste 70. 2005, pp. 57–74

F. den Heijer, M. A. Wolters, J. van Dorsser, H. Berger, and A. Hydra. "Developing a substitution strategy for hydraulic structures to meet the challenges of a new century". In: *Proceeedings of the 32nd PIANC MMX Congress*. Liverpool, 2010

F. den Heijer, M. Boomgaard, M. van Buren, T. E. van der Lei, J. K. van Deen, and J. IJmker. "An asset management strategy for a Dutch inland water system". In: *Life-Cycle of Structural Systems: Design, Assessment, Maintenance and Management - Proceedings of the 4th International Symposium on Life-Cycle Civil Engineering, IALCCE 2014* (2015), pp. 1883–1890. doi: 10.1201/b17618-280

W. J. Klerk, **F. den Heijer**, and T. Schweckendiek. "Value of information in life cycle management of flood defences". In: *Safety and Reliability of Complex Engineered Systems - Proceedings of the 25th European Safety and Reliability Conference, ESREL 2015* (2015), pp. 931–938. doi: 10.1201/B19094-125

W. Klerk and **F. den Heijer**. "A framework for life-cycle management of public infrastructure". In: *Life-Cycle of Engineering Systems: Emphasis on Sustainable Civil Infrastructure - 5th International Symposium on Life-Cycle Engineering, IALCCE 2016*. 2017. doi: 10.1201/9781315375175-63

M. Barciela-Rial, **F. den Heijer**, and J. Rijke. "A way forward for Building with Nature in river areas". In: *River Flow 2020 - Proceedings of the 10th Conference on Fluvial Hydraulics*. Ed. by W. Uijttewaal, M. Franca, D. Valero, V. Chavarrias, C. Arbós, R. Schielen, and A. Crosato. CRC Press/Balkema, 2020, pp. 1797–1804. isbn: 9780367627737. doi: doi.org/10.1201/b22619

F. den Heijer, J. Rijke, and M. Barciela Rial. "Serious gaming as an innovative means for handling complexity in flood risk reduction". In: *4th European conference on flood risk management*. 2020. doi: 10.3311/FloodRisk2020.14.9

F. den Heijer and M. Van. "Climate robust ductile dikes". In: *River Flow 2024*. Ed. by I. Carnacina, M. Abdellatif, M. Andredaki, J. Cooper, D. Lumbroso, and V. Ruiz-Villanueva. CRC Press, 2025, pp. 902–908. doi: 10.1201/9781003475378-131. url: ISBN%20978-1-032-75721-6